AD-A193 232 VERTICAL DIRECTIONALITY OF AMBIENT NOISE AT 32 DEG N AS A FUNCTION OF LON..(U) SCRIPPS INSTITUTION OF OCEANOGRAPHY LA JOLLA CA MARINE PHYSIC.. 1/2

UNCLASSIFIED W S HODGKISS ET AL. JAN 88 MPL-TM-387-A F/G 20/1 NL

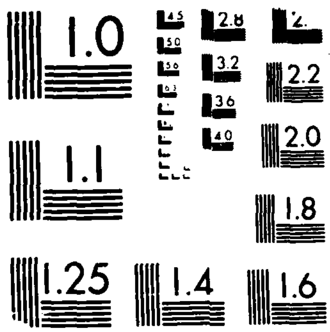

MICROCOPY RESOLUTION TEST CHART

MARINE PHYSICAL LABORATORY

SCRIPPS INSTITUTION OF OCEANOGRAPHY

San Diego, California 92152

VERTICAL DIRECTIONALITY OF AMBIENT NOISE AT 32°N AS A FUNCTION OF LONGITUDE

W. S. Hodgkiss and F. H. Fisher

MPL TECHNICAL MEMORANDUM 387-A

MPL-U-32/86

Approved for public release; distribution unlimited.

January 1988

SECURITY CLASSIFICATION OF THIS PAGE

REPORT DOCUMENTATION PAGE

1a. REPORT SECURITY CLASSIFICATION: UNCLASSIFIED	1b. RESTRICTIVE MARKINGS
2a. SECURITY CLASSIFICATION AUTHORITY	3. DISTRIBUTION/AVAILABILITY OF REPORT: Approved for public release; distribution unlimited.
2b. DECLASSIFICATION/DOWNGRADING SCHEDULE	
4. PERFORMING ORGANIZATION REPORT NUMBER(S): MPL TECHNICAL MEMORANDUM 387-A [MPL-U-32/86]	5. MONITORING ORGANIZATION REPORT NUMBER(S)
6a. NAME OF PERFORMING ORGANIZATION: Marine Physical Laboratory; 6b. OFFICE SYMBOL (If applicable): MPL	7a. NAME OF MONITORING ORGANIZATION: Office of Naval Research, Department of the Navy
6c. ADDRESS (City, State, and ZIP Code): University of California, San Diego, Scripps Institution of Oceanography, San Diego, CA 92152	7b. ADDRESS (City, State, and ZIP Code): 800 North Quincy Street, Arlington, VA 22217-5000
8a. NAME OF FUNDING/SPONSORING ORGANIZATION: Office of Naval Research; 8b. OFFICE SYMBOL (If applicable): ONR	9. PROCUREMENT INSTRUMENT IDENTIFICATION NUMBER: N00014-84-K-0097 and N00014-87-C-0127
8c. ADDRESS (City, State, and ZIP Code): Department of the Navy, 800 North Quincy Street, Arlington, VA 22217-5000	10. SOURCE OF FUNDING NUMBERS: PROGRAM ELEMENT NO. / PROJECT NO. / TASK NO. / WORK UNIT ACCESSION NO.

11. TITLE (Include Security Classification)
Vertical Directionality of Ambient Noise at 32°N as a Function of Longitude

12. PERSONAL AUTHOR(S)
W. S. Hodgkiss and F. H. Fisher

13a. TYPE OF REPORT	13b. TIME COVERED	14. DATE OF REPORT (Year, Month, Day)	15. PAGE COUNT
tech memo	FROM ______ TO ______	January 1988	127

16. SUPPLEMENTARY NOTATION

17. COSATI CODES			18. SUBJECT TERMS (Continue on reverse if necessary and identify by block number)
FIELD	GROUP	SUB-GROUP	ambient noise, vertical arrays, vertical distribution

19. ABSTRACT (Continue on reverse if necessary and identify by block number)

Measurements have been made of the ambient noise field between 25 and 300 Hz with vertical arrays at 32°N (124°W, 136°W, and 150°W). Substantial differences in the vertical distribution of noise have been measured, especially at the higher frequencies which can be interpreted in the context of attenuation by seawater sound absorption of coastal shipping. Due to substantial differences in weather at the stations, these measurements also provide an opportunity to observe the effect of weather on the vertical distribution of ambient noise.

20. DISTRIBUTION/AVAILABILITY OF ABSTRACT: ☐ UNCLASSIFIED/UNLIMITED ☒ SAME AS RPT ☐ DTIC USERS	21. ABSTRACT SECURITY CLASSIFICATION: UNCLASSIFIED
22a. NAME OF RESPONSIBLE INDIVIDUAL: W. S. Hodgkiss	22b. TELEPHONE (Include Area Code): 619-534-1798; 22c. OFFICE SYMBOL: MPL

DD FORM 1473, 84 MAR — 83 APR edition may be used until exhausted. All other editions are obsolete

SECURITY CLASSIFICATION OF THIS PAGE

☆ U.S. Government Printing Office: 1986—607-044

Vertical Directionality of Ambient Noise

at 32°N as a Function of Longitude

W.S. Hodgkiss and F.H. Fisher

Marine Physical Laboratory
Scripps Institution of Oceanography
San Diego, CA 92152

Abstract

Measurements have been made of the ambient noise field between 25 and 300 Hz with vertical arrays at 32°N (124°W, 136°W, and 150°W). Substantial differences in the vertical distribution of noise have been measured, especially at the higher frequencies which can be interpreted in the context of attenuation by seawater sound absorption of coastal shipping. Due to substantial differences in weather at the stations, these measurements also provide an opportunity to observe the effect of weather on the vertical distribution of ambient noise.

I. Introduction

Ambient ocean noise in the low and mid-frequency regions has received a great deal of attention over the last 25 years. Although not intended to be complete, the references provide an indication of the wide scope of this work. In the unclassified literature, major comprehensive bibliographies include [1-4], books [5-8], workshops [9-10], the analysis of experimental data sets [11-43], ship radiated noise characteristics [44-47], theoretical models [48-64], and the performance of array processors operating in an ambient noise environment [65-73]. A representative view into the classified literature can be obtained by reviewing past issues of the U.S. Navy Journal of Underwater Acoustics and the proceedings of the Navy Symposium on Underwater Acoustics.

Downslope conversion of coastal shipping noise has been discussed as being a major contributor to the low-angle noise distribution in the vertical plane (angles close to the horizontal) [33,38-40,42]. If this is so, then sound absorption in seawater should produce changes in the distribution of low-angle noise in the vertical plane as a function of range from coastal shipping.

A decrease in the noise energy per unit angle in the vertical offers improved array performance as a function of distance from coastal shipping. In the Pacific for these latitudes (32°N), the attenuation is about 0.005 dB/km at 300 Hz and decreases to 0.00125 dB/km at 150 Hz. At a range of 1500 nmi (2778 km), the attenuation would be 13.9 dB at 300 Hz and only 3.5 dB at 150 Hz. Therefore, if we had data on vertical noise distribution at short and long ranges from coastal shipping, we would expect to see substantial absolute differences at low angles between the 300 Hz data and much less for the 150 Hz data.

We have made such measurements - two at 32°N 124°W (approximately 350 nmi due west of San Diego), and one each at 32°N 136°W (approximately 1000 nmi west) and 32°N 150°W (approximately 1700 nmi west). Due to substantial differences in weather at the stations, these measurements also provide an opportunity to observe the effect of weather on the vertical distribution of ambient noise.

A summary of the analysis results is contained in this volume (MPL-TM-387-A). Companion volumes (MPL-TM-387-B,C,D,E) contain the complete analysis results for the four data tapes examined (Tapes #85010, 86060, 86247, and 86180, respectively).

II. Experiment Description and Data Analysis

The data were obtained with two uniformly spaced arrays suspended in the vertical from FLIP and centered on the sound axis ($z = 750$ m) - the 48 element NORDA VEKA array cut for 309 Hz ($d = 2.4$ m) and the 27 element MPL digital array cut for 217 Hz ($d = 3.46$ m). FLIP was in a tight, three-point moor at 32°N, 124°W for the October 1985 data taken with the NORDA VEKA array and drifting slowly at 32° 124°W, 32° 136°W, and 32° 150°W for the April/May 1986 data taken with the MPL digital array. Figure 1 shows the array deployment geometry superimposed on a representative sound velocity profile. The locations of the FLIP stations are indicated on the chart in Figure 2.

The NORDA VEKA array data discussed here were taken on 18 October 1985 starting at 20:05 PDT (Tape #85010, position 32° 124°W, wind speed 6 kts). Twenty-one data segments each of length 72 s were analyzed (25.2 min total). With a sampling rate $f_s = 907.8$ Hz, each segment consisted of 65536 samples/channel.

Figures 5-6 display the power spectra of Channels #1, 16, 32, and 48 from the first segment of the NORDA VEKA array data (Channel #1 corresponds to the hydrophone at the top of the array). They were derived from the incoherent addition of 15, 50% overlapped, 8192-point FFT's (111 mHz bin width). A Kaiser-Bessel window ($\alpha = 2.5$) weighted the data prior to each FFT. For this value of α, the highest sidelobe level is -57 dB [74]. The values reported in these figures are properly calibrated (dB re 1 μPa/$\sqrt{\text{Hz}}$). The 90% confidence interval for these results is +2.0/-1.6 dB. The very prominent line at slightly less than 250 Hz was projected from a support ship as part of the experiment. The line at 174 Hz was generated on board FLIP.

The MPL digital array data discussed here were taken on 27 April 1986 starting at 06:34 PDT (Tape #86060, position 32° 124°W, wind speed 22 kts), 9 May 1986 starting at 13:38 PDT (Tape #86247, position 32° 136°W, wind speed 17 kts), and 5 May 1986 starting at 10:09 PDT (Tape #86180, position 32° 150°W, wind speed 10 kts). Twenty data segments each of length 55.7 s were analyzed (18.6 min total) from each tape. With a sampling rate of $f_s = 1176$ Hz, each segment consisted of 65536 samples/channel.

Figures 9-10, 13-14, and 17-18 display the power spectra of Channels #1, 10, 20, and 27 from the first segment of each of the MPL digital array data tapes (Channel #1 corresponds to the hydrophone at the top of the array). They were derived from the incoherent addition of 15, 50% overlapped, 8192-point FFT's (144 mHz bin width). A Kaiser-Bessel window ($\alpha = 2.5$) weighted the data prior to each FFT. The values reported in these figures are properly calibrated (dB re 1 μPa/$\sqrt{\text{Hz}}$). The 90% confidence interval for these results is +2.0/-1.6 dB.

The results in the next section were produced with a FFT beamformer [75]. The along-channel FFT's were 50% overlapped and 8192-points in length. A Kaiser-Bessel window ($\alpha = 2.5$) weighted the data prior to each FFT. The cross-channel FFT's were 512-points in length where the (complex) data first was windowed with a 48-point (NORDA VEKA array data) or a 27-point (MPL digital array data) Kaiser-Bessel window ($\alpha = 1.5$) and then zero-padded out to the FFT length. For this value of α, the first sidelobe is -35 dB [74]. Figures 3-4 display the beam patterns of both arrays at several frequencies.

III. Discussion

Figures 7-8, 11-12, 15-16, and 19-20 report the time-evolving character of ambient noise vertical directionality at three stations due west of San Diego. Tape #85010 is from the NORDA VEKA array at 124°W. Tapes #86060, 86247, and 86180 are from the MPL digital array at 124°W, 136°W, and 150°W, respectively. The waterfall plots represent a (time) FFT bin width of 111 mHz (NORDA VEKA array) and 144 mHz (MPL digital array) centered every 25 Hz from 25 Hz through 300 Hz. Multi-panel plots of the same results are included for $f = 75$ Hz, $f = 150$ Hz, and $f = 300$ Hz. Positive angies refer to downward looking beams. The plots have been calibrated to report ambient noise power spectral density per Hz per degree of vertical angle (dB re 1 $\mu Pa/\sqrt{HzDeg}$).

A number of observations can be made by comparing the waterfall and multi-panel plots from the three stations. Under calm weather conditions (Tapes #85010 and #86180), the vertical distribution of ambient noise clearly is concentrated within approximately ±15° of the horizontal. Under poor weather conditions (Tape #86060), high wind speed has the effect of filling in the higher vertical angles while leaving the level within the low-angular region unchanged. Under intermediate weather conditions (Tape #86247), a transition between these two characteristics occurs which is frequency dependent (in the case of Tape #86247, the transition occurs in the the 125-150 Hz region). This frequency-dependent transition characteristic is consistent with single hydrophone measurements reported in the literature (e.g. see [24] where ambient noise levels above 100 Hz were very sensitive to wind speed while ambient noise levels below 100 Hz showed no wind speed dependence at all).

In the low-angular region at the higher frequencies, significant differences can be seen in the vertical distribution of ambient noise as a function of distance from the coast. There is a clear decrease in absolute level with distance. Furthermore, a concave character to the angular distribution of ambient noise centered on the horizontal begins to appear. Both of these observations are consistent with the hypothesis that downslope conversion of coastal shipping noise constitutes a major portion of the low-angle energy and that this kind of noise is diminished by sound absorption as a function of distance from the coast.

IV. Summary

Downslope conversion of coastal shipping noise has been discussed as being a major contributor to the low-angle noise distribution in the vertical plane (angles close to the horizontal). The results reported here on the vertical directionality of ambient noise as a function of longitude are consistent with this hypothesis. Sound absorption in seawater appears to diminish the low-angle energy as a function of distance from the coast with the effect being more pronounced at higher frequencies than at lower frequencies.

Due to substantial differences in weather at the stations, these measurements also provided an opportunity to observe the effect of weather on the vertical distribution of ambient noise. Under calm weather conditions, the vertical distribution of ambient noise clearly is concentrated within approximately $\pm 15^\circ$ of the horizontal. Under poor weather conditions, high wind speed has the effect of filling in the higher vertical angles while leaving the level within the low-angular region unchanged. Under intermediate weather conditions, a frequency-dependent transition between these two characteristics occurs which is consistent with single hydrophone measurements of wind speed dependence.

Acknowledgements

This work was supported by the Office of Naval Research under contract N00014-84-K-0097 and the Naval Air Systems Command under contract N00014-87-C-0127. The NORDA VEKA array was augmented by Neptune Ocean Engineering under the supervision of Dr. Tom Tunnell of NORDA. Dr. Tunnell was in charge of the NORDA and Neptune Ocean Engineering personnel which included Cecil Watkins and Andrew Monks of NORDA and Dr. Norman Gholson and Tony Jarrell of Neptune. Subcontracts from MPL to NORDA and Neptune Ocean Engineering were let in order to collect the data discussed here. Dr. Fred Fisher was chief scientist for CONTRACK VIII and IX and Dr. Bill Hodgkiss was in charge of data analysis. We wish to thank Mr. Dewitt Efird, the Officer-in-Charge of FLIP and his crew for their excellent cooperation.

References

[1] G.M. Wenz, "Review of Underwater Acoustics Research: Noise," J. Acoust. Soc. Am. 51:3(2):1010-1024 (1972).

[2] W. Crouch, "Ambient Sea Noise: A Review of the Literature," NUSC TR-4179, Naval Underwater Systems Center, New London, CT (1972).

[3] R.A. Wagstaff, "A Comprehensive Ambient Noise Bibliography," NUC TR-333, Naval Undersea Center, San Diego, CA (1973).

[4] Tery E. Ingalsbe, "The Ambient Noise Bibliographic Data Bank," AESD TN-75-03, Acoustic Environmental Support Detachment, Office of Naval Research, Arlington, VA (1975).

[5] D. Ross, "Mechanics of Underwater Noise," Pergamon Press (1976).

[6] R.J. Urick, "Sound Propagation in the Sea," Defense Advanced Research Projects Agency, Washington, DC (1979).

[7] R.J. Urick. Principles of Underwater Sound. NY: McGraw-Hill, 1983.

[8] R.J. Urick, "Ambient Noise in the Sea," Undersea Warfare Technology Office, Naval Sea Systems Command, Dept. of the Navy, Washington, DC (1984).

[9] "International Workshop on Low-Frequency Propagation and Noise," 14-19 October 1974, Woods Hole, MA (Coordinated by the Maury Center for Ocean Science, Office of Naval Research).

[10] R.A. Wagstaff and O.Z. Bluy, "Proceedings SACLANTCEN Conference on Underwater Ambient Noise," 15 June 1982 La Spezia, Italy.

[11] G.M. Wenz, "Acoustic Ambient Noise in the Ocean: Spectra and Sources," J. Acoust. Soc. Am. 34(2): 1936-1956 (1962).

[12] G.R. Fox, "Ambient-Noise Directivity Measurements," J. Acoust. Soc. Am. 36(3): 1537-1540 (1964).

[13] R.J. Talham, "Ambient-Sea-Noise Model," J. Acoust. Soc. Am. 36(8): 1541-1544 (1964).

[14] C.L. Piggott, "Ambient Sea Noise at Low Frequencies in shallow Water off the Scotian Shelf," J. Acoust. Soc. Am. 36(11): 2152-2163 (1964).

[15] E.H. Axelrod, B.A. Schoomer, and W.A. Von Winkle, "Vertical Directionality of Ambient Noise in the Deep Ocean at a Site near Bermuda," J. Acoust. Soc. Am. 37(1): 77-83 (1965).

[16] R. Rudnick and E.D. Squier, "Fluctuations and Directionality in Ambient Sea Noise," J. Acoust. Soc. Am. 41(5): 1347-1351 (1967).

[17] A.J. Perrone, "Deep-ocean ambient-noise spectra in the northwest Atlantic," J. Acoust. Soc. Am. 46: 762-770 (1969).

[18] A.J. Perrone, "Ambient noise spectrum levels as a function of water-depth," J. Acoust. Soc. Am. 48: 362-370 (1970).

[19] A.J. Perrone, "Infransonic and low-frequency ambient noise measurements on the Grand Banks," J. Acoust. Soc. Am. 55: 754-758 (1974).

[20] R. Martin and A. Perrone, "Geographical variation of ambient noise in the ocean for the frequency range from 1 Hz to 5 kHz," International Workshop on Low-Frequency Propagation and Noise, Vol. 2, 14-19 October 1974, Woods Hole, MA, pp. 817-841.

[21] G. B. Morris, "Preliminary Results on Seamount and Continental Slope Reflection Ennhancement of Shipping Noise," MPL-U-57/75, Marine Physical Laboratory, Scripps Institution of Oceanography, San Diego, CA (1975).

[22] A.C. Kibblewhite, J.A. Shooter, and S.L. Watkins, "Examination of attenuation at very low frequencies using the deep-water ambient noise field," J. Acoust. Soc. Am. 60(5): 1040-1047 (1976).

[23] D.H. Cato, "Ambient sea noise in waters near Australia," J.Acoust. Soc. Am. 60(2): 320-328 (1976).

[24] G. B. Morris, "Depth dependence of ambient noise in the northeast Pacific Ocean," J. Acoust. Soc. Am. 64: 581-590 (1978).

[25] R.A. Wagstaff, "Iterative technique for ambient-noise horizontal-directionality estimation from towed line-array data," J. Acoust. Soc. Am. 63(3): 863-869 (1978).

[26] V.C. Anderson, "Envelope spectra for signals and noise in vertically directional beams," J. Acoust. Soc. Am. 65(6): 1480-1487 (1979).

[27] V.C. Anderson, "Variation of the vertical directionality of noise with depth in the North Pacific," J. Acoust. Soc. Am. 66(5): 1446-1452 (1979).

[28] R.W. Bannister, R. N. Denham, K. M. Guthrie, D. G. Browning, A. J. Perrone, "Variability of low-frequency ambient sea noise," J. Acoust. Soc. Am. 65: 1156-1163 (1979).

[29] V.C. Anderson, "Nonstationary and nonuniform oceanic background in a high-gain acoustic array," J. Acoust. Soc. Am. 67(4): 1170-1179 (1980).

[30] W.S. Hodgkiss and V.C. Anderson, "Detection of sinusoids in ocean acoustic background noise," J. Acoust. Soc. Am. 67(1): 214-219 (1980).

[31] R.A. Wagstaff, "Horizontal directionality estimation considering array tilt and noise field vertical arrival structure," J. Acoust. Soc. Am. 67(4): 1287-1294 (1980).

[32] J.A. Shooter and M. Gentry, "Wind generated noise in the Parece Vela Basin," J. Acoust. Soc. Am. 70(6): 1757-1761 (1981).

[33] R.A. Wagstaff, "Low-frequency ambient noise in the deep sound channel - The missing component," J. Acoust. Soc. Am. 69(4): 1009-1014 (1981).

[34] S.C. Wales and O.I. Diachok, "Ambient noise vertical directionality in the northwest Atlantic," J. Acoust. Soc. Am. 70(2): 577-582 (1981).

[35] R.C. Tyce, "Depth Dependence of Directionality of Ambient Noise in the North Pacific: Experimental Data And Equipment Design," SACLANTCEN Conference Proceedings No. 32 (Underwater Ambient Noise), 15 June 1982, SACLANT ASW Research Centre, San Bartolomeo, Italy.

[36] A.S. Burgess and D.J. Kewley, "Wind-generated surface noise source levels in deep water east of Australia," J. Acoust. Soc. Am. 73(1): 201-210 (1983).

[37] W.A. Kuperman and M.C. Ferla, "A shallow water experiment to determine the source spectrum level of wind-generated noise," J. Acoust. Soc. Am. 77(6): 2067-2073 (1985).

[38] W.M. Carey, R.A. Wagstaff, B.A. Brunson, and M.R. Bradley, "Low-Frequency Noise Fields and Signal Characteristics," NORDA TR-131, Naval Ocean Research and Development Activity,

NSTL, MS (1985).

[39] W.M. Carey and R.A. Wagstaff, "Low-frequency noise fields," J. Acoust. Soc. Am. 80(5): 1523-1526 (1986).

[40] W.M. Carey, "Measurement of down-slope sound propagation from a shallow source to a deep ocean receiver," J.Acoust. Soc. Am. 79(1): 49-59 (1986).

[41] R.W. Bannister, "Deep sound channel noise from high-latitude winds," J. Acoust. Soc. Am. 79(1): 41-48 (1986).

[42] W.M. Carey, I.B. Gereben, and B.A. Brunson, "Measurement of sound propagation downslope to a bottom-limited sound channel," J. Acoust. Soc. Am. 81(2): 244-257 (1987).

[43] M.J. Buckingham, "A new shallow-ocean technique for determining the critical angle of the seabed from the vertical directionality of the ambient noise in the water column," J. Acoust. Soc. Am. 81(4): 938-946 (1987).

[44] J. Cybulski, "Probable Origin of Measured Supertanker Radiated Noise Spectra," Oceans '77, pp. 15c-1 to 15c-8 (1977).

[45] B. Schmalfeldt and D. Rauch, "Ambient and Ship-Induced Low-Frequency Noise in Shallow Water," appears in: W. Kuperman and F. Jensen, "Bottom-Interacting Ocean Acoustics," pp. 329-343, NY: Plenum Press (1980).

[46] L.M. Gray and D.S. Greeley, "Source level model for propeller blade rate radiation for the world's merchant fleet," J. Acoust. Soc. Am. 67(2): 516-522 (1980).

[47] J.C. Heine, "Acoustic Source Characteristics of Merchant Ships," SACLANTCEN Conference Proceedings No. 32 (Underwater Ambient Noise), 15 June 1982, SACLANT ASW Research Centre, San Bartolomeo, Italy.

[48] W.S. Liggett and M.J. Jacobson, "Covarieance of Noise in Attenuating Media," J. Acoust. Soc. Am. 36: 1183-1194 (1964).

[49] W.S. Liggett and M.J. Jacobson, "Covariance of Surface-Generated Noise in a Deep Ocean," J. Acoust. Soc. Am. 38: 303-312 (1965).

[50] H. Cox, "Spatial correlation in arbitrary noise fields with application to ambient sea noise," J. Acoust. Soc. Am. 54(5): 1289-1301 (1973).

[51] H. Cox, "Spatial correlation in arbitrary noise fields with application to ambient sea noise," J. Acoust. Soc. Am. 54(5): 1289-1301 (1973).

[52] W.A. Kuperman and F. Ingenito, "Spatial correlation of surface generated noise in a stratified ocean," J. Acoust. Soc. Am. 67(6): 1988-1996 (1980).

[53] M.J. Buckingham, "A theoretical model of ambient noise in a low-loss, shallow water channel," J. Acoust. Soc. Am. 67(4): 1186-1192 (1980).

[54] R.C. Cavanagh and W.W. Renner, "Vertical directionality and depth dependence of averaged acoustic signals and noise," J.Acoust. Soc. Am. 68(5): 1467-1474 (1980).

[55] D.E. Weston, "Ambient noise depth-dependence models and their relation to low-frequency attenuation," J. Acoust. Soc. Am. 67(2): 530-537 (1980).

[56] C.I. Oelkers, "Noise correlation functions for arbitrary receiver orientation and steering direction in vertically anisotropic, azimuthally isotropic noise fields," J. Acoust. Soc. Am. 67(3): 864-867 (1980).

[57] R.J. Talham, "Noise correlation functions for anisotropic noise fields," J. Acoust. Soc. Am. 69(1): 213-214 (1981).

[58] R.J. Talham, "Noise correlation functions for anisotropic noise fields," J. Acoust. Soc. Am. 69(1): 213-214 (1981).

[59] M.J. Buckingham, "Spatial coherence of wind-generated noise in a shallow ocean channel," J. Acoust. Soc. Am. 70(5): 1412-1420 (1981).

[60] R.A. Wagstaff, "Noise Field Calculation or Measurement Simulation: Some Comments on Ambient Noise Modeling," Oceans '82, pp. 187-191 (1982).

[61] D. Ross, "Role of Propagation in Ambient Noise," SACLANTCEN Conference Proceedings No. 32 (Underwater Ambient Noise), 15 June 1982, SACLANT ASW Research Centre, San Bartolomeo, Italy.

[62] J.H. Wilson, "Wind-generated noise modeling," J. Acoust. Soc. Am. 73(1):211-216 (1983).

[63] R. Dashen and W. Munk, "Three models of ocean noise," J. Acoust. Soc. Am. 76(2): 540-554 (1984).

[64] M.J. Buckingham, "A theoretical model of surface-generated noise in a wedge-shaped ocean with pressure-release boundaries," J. Acoust. Soc. Am. 78(1): 143-148 (1985).

[65] H. Cox, "Line array performance when the signal coherence is spatially dependent," J.Acoust. Soc. Am. 54(6): 1743-1746 (1973).

[66] E.R. Floyd and D.F. Gordon, "Effects of Propagation on Linear Array Performance," NUC TN 1774, Naval Undersea Center, San Diego, CA (1976).

[67] M.J. Buckingham, "On the response of steered vertical line arrays to anisotropic noise," Proc. R. Soc. Lond. A 367: 539-547 (1979).

[68] M.J. Buckingham, "Array gain of a broadside vertical line array in shallow water," J.Acoust. Soc. Am. 65(1): 148-161 (1979).

[69] R.M. Hamson, "The theoretical gain limitations of a passive vertical line array in shallow water," J.Acoust. Soc. Am. 68(1): 156-164 (1980).

[70] F. Ingenito, "Calculations of the Spatial coherence and Array Noise Gain of Wind-Generated Noise," Oceans '82, pp. 166-171 (1982).

[71] M.J. Buckingham, "On the response of a towed array to the acoustic field in shallow water," IEE Proc 131 F (3): 298-307 (1984).

[72] R.M. Hamson, "The theoretical responses of vertical and horizontal line arrays to wind-induced noise in shallow water," J.Acoust. Soc. Am. 78(5): 1702-1712 (1985).

[73] B.G. Ferguson and D.V. Wyllie, "Comparison of observed and theoretical responses of a horizontal line array to wind-induced noise in the deep ocean," J. Acoust. Soc. Am. 82(2): 601-605 (1987).

[74] F.J. Harris, "On the Use of Windows for Harmonic Analysis with the Discrete Fourier Transform," Proc. IEEE 66(1): 51-83 (1978).

[75] J.R. Williams, "Fast Beam-Forming Algorithm," J. Acoust. Soc. Am. 44(5): 1454-1455 (1968).

Figure Captions

Figure 1. Array Deployment Geometry and Representative Sound Velocity Profile.

Figure 2. FLIP Stations for October 1985 and April/May 1986 Experiments.

Figure 3. Beam Patterns: NORDA VEKA Array. (a) Kaiser-Bessel ($\alpha = 1.5$) shading function and (b) Rectangular shading function.

Figure 4. Beam Patterns: MPL Digital Array. (a) Kaiser-Bessel ($\alpha = 1.5$) shading function and (b) Rectangular shading function.

Figure 5. Power Spectra: Tape #85010. FFT Bin Width = 111 mHz. Calibration: dB//μPa/$\sqrt{}$Hz. Channels #1, 16, 32, and 48.

Figure 6. Power Spectra: Tape #85010. FFT Bin Width = 111 mHz. Calibration: dB//μPa/$\sqrt{}$Hz. (a) Channel #1, (b) Channel #16, (c) Channel #32, and (d) Channel #48.

Figure 7. Ambient Noise Vertical Directionality: Tape #85010. 32°N 124°W. Wind speed 6 kts. 18 October 1985, 20:05 PDT. Kaiser-Bessel ($\alpha = 1.5$) shading function. Positive angles refer to downward looking beams. Calibration: dB//μPa/$\sqrt{}$HzDeg. (a) f = 25 Hz, (b) f = 50 Hz, (c) f = 75 Hz, (d) f = 100 Hz, (e) f = 125 Hz, (f) f = 150 Hz, (g) f = 175 Hz, (h) f = 200 Hz, (i) f = 225 Hz, (j) f = 250 Hz, (k) f = 275 Hz, and (l) f = 300 Hz.

Figure 8. Ambient Noise Vertical Directionality: Tape #85010. 32°N 124°W. Wind speed 6 kts. 18 October 1985, 20:05 PDT. Kaiser-Bessel ($\alpha = 1.5$) shading function. Positive angles refer to downward looking beams. Calibration: dB//μPa/$\sqrt{}$HzDeg. (a) f = 75 Hz, (b) f = 150 Hz, and (c) f = 300 Hz.

Figure 9. Power Spectra: Tape #86060. FFT Bin Width = 144 mHz. Calibration: dB//μPa/$\sqrt{}$Hz. Channels #1, 10, 20, and 27.

Figure 17. Power Spectra: Tape #86180. FFT Bin Width = 144 mHz. Calibration: dB//μPa/$\sqrt{}$Hz. Channels #1, 10, 20, and 27.

Figure 18. Power Spectra: Tape #86180. FFT Bin Width = 144 mHz. Calibration: dB//μPa/$\sqrt{}$Hz. (a) Channel #1, (b) Channel #10, (c) Channel #20, and (d) Channel #27.

Figure 19. Ambient Noise Vertical Directionality: Tape #86180. 32°N 150°W. Wind speed 10 kts. 5 May 1986, 10:09 PDT. Kaiser-Bessel (α = 1.5) shading function. Positive angles refer to downward looking beams. Calibration: dB//μPa/$\sqrt{}$HzDeg. (a) f = 25 Hz, (b) f = 50 Hz, (c) f = 75 Hz, (d) f = 100 Hz, (e) f = 125 Hz, (f) f = 150 Hz, (g) f = 175 Hz, (h) f = 200 Hz, (i) f = 225 Hz, (j) f = 250 Hz, (k) f = 275 Hz, and (l) f = 300 Hz.

Figure 20. Ambient Noise Vertical Directionality: Tape #86180. 32°N 150°W. Wind speed 10 kts. 5 May 1986, 10:09 PDT. Kaiser-Bessel (α = 1.5) shading function. Positive angles refer to downward looking beams. Calibration: dB//μPa/$\sqrt{}$HzDeg. (a) f = 75 Hz, (b) f = 150 Hz, and (c) f = 300 Hz.

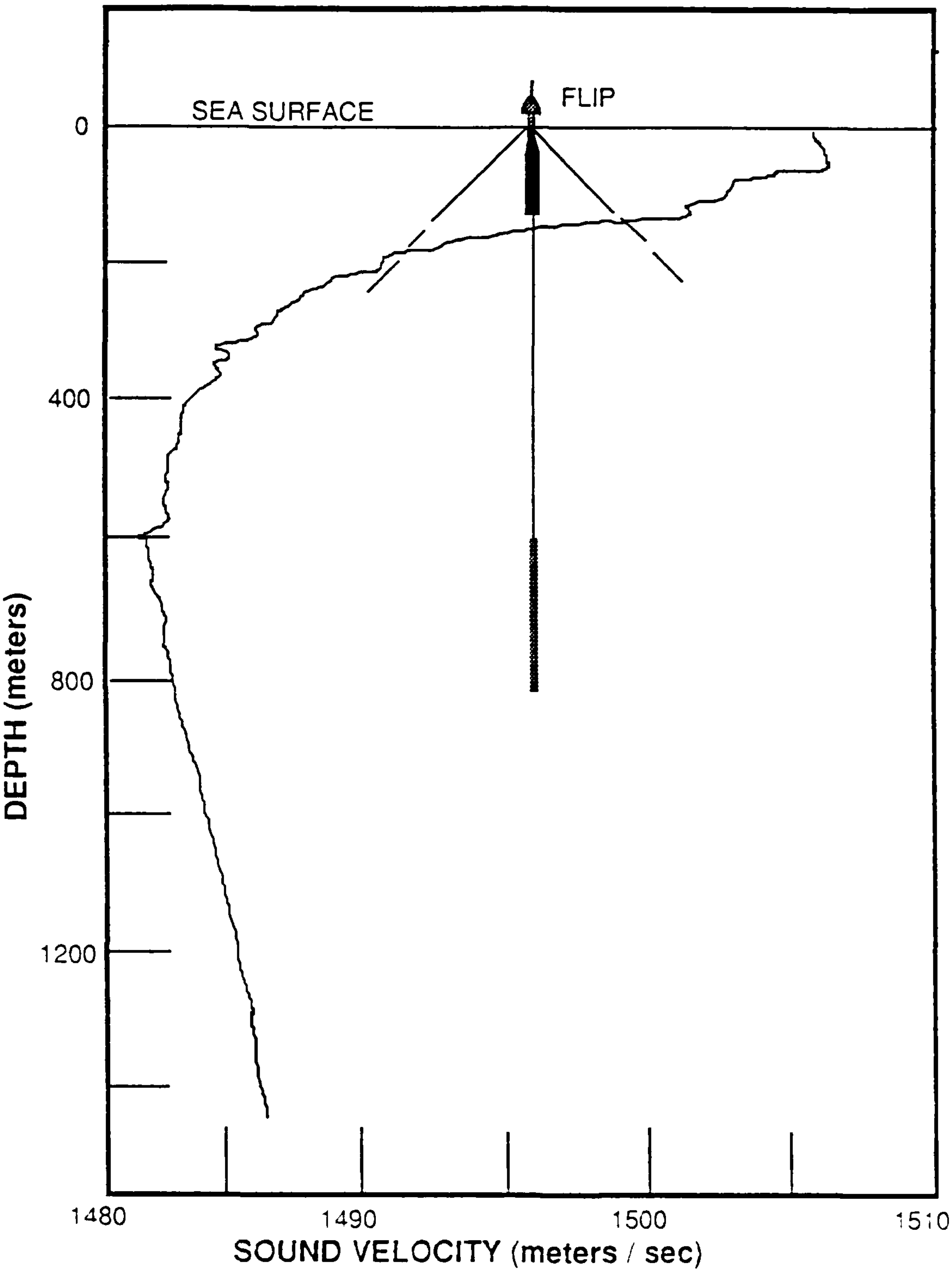
SEA SURFACE
FLIP
0
400
800
1200
DEPTH (meters)
1480
1490
1500
1510
SOUND VELOCITY (meters / sec)

Figure 1.

Hawaii to California

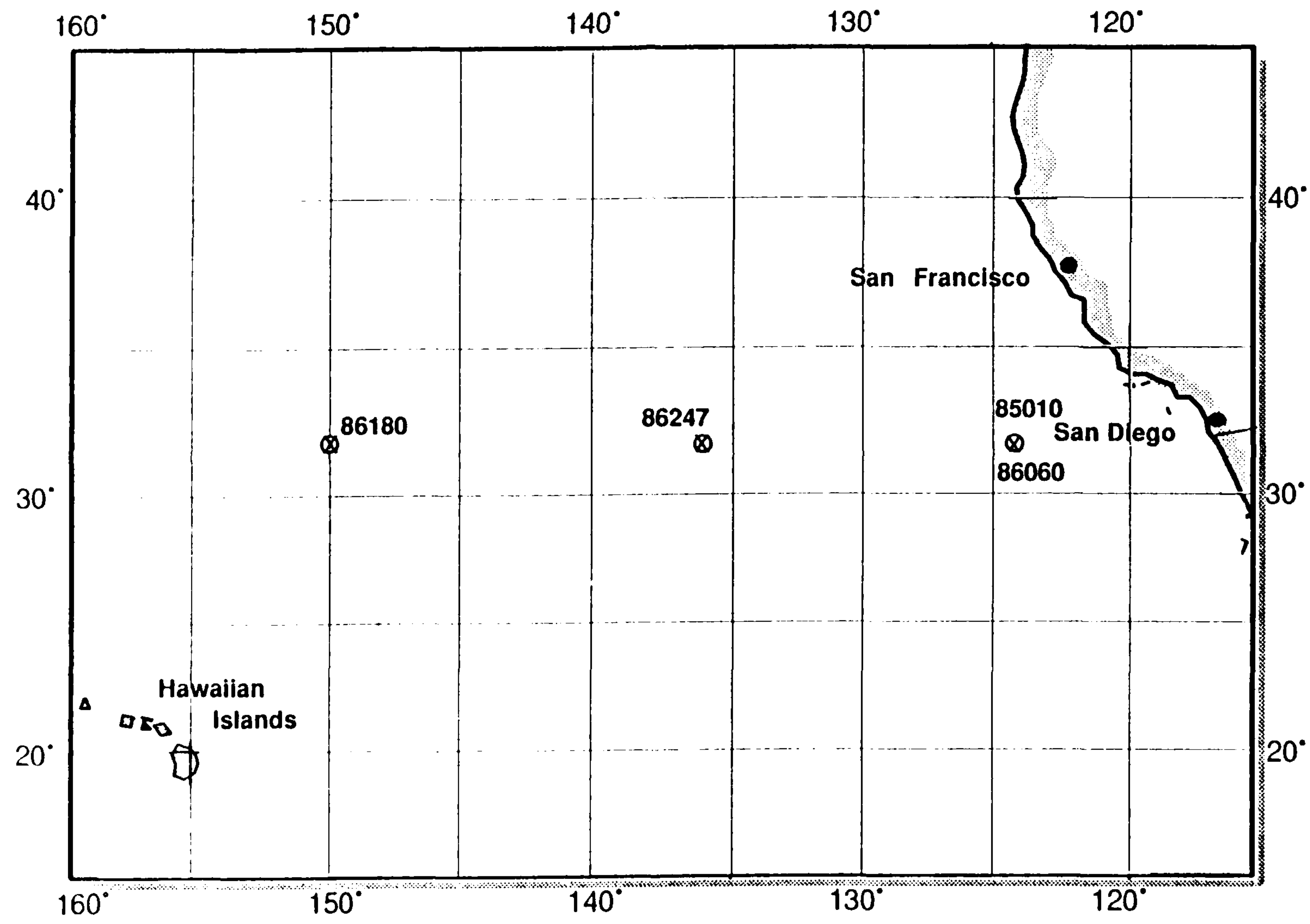

Figure 2.

VLKA Array Beam Pattern: Kb window (alpha = 1.5)

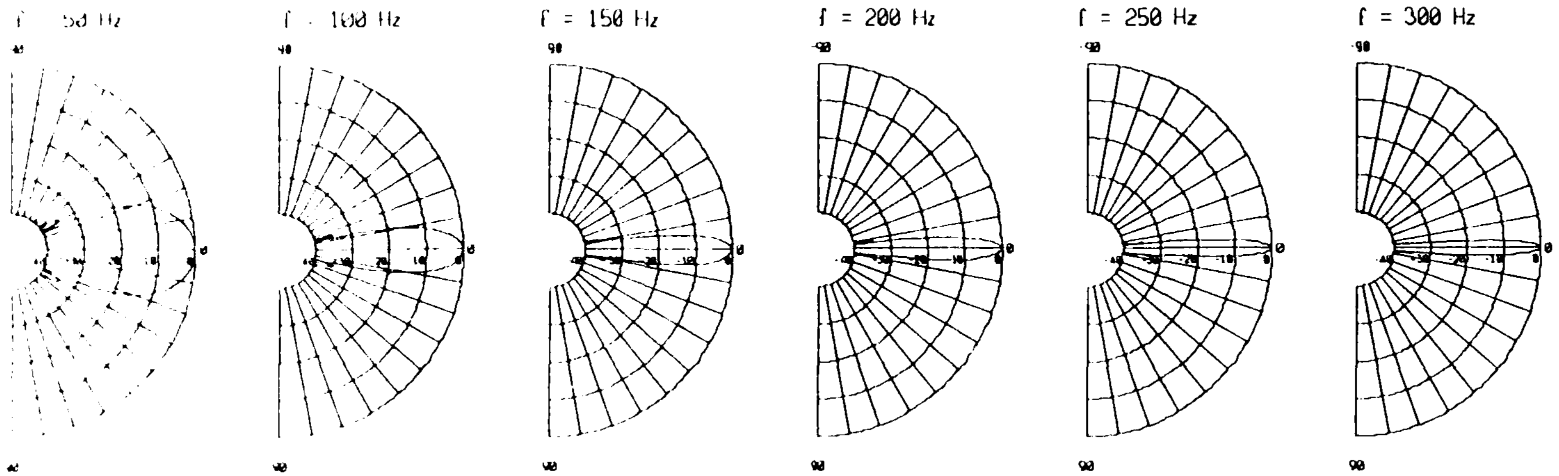

Figure 3(a).

VLKA Array Beam Pattern: rect window

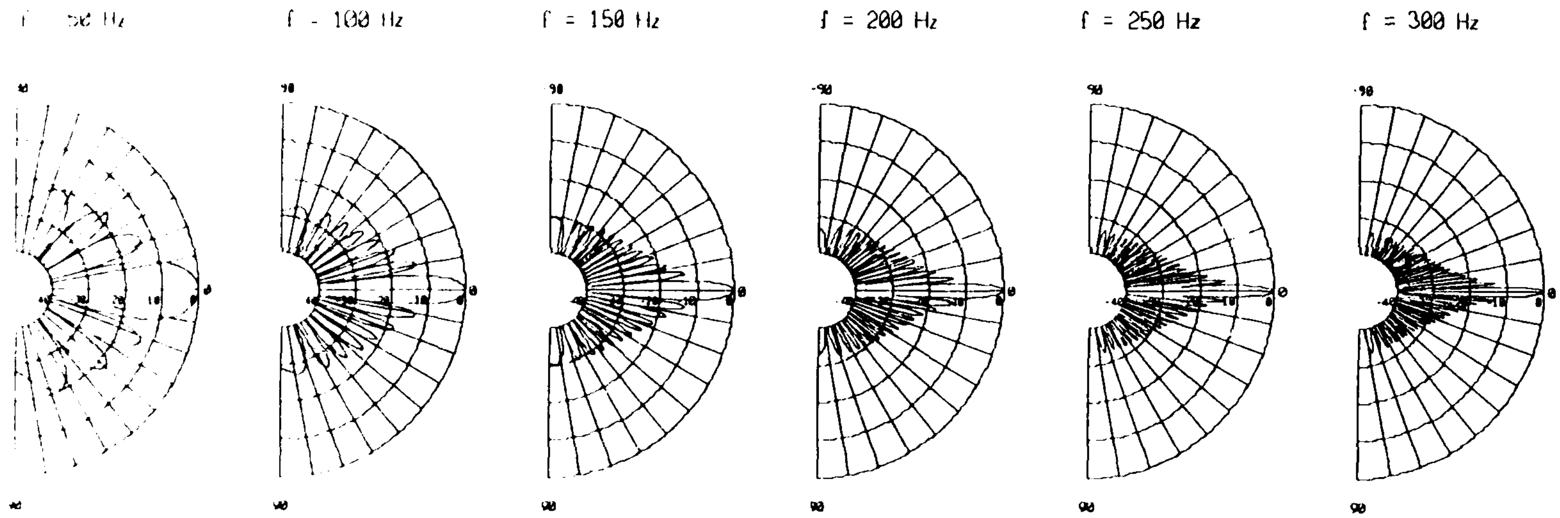

Figure 3(b).

MPA Array Beam Pattern: Kb window (alpha = 1.5)

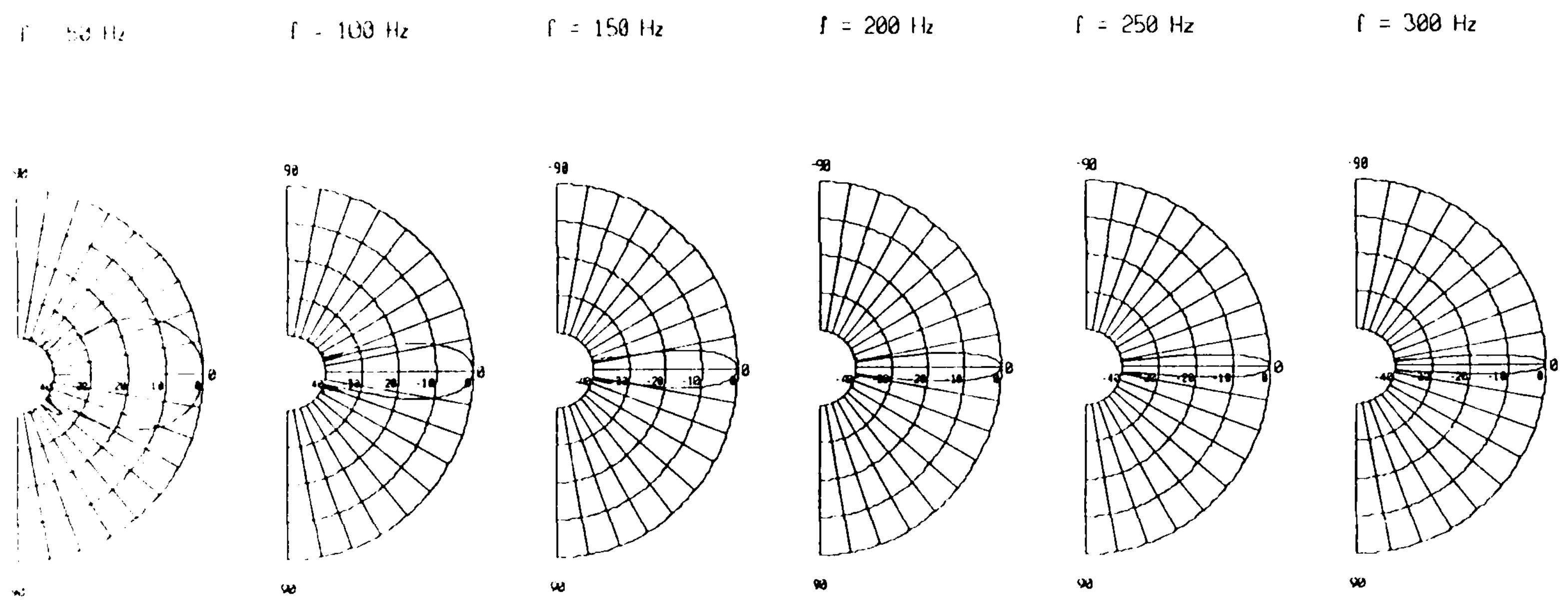

Figure 4(a).

MPA Array Beam Pattern: rect window

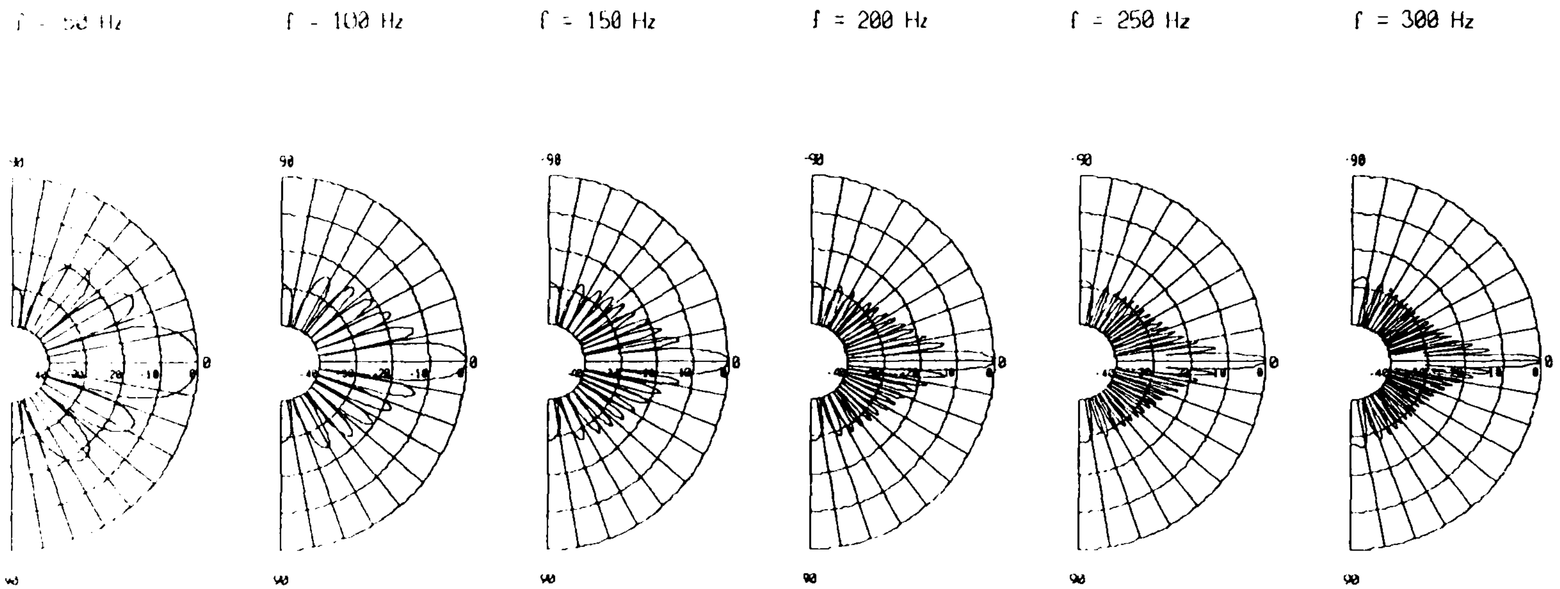

Figure 4(b).

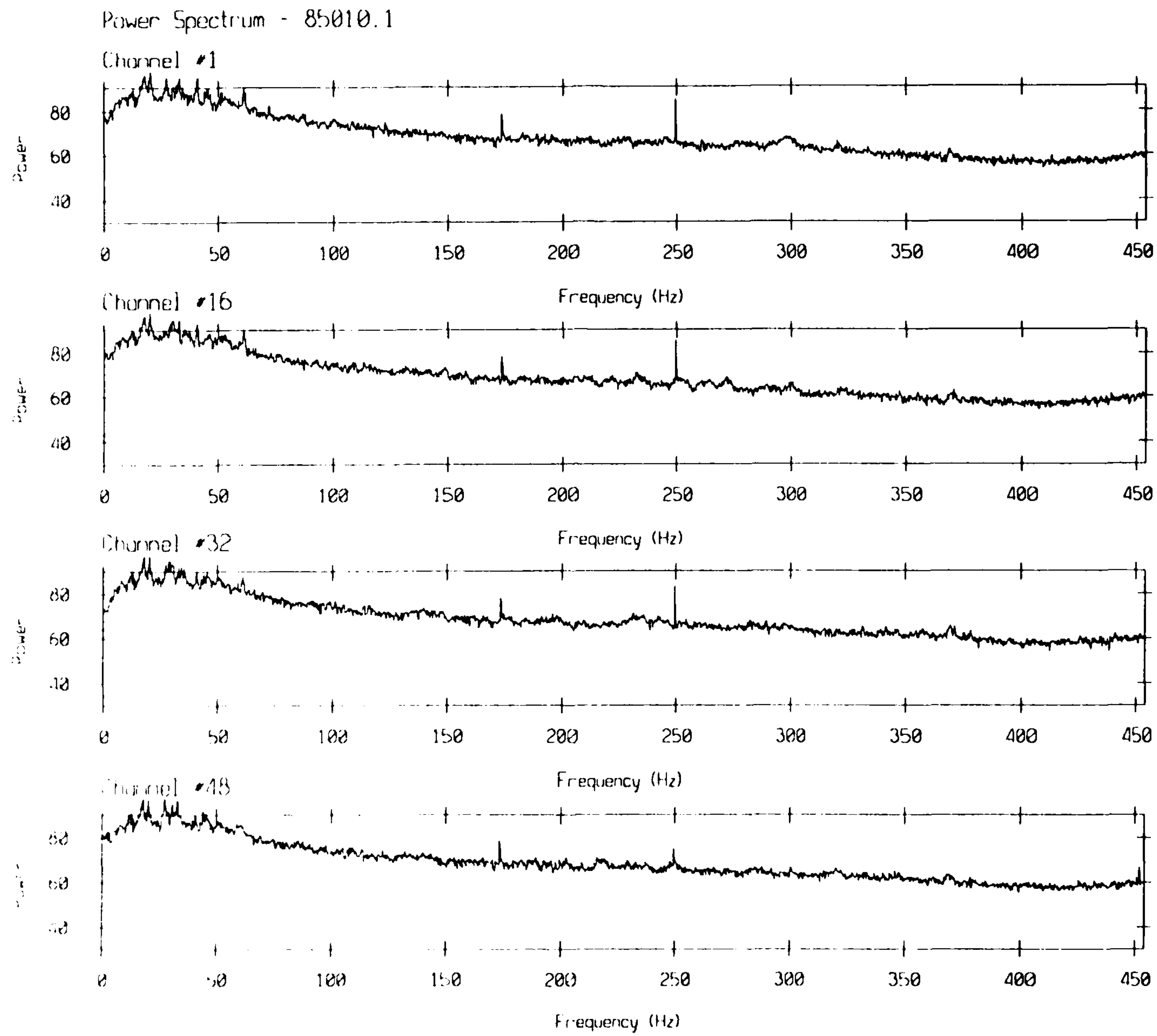
Power Spectrum - 85010.1
Channel #1
Channel #16
Channel #32
Channel #48
Power
80
60
40
0
50
100
150
200
250
300
350
400
450
Frequency (Hz)

Figure 5.

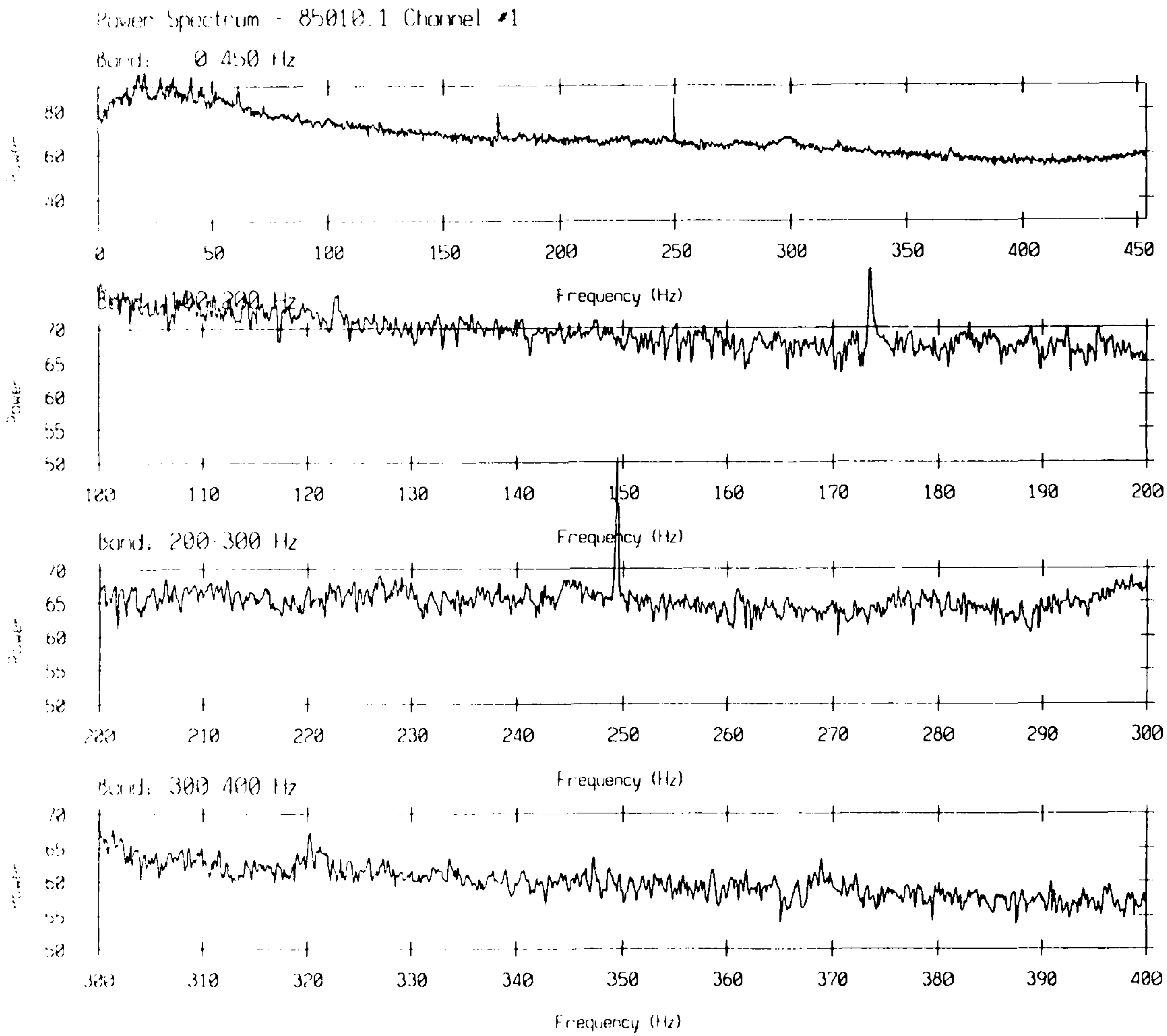
Power Spectrum - 85010.1 Channel #1
Band: 0 450 Hz
Band: 100 200 Hz
Band: 200 300 Hz
Band: 300 400 Hz
Frequency (Hz)
Power

Figure 6(a).

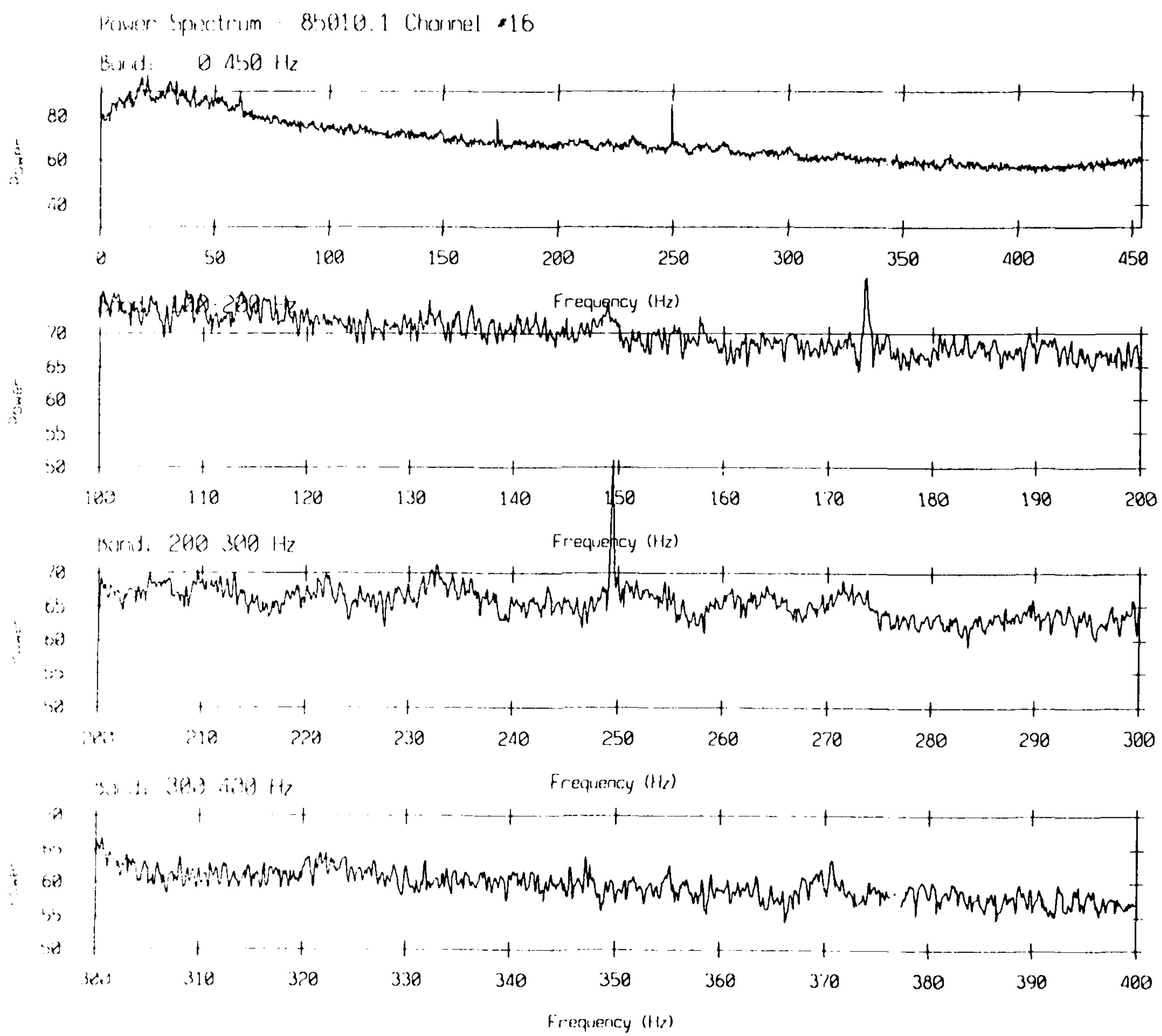
Power Spectrum 85010.1 Channel #16
Band: 0 450 Hz
Power
80
60
40
0
50
100
150
200
250
300
350
400
450
Frequency (Hz)
Band: 100 200 Hz
Power
70
65
60
55
50
100
110
120
130
140
150
160
170
180
190
200
Frequency (Hz)
Band: 200 300 Hz
70
65
60
55
50
210
220
230
240
250
260
270
280
290
300
Frequency (Hz)
Band: 300 400 Hz
60
55
50
310
320
330
340
350
360
370
380
390
400
Frequency (Hz)

Figure 6(b).

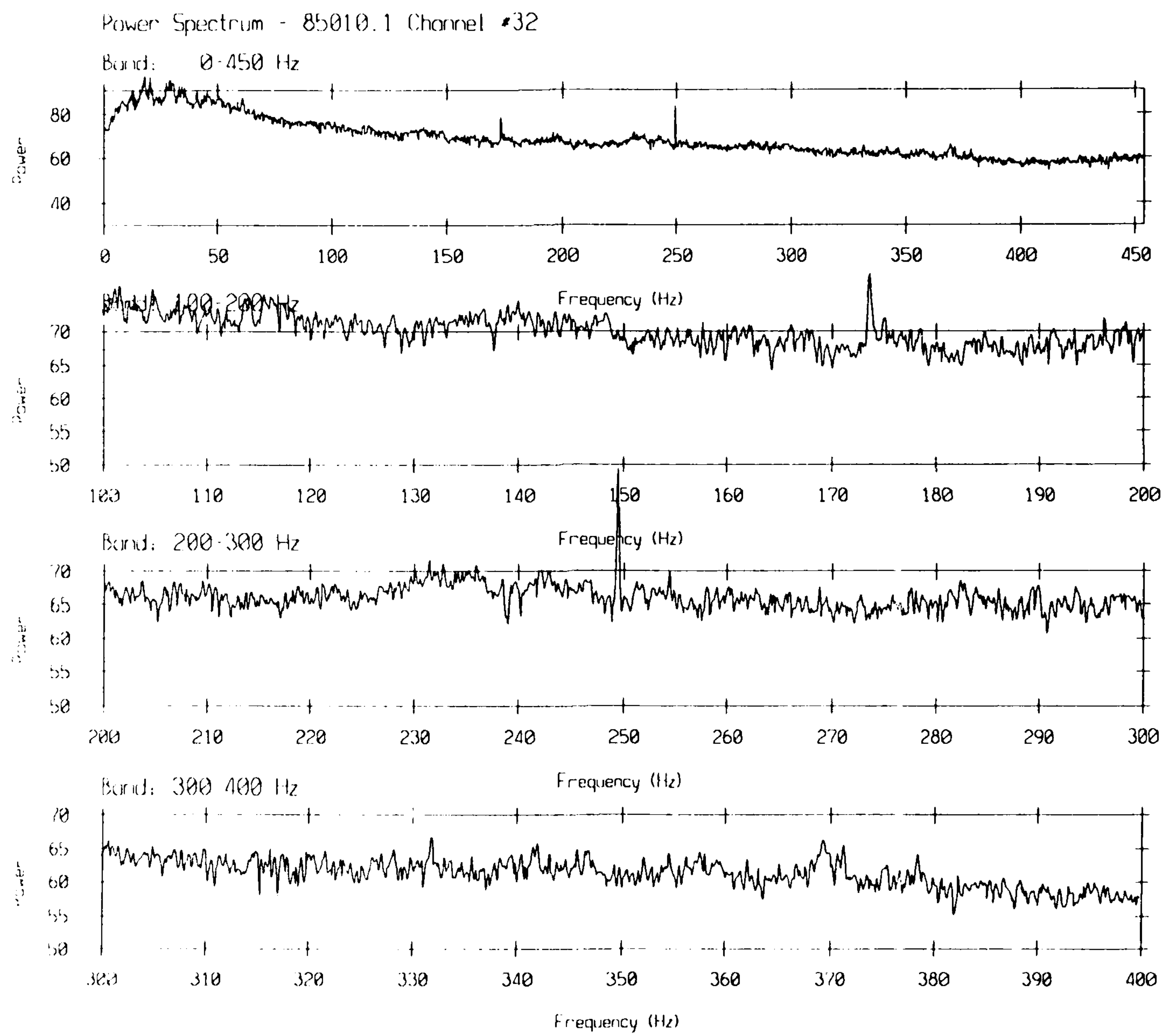

Power Spectrum - 85010.1 Channel #32
Band: 0-450 Hz
Band: 100-200 Hz
Band: 200-300 Hz
Band: 300-400 Hz
Power
Frequency (Hz)

Figure 6(c).

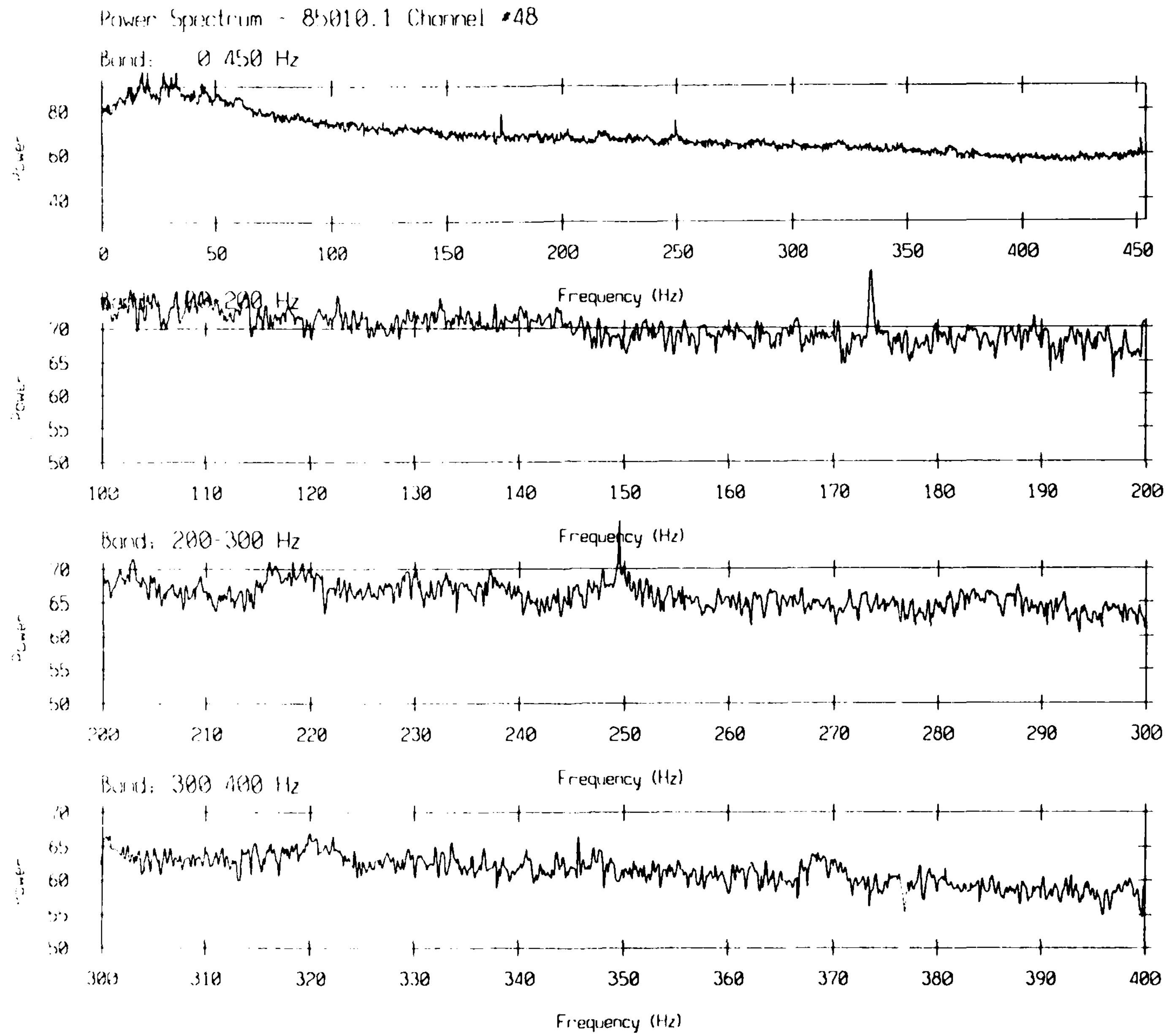

Power Spectrum - 85010.1 Channel #48
Band: 0 450 Hz
Band: 100-200 Hz
Band: 200-300 Hz
Band: 300 400 Hz
Frequency (Hz)
Power

Figure 6(d).

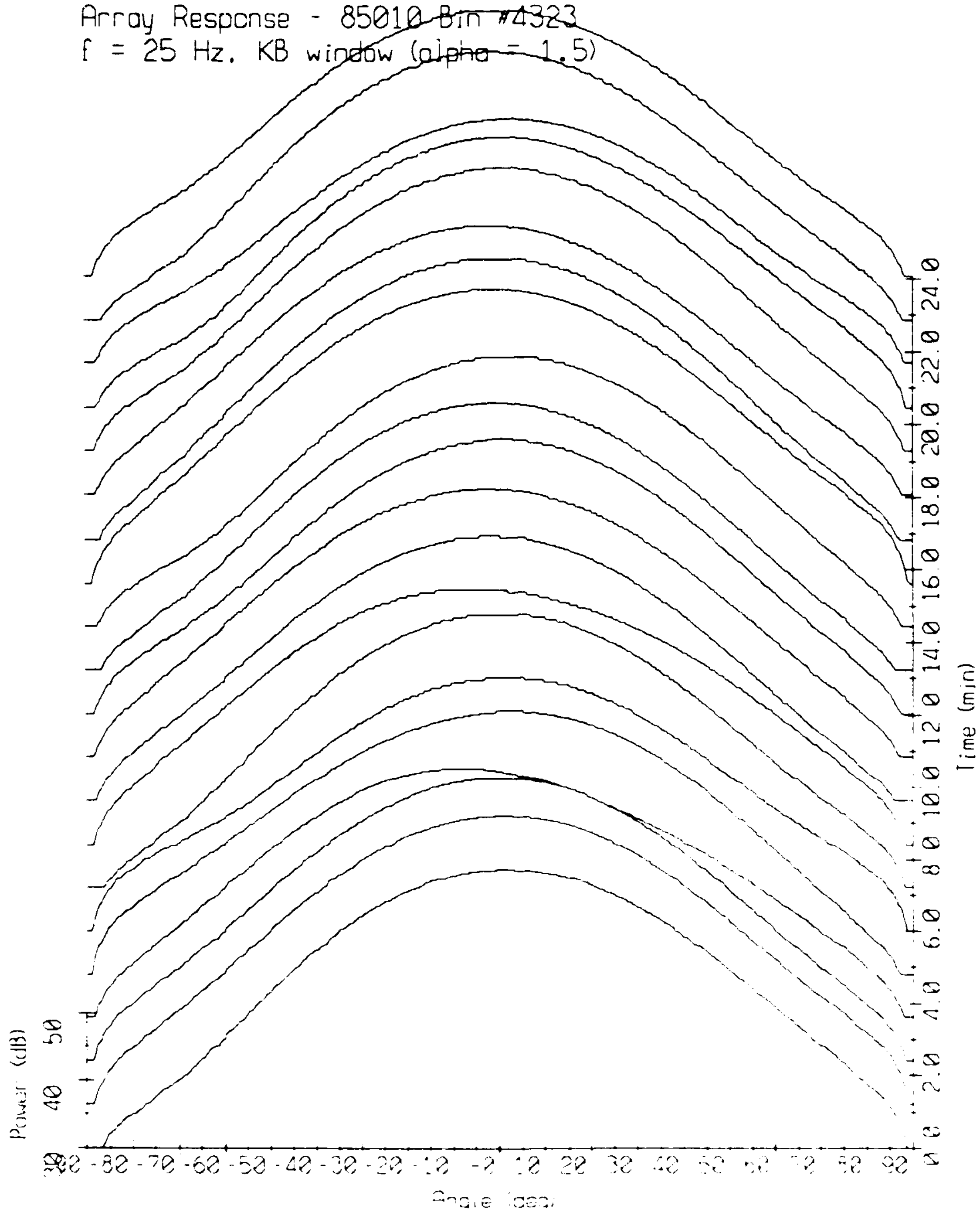
Array Response - 85010 Bin #4323
f = 25 Hz, KB window (alpha = 1.5)
Power (dB)
Time (min)
Angle (deg)

Figure 7(a).

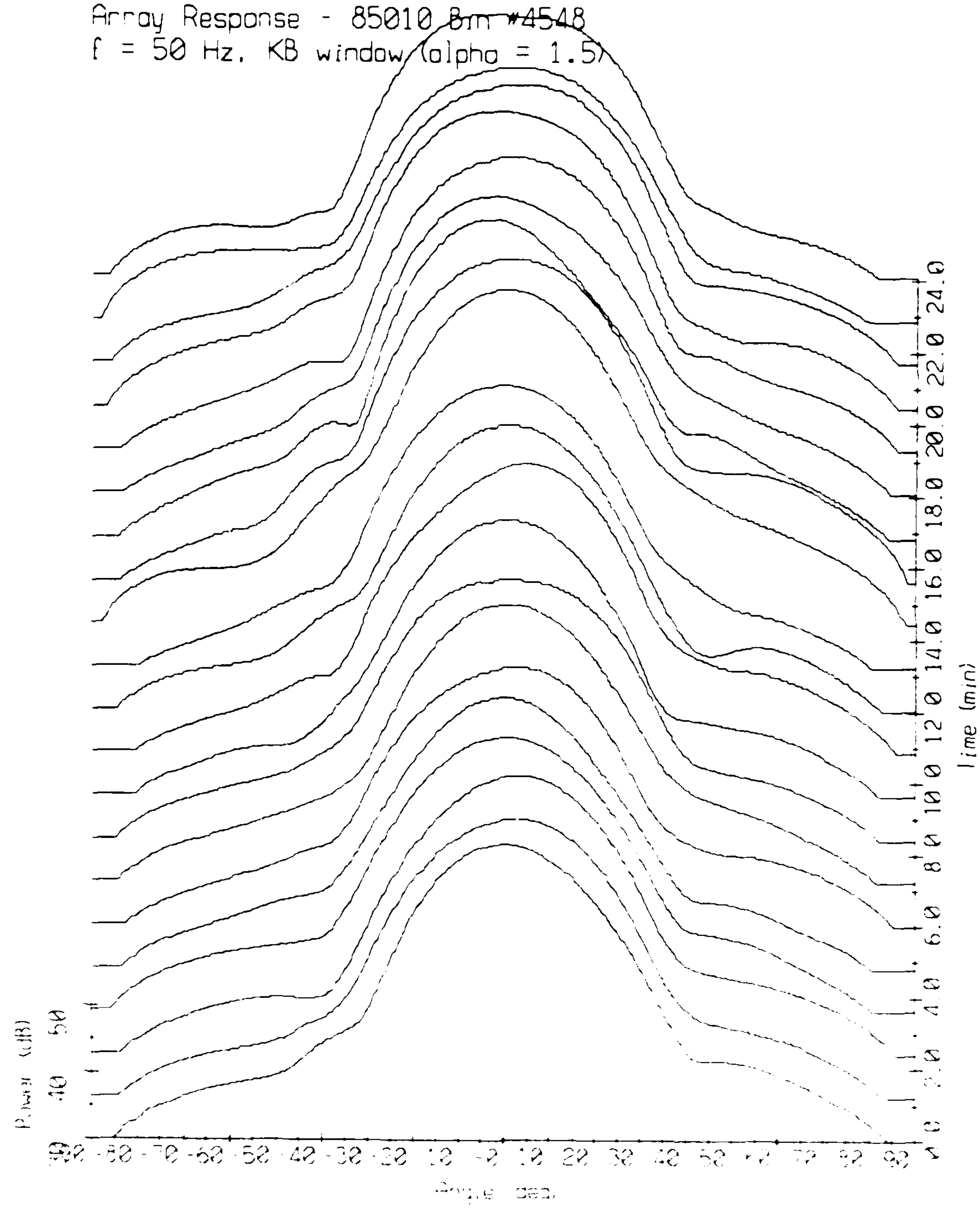
Array Response - 85010 8m #4548
f = 50 Hz, KB window (alpha = 1.5)
Power (dB)
40
50
Time (min)
24.0
22.0
20.0
18.0
16.0
14.0
12.0
10.0
8.0
6.0
4.0
2.0
0

Figure 7(b).

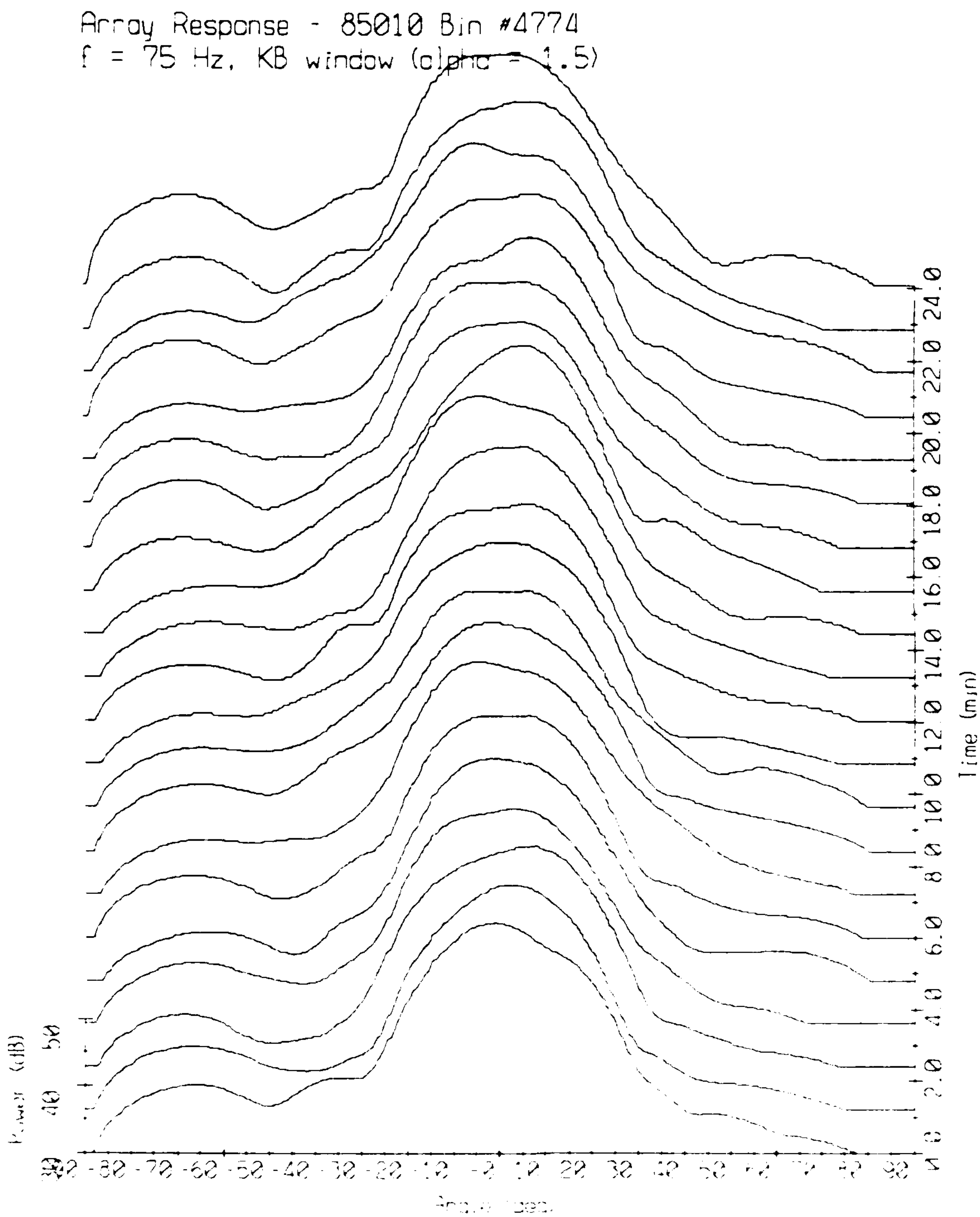
Array Response - 85010 Bin #4774
f = 75 Hz, KB window (alpha = 1.5)
Time (min)
0.0 2.0 4.0 6.0 8.0 10.0 12.0 14.0 16.0 18.0 20.0 22.0 24.0
Power (dB)
40 50
-90 -80 -70 -60 -50 -40 -30 -20 -10 0 10 20 30 40 50 60 70 80 90

Figure 7(c).

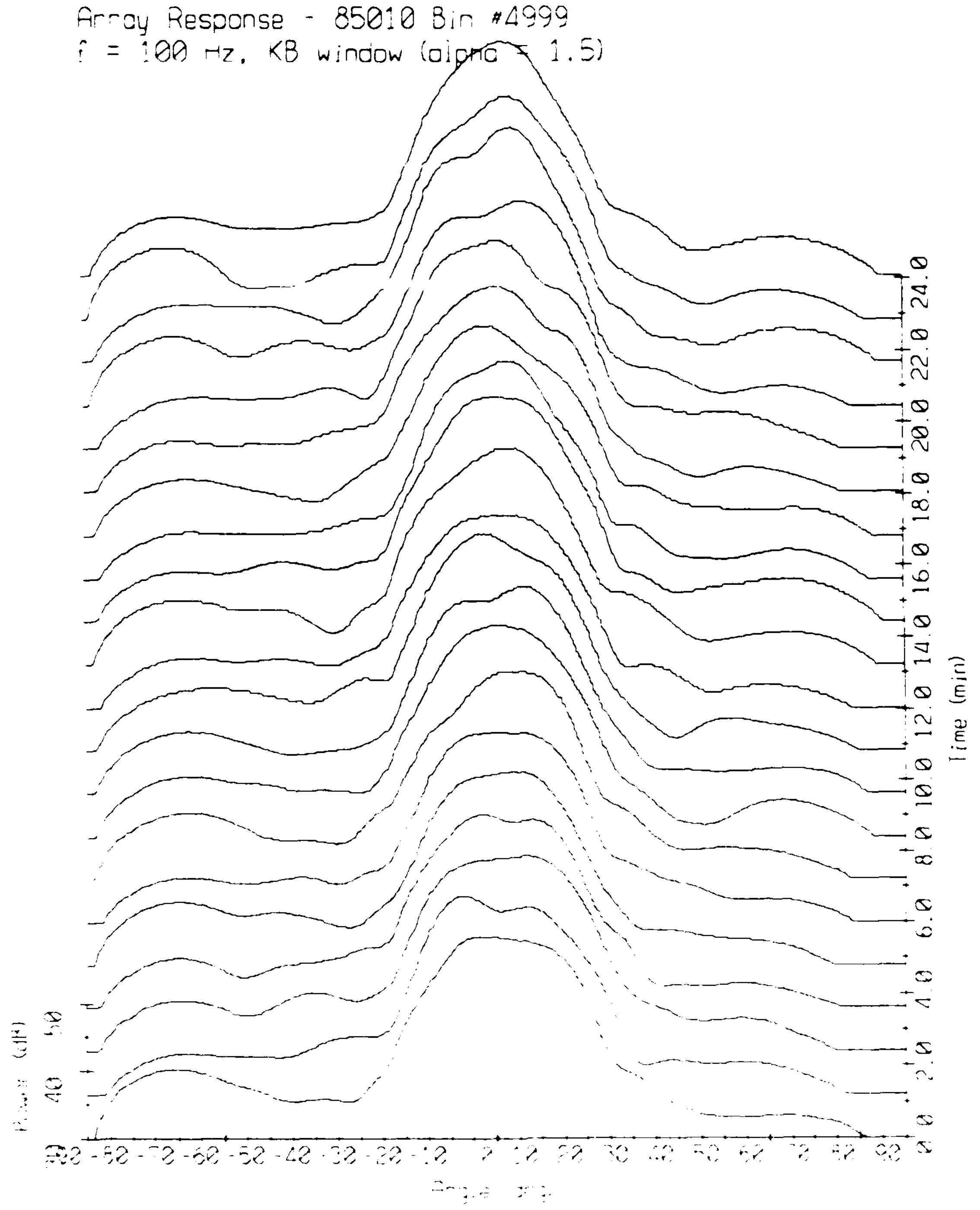

Array Response - 85010 Bin #4999
f = 100 Hz, KB window (alpha = 1.5)
Time (min)

Figure 7(d).

Array Response - 85010 Bin #5225
f = 125 Hz, KB window (alpha = 1.5)

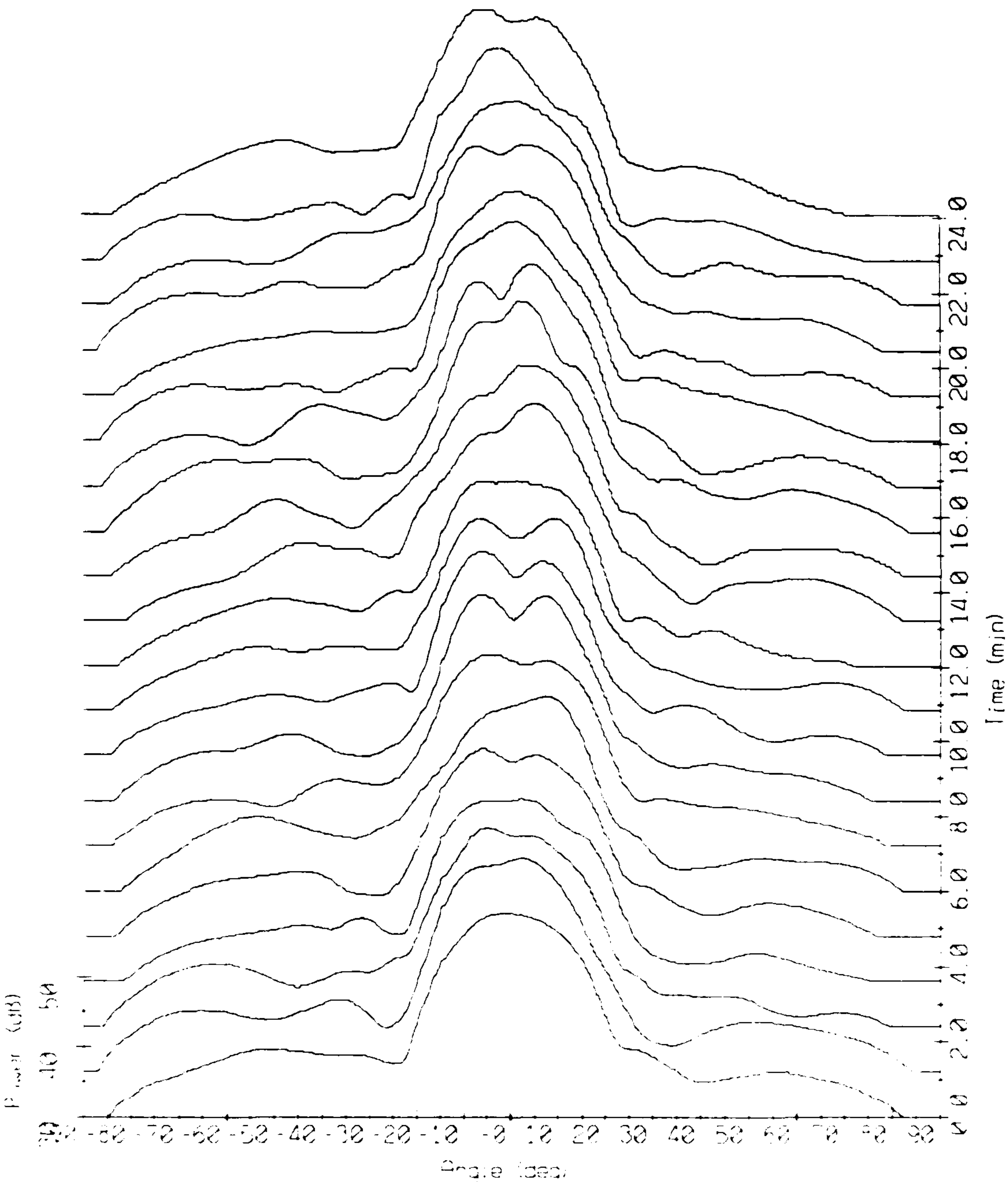

Figure 7(e).

Array Response - 85010 Bin #5451
f = 150 Hz, KB window (alpha = 1.5)

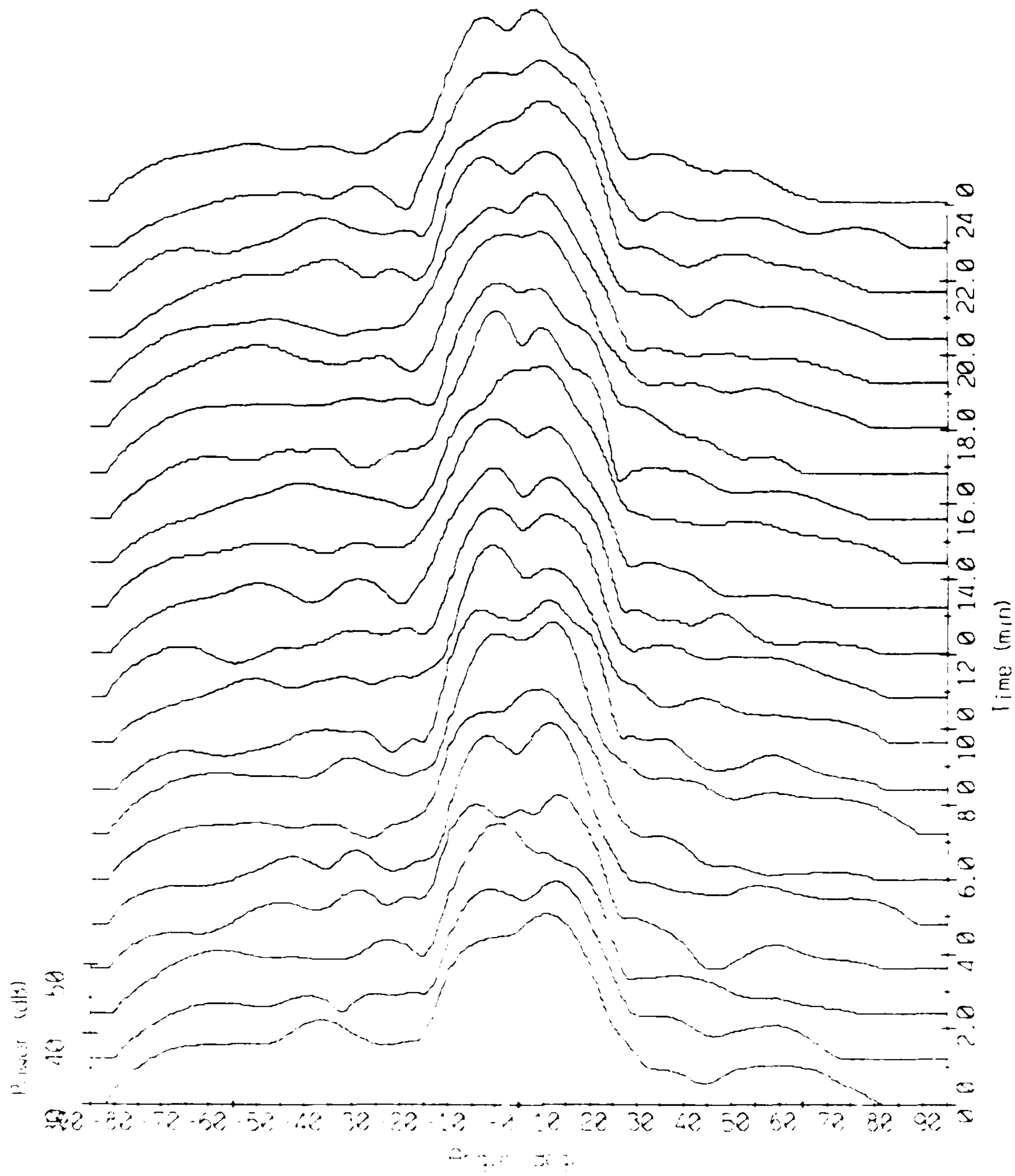

Figure 7(f)

Array Response - 85010 Bin #5676
f = 175 Hz, KB window (alpha = 1.5)

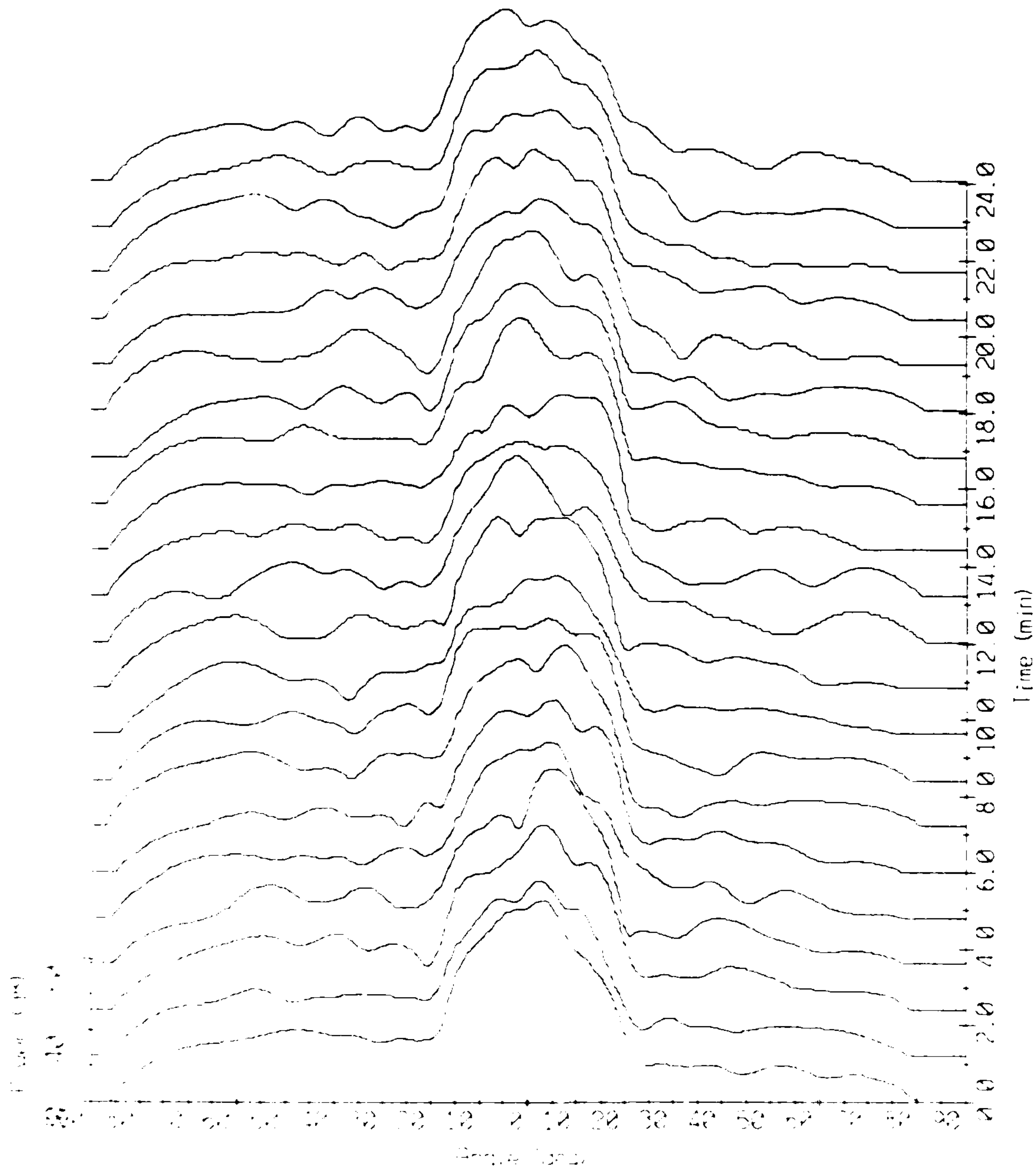

Figure 7(a).

Array Response - 85010 Bin #5902
f = 200 Hz, KB window (alpha = 1.5)

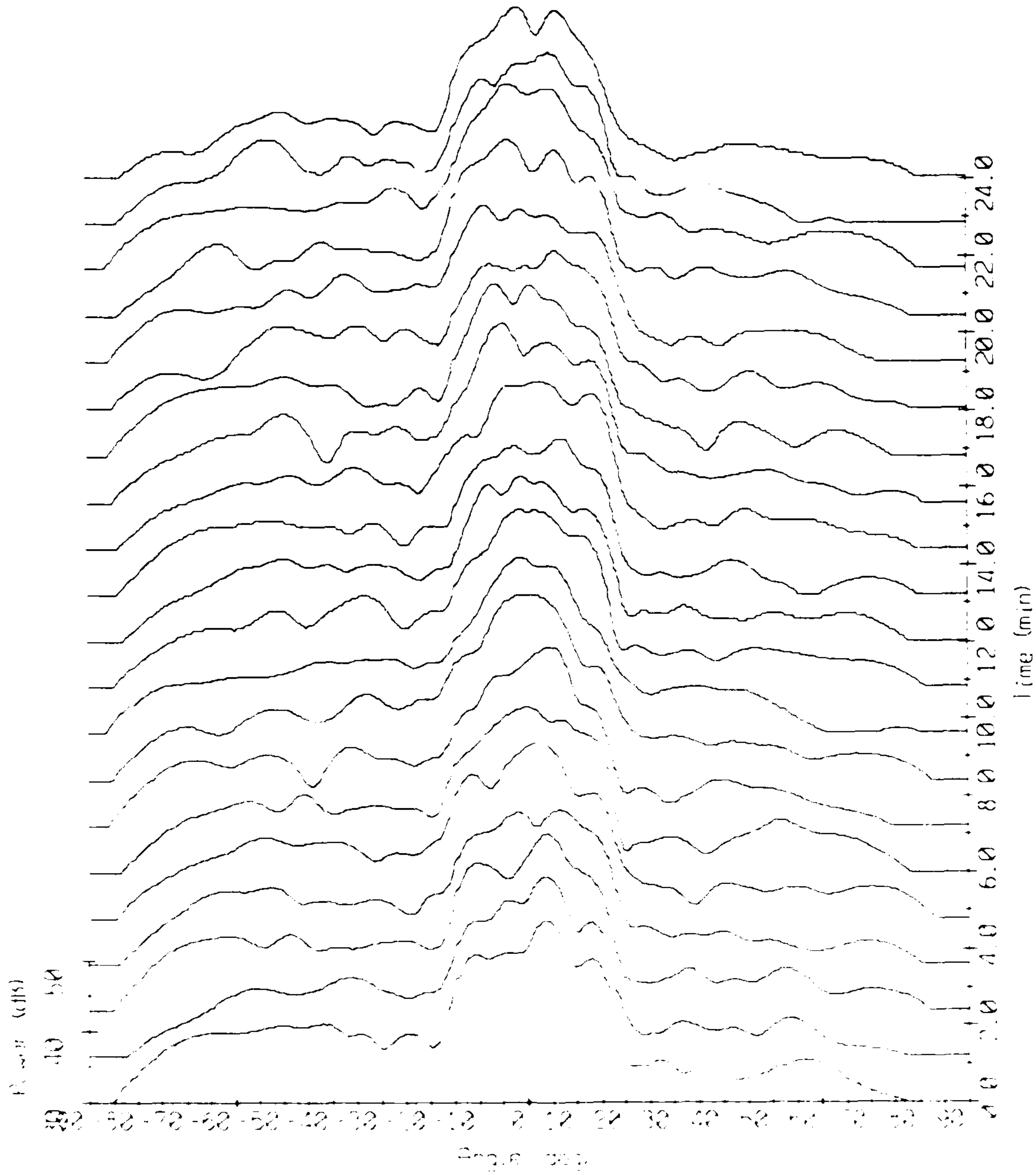

Figure 7(h).

Array Response - 85010 Bin #6127
f = 225 Hz, KB window (alpha = 1.5)

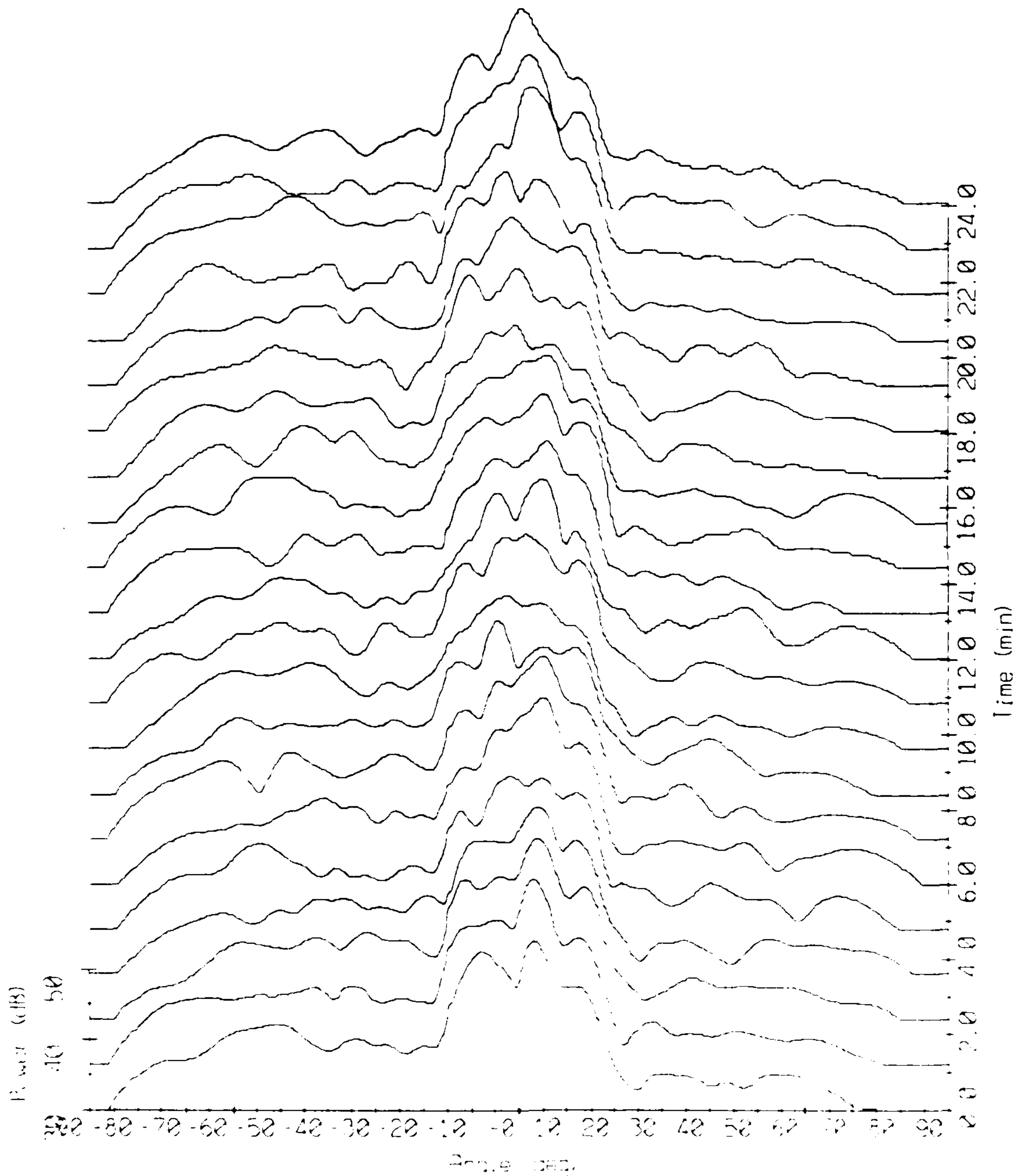

Figure 7(i).

Array Response - 85010 Bin #6354
f = 250 Hz, KB window (alpha = 1.5)

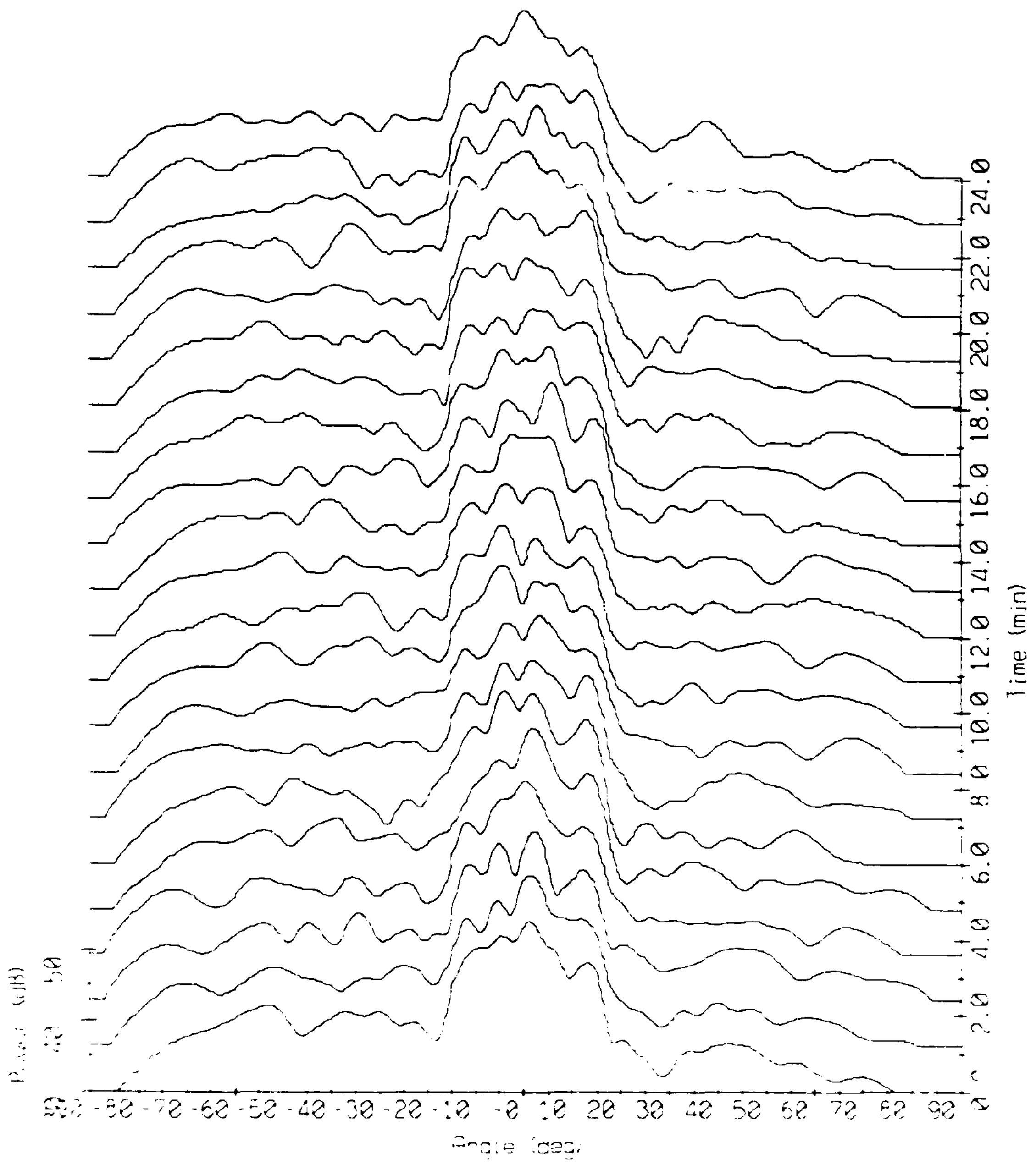

Figure 7(j).

Array Response - 85010 Bin #6579
f = 275 Hz, KB window (alpha = 1.5)

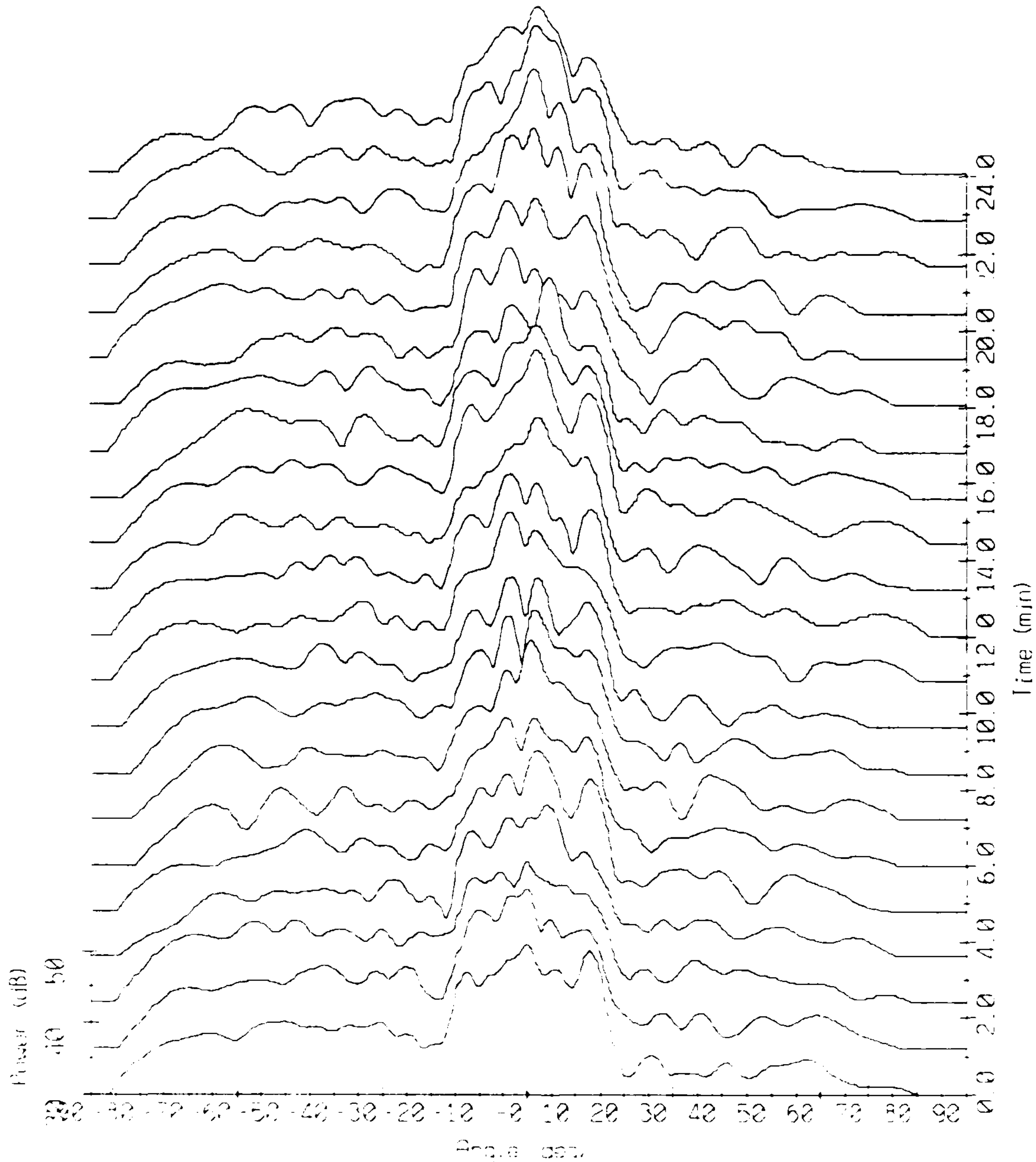

Figure 7(k).

Array Response - 85010 Bin #6804
f = 300 Hz, KB window (alpha = 1.5)

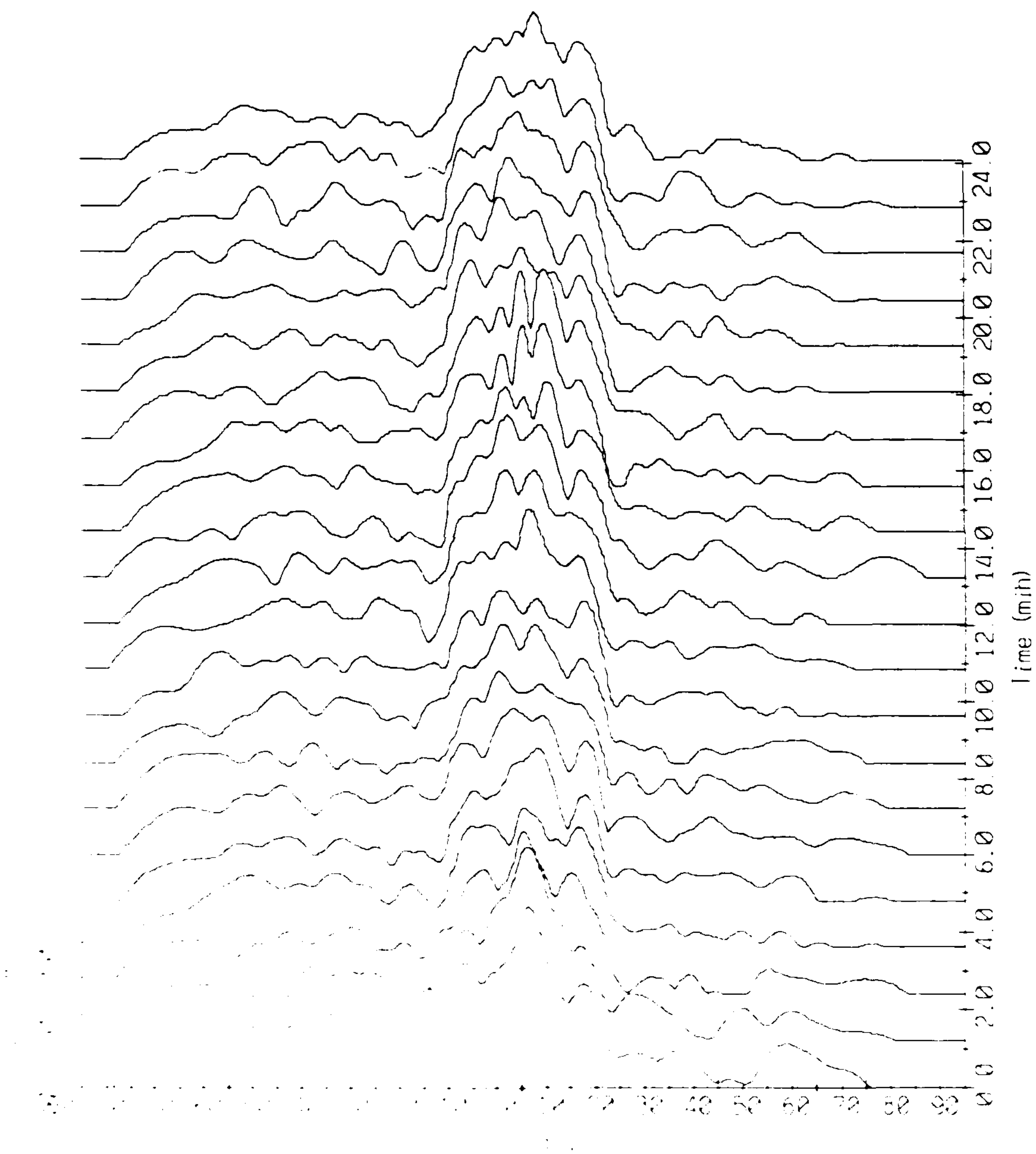

Figure 7(1).

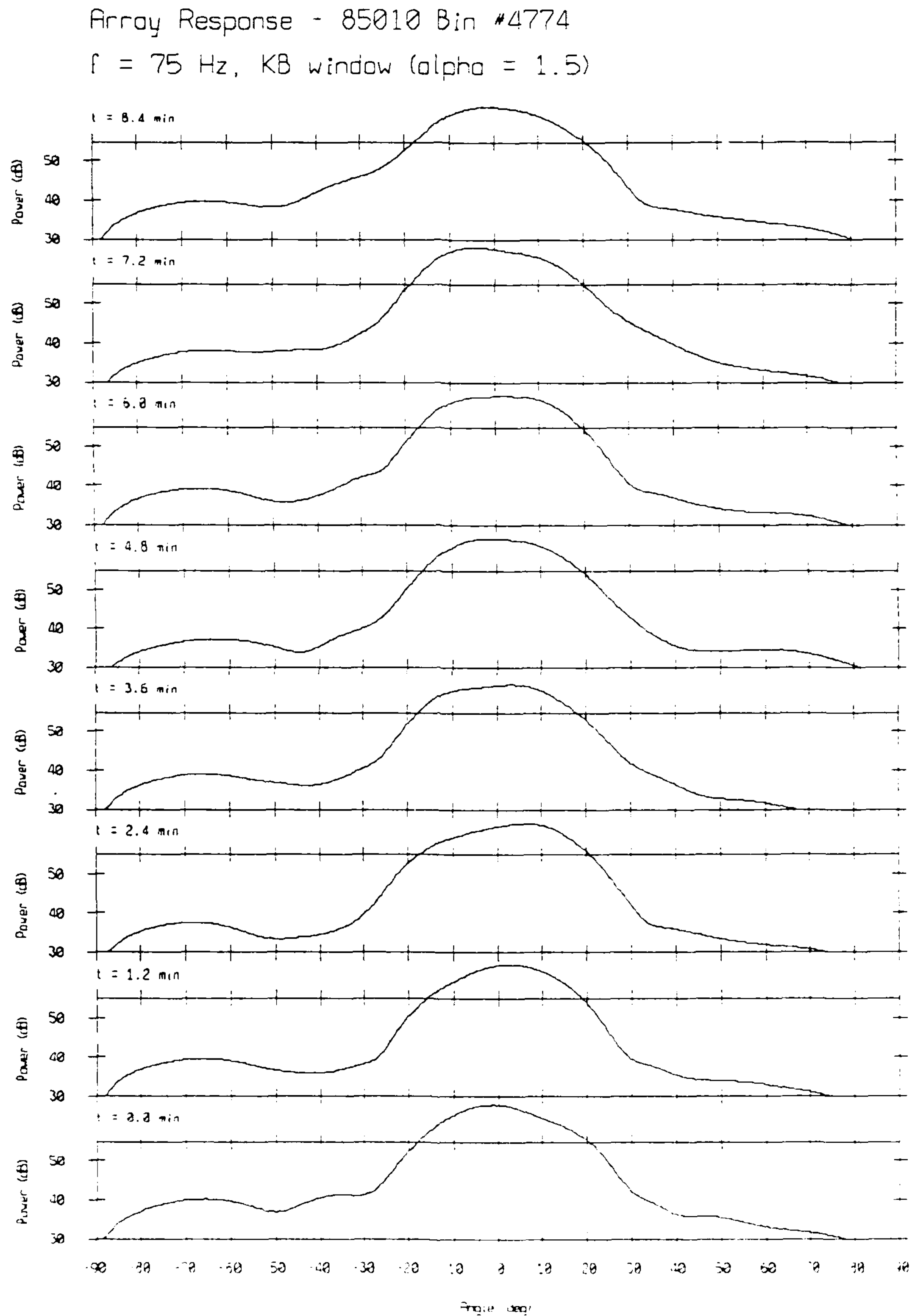

Array Response - 85010 Bin #4774
f = 75 Hz, KB window (alpha = 1.5)
t = 8.4 min
t = 7.2 min
t = 6.0 min
t = 4.8 min
t = 3.6 min
t = 2.4 min
t = 1.2 min
t = 0.0 min
Power (dB)
50
40
30

Figure 3(a).

Array Response - 85010 Bin #4774

f = 75 Hz, KB window (alpha = 1.5)

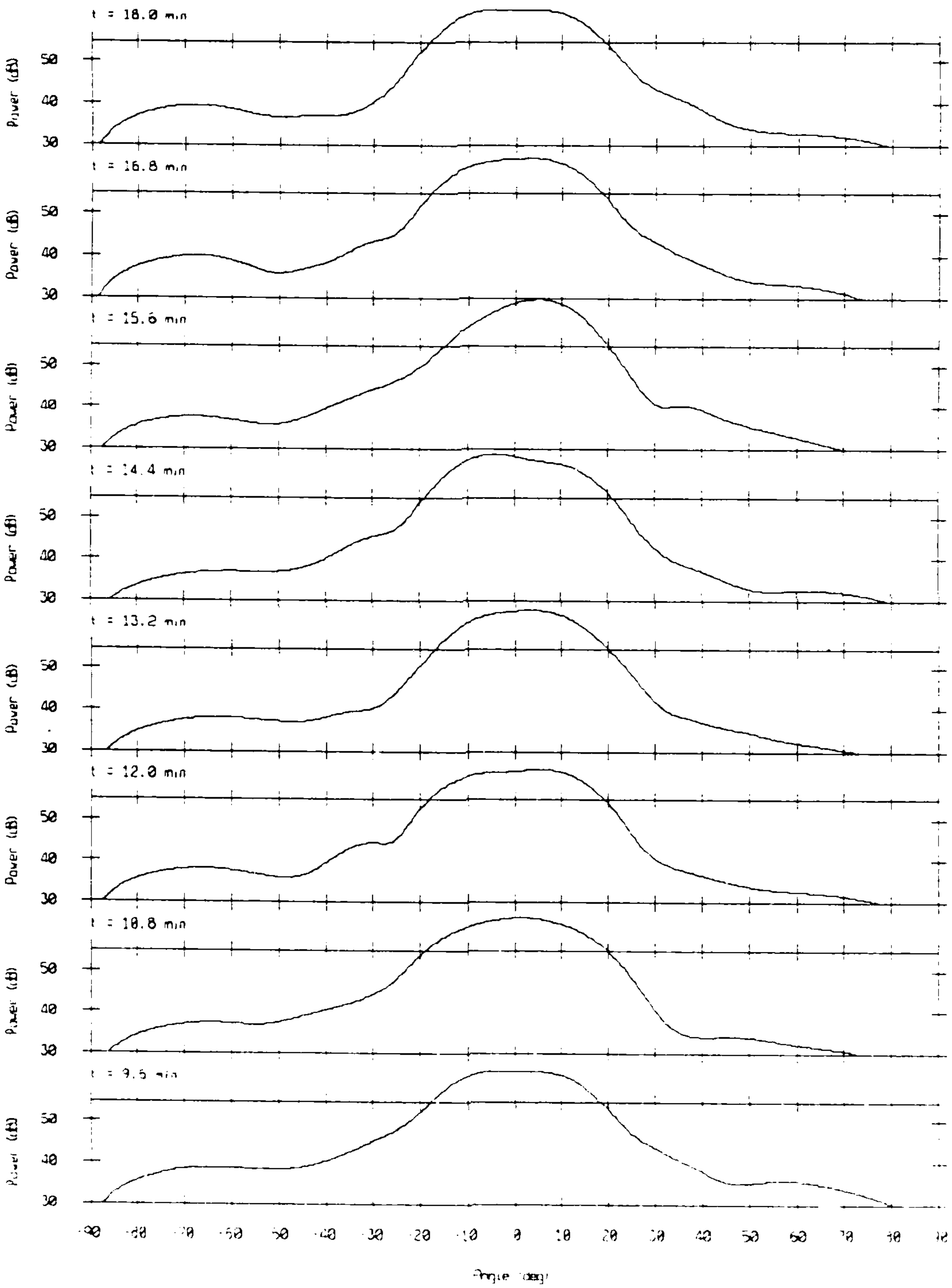

Array Response - 85010 Bin #4774

f = 75 Hz, KB window (alpha = 1.5)

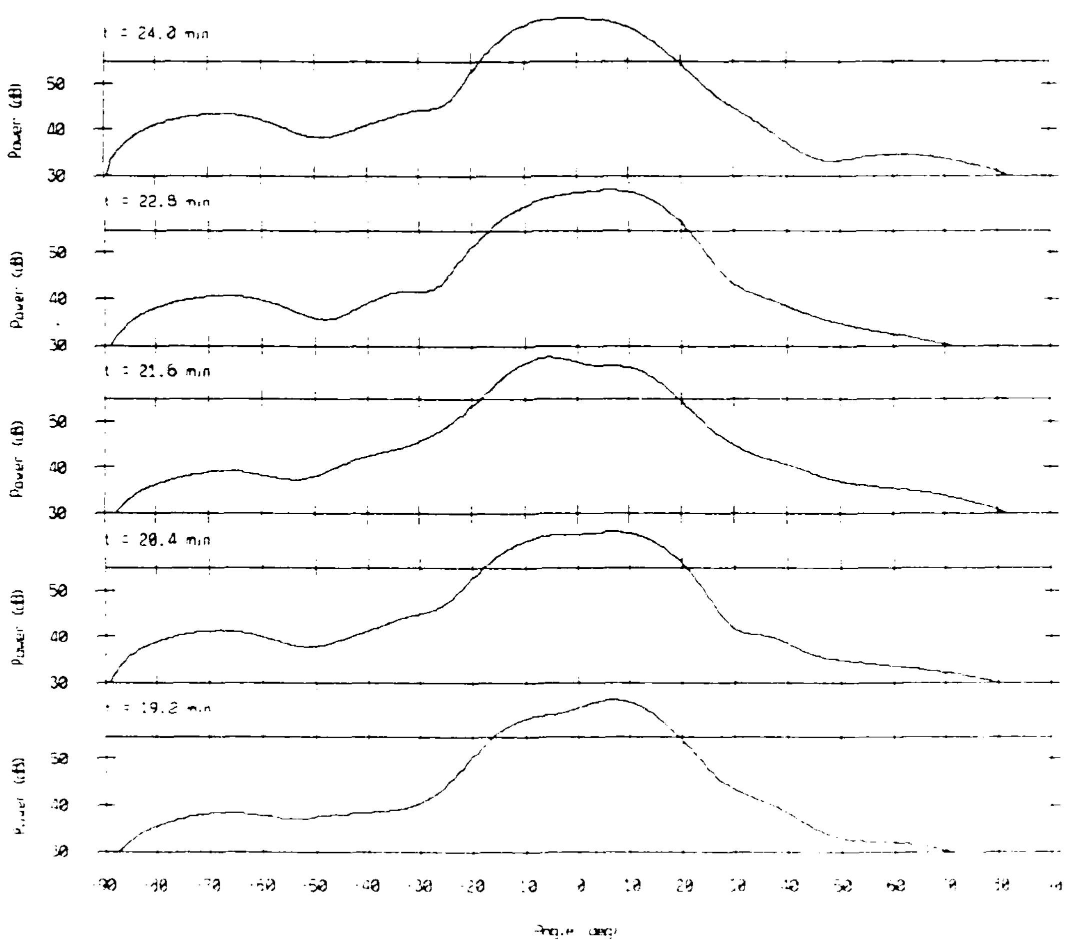

Array Response - 85010 Bin #5451

f = 150 Hz, KB window (alpha = 1.5)

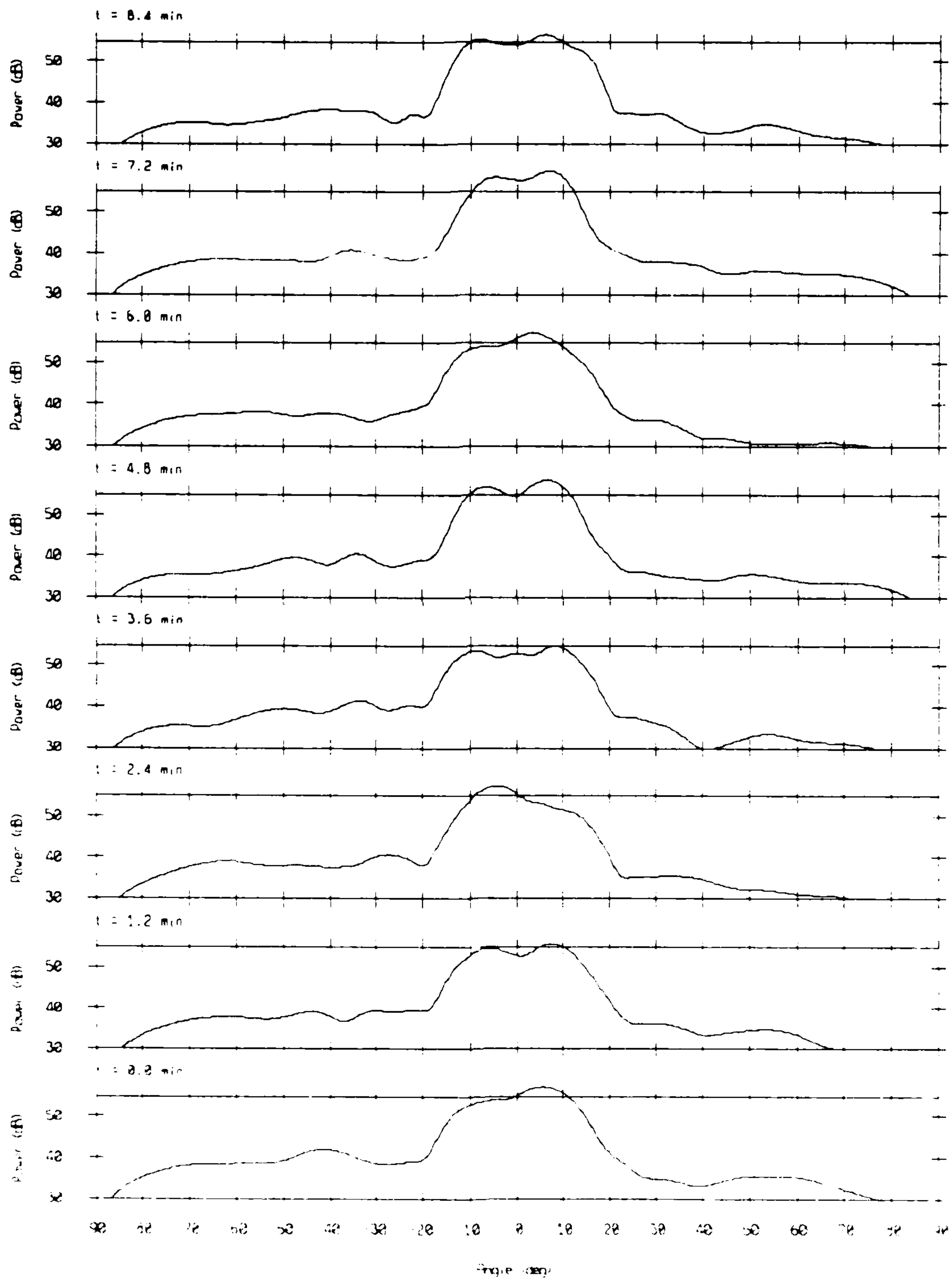

Figure 8(b).

Array Response - 85010 Bin #5451

f = 150 Hz, KB window (alpha = 1.5)

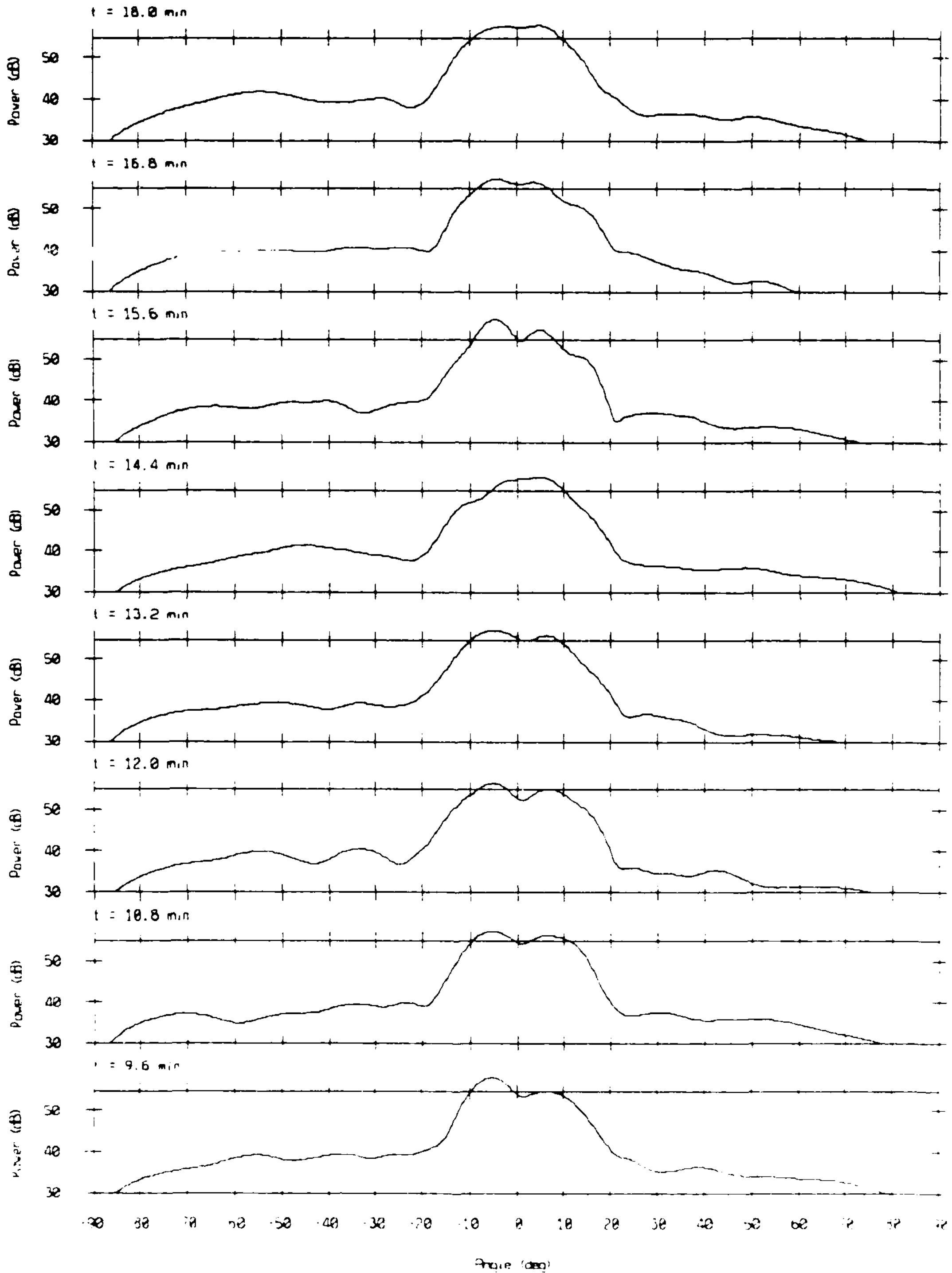

Array Response - 85010 Bin #5451

f = 150 Hz, KB window (alpha = 1.5)

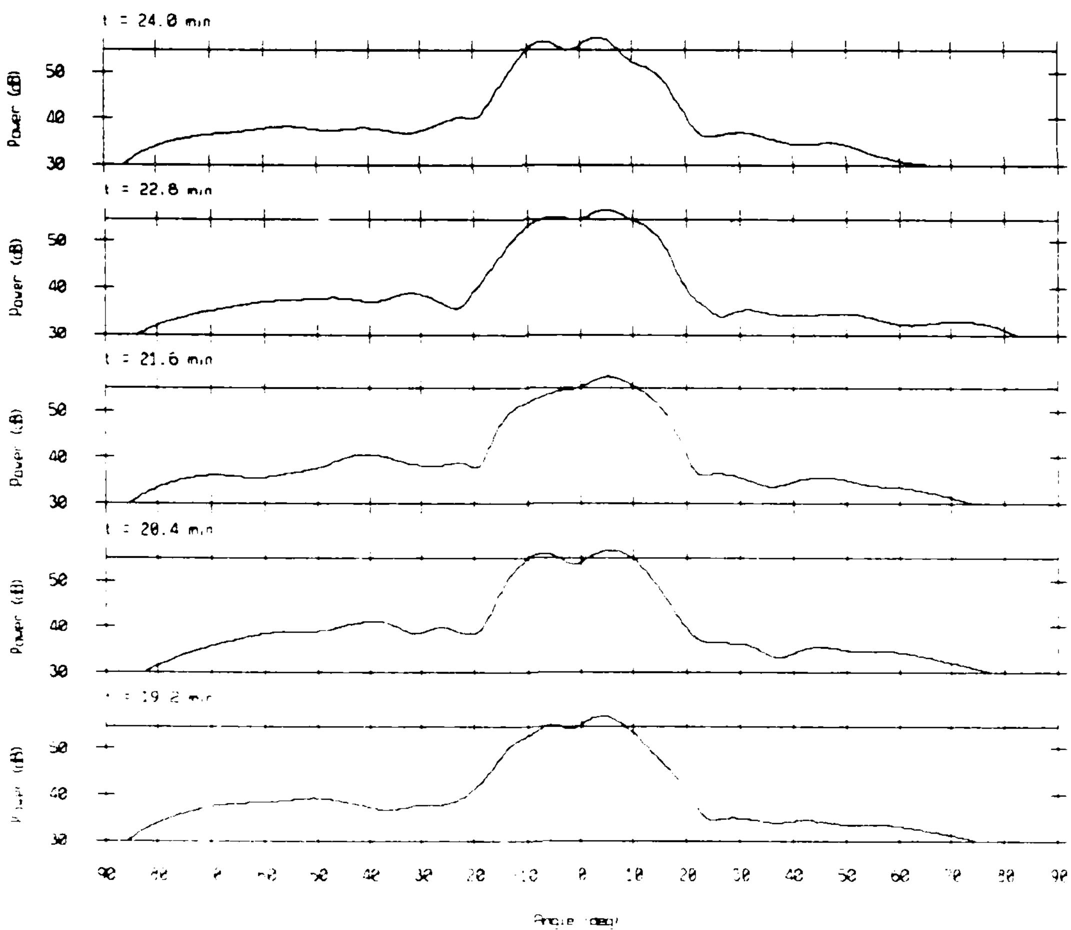

Array Response - 85010 Bin #6804

f = 300 Hz, KB window (alpha = 1.5)

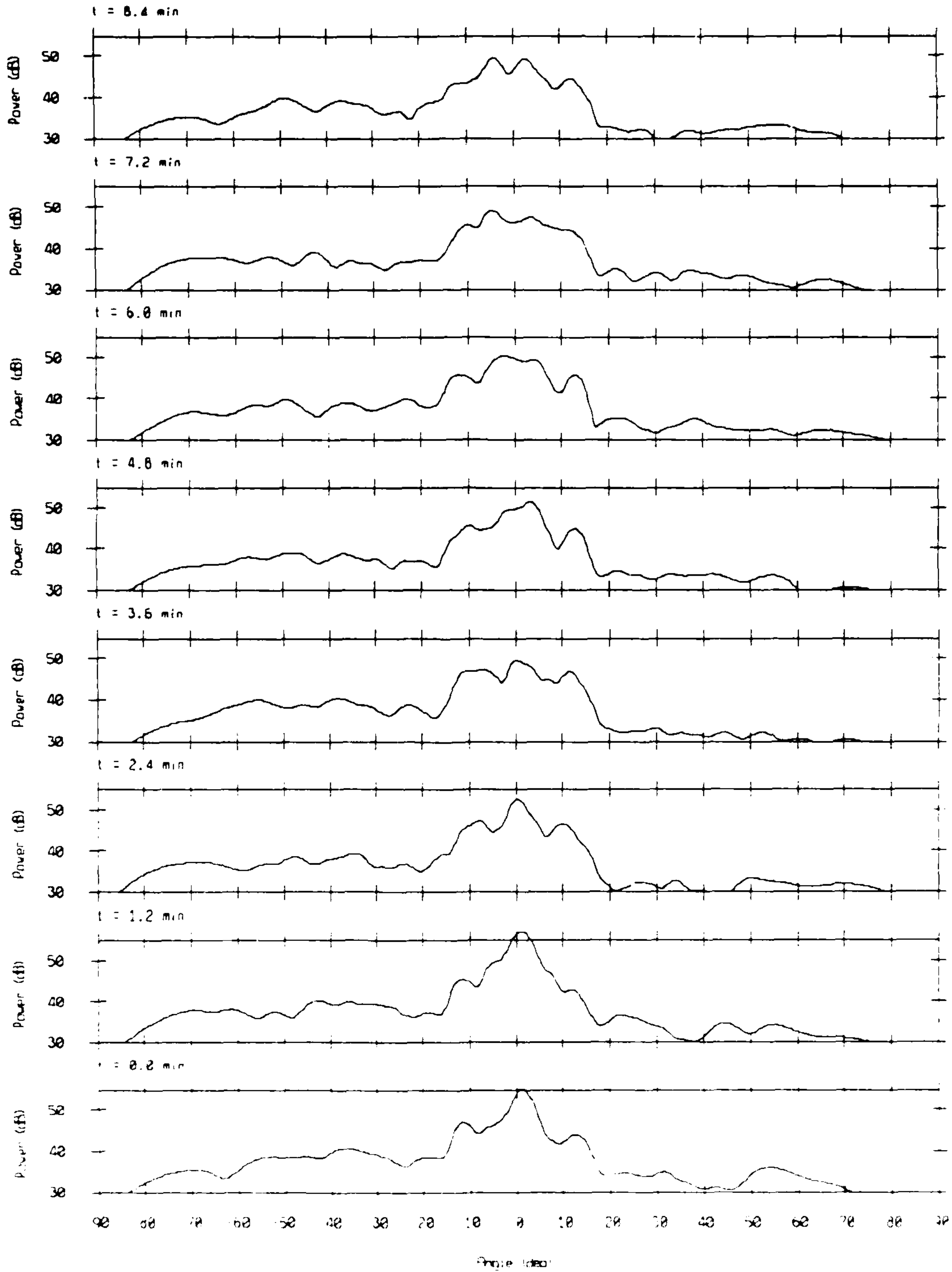

Figure 8(c).

Array Response - 85010 Bin #6804

f = 300 Hz, KB window (alpha = 1.5)

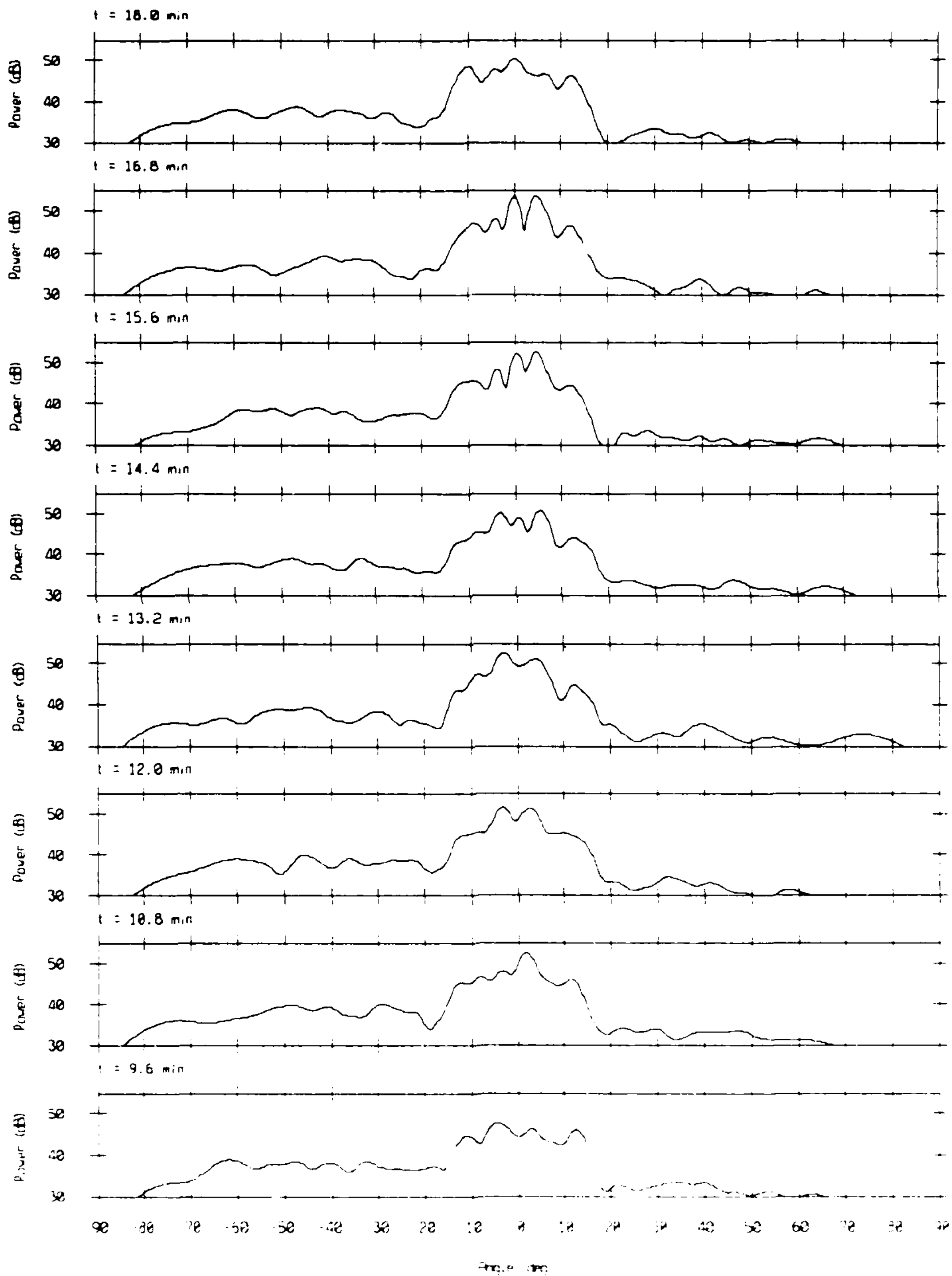

Array Response - 85010 Bin #6804
f = 300 Hz, KB window (alpha = 1.5)

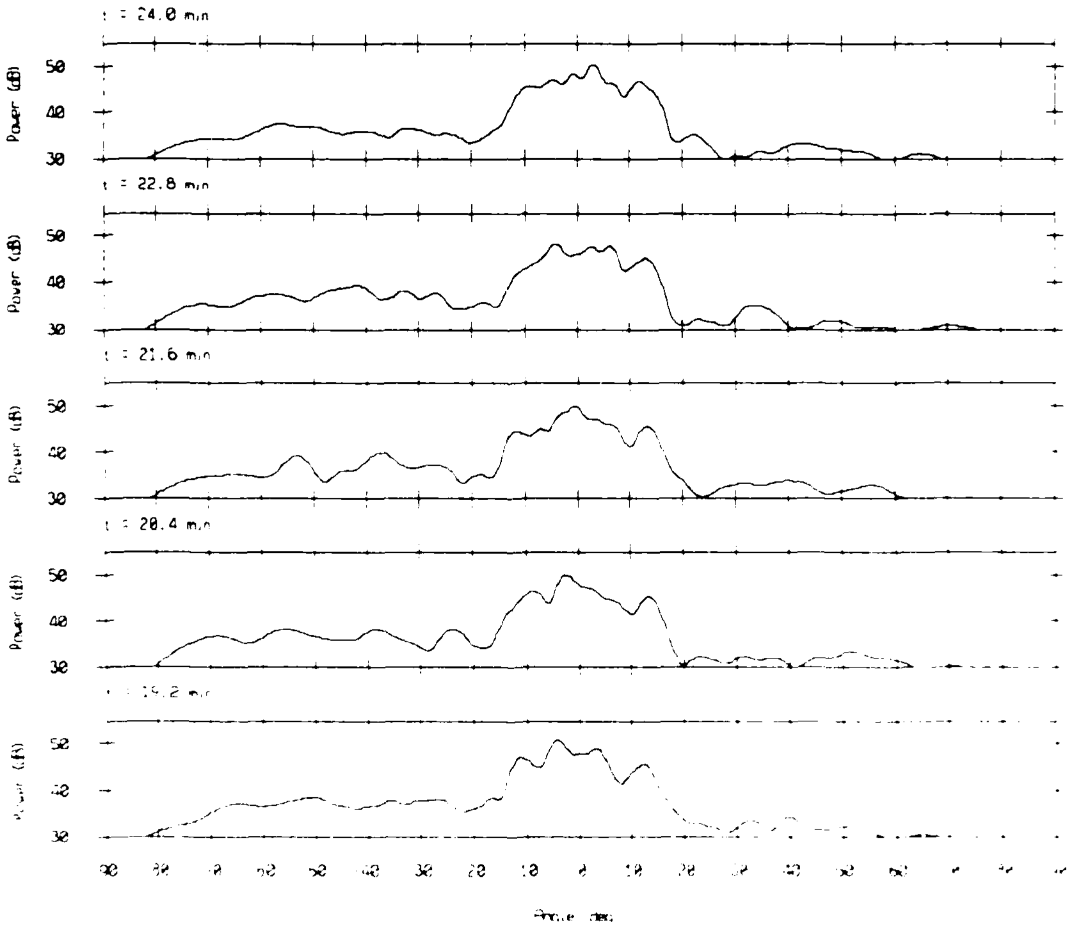

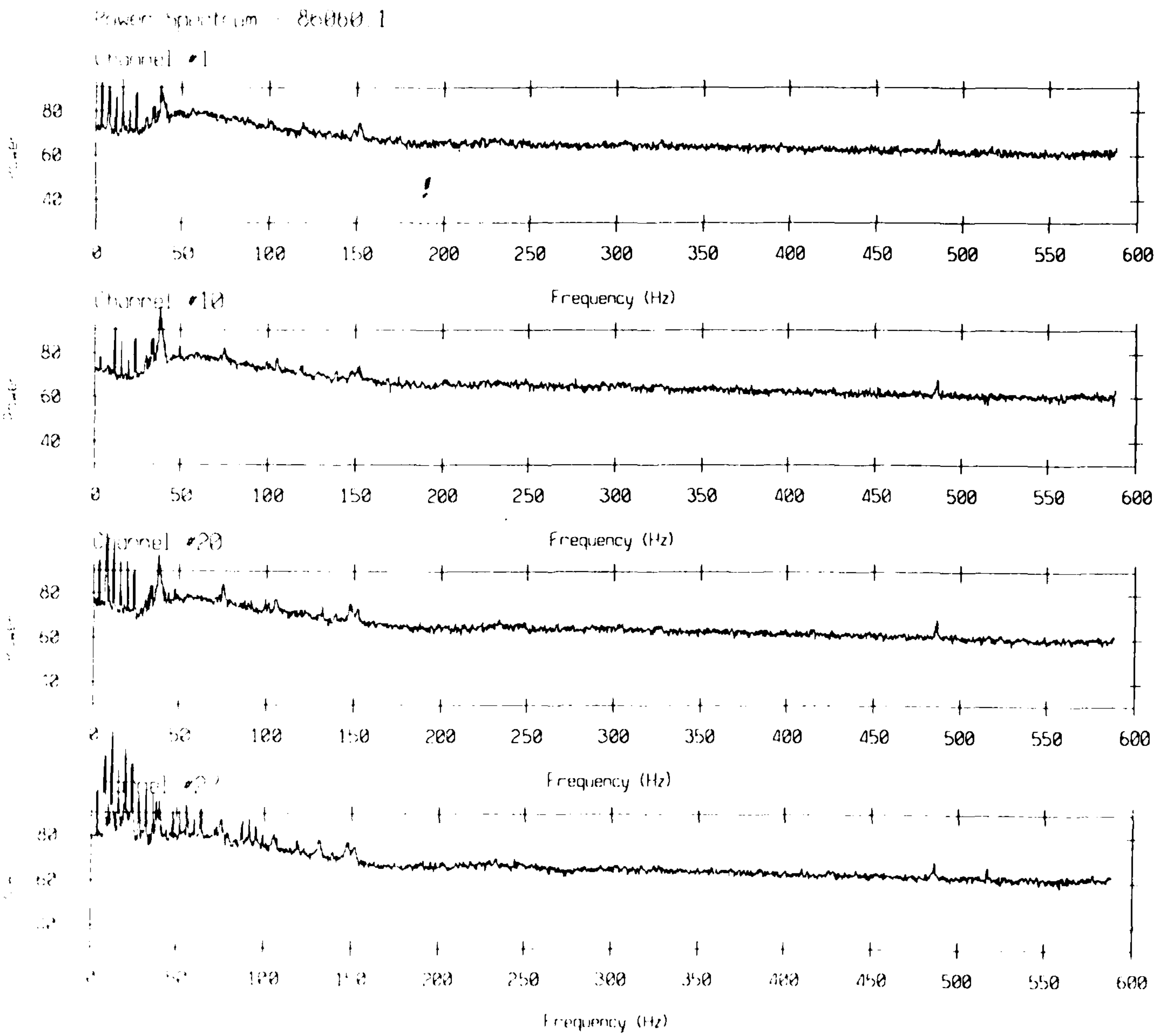
Channel #1
80
60
40
0
50
100
150
200
250
300
350
400
450
500
550
600
Frequency (Hz)
Channel #10
Frequency (Hz)
Channel #20
Frequency (Hz)
Frequency (Hz)

Figure 9.

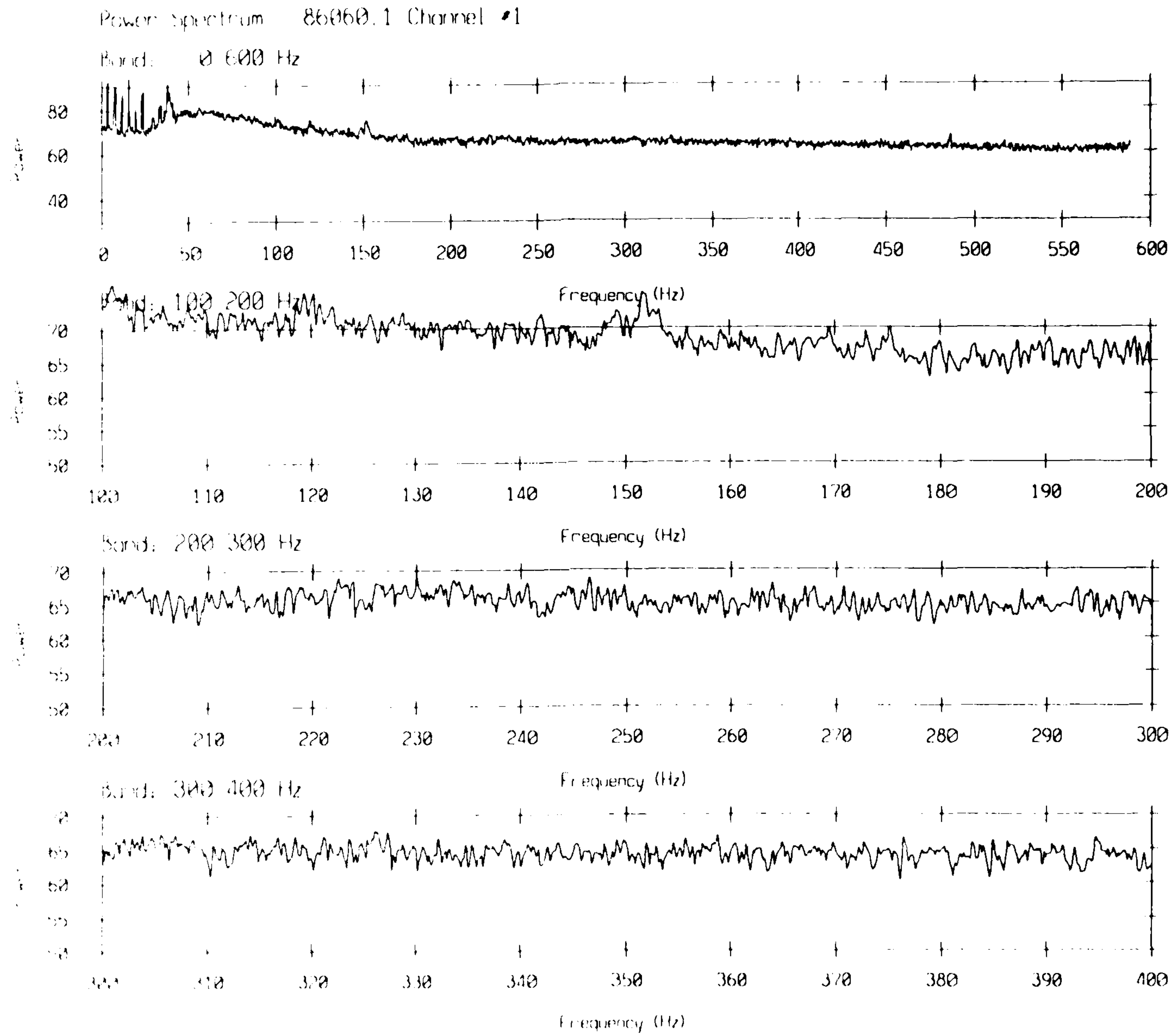
Power Spectrum 86060.1 Channel #1
Band: 0 600 Hz
Band: 100 200 Hz
Band: 200 300 Hz
Band: 300 400 Hz
Frequency (Hz)

Figure 10(a).

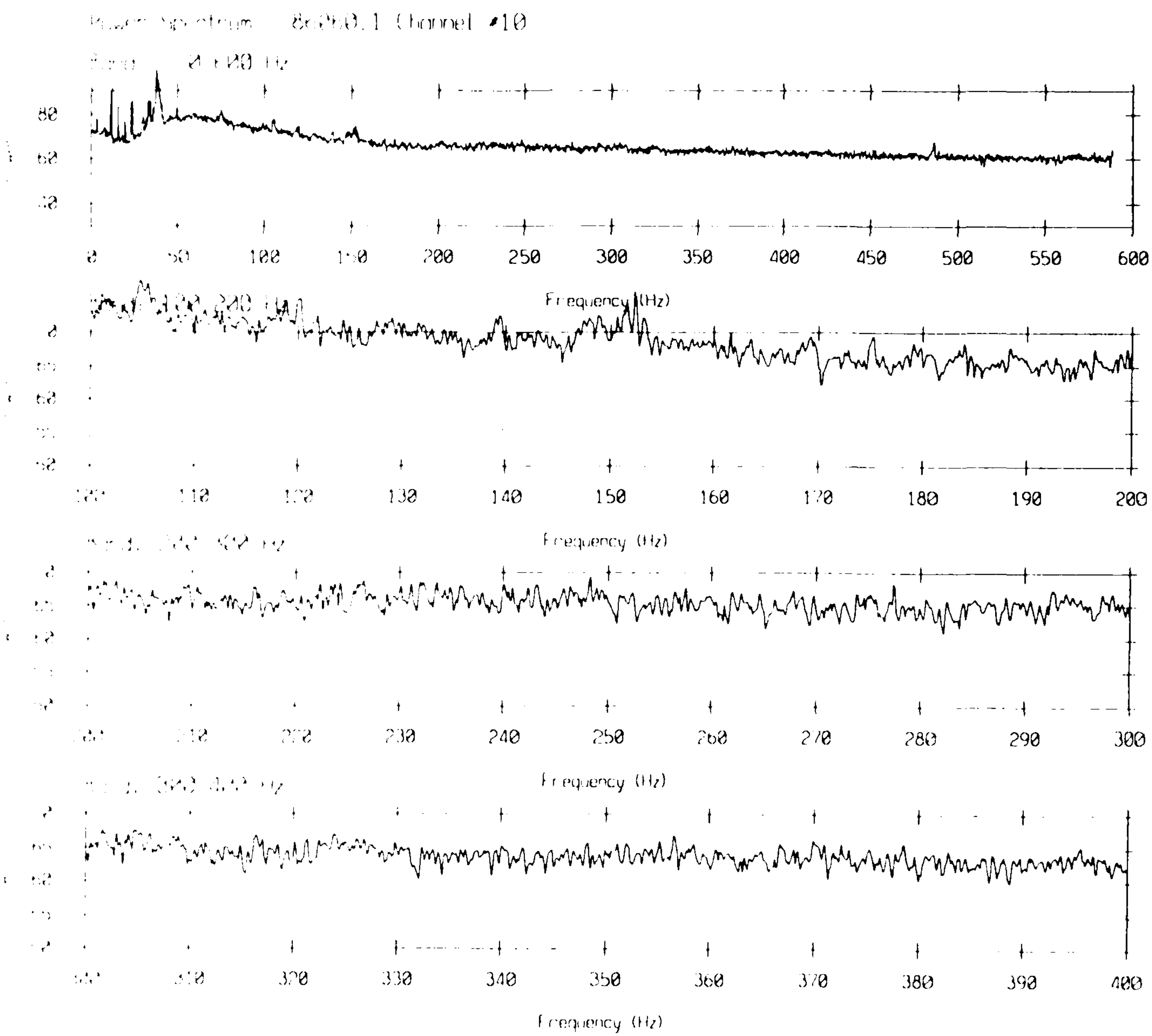
Channel #10
0 600 Hz
80
60
0
50
100
150
200
250
300
350
400
450
500
550
600
Frequency (Hz)
110
120
130
140
150
160
170
180
190
200
Frequency (Hz)
230
240
250
260
270
280
290
300
Frequency (Hz)
310
320
330
340
350
360
370
380
390
400
Frequency (Hz)

Figure 10(b).

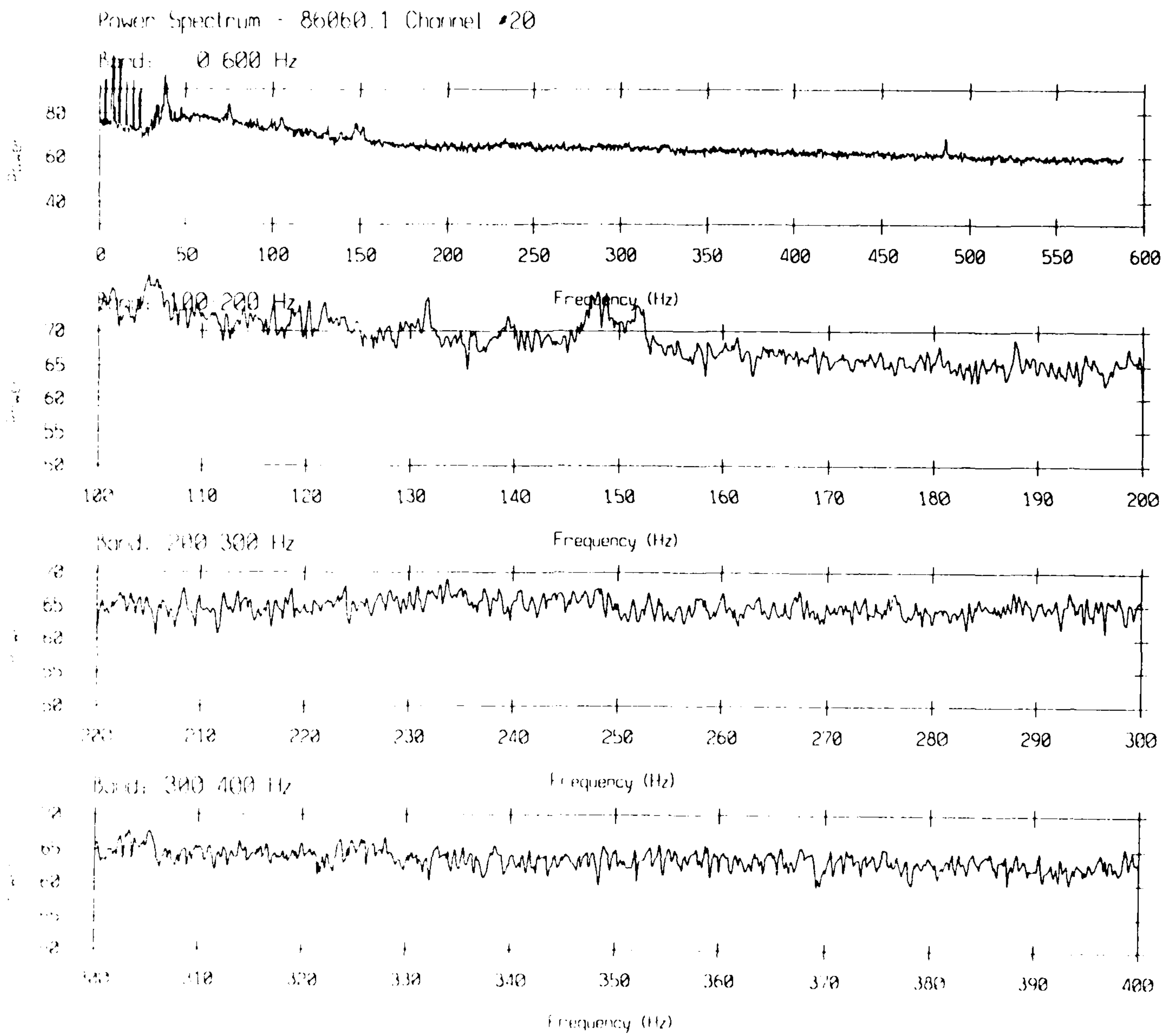

Power Spectrum - 86060.1 Channel #20
Band: 0 600 Hz
80
60
40
0
50
100
150
200
250
300
350
400
450
500
550
600
Frequency (Hz)
Band: 100 200 Hz
70
65
60
55
50
100
110
120
130
140
150
160
170
180
190
200
Frequency (Hz)
Band: 200 300 Hz
65
60
210
220
230
240
250
260
270
280
290
300
Frequency (Hz)
Band: 300 400 Hz
310
320
330
340
350
360
370
380
390
400
Frequency (Hz)

Figure 10(c).

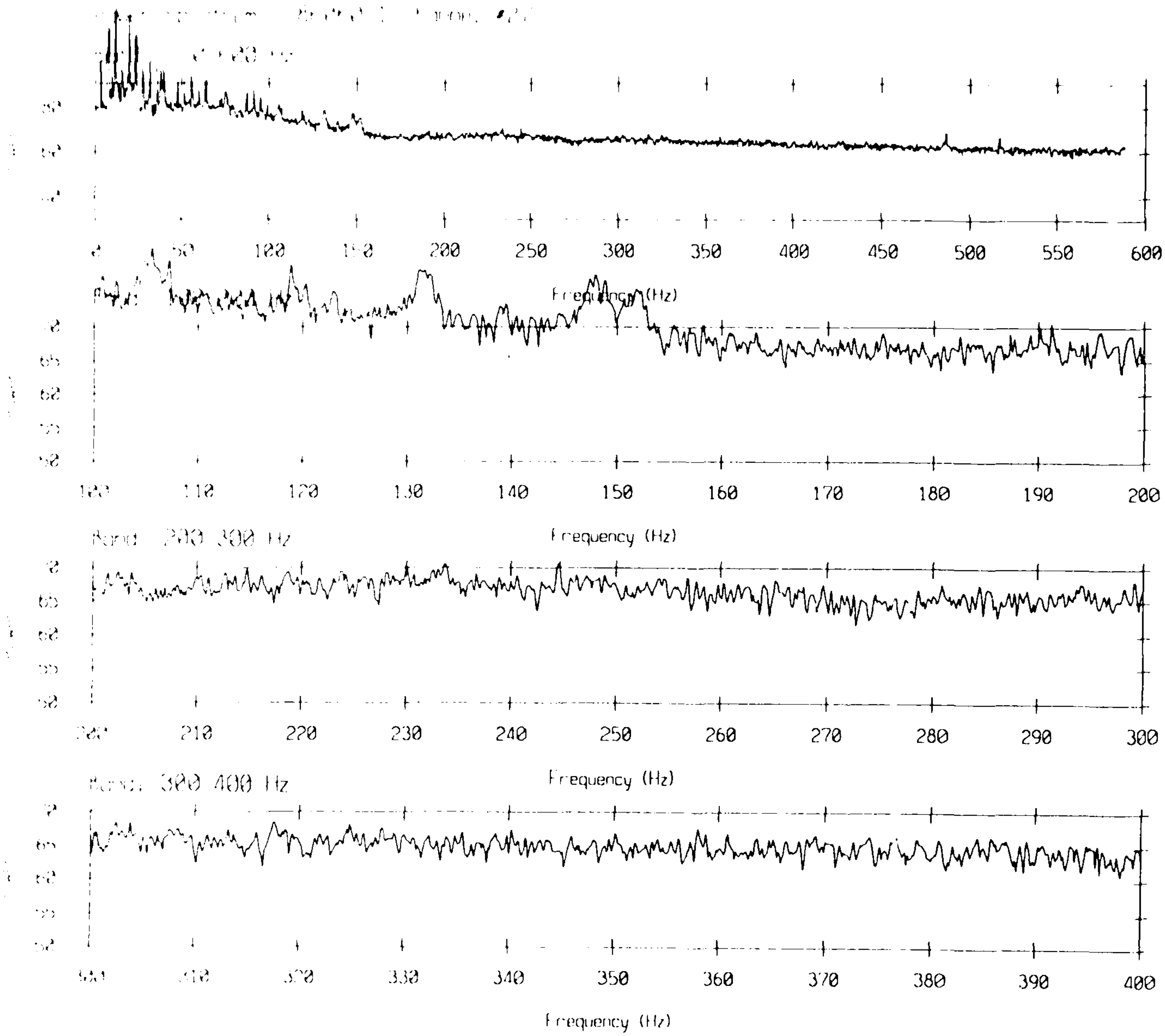
Frequency (Hz)
Frequency (Hz)
Band: 200 300 Hz
Frequency (Hz)
300 400 Hz
Frequency (Hz)

Figure 10(d).

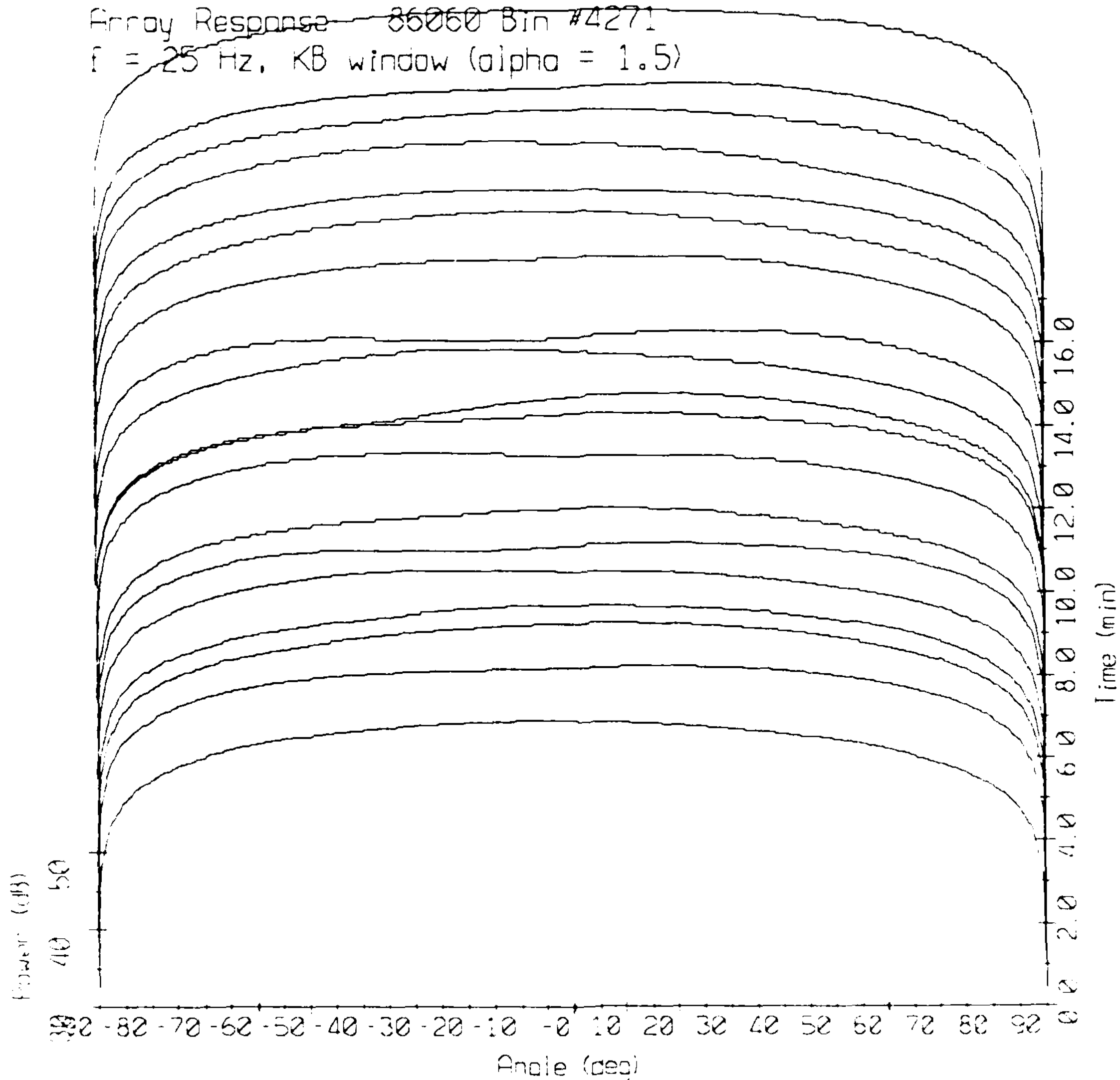
Array Response 86060 Bin #4271
f = 25 Hz, KB window (alpha = 1.5)
Power (dB)
40 50
0.0 2.0 4.0 6.0 8.0 10.0 12.0 14.0 16.0
Time (min)
-90 -80 -70 -60 -50 -40 -30 -20 -10 -0 10 20 30 40 50 60 70 80 90
Angle (deg)

Figure 11(a).

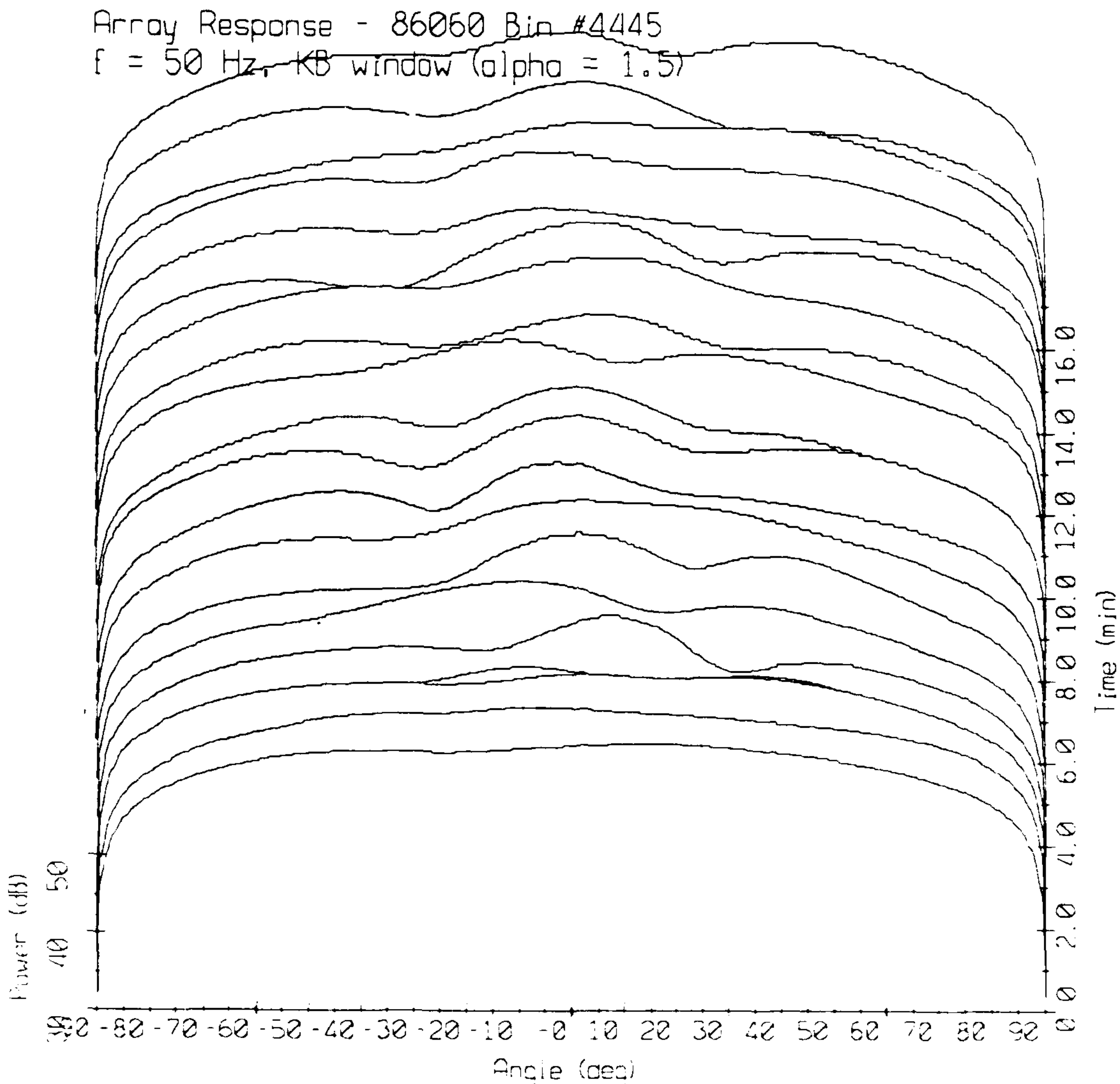

Array Response - 86060 Bin #4445
f = 50 Hz, KB window (alpha = 1.5)
Power (dB)
40
50
-80 -70 -60 -50 -40 -30 -20 -10 -0 10 20 30 40 50 60 70 80 90
Angle (deg)
0 2.0 4.0 6.0 8.0 10.0 12.0 14.0 16.0
Time (min)

Figure 11(b).

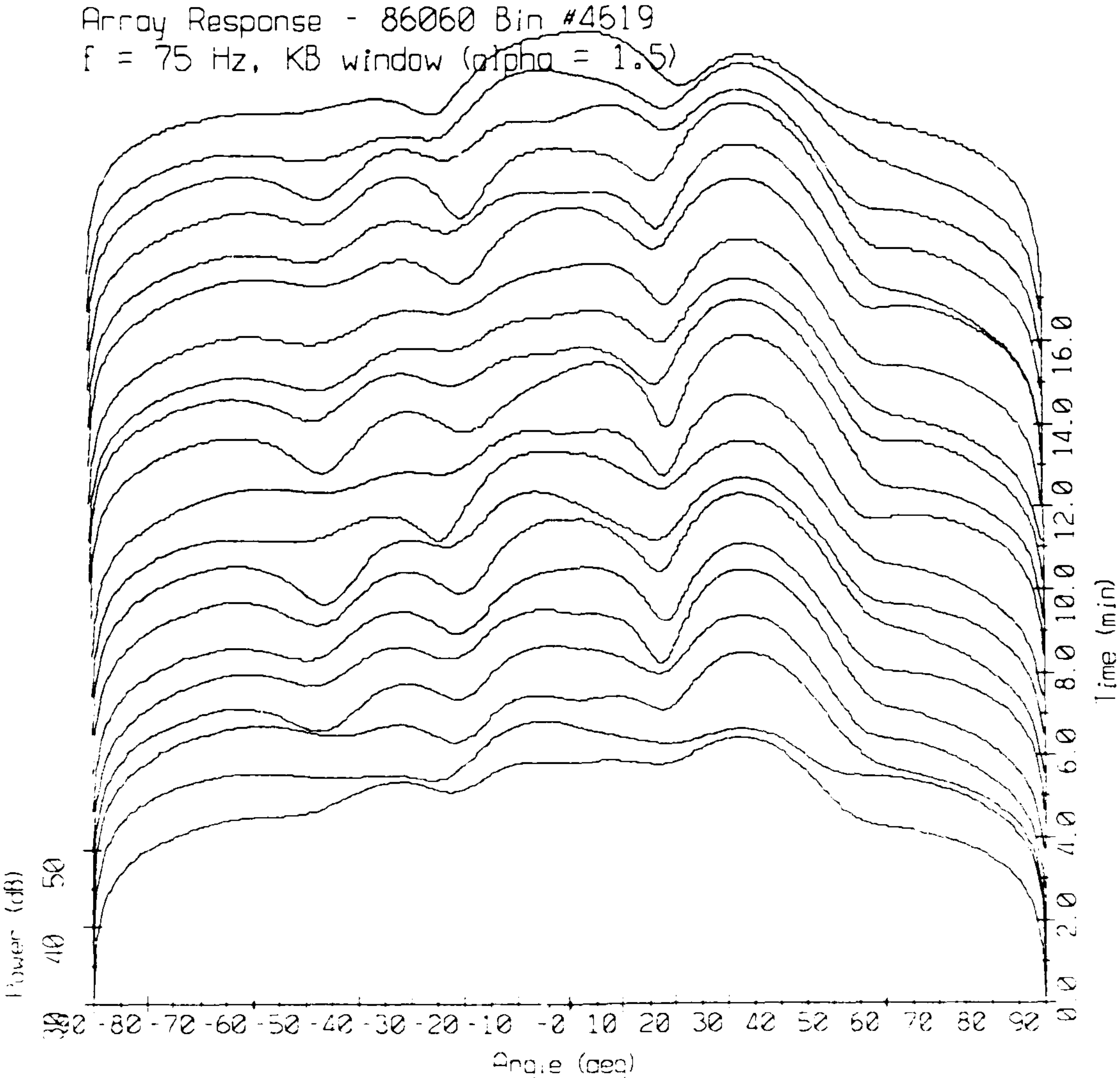

Array Response - 86060 Bin #4519
f = 75 Hz, KB window (alpha = 1.5)
Power (dB)
40
50
-82 -72 -62 -52 -42 -32 -22 -12 -2 12 22 32 42 52 62 72 82 92
Angle (deg)
0.0 2.0 4.0 6.0 8.0 10.0 12.0 14.0 16.0
Time (min)

Figure 11(c).

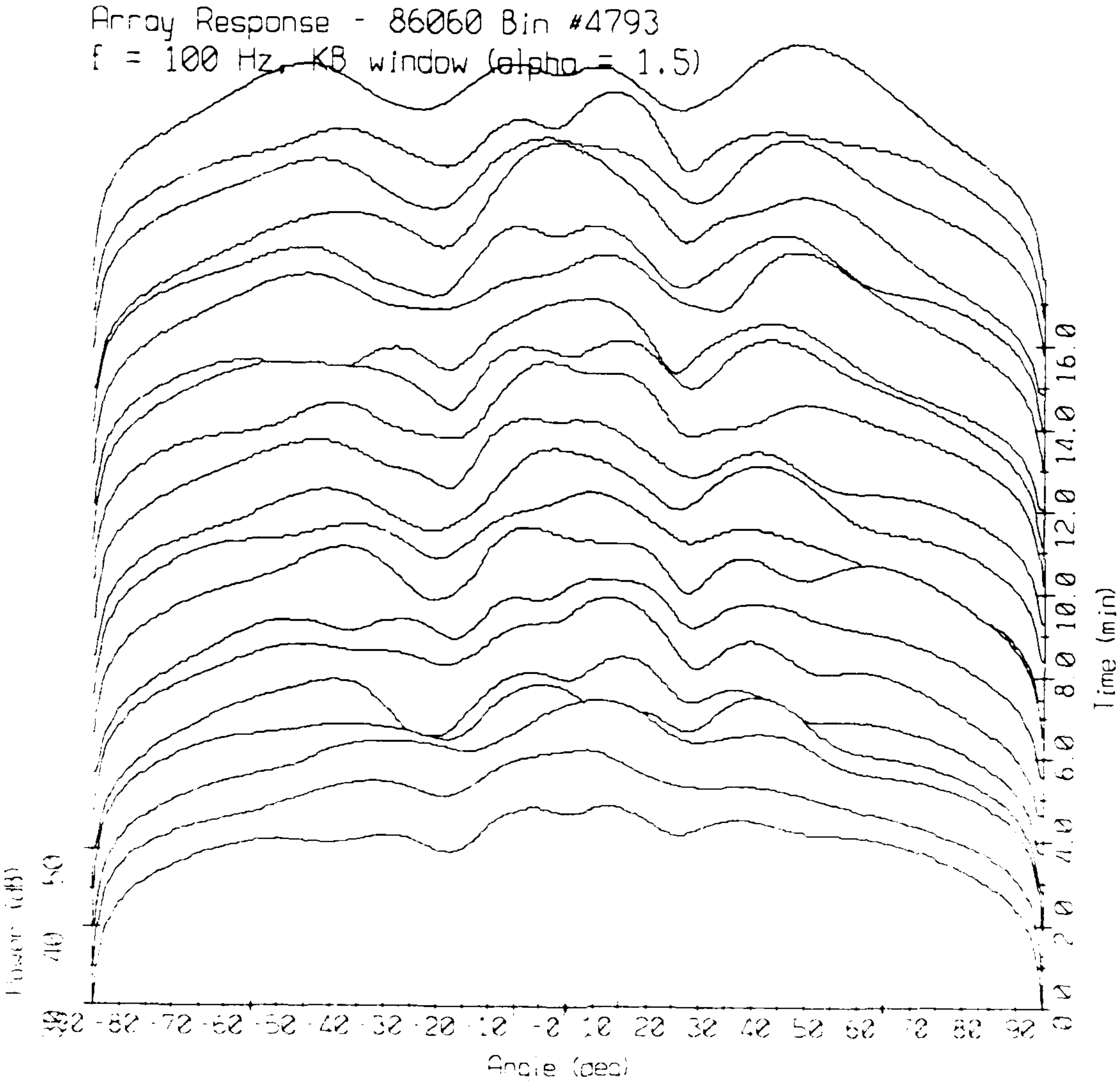
Array Response - 86060 Bin #4793
f = 100 Hz, KB window (alpha = 1.5)
Power (dB)
40
50
Time (min)
0.0
2.0
4.0
6.0
8.0
10.0
12.0
14.0
16.0
-80 -70 -60 -50 -40 -30 -20 -10 0 10 20 30 40 50 60 70 80 90
Angle (deg)

Figure 11(d).

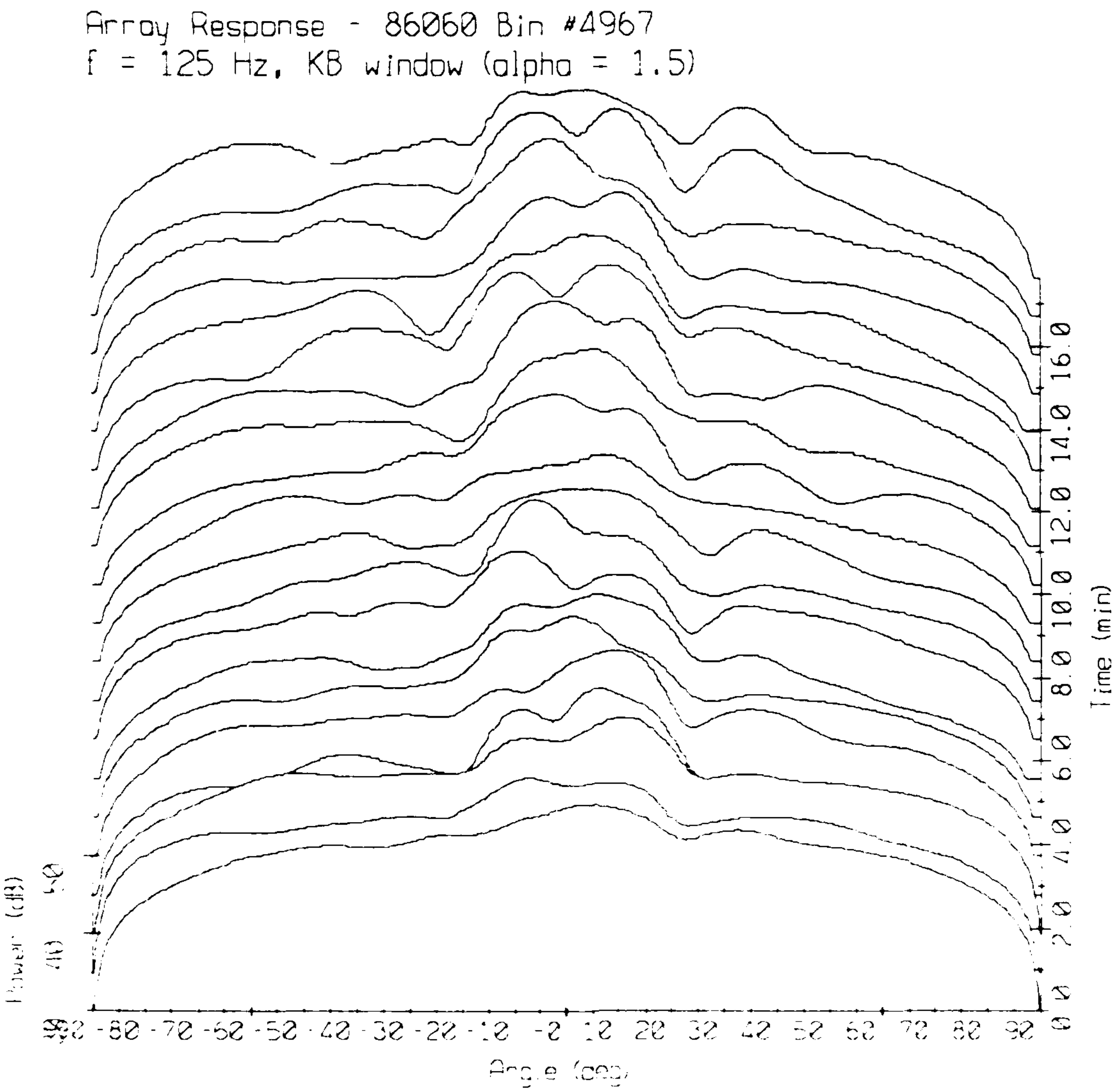
Array Response - 86060 Bin #4967
f = 125 Hz, KB window (alpha = 1.5)
Time (min)
Power (dB)
Angle (deg)

Figure 11(e).

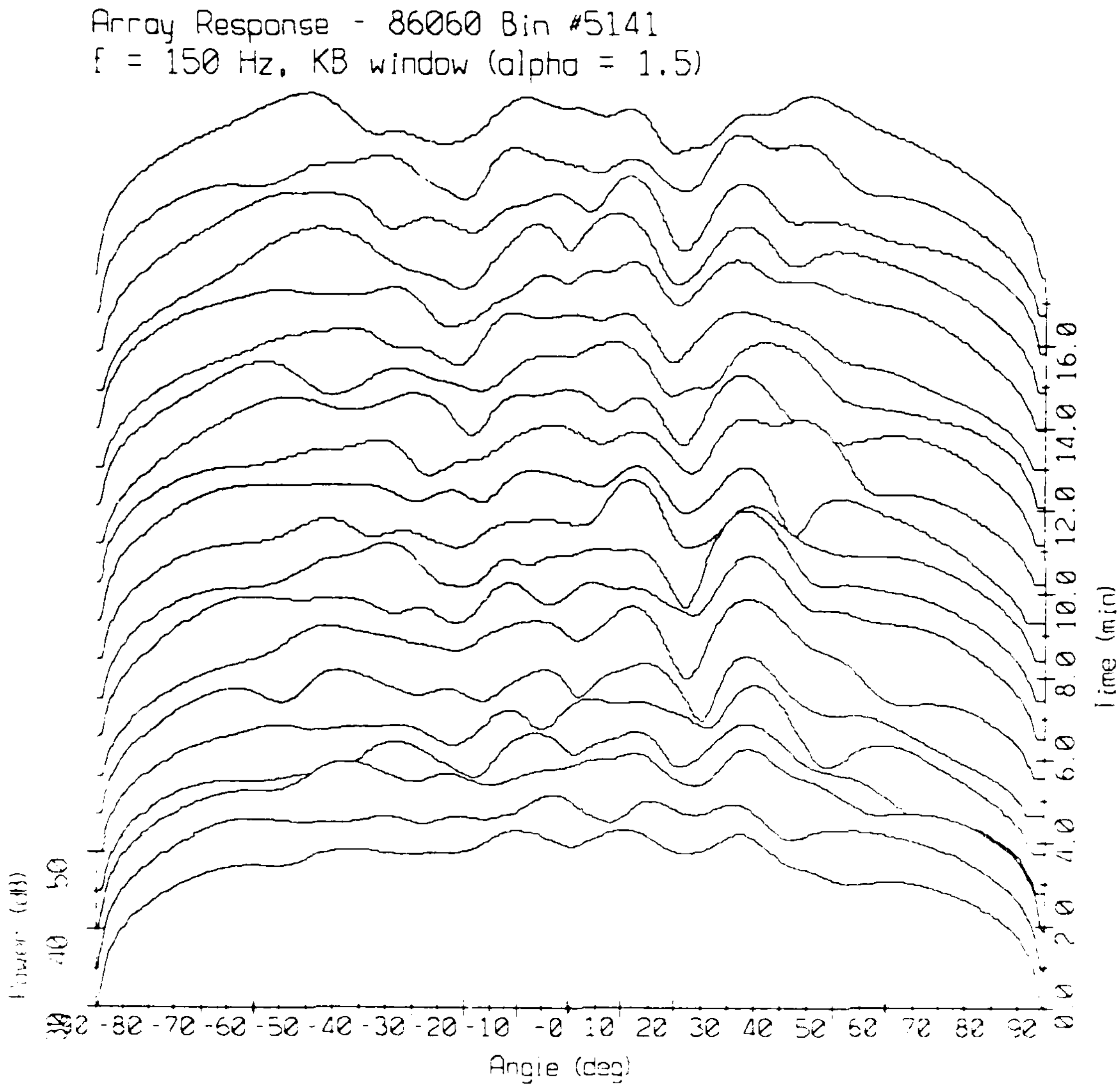
Array Response - 86060 Bin #5141
f = 150 Hz, KB window (alpha = 1.5)
Power (dB)
40
50
-82 -80 -70 -60 -50 -40 -30 -20 -10 -0 10 20 30 40 50 60 70 80 90
Angle (deg)
0 2.0 4.0 6.0 8.0 10.0 12.0 14.0 16.0
Time (min)

Figure 11(f).

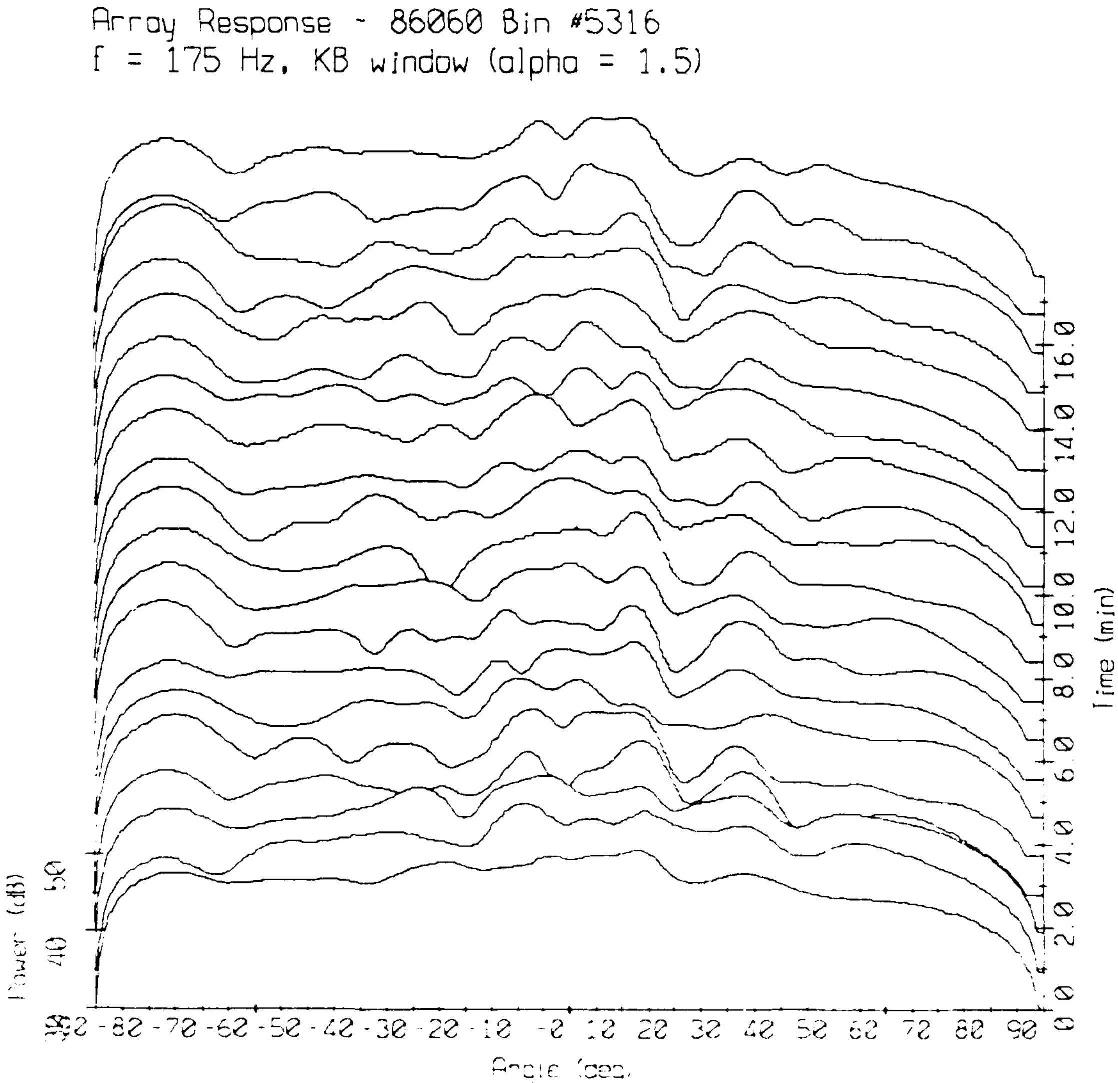
Array Response - 86060 Bin #5316
f = 175 Hz, KB window (alpha = 1.5)
Power (dB)
40
50
-82 -72 -62 -52 -42 -32 -22 -12 -2 12 22 32 42 52 62 72 82 92
Angle (deg)
0.0 2.0 4.0 6.0 8.0 10.0 12.0 14.0 16.0
Time (min)

Figure 11(a).

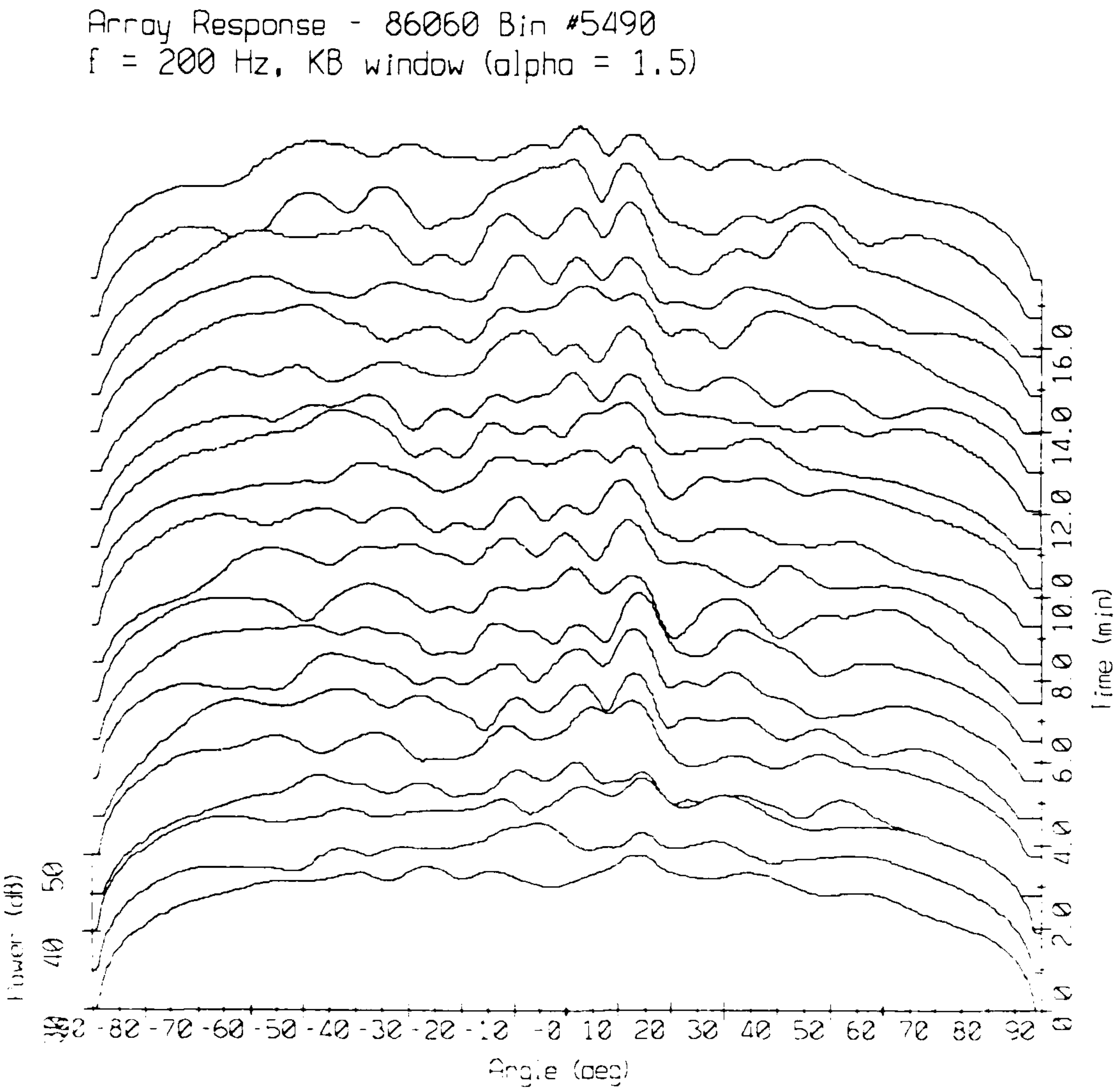

Array Response - 86060 Bin #5490
f = 200 Hz, KB window (alpha = 1.5)
Power (dB)
40
50
-82 -70 -60 -50 -40 -30 -20 -10 -0 10 20 30 40 50 60 70 80 90
Angle (deg)
0.0
2.0
4.0
6.0
8.0
10.0
12.0
14.0
16.0
Time (min)

Figure 11(b).

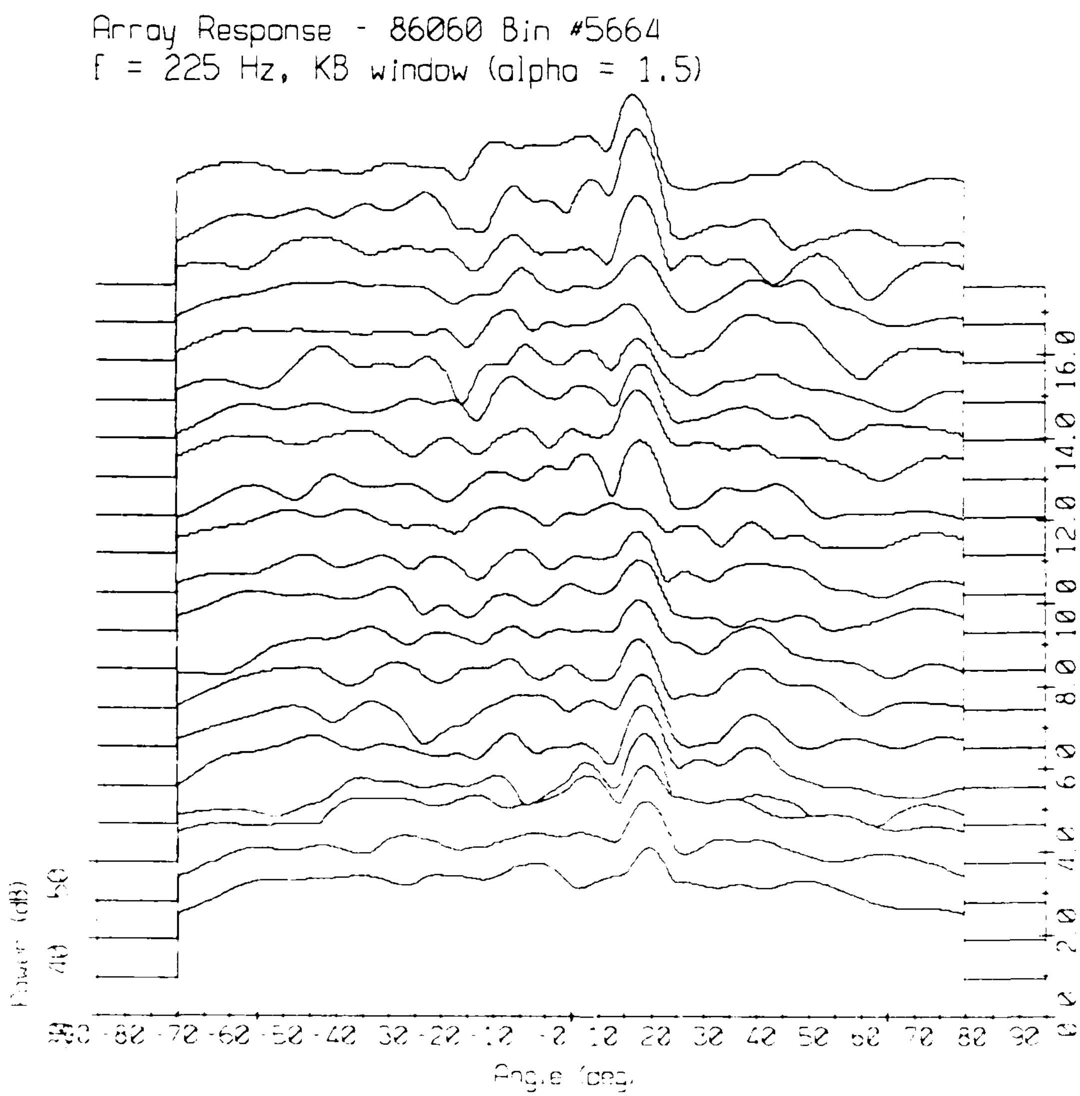
Array Response - 86060 Bin #5664
f = 225 Hz, KB window (alpha = 1.5)
-82 -72 -62 -52 -42 -32 -22 -12 -2 12 22 32 42 52 62 72 82 92
Angle (deg)
Power (dB)
40 50
0 2.0 4.0 6.0 8.0 10.0 12.0 14.0 16.0
Time (min)

Figure 11(i).

Array Response - 86060 Bin #5832
f = 250 Hz, KB window (alpha = 1.5)

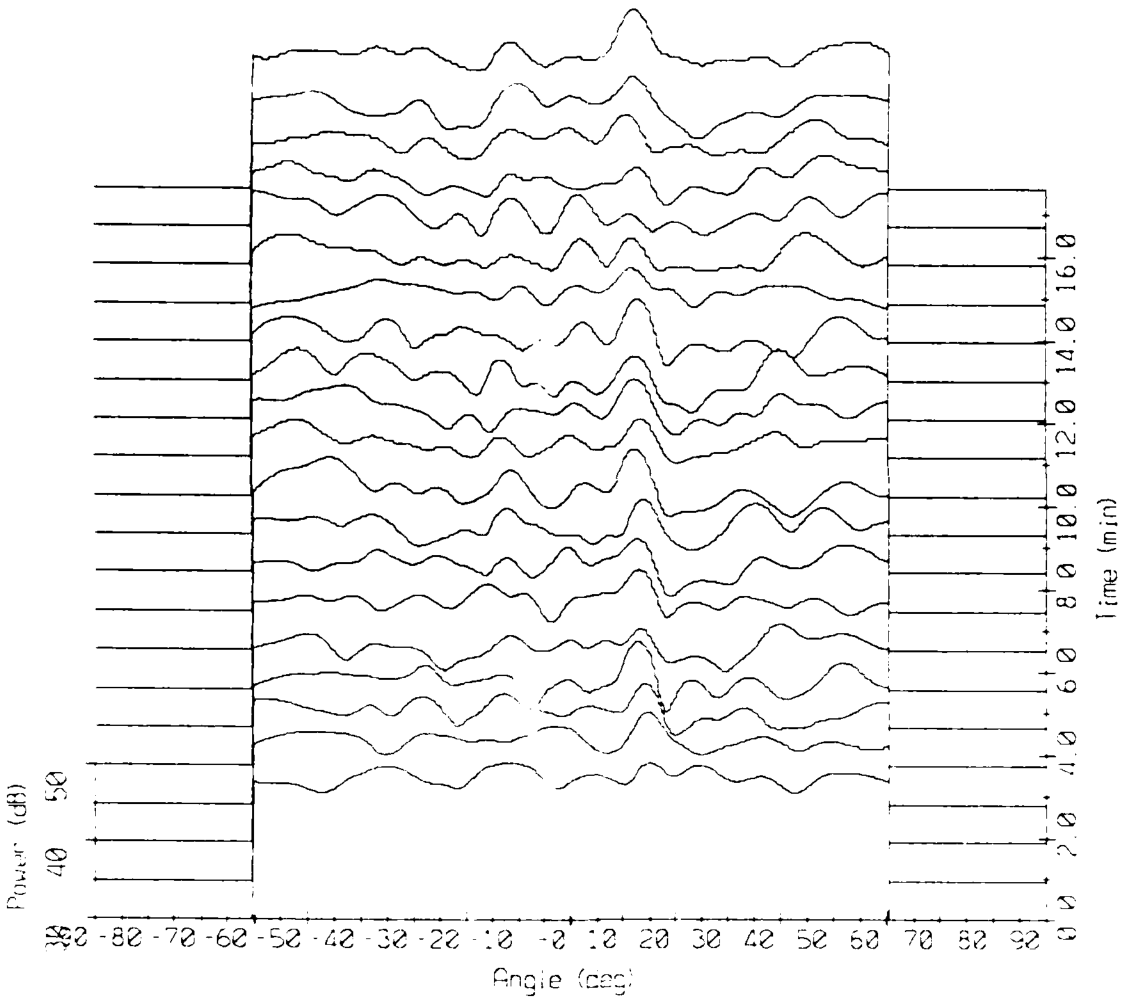

Figure 11(?).

Array Response - 86060 Bin #6012
f = 275 Hz, KB window (alpha = 1.5)

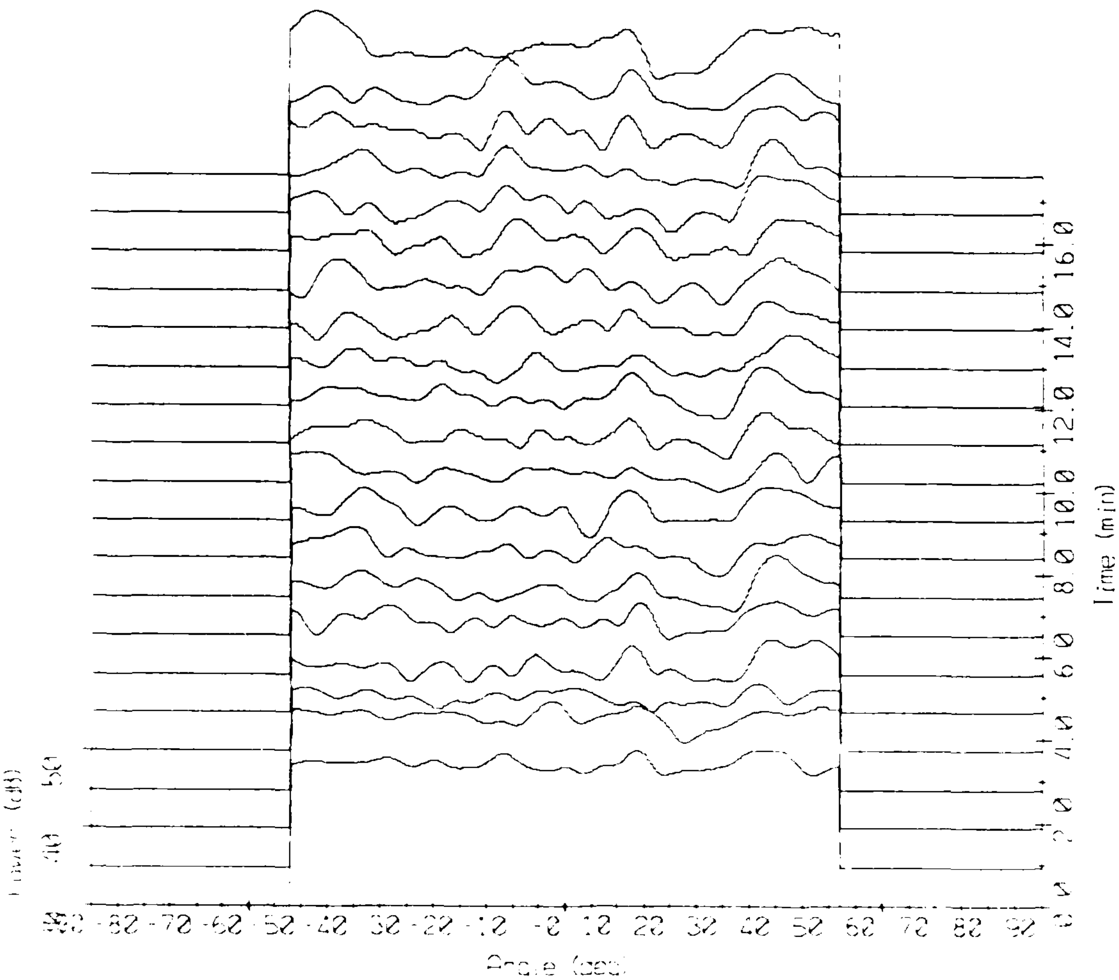

Figure 11(k).

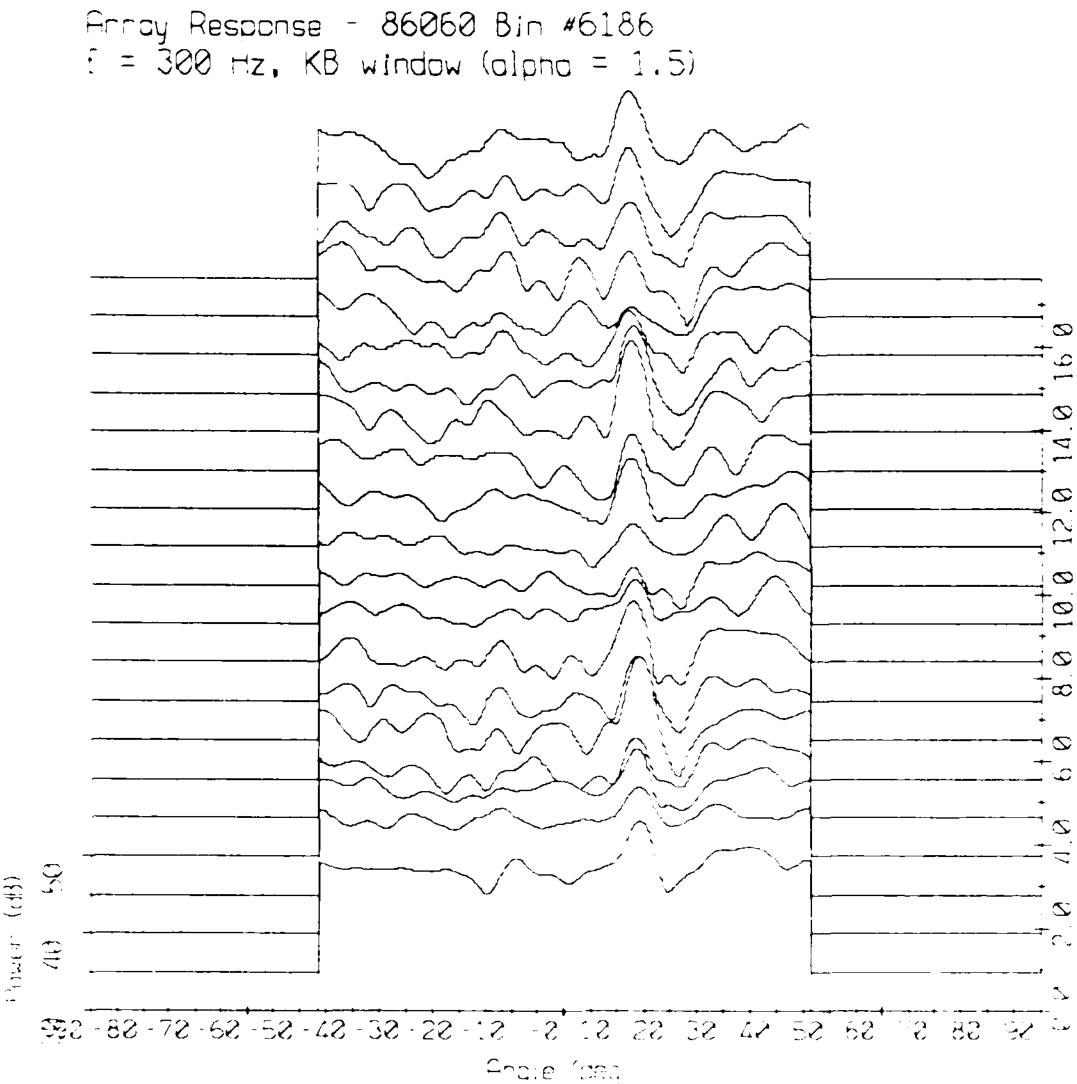

Array Response - 86060 Bin #6186
f = 300 Hz, KB window (alpha = 1.5)
Power (dB)
40
50
Time (min)
2.0 4.0 6.0 8.0 10.0 12.0 14.0 16.0
-82 -72 -62 -52 -42 -32 -22 -12 -2 12 22 32 42 52 62 82 92
Angle (deg)

Array Response - 86060 Bin #4619

f = 75 Hz, KB window (alpha = 1.5)

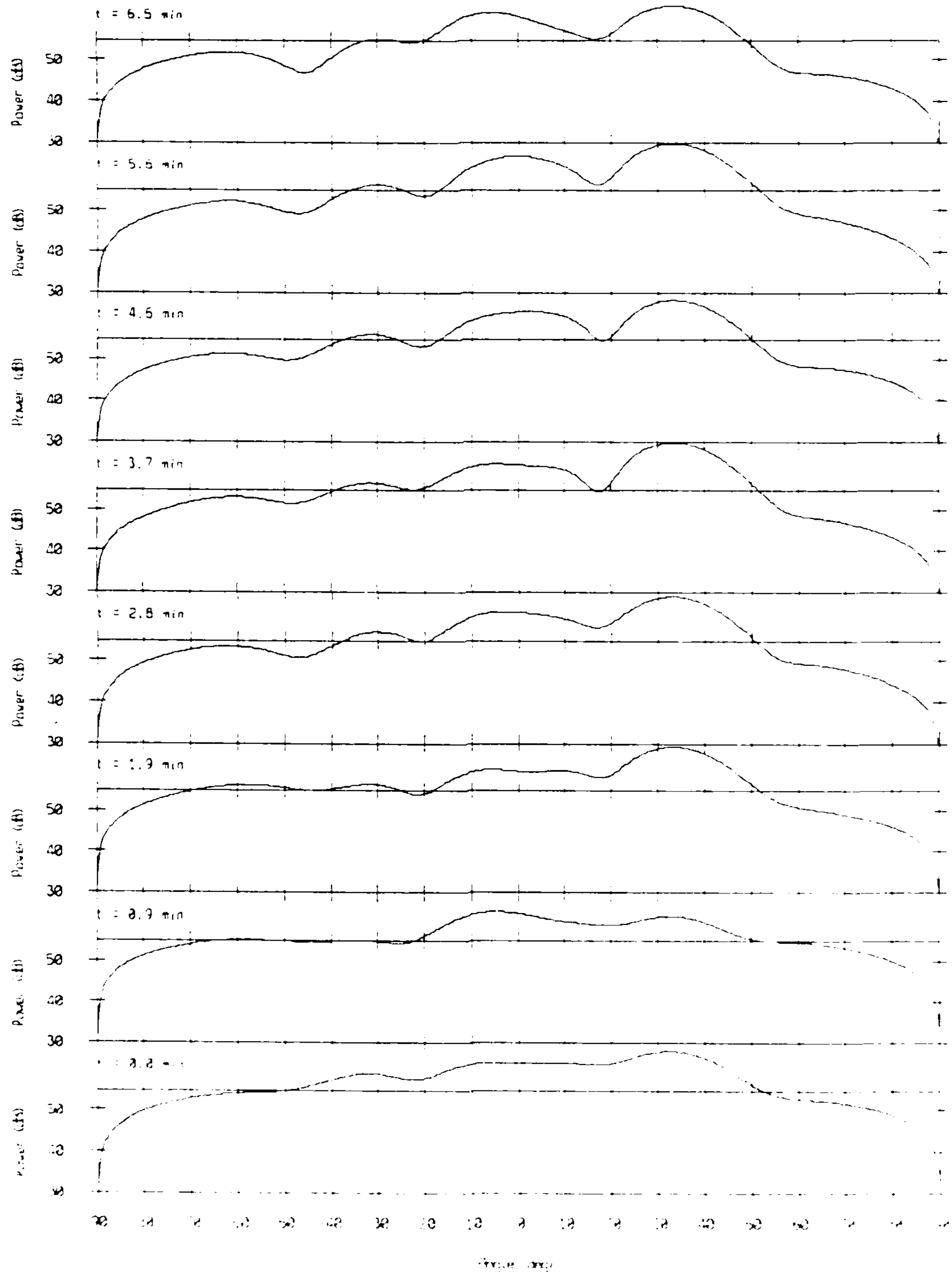

Array Response - 86260 Bin #4619

f = 75 Hz, KB window (alpha = 1.5)

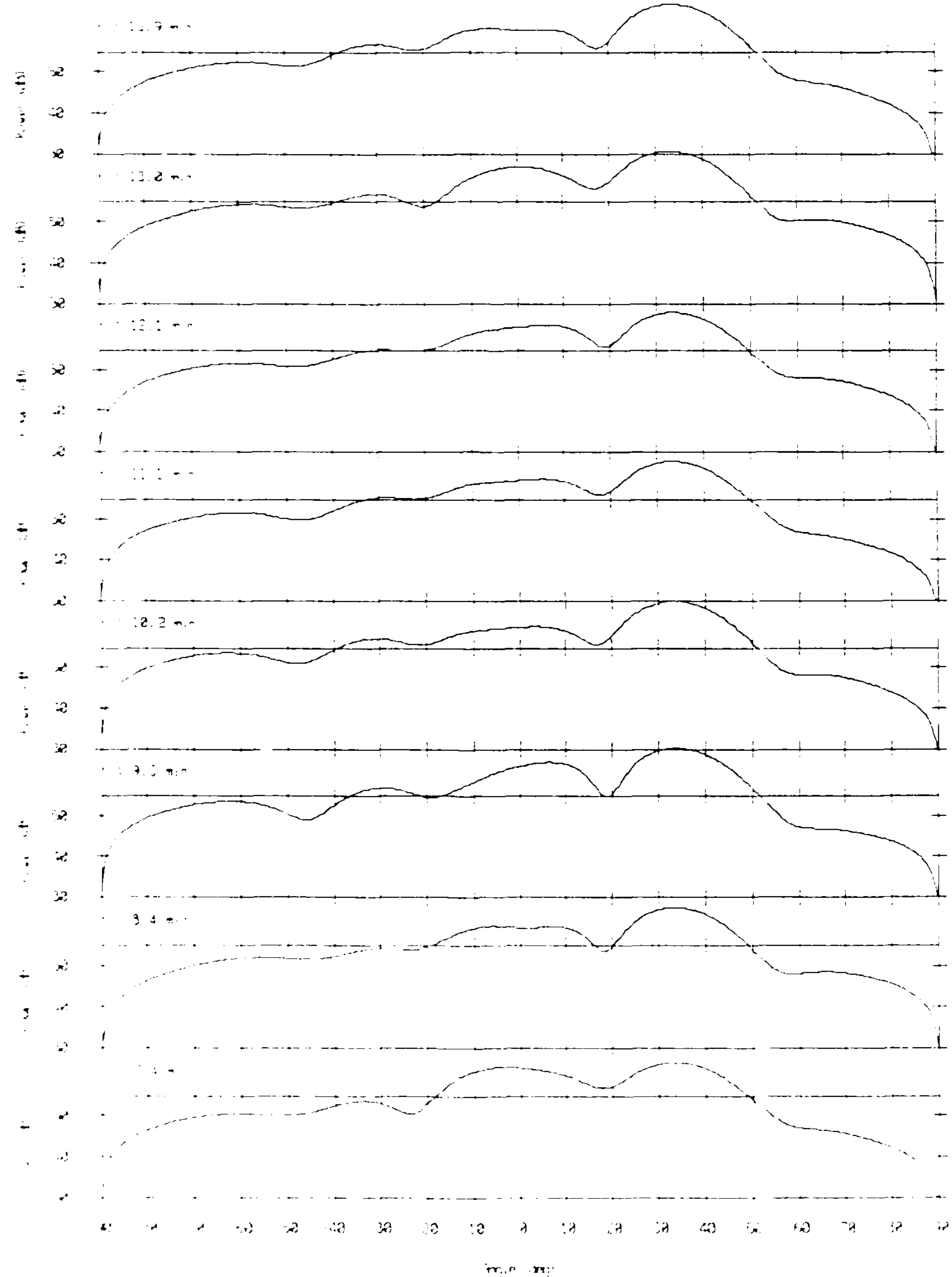

Array Response - 86060 Bin #4619

f = 75 Hz, KB window (alpha = 1.5)

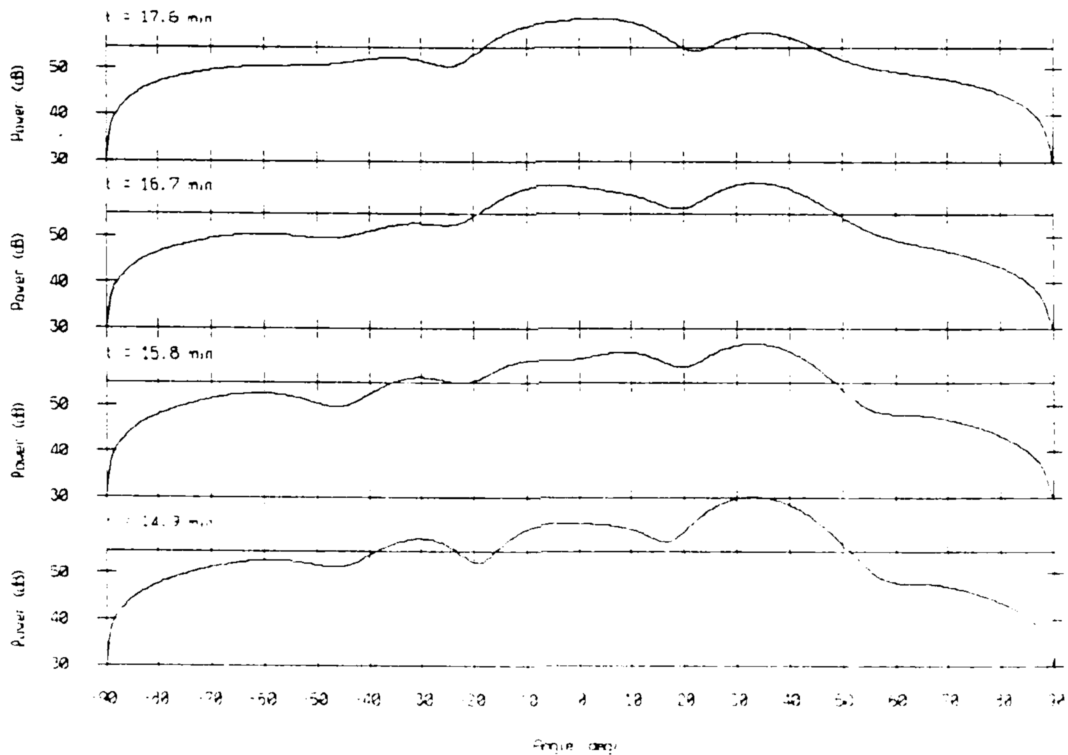

Array Response - 86060 Bin #5141

f = 150 Hz, KB window (alpha = 1.5)

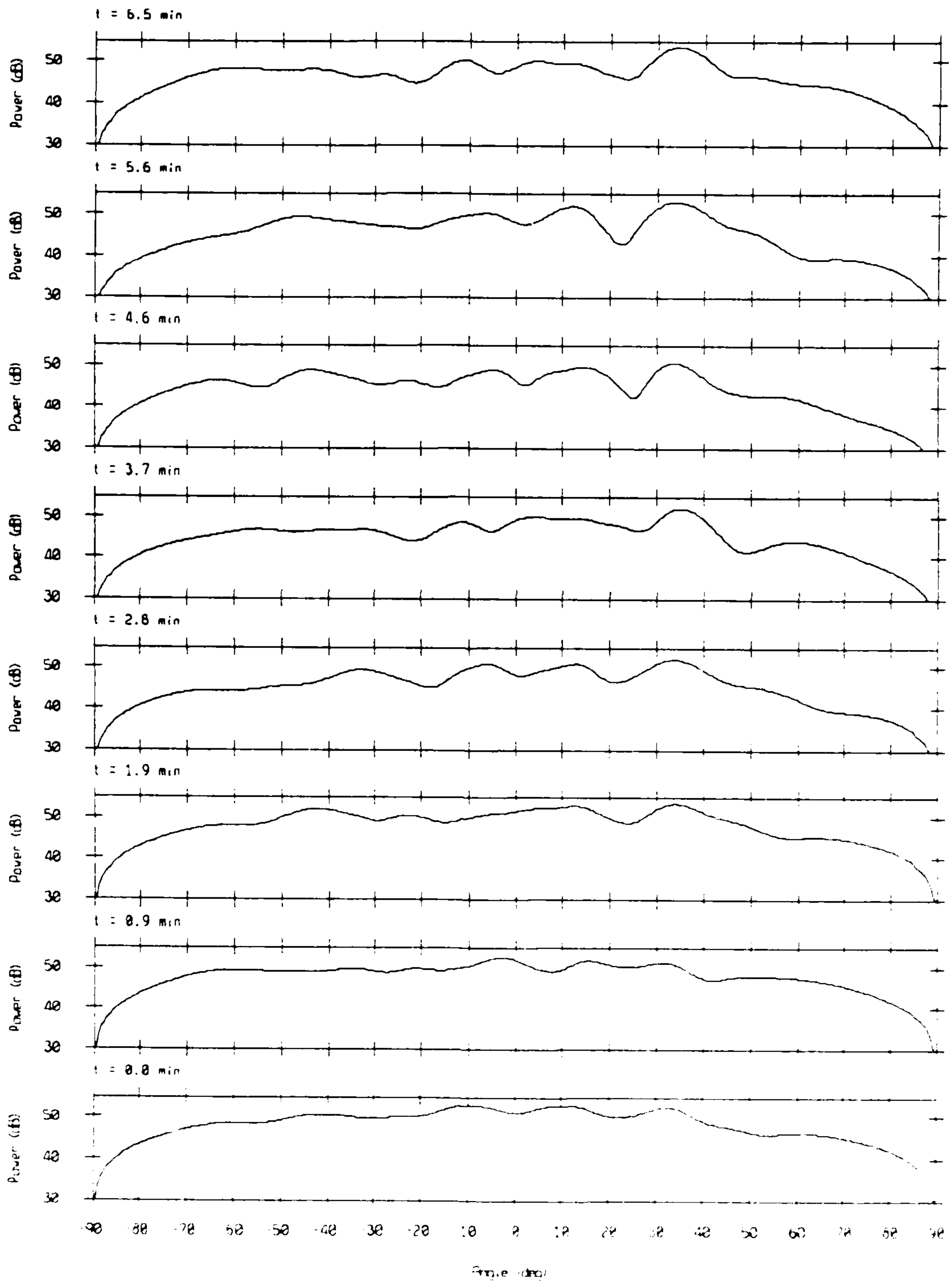

Figure 12(b).

Array Response - 86060 Bin #5141

f = 150 Hz, KB window (alpha = 1.5)

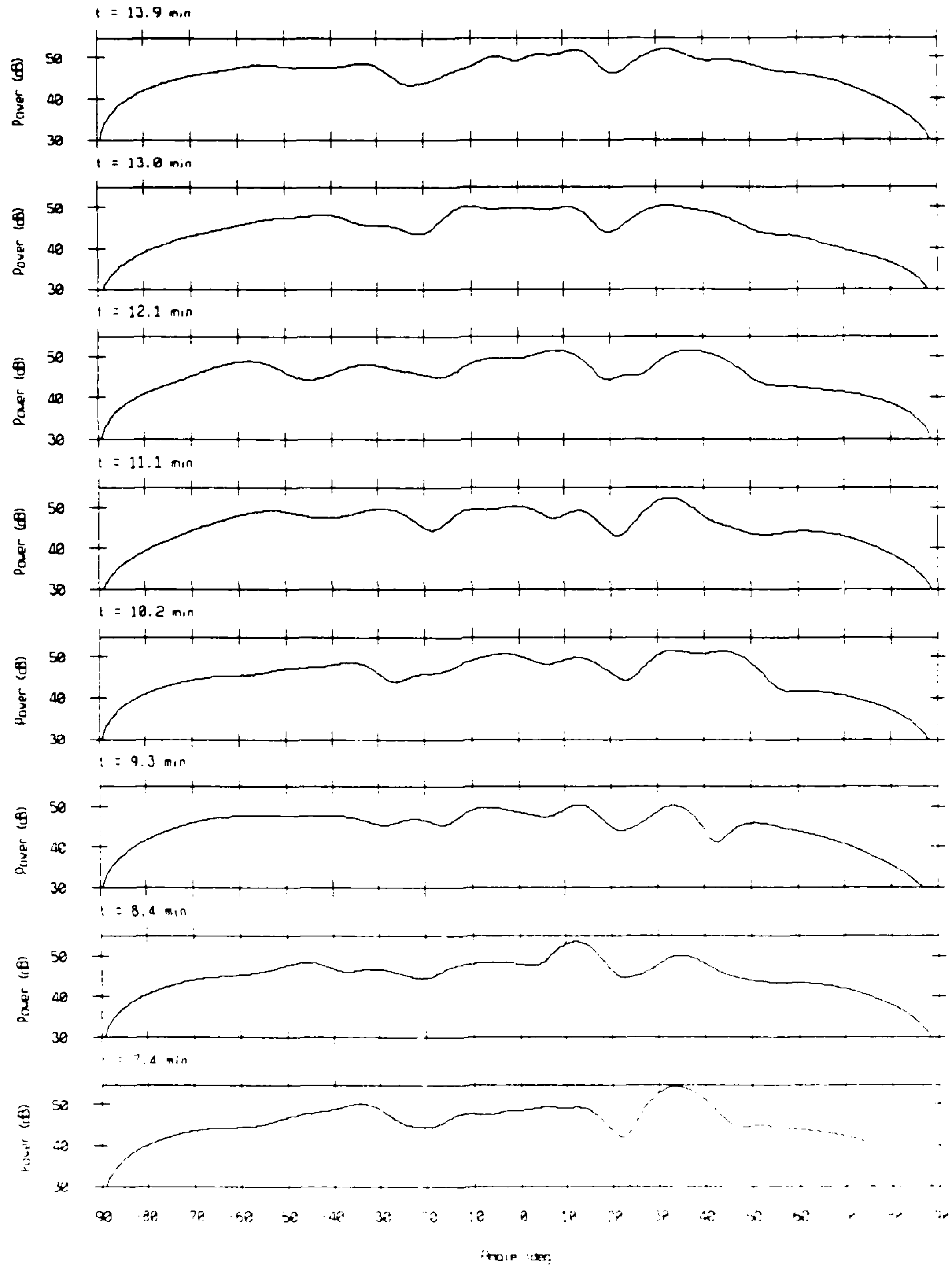

Array Response - 86060 Bin #5141

f = 150 Hz, KB window (alpha = 1.5)

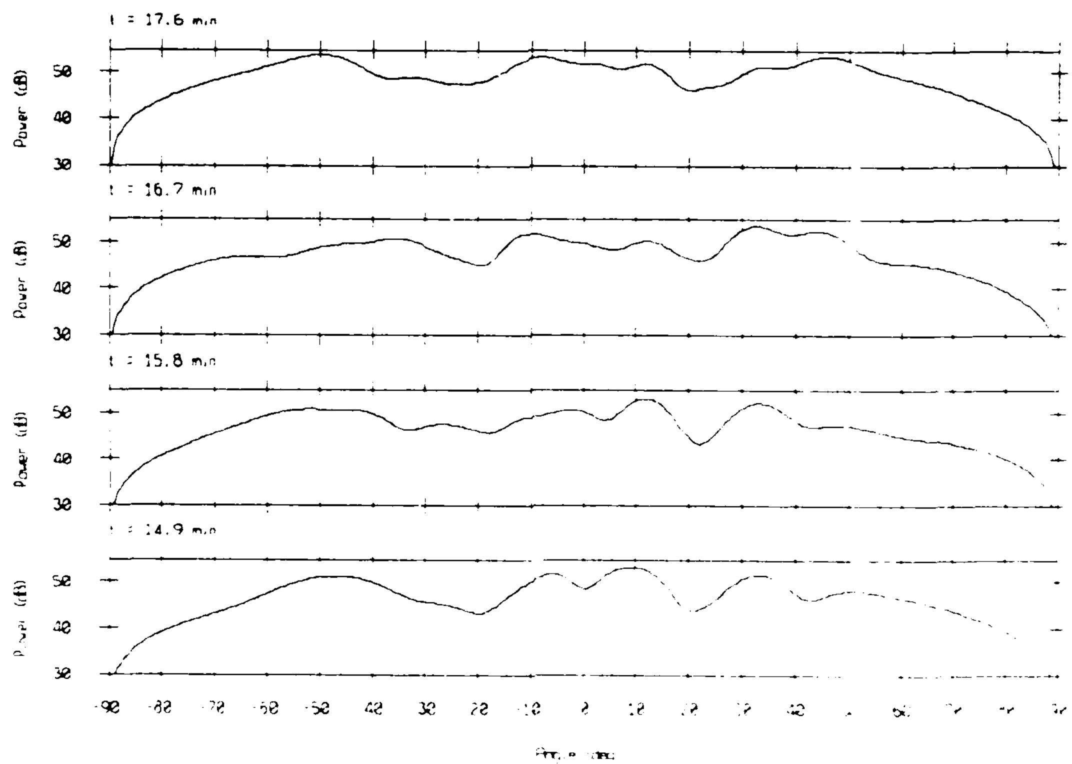

Array Response - 86060 Bin #6186

f = 300 Hz, KB window (alpha = 1.5)

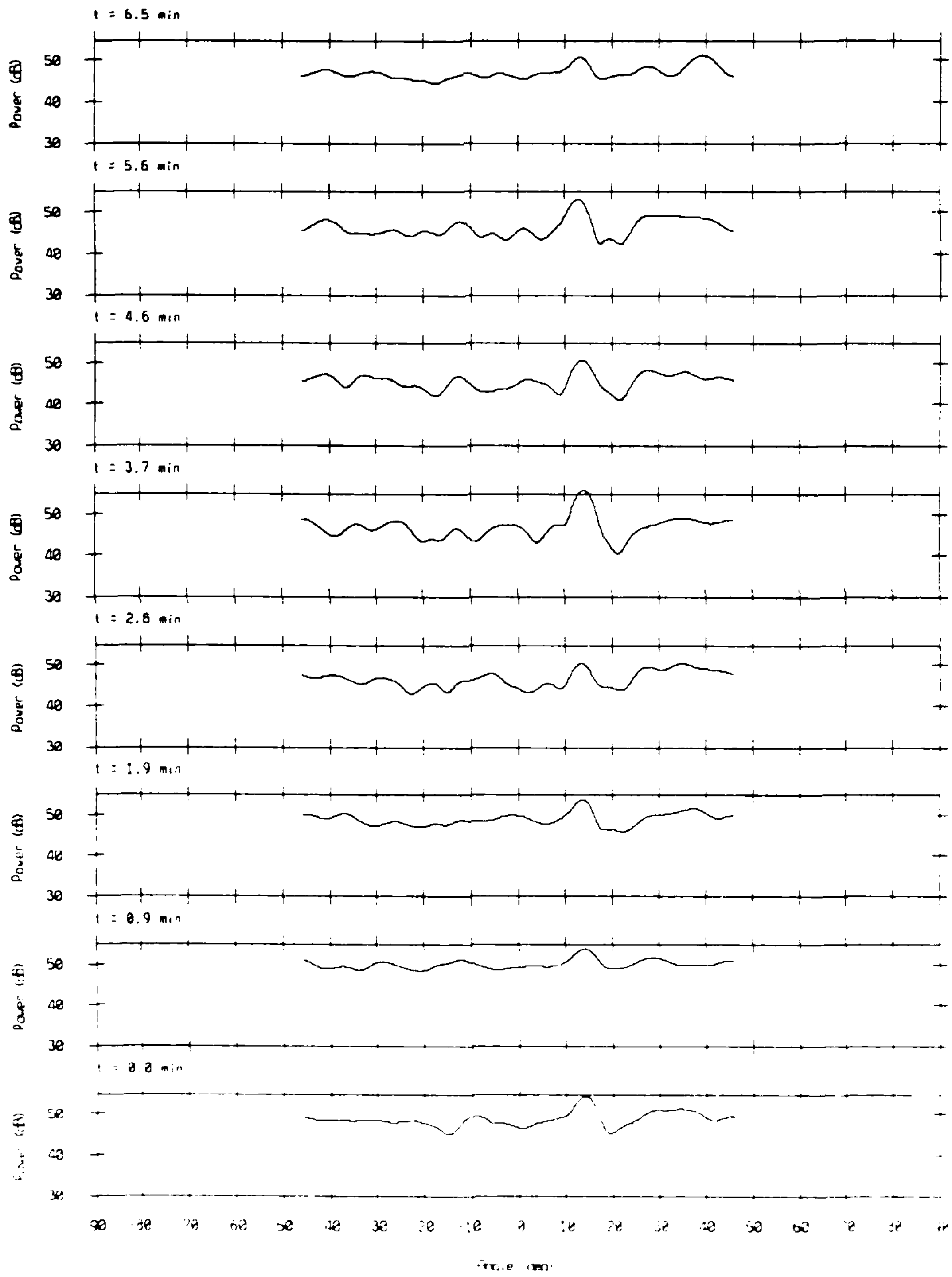

Figure 12(c).

Array Response - 86060 Bin #6186

f = 300 Hz, KB window (alpha = 1.5)

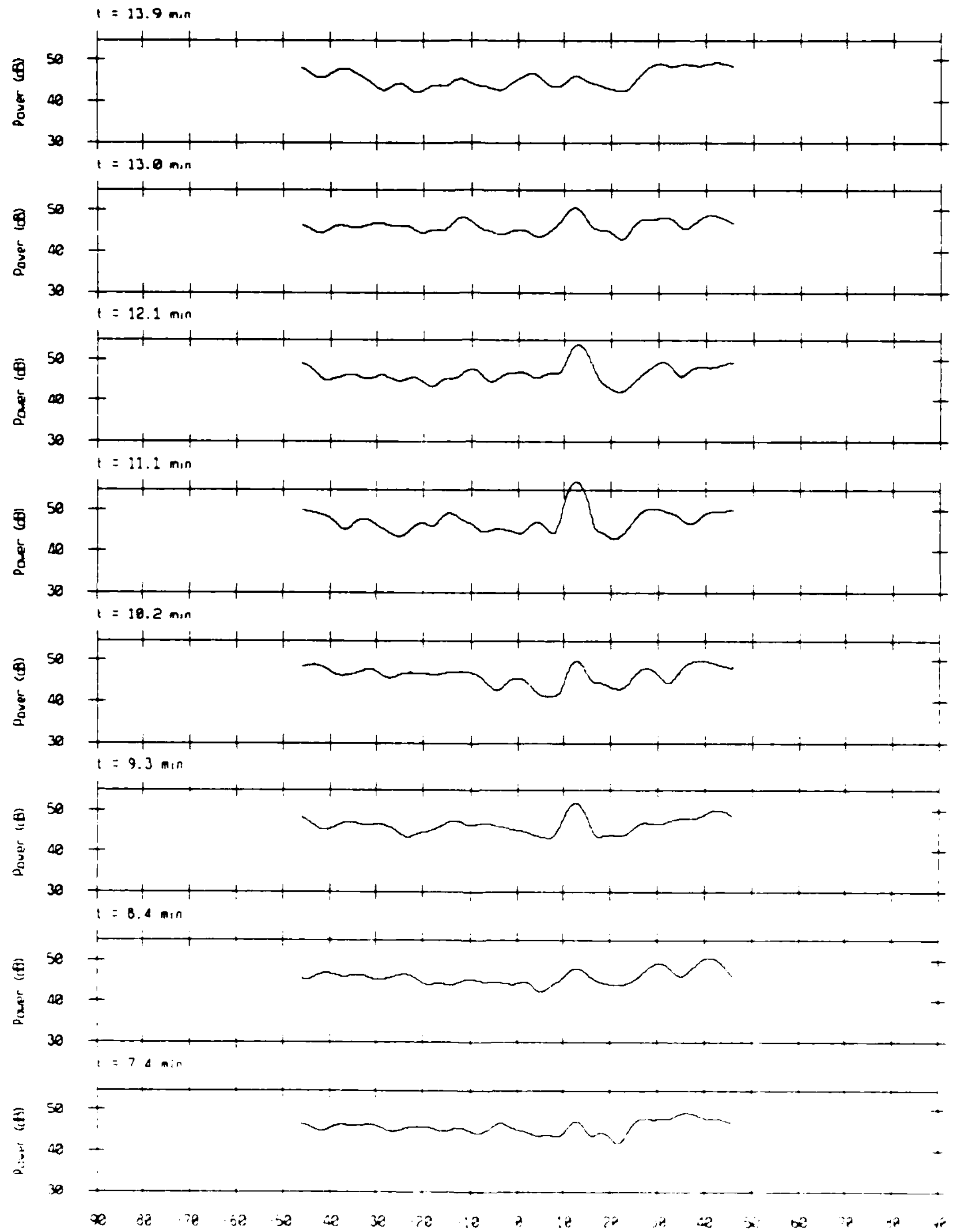

Array Response - 86060 Bin #6186

f = 300 Hz, KB window (alpha = 1.5)

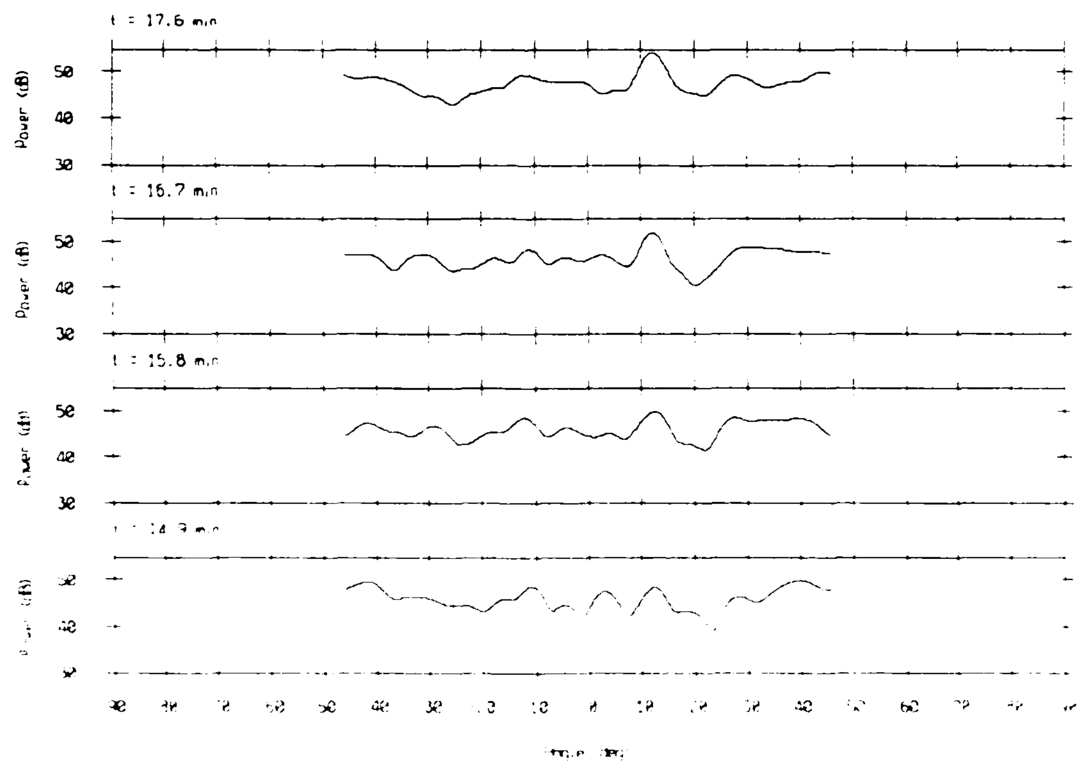

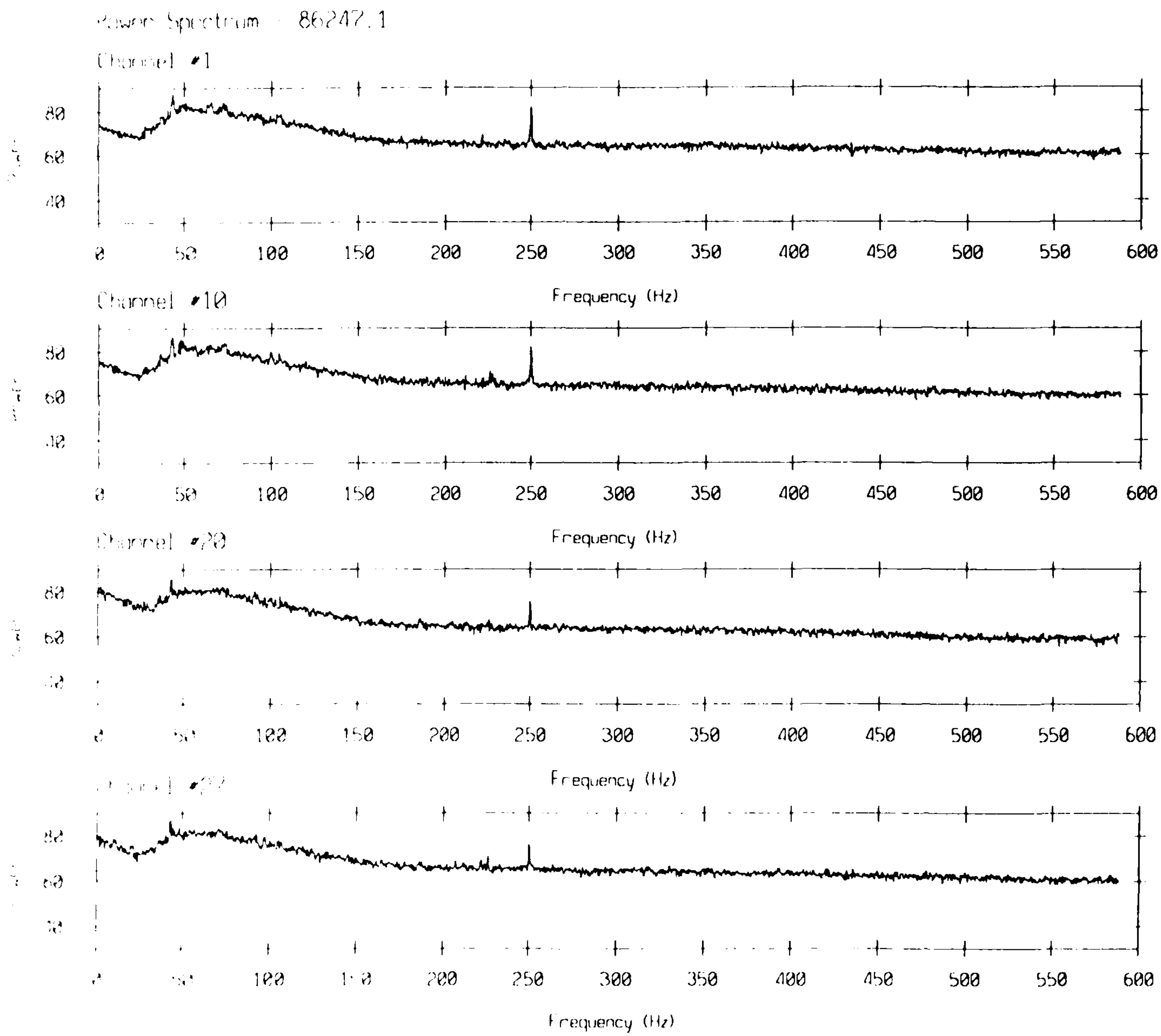

Power Spectrum 86247.1
Channel #1
Channel #10
Channel #20
Frequency (Hz)

Figure 13.

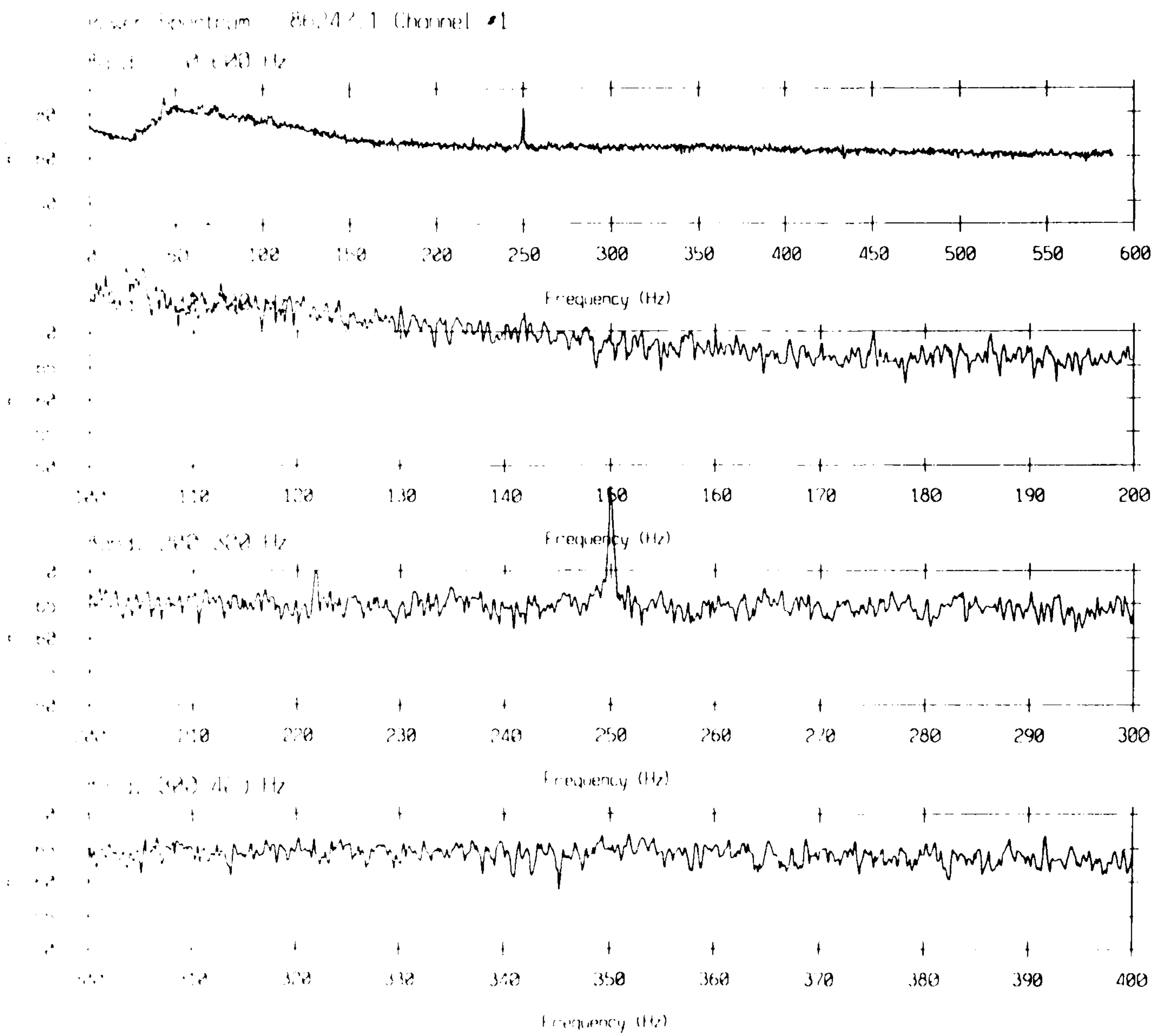
Channel #1
Frequency (Hz)
Frequency (Hz)
Frequency (Hz)
Frequency (Hz)

Figure 14(a).

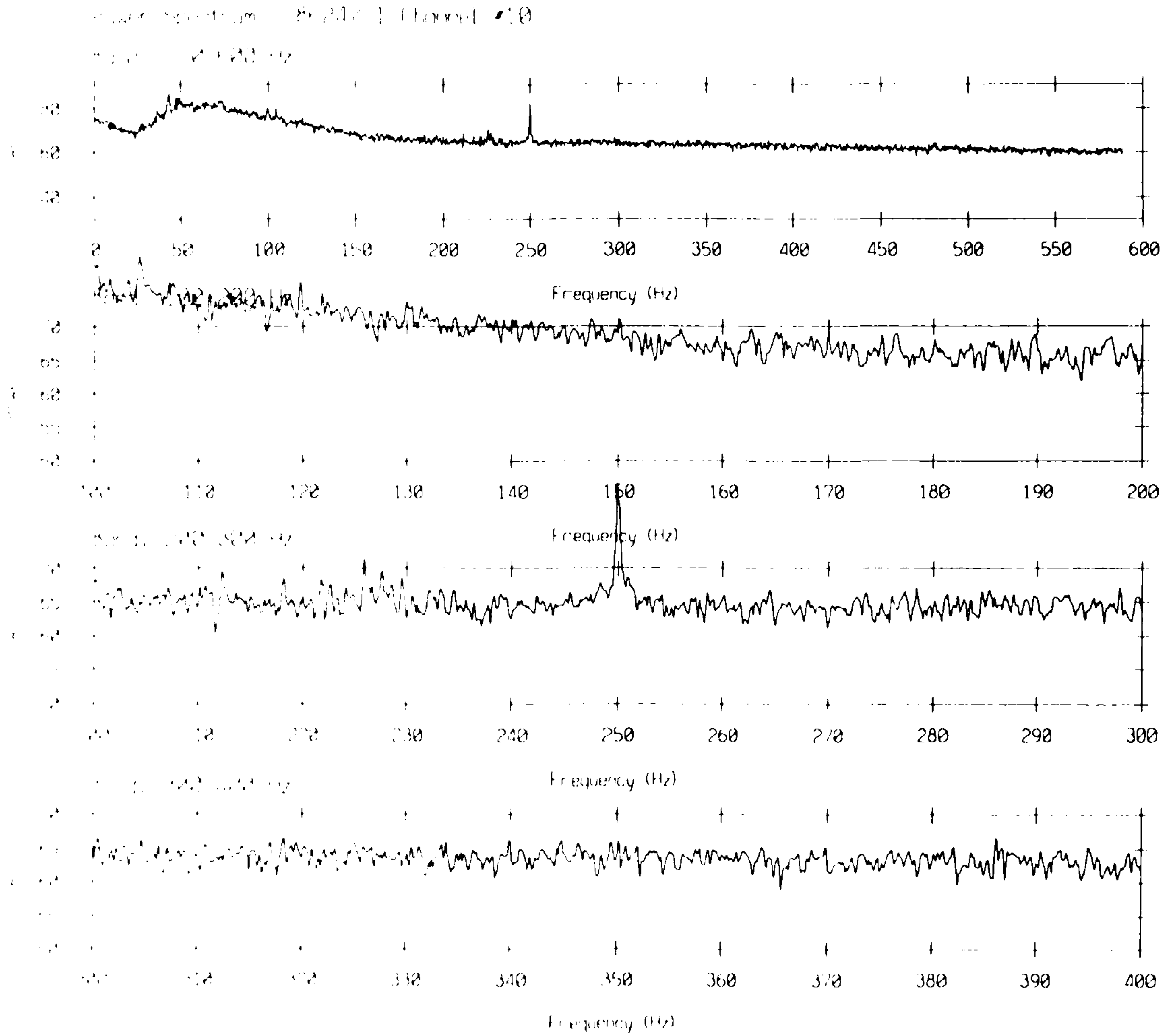
0
50
100
150
200
250
300
350
400
450
500
550
600
Frequency (Hz)
140
150
160
170
180
190
200
Frequency (Hz)
240
250
260
270
280
290
300
Frequency (Hz)
340
350
360
370
380
390
400

Figure 14(b).

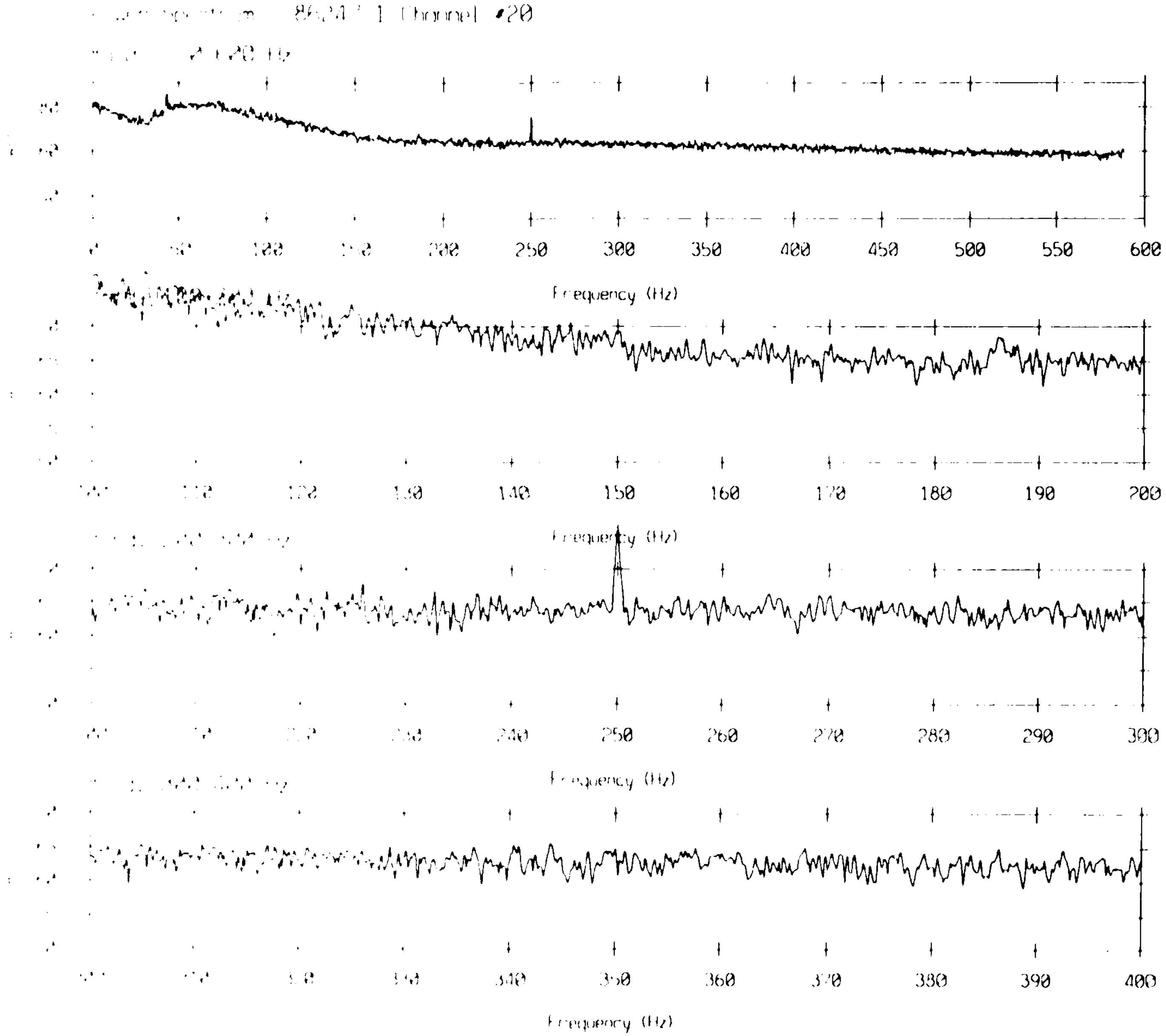
Channel #20
0 50 100 150 200 250 300 350 400 450 500 550 600
Frequency (Hz)
100 110 120 130 140 150 160 170 180 190 200
Frequency (Hz)
200 210 220 230 240 250 260 270 280 290 300
Frequency (Hz)
300 310 320 330 340 350 360 370 380 390 400
Frequency (Hz)

Figure 14(c).

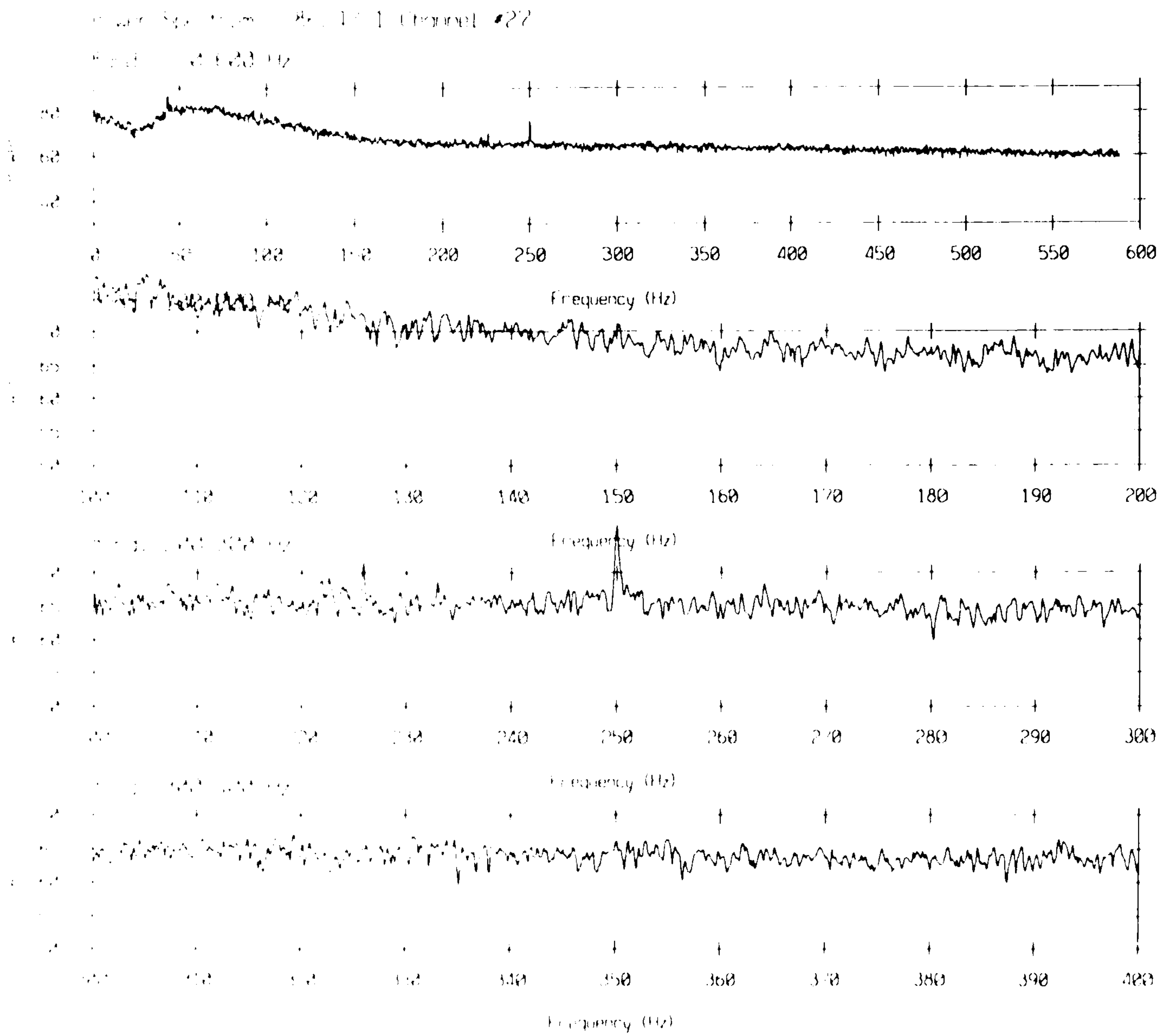
Channel #22
Frequency (Hz)
Frequency (Hz)
Frequency (Hz)
Frequency (Hz)

Figure 14

Array Response - 86247 Bin #4271
f = 25 Hz, KB window (alpha = 1.5)

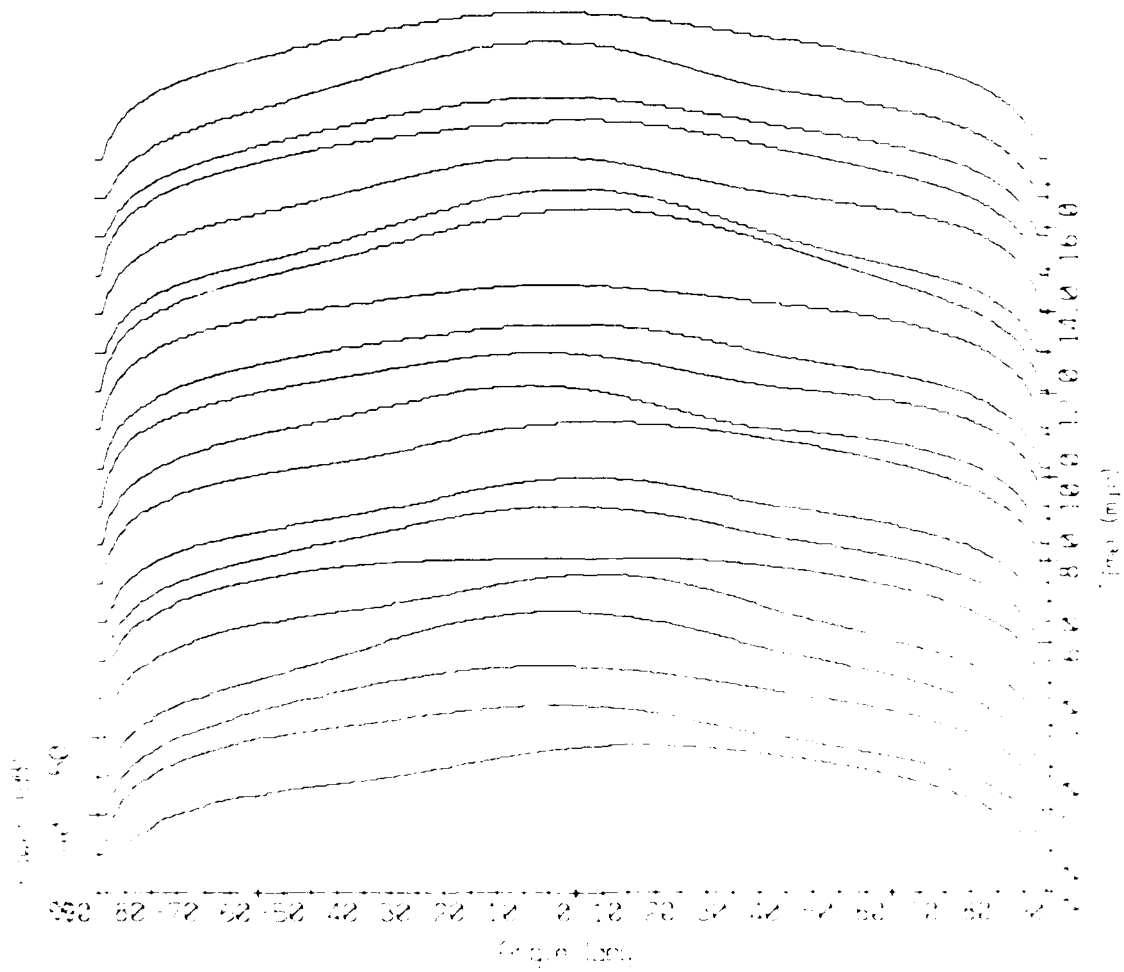

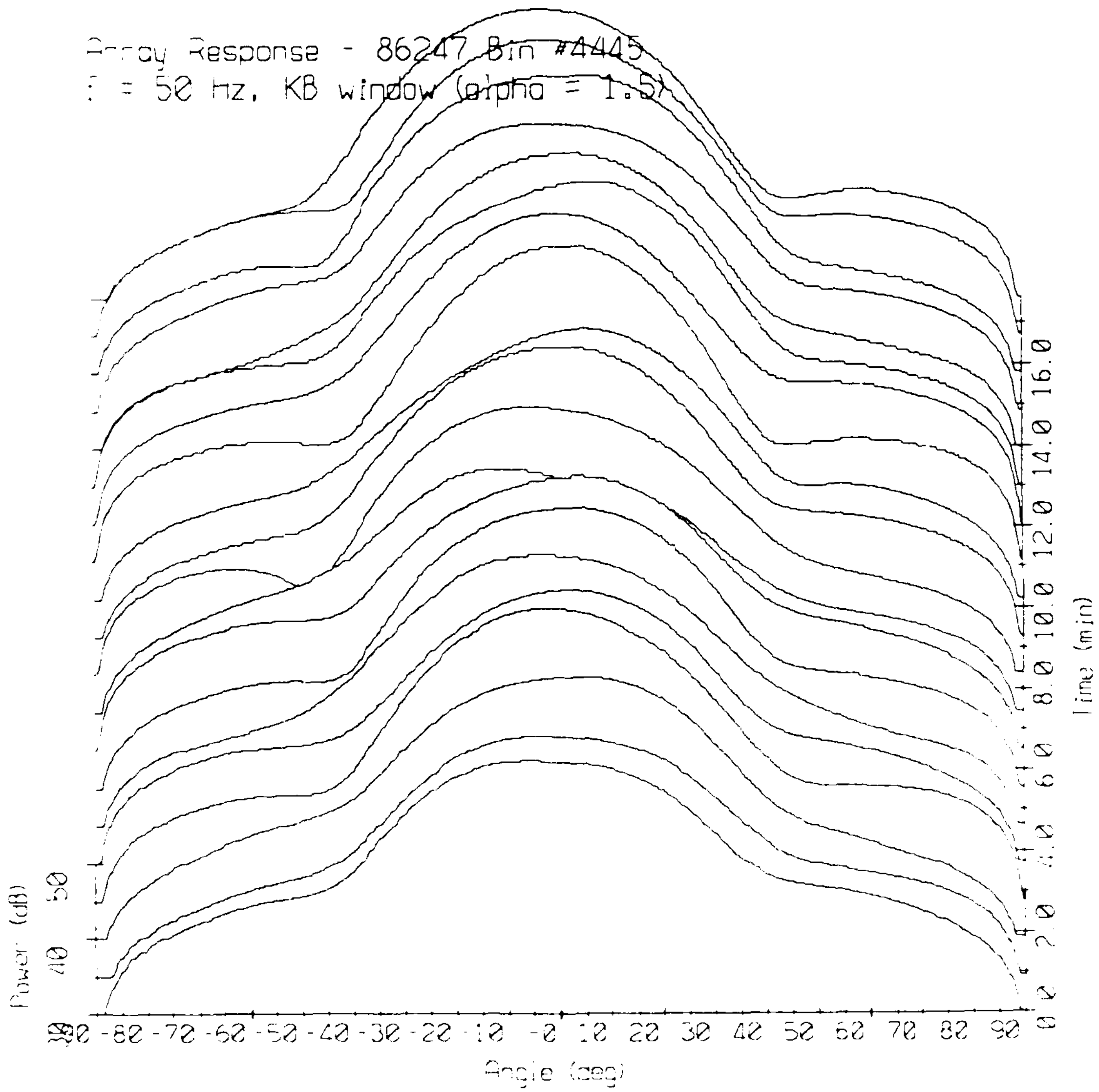
Array Response - 86247 Bin #4445
f = 50 Hz, KB window (alpha = 1.5)
Power (dB)
40 50
-90 -80 -70 -60 -50 -40 -30 -20 -10 -0 10 20 30 40 50 60 70 80 90
Angle (deg)
0 2.0 4.0 6.0 8.0 10.0 12.0 14.0 16.0
Time (min)

Figure 15(b).

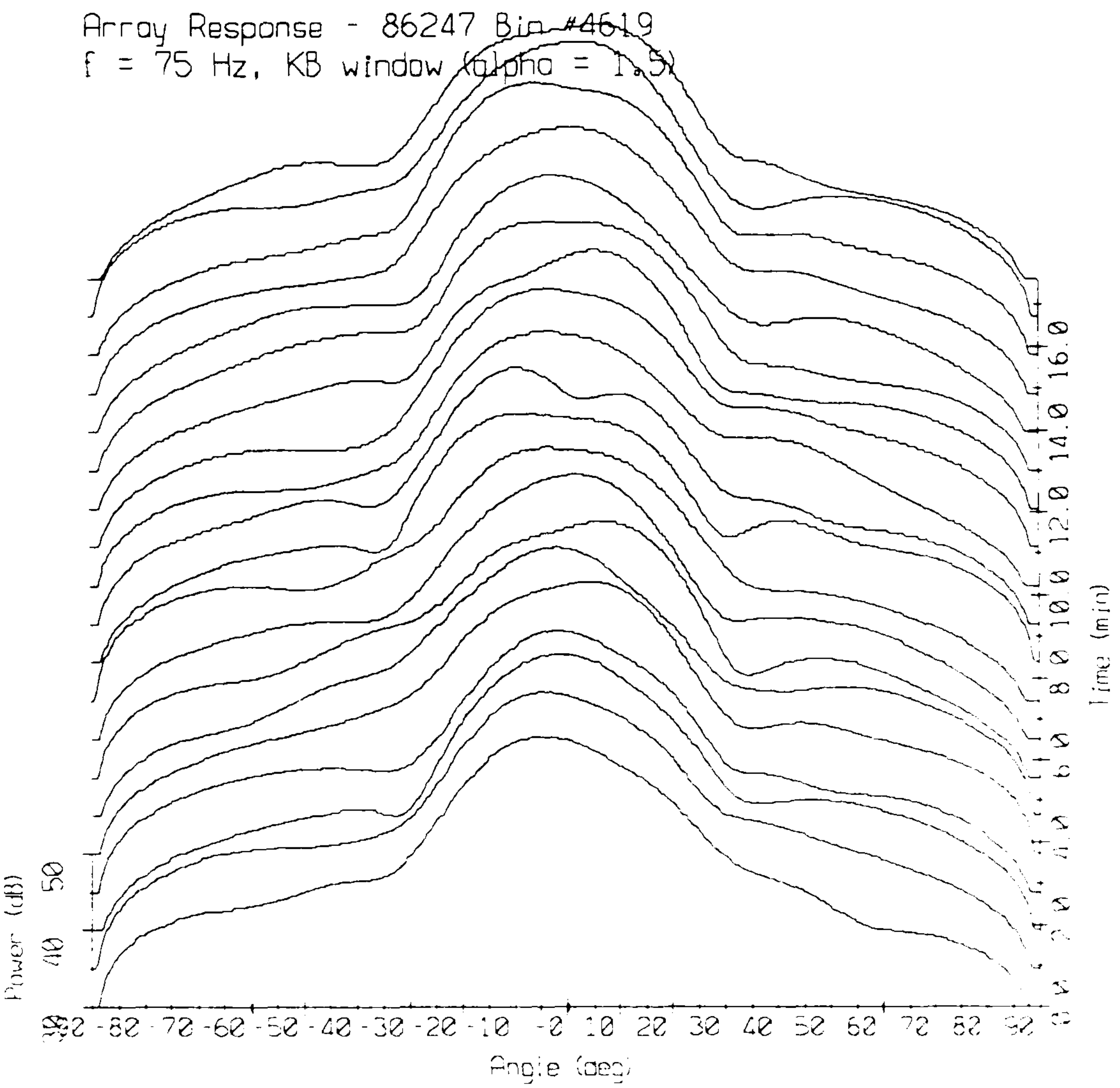
Array Response - 86247 Bin #4619
f = 75 Hz, KB window (alpha = 1.5)
Power (dB)
40
50
Time (min)
16.0
14.0
12.0
10.0
8.0
Angle (deg)
-82
-72
-62
-52
-42
-32
-22
-12
-2
10
20
30
40
50
60
70
80
90

Figure 15(c).

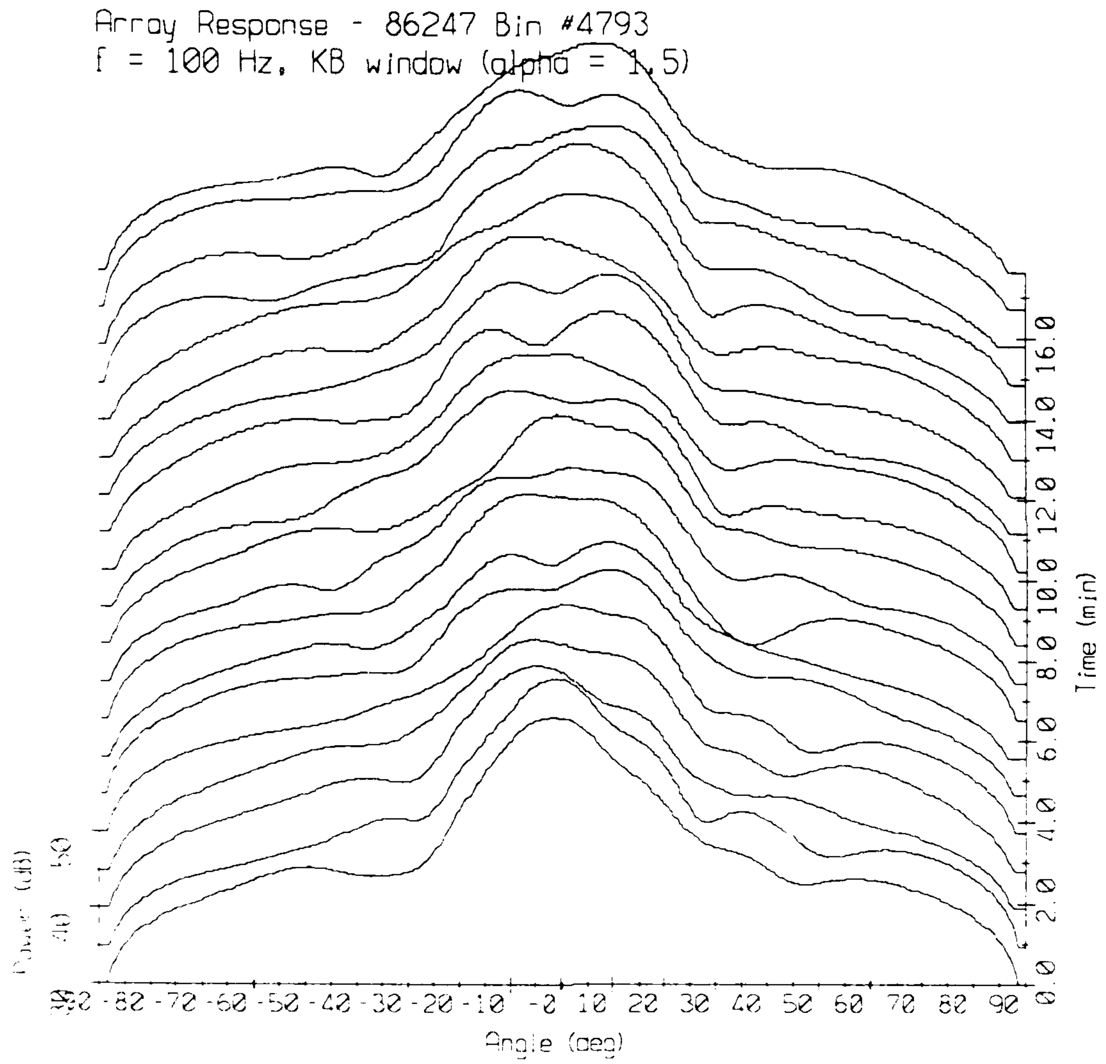

Array Response - 86247 Bin #4793
f = 100 Hz, KB window (alpha = 1.5)
Power (dB)
40
50
-92 -82 -72 -62 -52 -42 -32 -22 -12 -2 12 22 32 42 52 62 72 82 92
Angle (deg)
0 2.0 4.0 6.0 8.0 10.0 12.0 14.0 16.0
Time (min)

Figure 15(d).

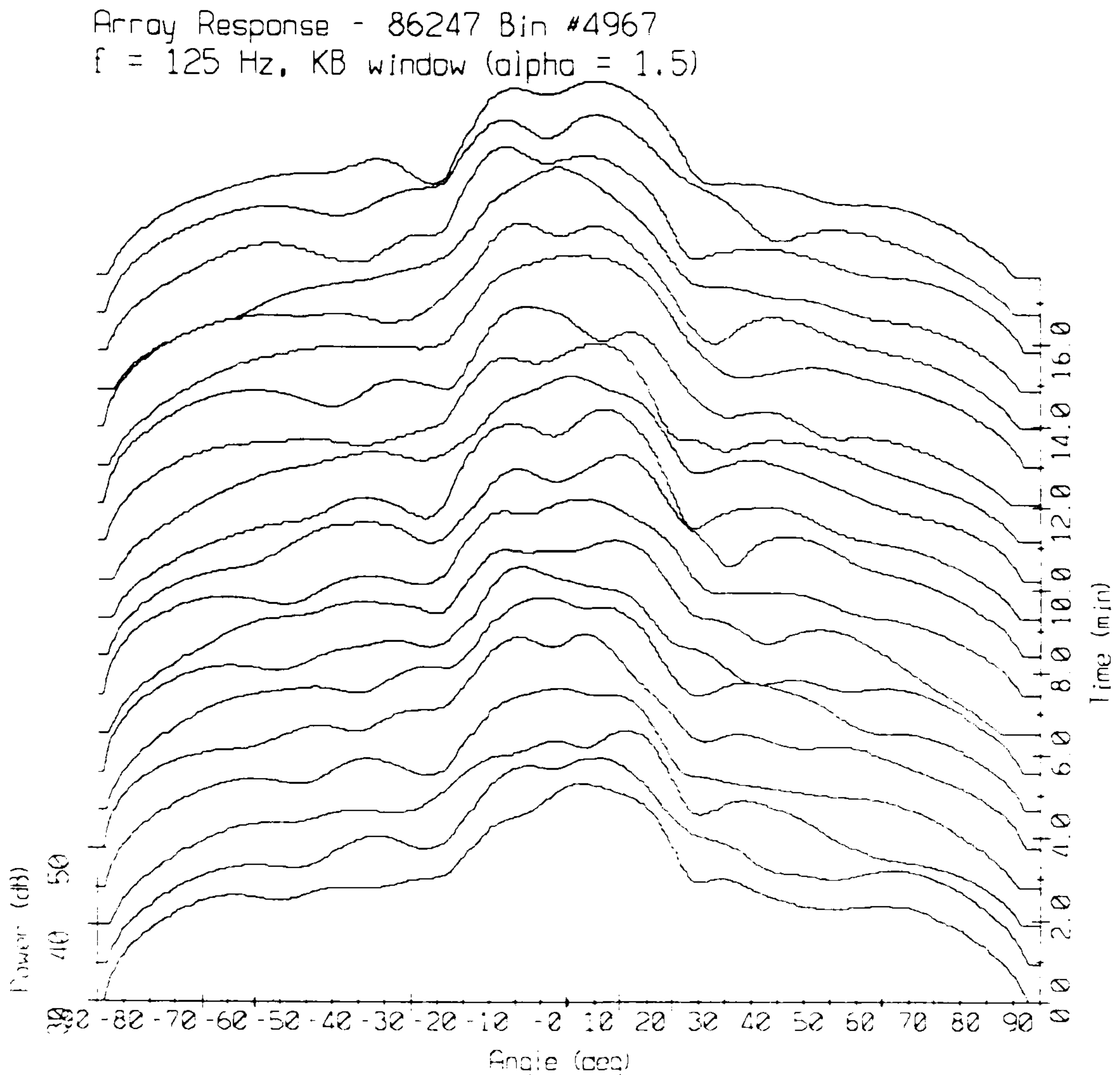
Array Response - 86247 Bin #4967
f = 125 Hz, KB window (alpha = 1.5)
Power (dB)
40
50
-82 -70 -60 -50 -40 -30 -20 -10 -0 10 20 30 40 50 60 70 80 90
Angle (deg)
0 2.0 4.0 6.0 8.0 10.0 12.0 14.0 16.0
Time (min)

Figure 15(e).

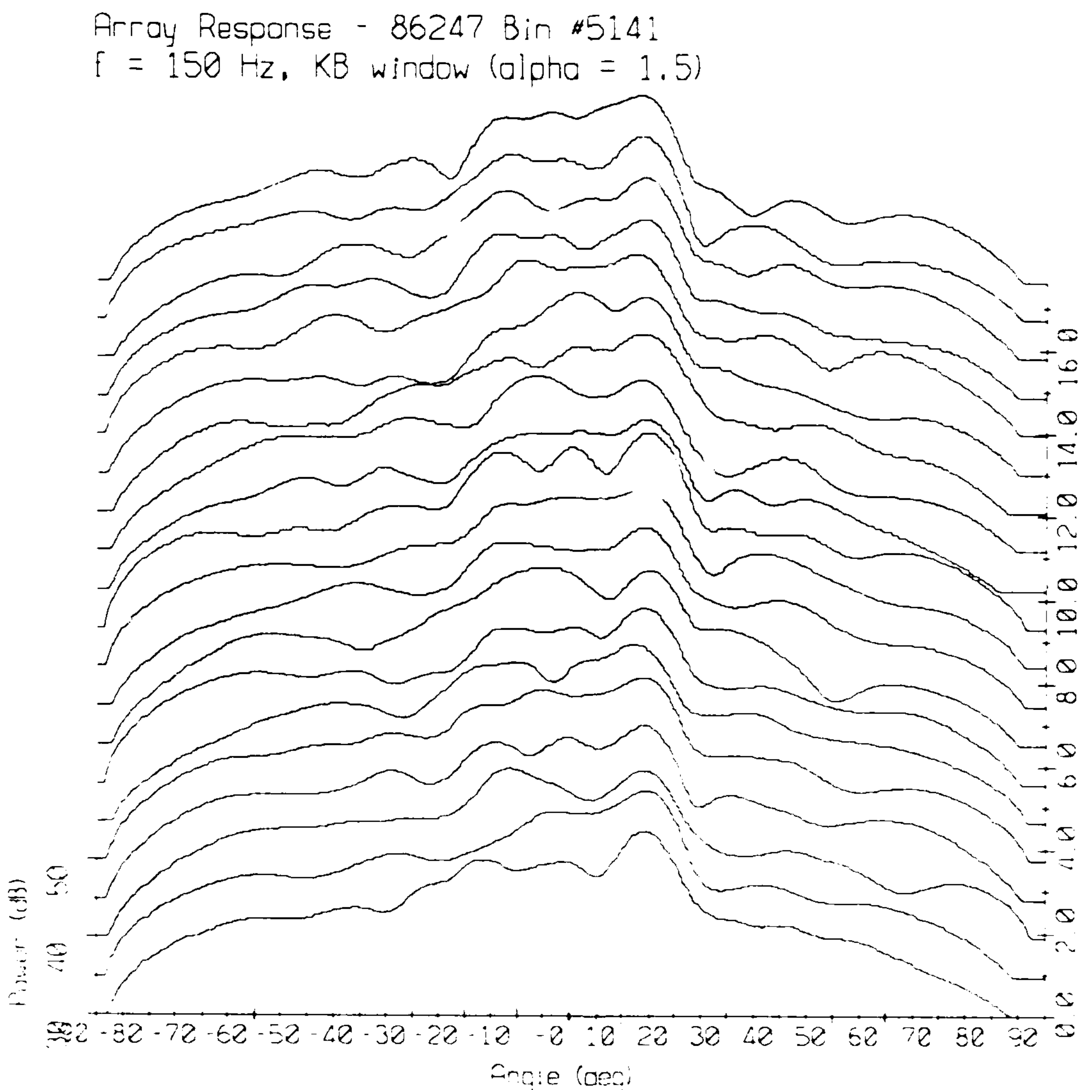

Array Response - 86247 Bin #5141
f = 150 Hz, KB window (alpha = 1.5)
Power (dB)
40
50
-82 -72 -62 -52 -42 -32 -22 -12 -2 12 22 32 42 52 62 72 82 92
Angle (deg)
0.0 2.0 4.0 6.0 8.0 10.0 12.0 14.0 16.0
Time (min)

Figure 15(f).

Array Response - 86247 Bin #5316
f = 175 Hz, KB window (alpha = 1.5)

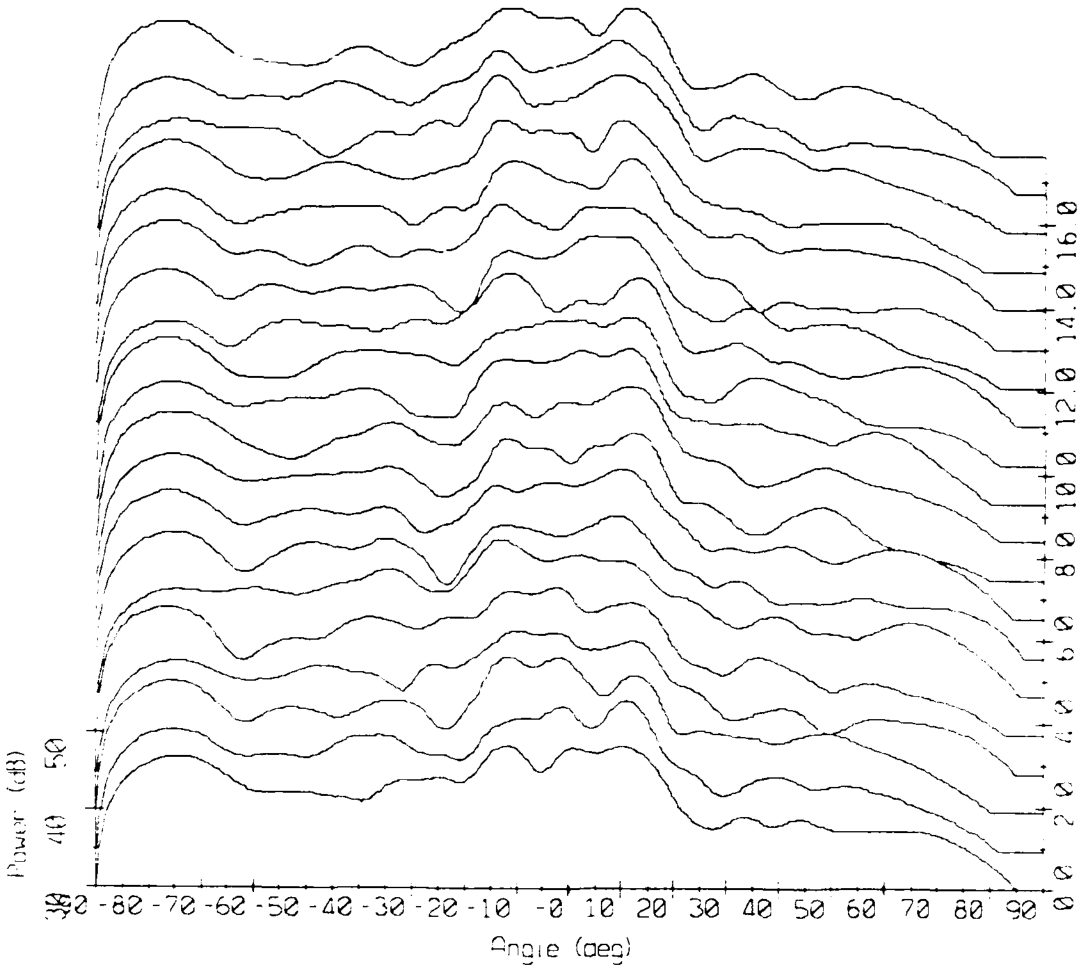

Figure 15(g).

Array Response - 86247 Bin #5490
f = 200 Hz, KB window (alpha = 1.5)

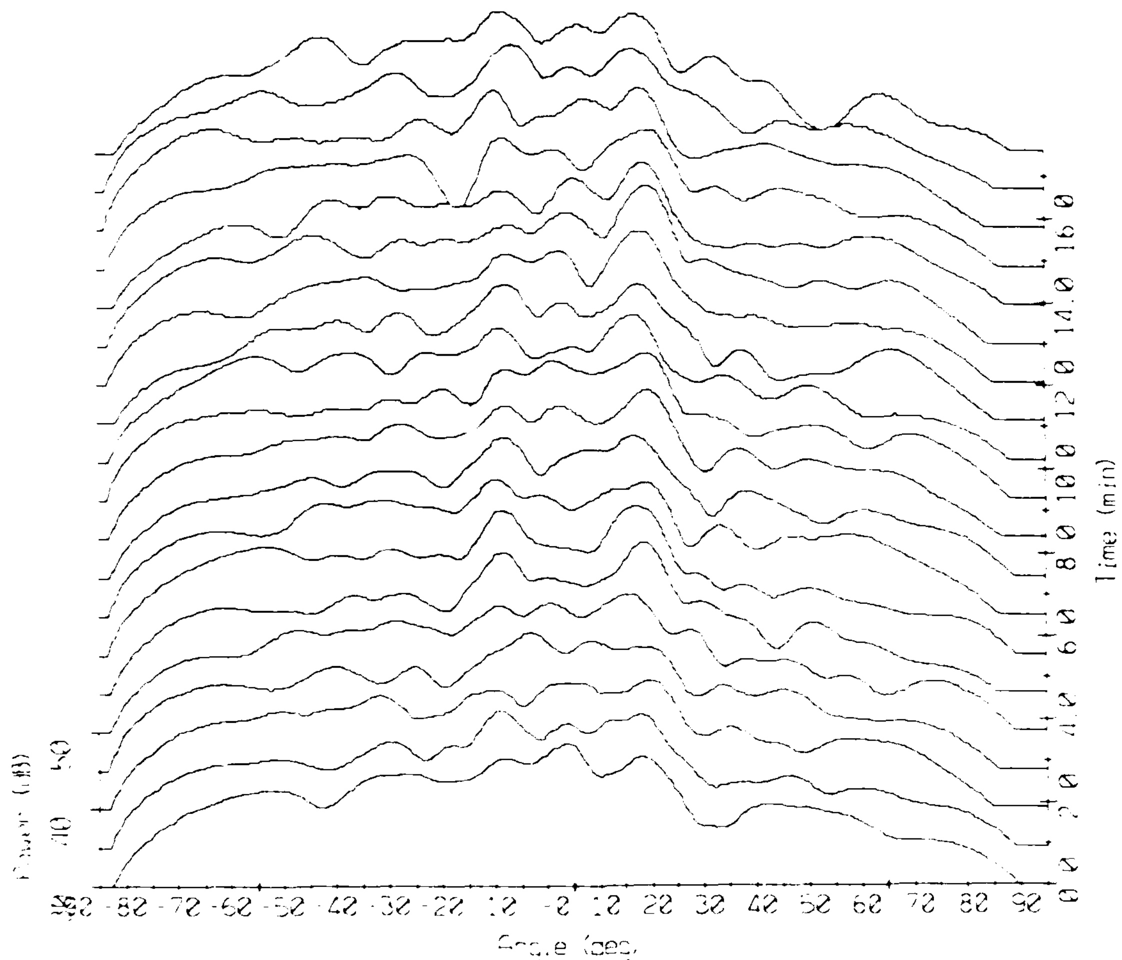

Figure 15(h).

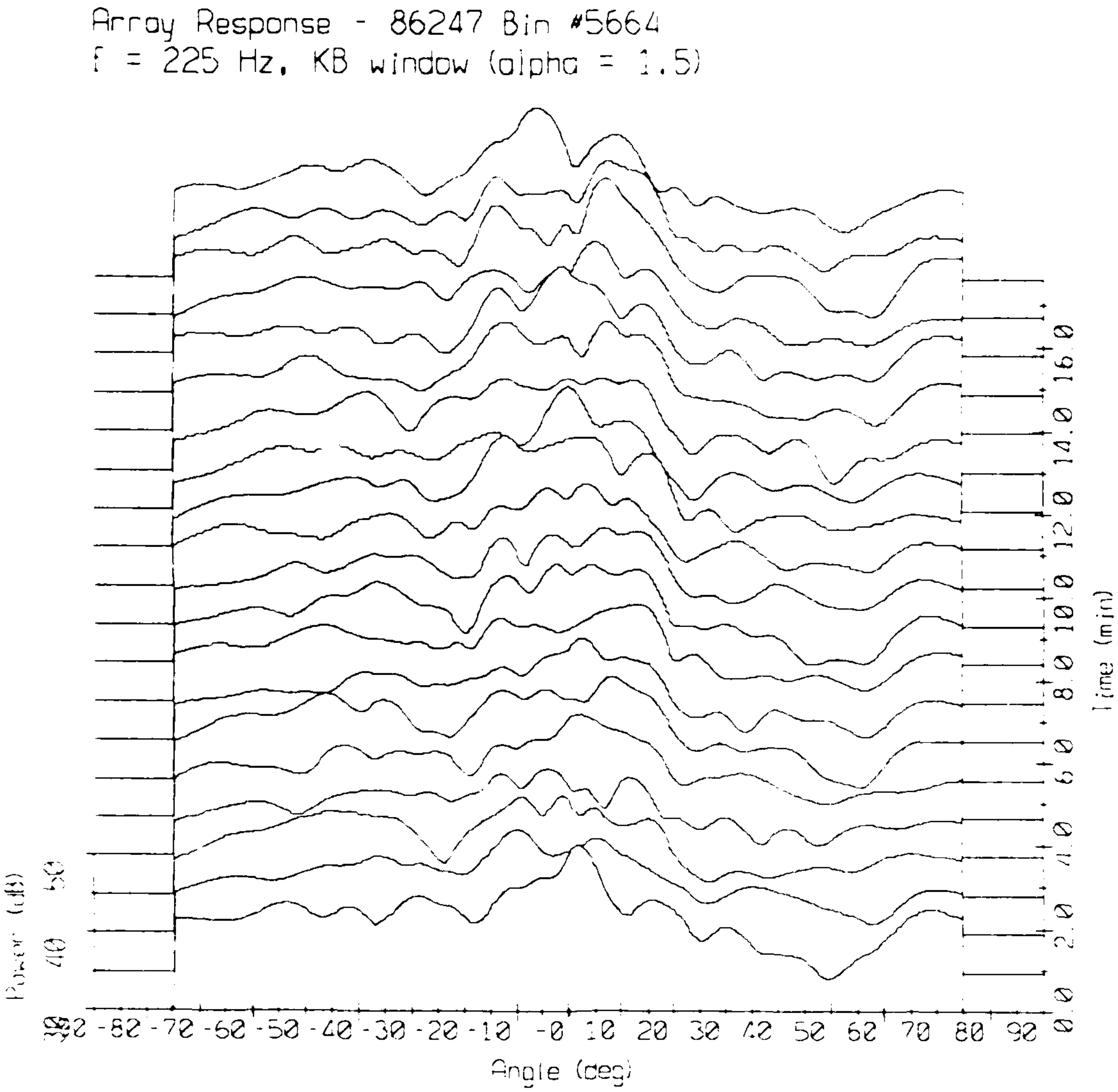
Array Response - 86247 Bin #5664
f = 225 Hz, KB window (alpha = 1.5)
Power (dB)
40
50
-82 -72 -62 -52 -42 -32 -22 -12 -0 12 22 32 42 52 62 72 82 92
Angle (deg)
0.0 2.0 4.0 6.0 8.0 10.0 12.0 14.0 16.0
Time (min)

Figure 15(i).

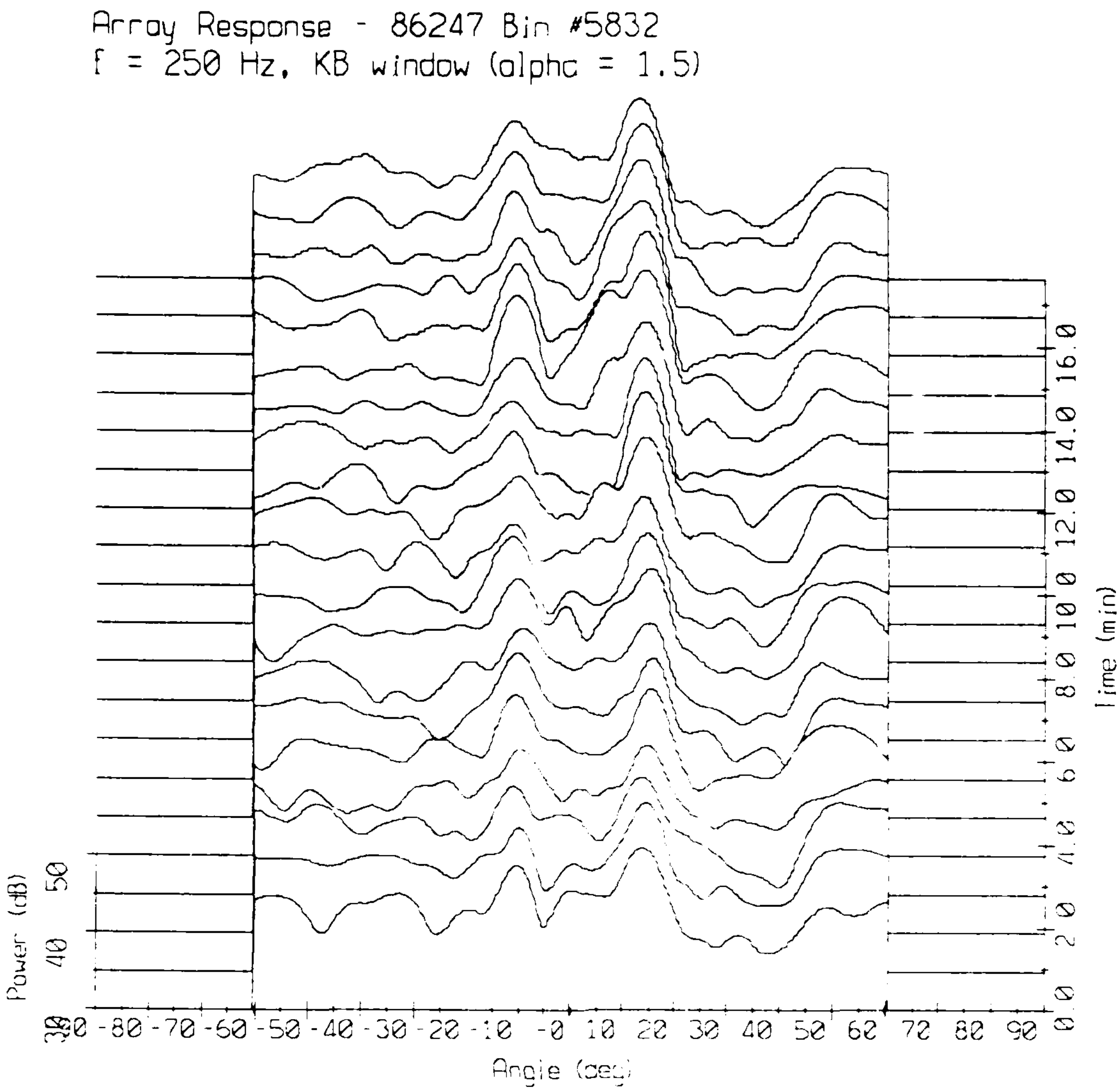
Array Response - 86247 Bin #5832
f = 250 Hz, KB window (alpha = 1.5)
Power (dB)
40
50
-80 -70 -60 -50 -40 -30 -20 -10 -0 10 20 30 40 50 60 70 80 90
Angle (deg)
0.0 2.0 4.0 6.0 8.0 10.0 12.0 14.0 16.0
Time (min)

Figure 15(j).

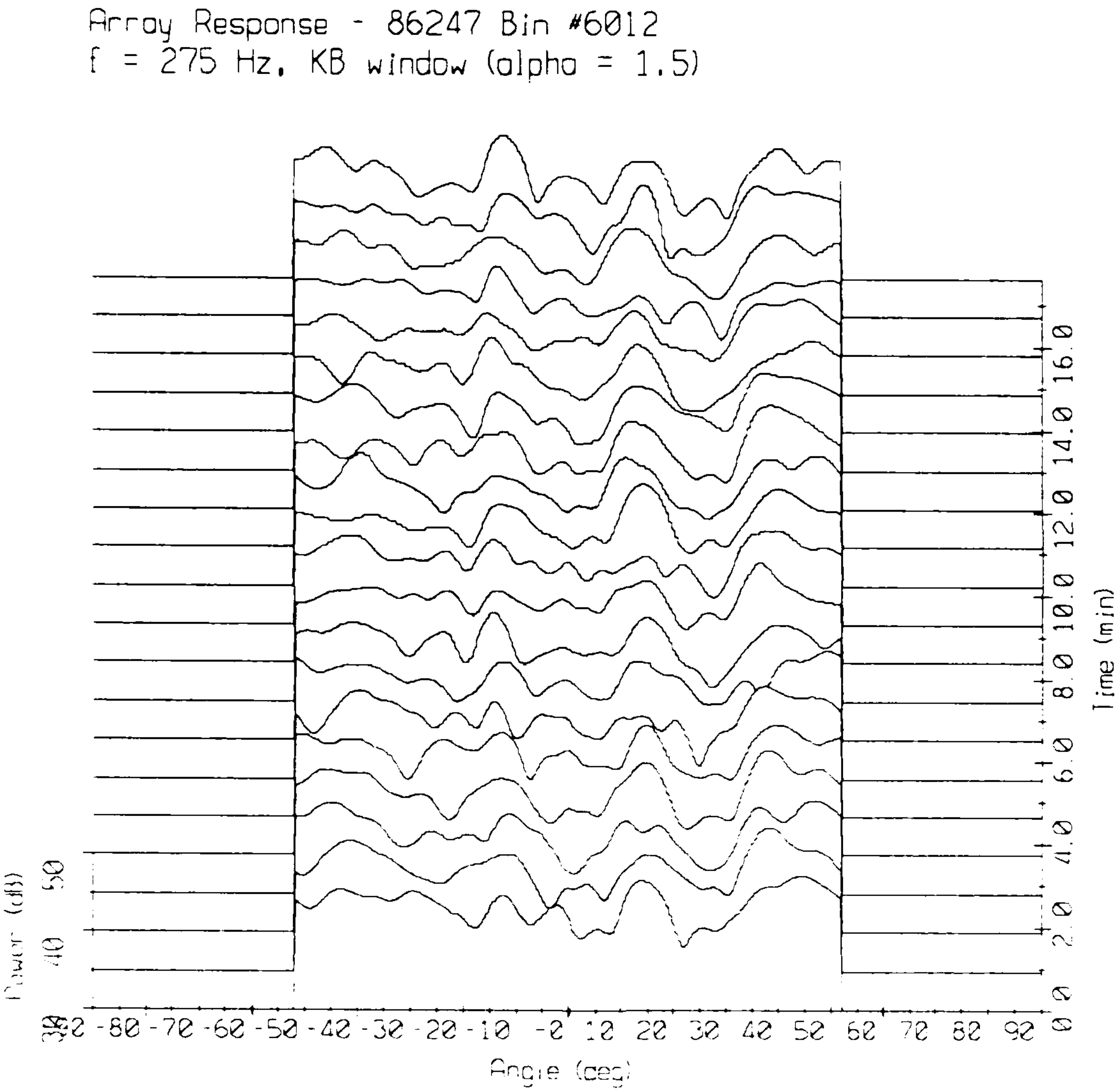

Array Response - 86247 Bin #6012
f = 275 Hz, KB window (alpha = 1.5)
Power (dB)
40
50
-80 -70 -60 -50 -40 -30 -20 -10 -0 10 20 30 40 50 60 70 80 90
Angle (deg)
0.0 2.0 4.0 6.0 8.0 10.0 12.0 14.0 16.0
Time (min)

Figure 15(k).

Array Response - 86247 Bin #6186
f = 300 Hz, KB window (alpha = 1.5)

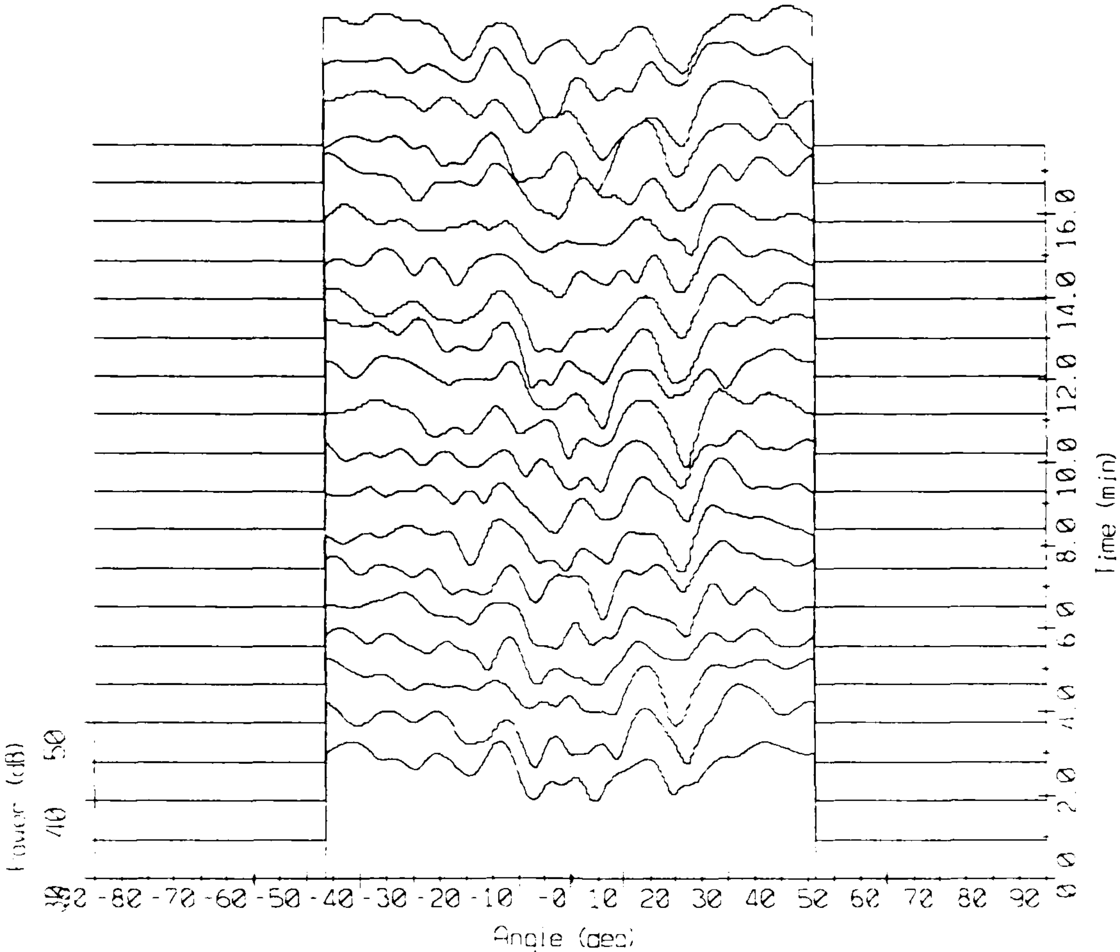

Figure 15(1).

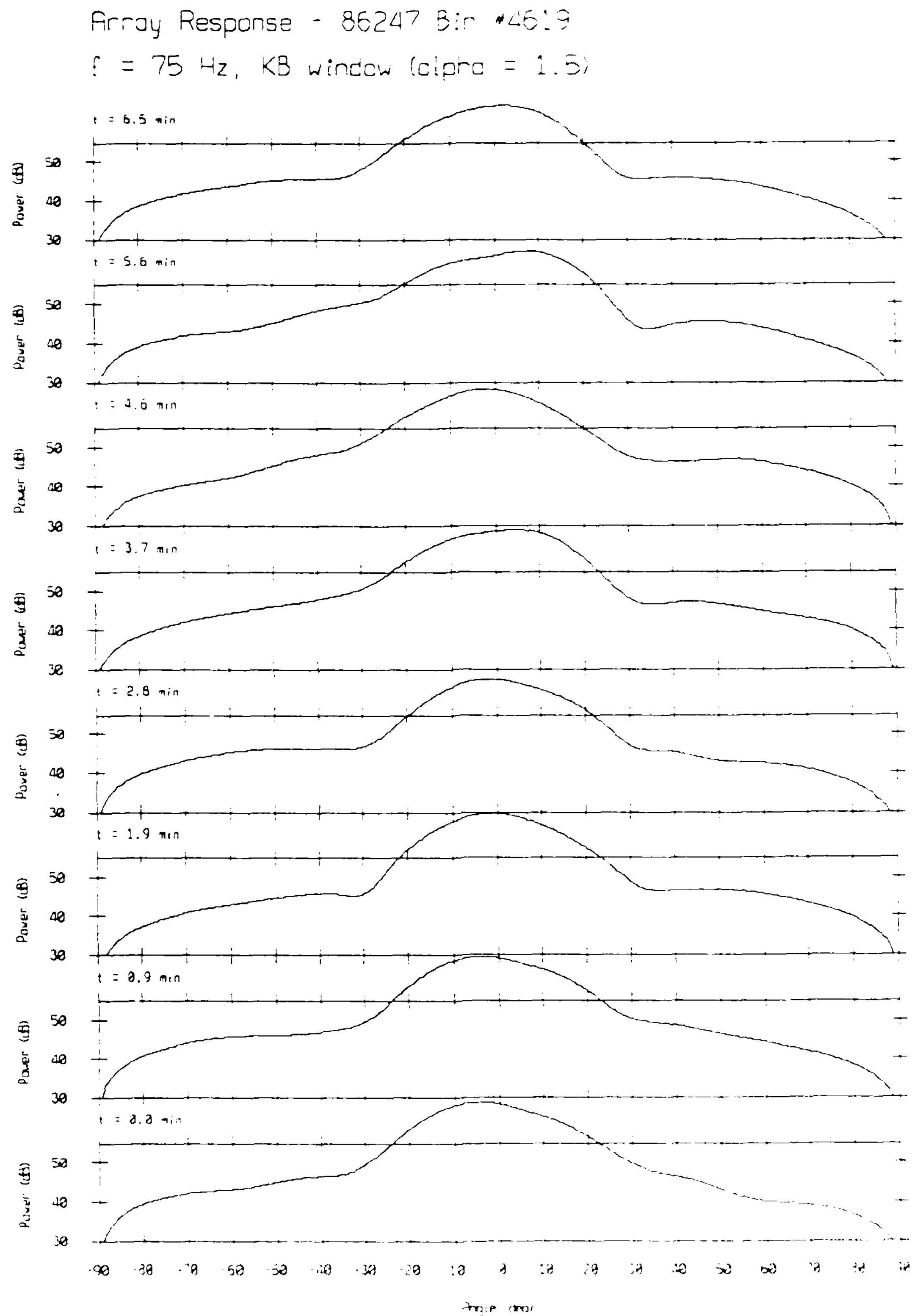
Array Response - 86247 Bin #4619
f = 75 Hz, KB window (alpha = 1.5)
t = 6.5 min
t = 5.6 min
t = 4.6 min
t = 3.7 min
t = 2.8 min
t = 1.9 min
t = 0.9 min
t = 0.0 min
Power (dB)
30
40
50
-90
-80
-70
-60
-50
-40
-30
-20
-10
0
10
20
30
40
50
60
70
80
90

Figure 16(a).

Array Response - 86247 Bin #4619

f = 75 Hz, KS window (alpha = 1.5)

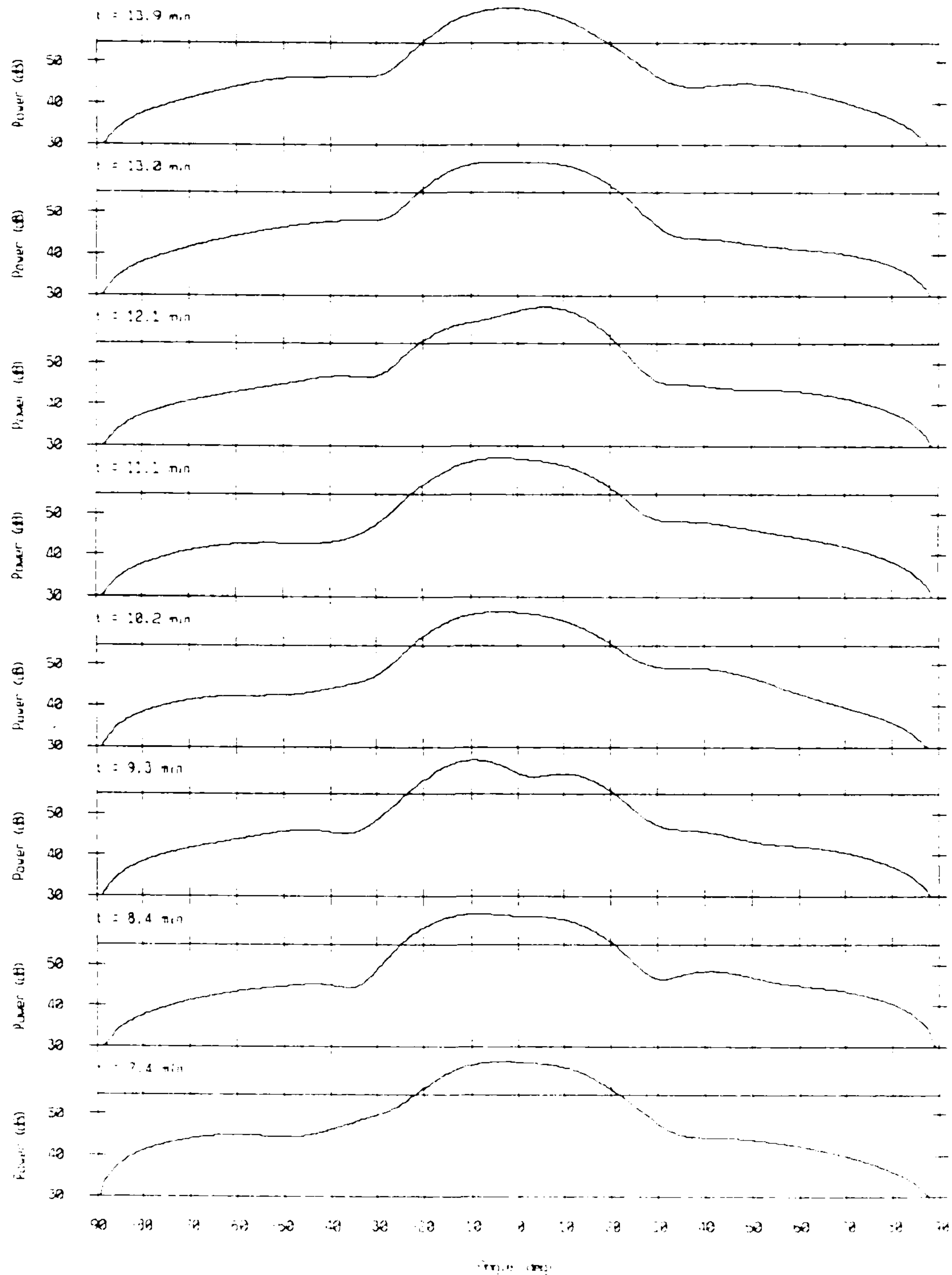

Array Response - 86247 Bin #4619

f = 75 Hz, KB window (alpha = 1.5)

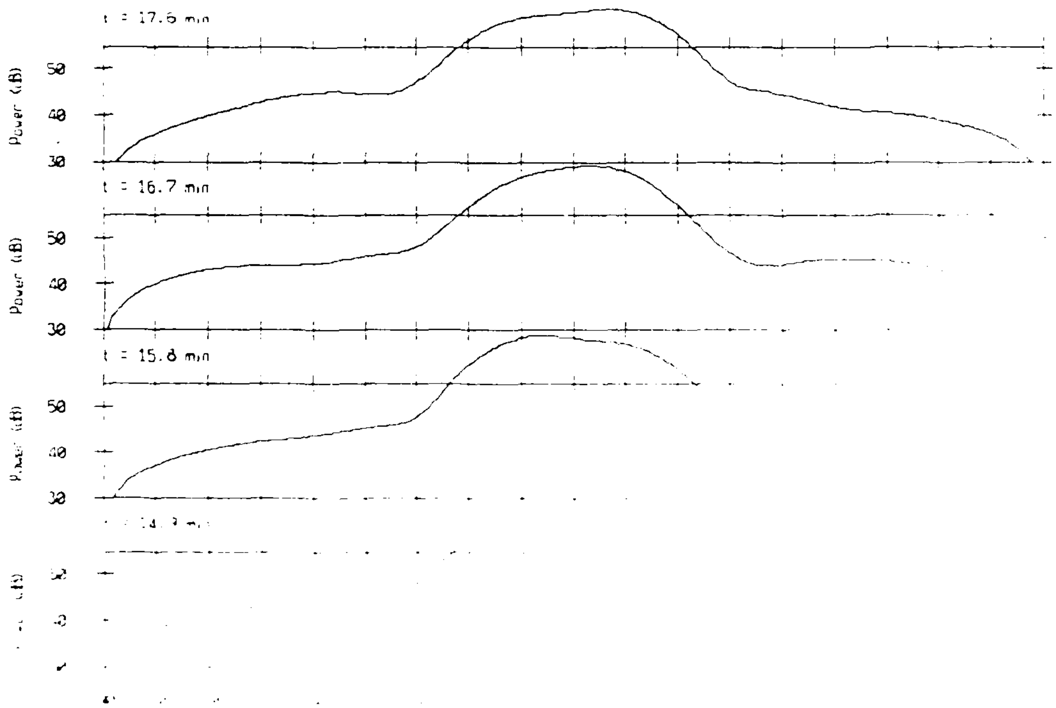

AD-A193 232 VERTICAL DIRECTIONALITY OF AMBIENT NOISE AT 32 DEG N AS 2/2
A FUNCTION OF LON.. (U) SCRIPPS INSTITUTION OF
OCEANOGRAPHY LA JOLLA CA MARINE PHYSIC..
UNCLASSIFIED W S HODGKISS ET AL. JAN 88 MPL-TM-387-A F/G 20/1 NL

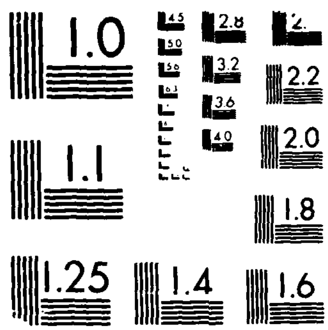

MICROCOPY RESOLUTION TEST CHART
IREAU STANDARDS 1963 A

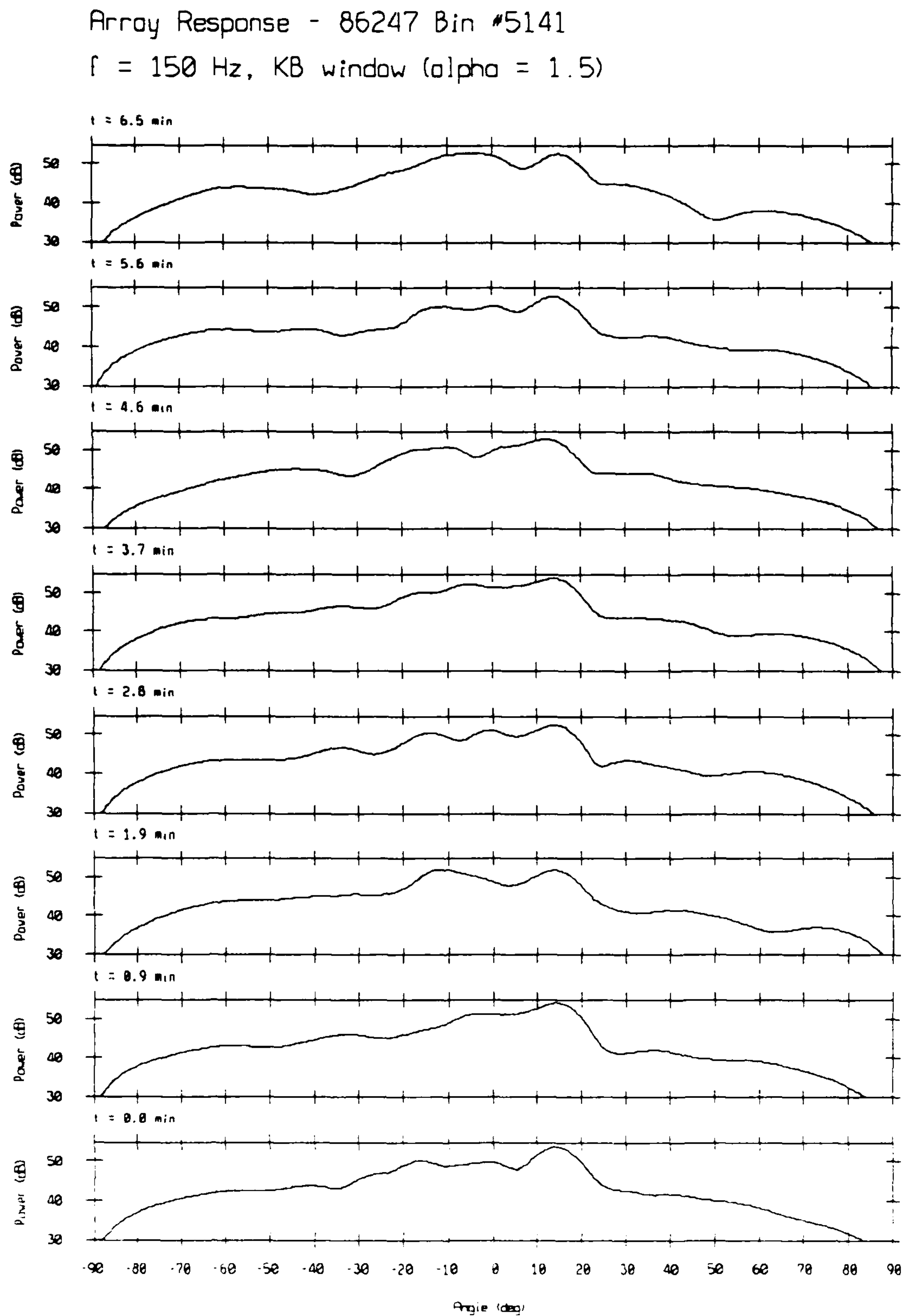
Array Response - 86247 Bin #5141
f = 150 Hz, KB window (alpha = 1.5)
t = 6.5 min
t = 5.6 min
t = 4.6 min
t = 3.7 min
t = 2.8 min
t = 1.9 min
t = 0.9 min
t = 0.0 min
Power (dB)
50
40
30
-90 -80 -70 -60 -50 -40 -30 -20 -10 0 10 20 30 40 50 60 70 80 90
Angle (deg)

Figure 16(b).

Array Response - 86247 Bin #5141

f = 150 Hz, KB window (alpha = 1.5)

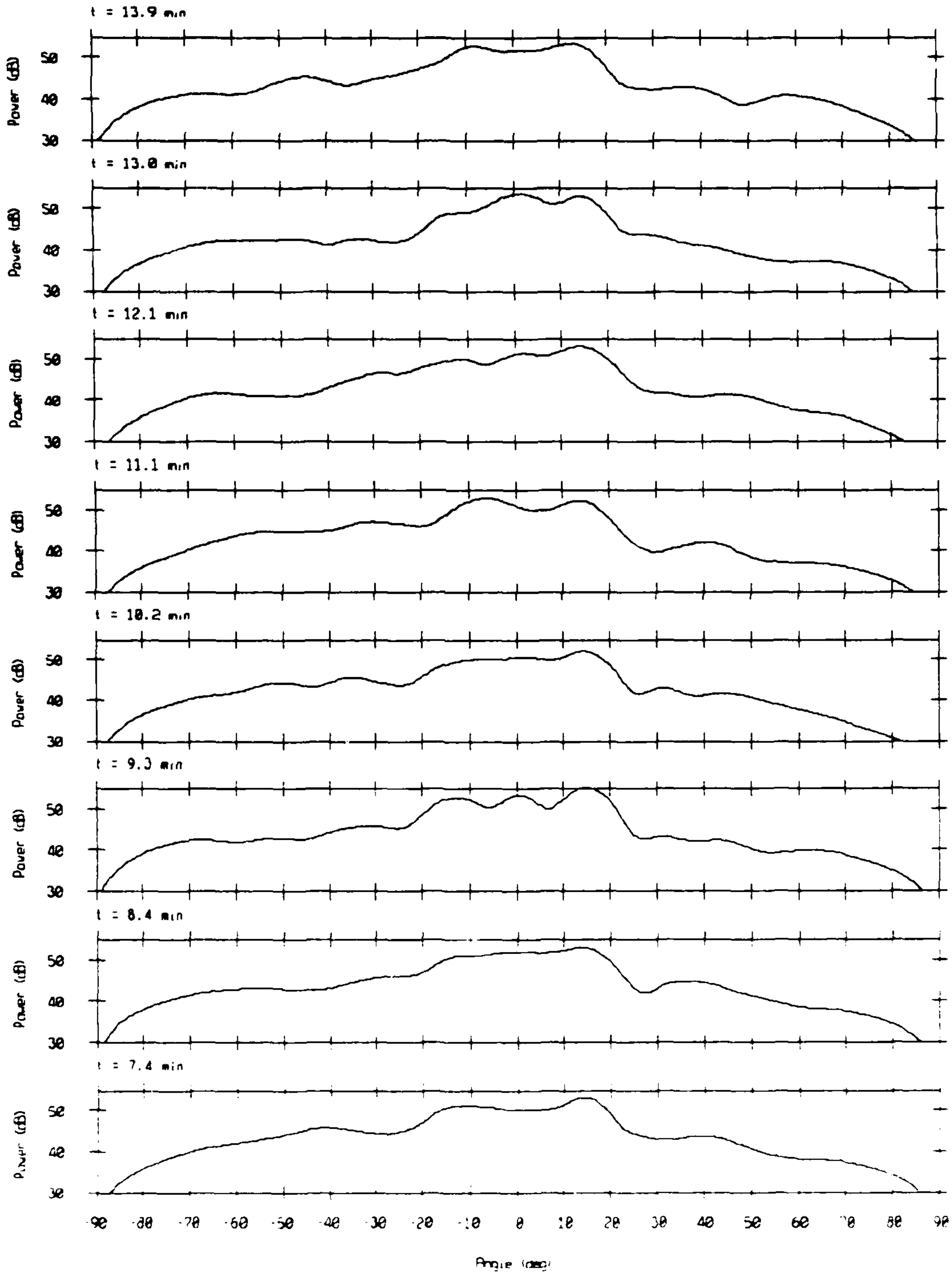

Array Response - 86247 Bin #5141

f = 150 Hz, KB window (alpha = 1.5)

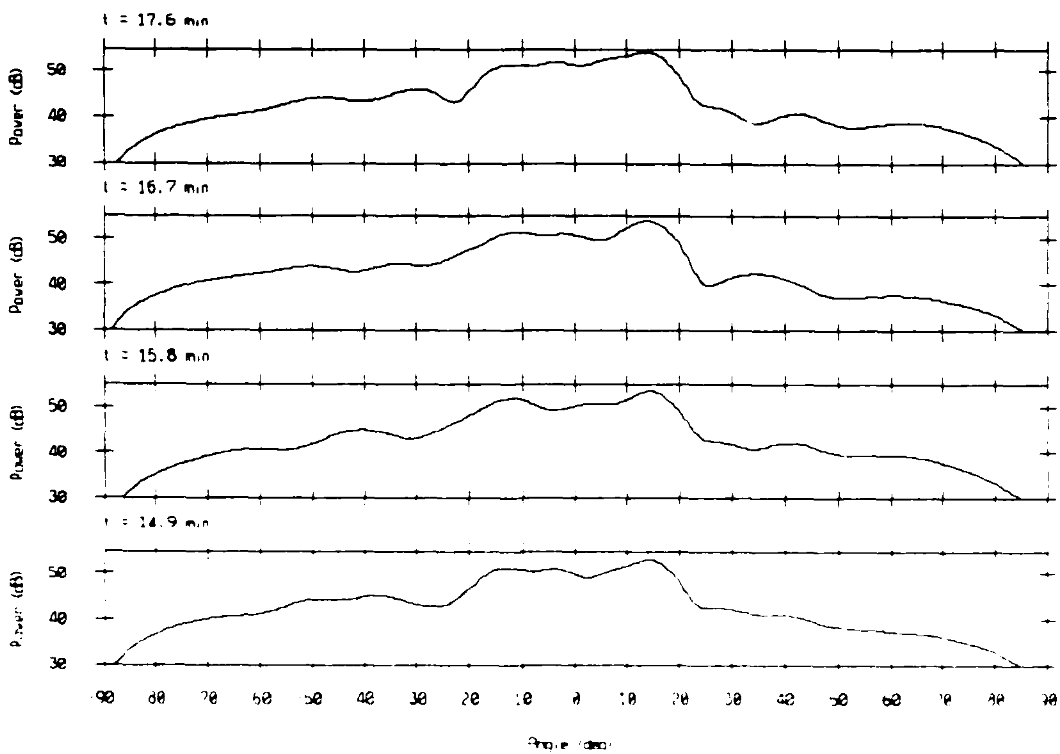

Array Response - 86247 Bin #6186

f = 300 Hz, KB window (alpha = 1.5)

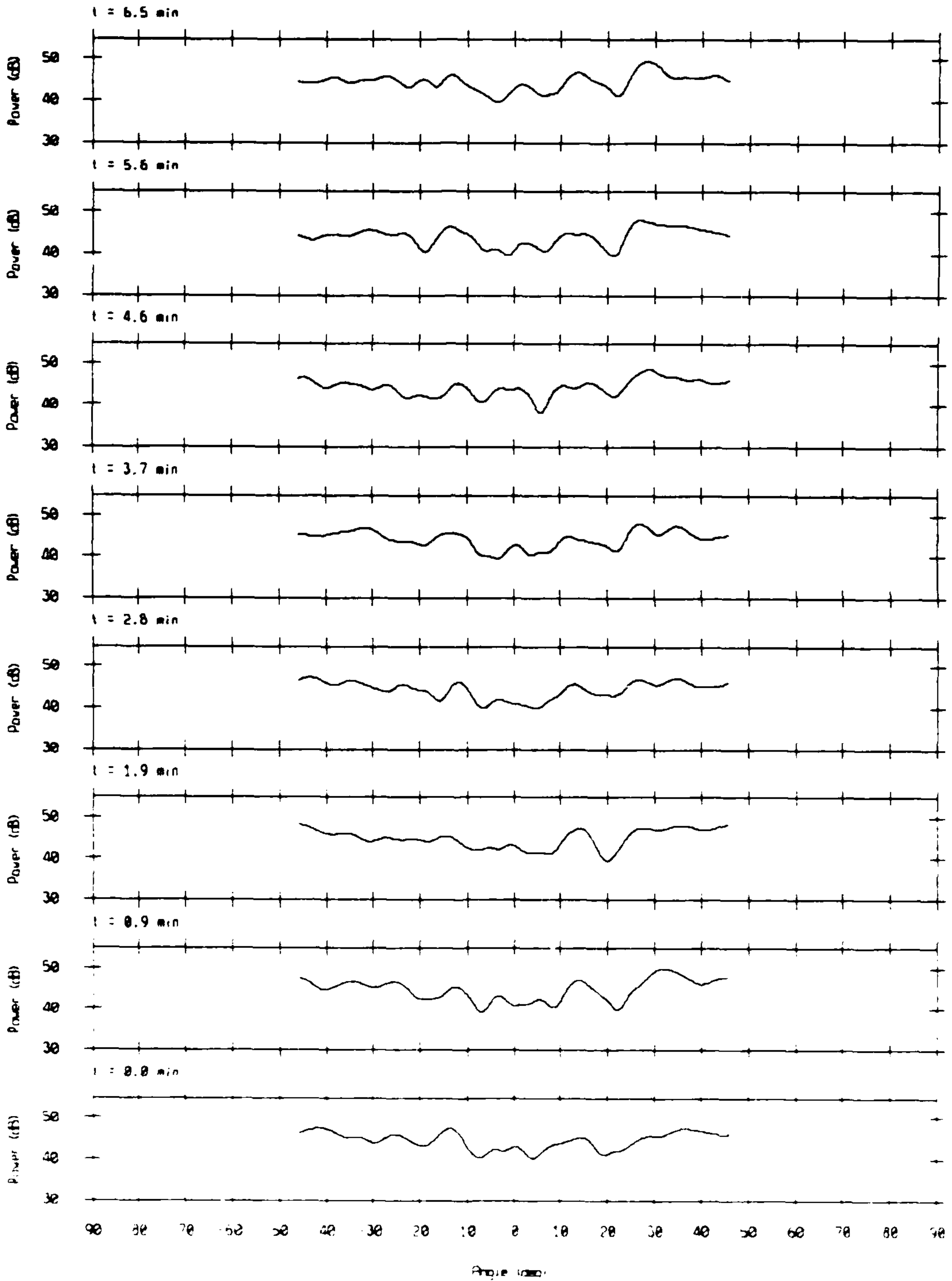

Figure 16(c).

Array Response - 86247 Bin #6186

f = 300 Hz, KB window (alpha = 1.5)

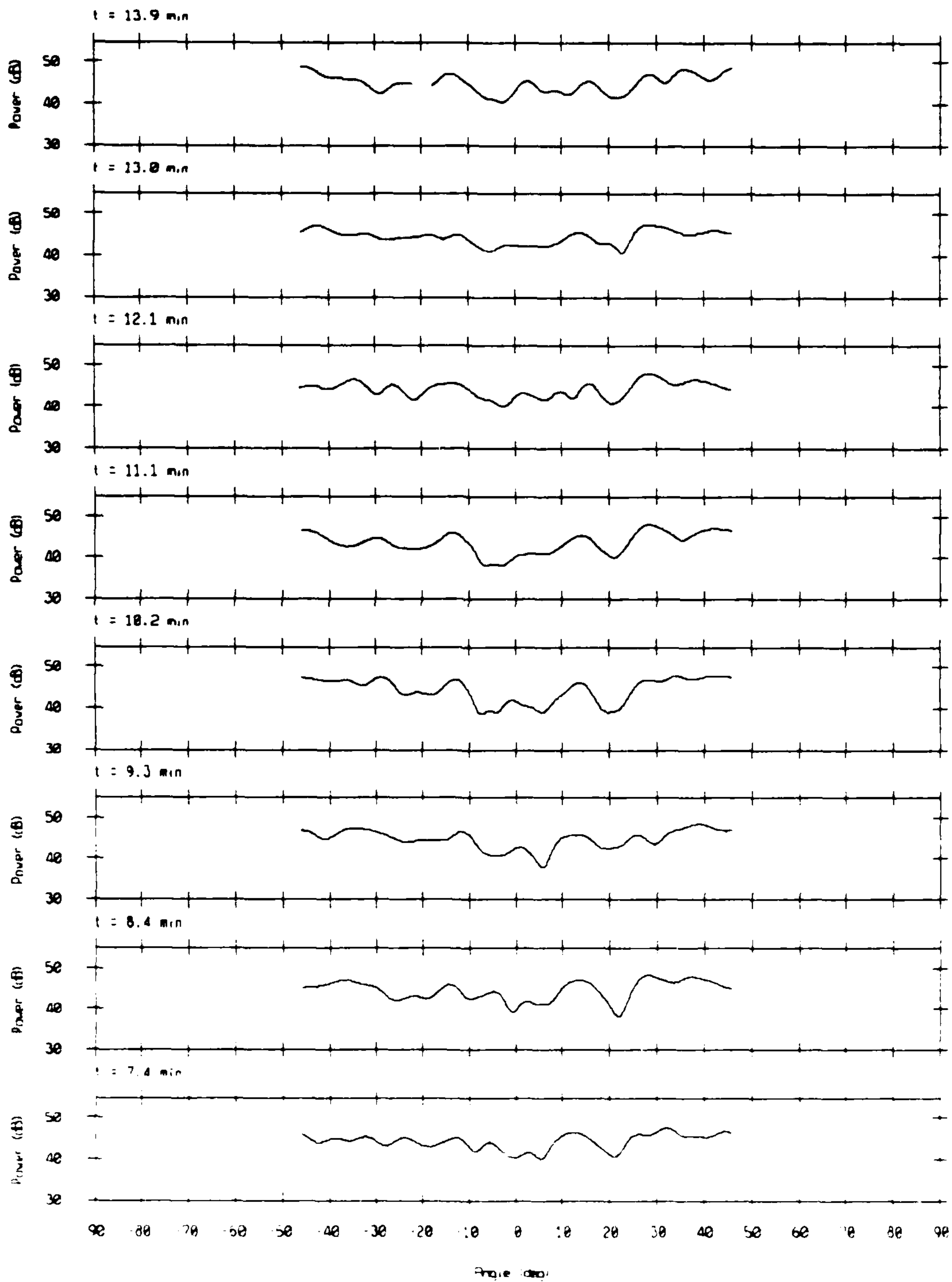

Array Response - 86247 Bin #6186

f = 300 Hz, KB window (alpha = 1.5)

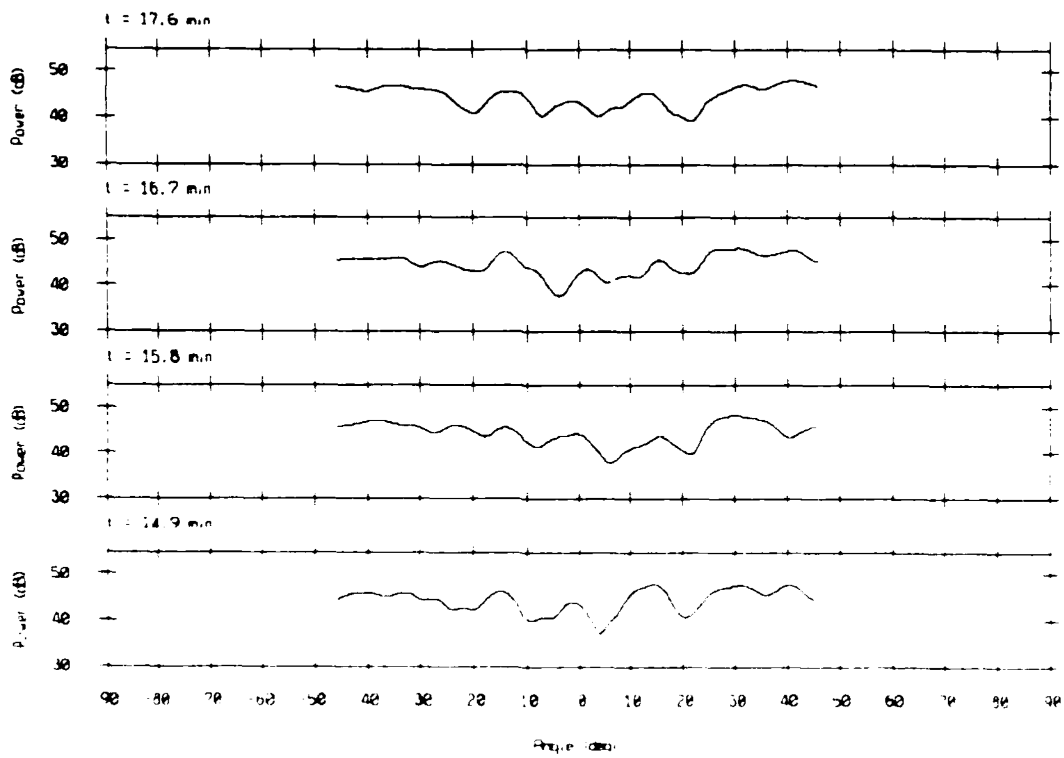

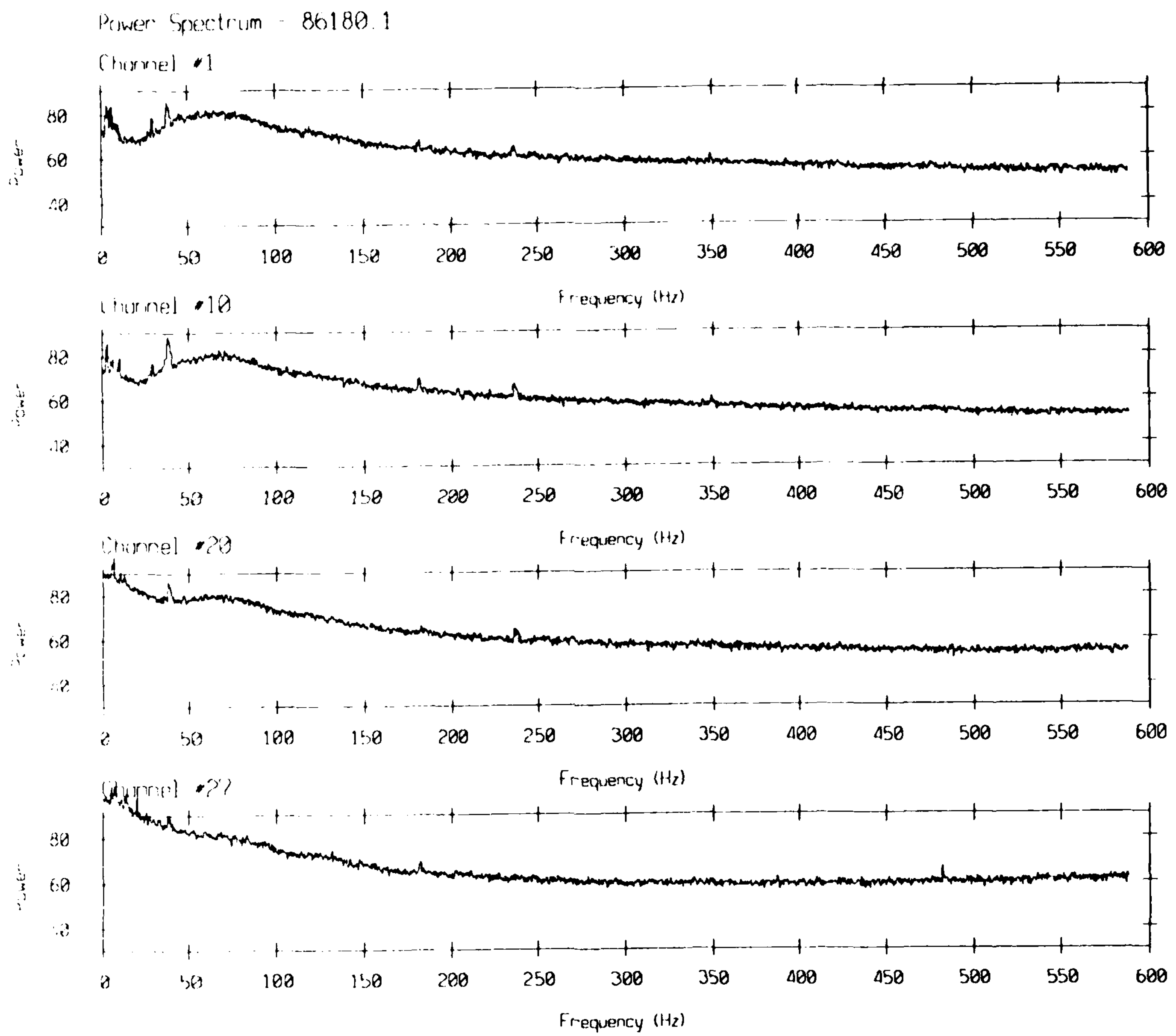
Power Spectrum - 86180.1
Channel #1
Channel #10
Channel #20
Channel #27
80
60
40
0
50
100
150
200
250
300
350
400
450
500
550
600
Frequency (Hz)

Figure 17.

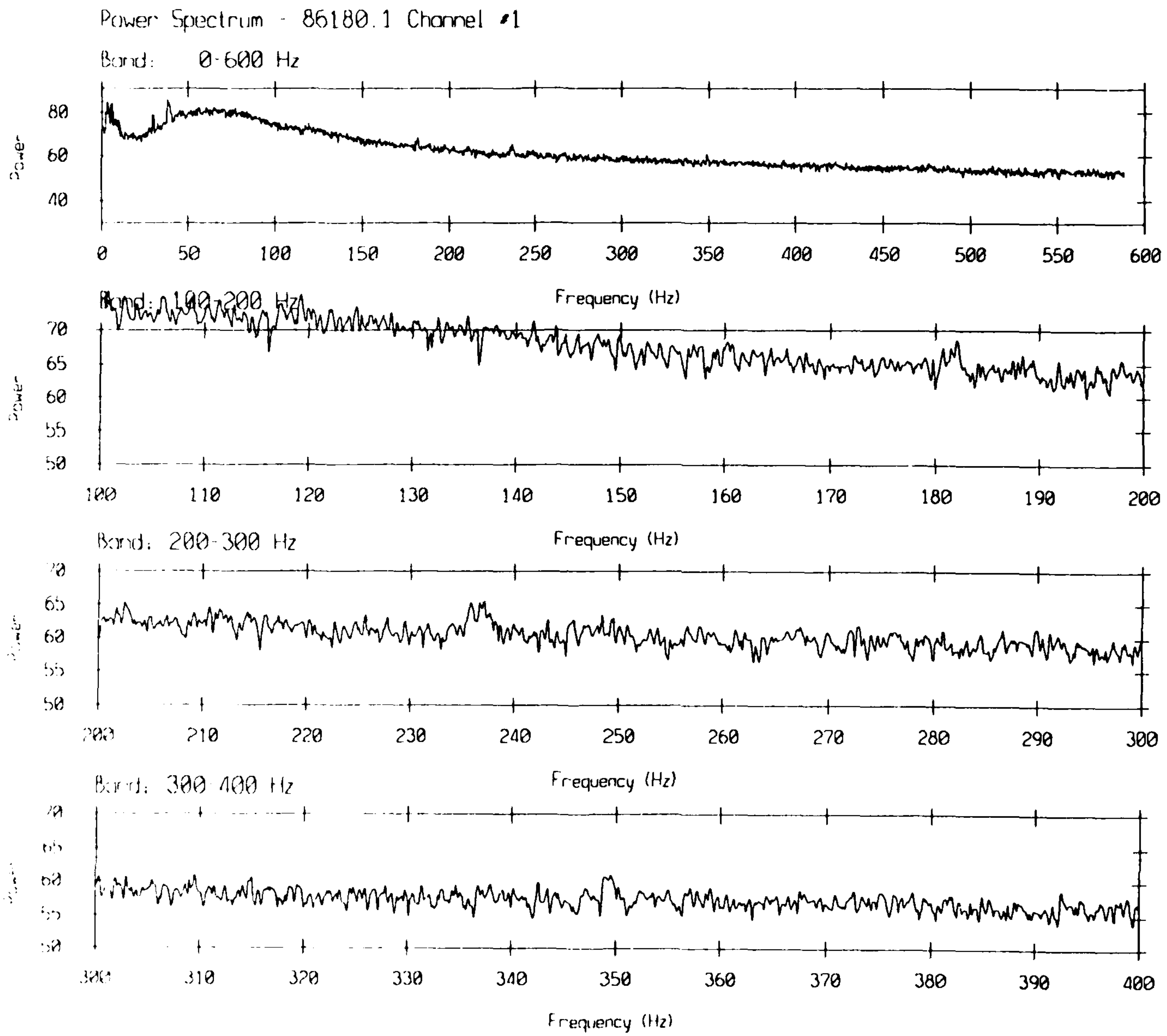
Power Spectrum - 86180.1 Channel #1
Band: 0-600 Hz
Band: 100-200 Hz
Band: 200-300 Hz
Band: 300 400 Hz
Power
Frequency (Hz)

Figure 18(a).

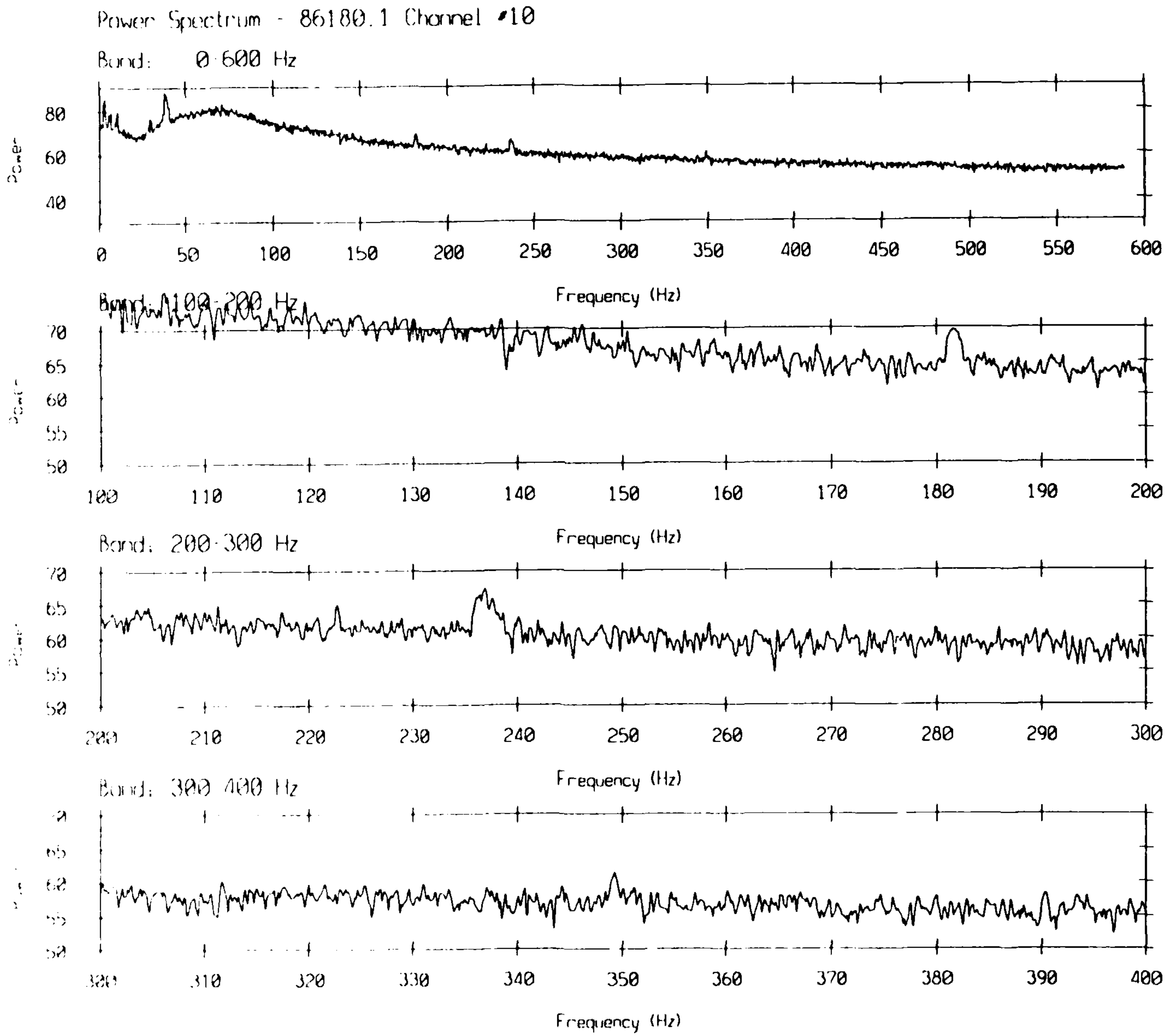
Power Spectrum - 86180.1 Channel #10
Band: 0-600 Hz
Band: 100-200 Hz
Band: 200-300 Hz
Band: 300-400 Hz
Frequency (Hz)
Power

Figure 18(b).

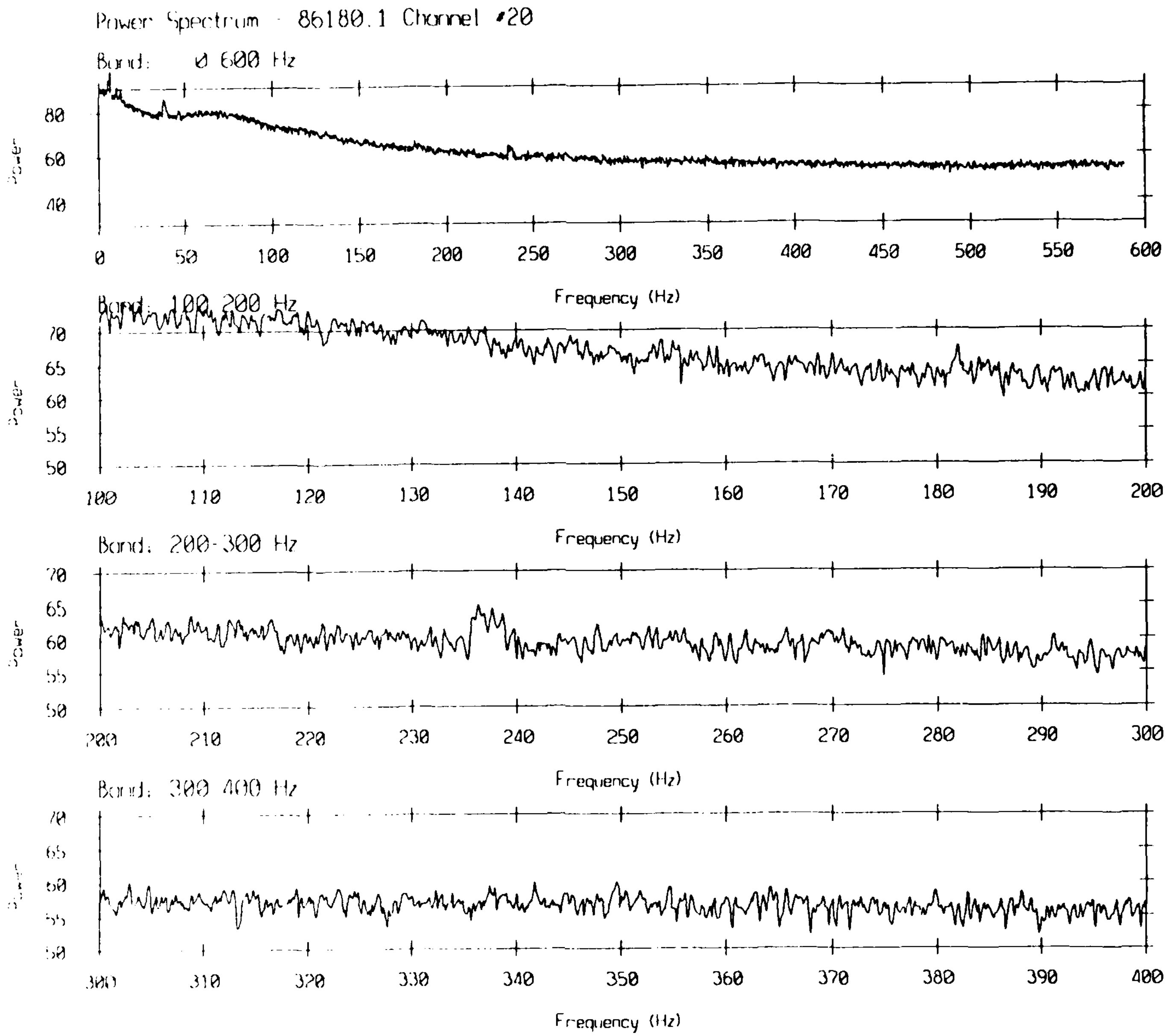

Power Spectrum - 86180.1 Channel #20
Band: 0 600 Hz
Band: 100 200 Hz
Band: 200-300 Hz
Band: 300 400 Hz
Power
Frequency (Hz)

Figure 18(c).

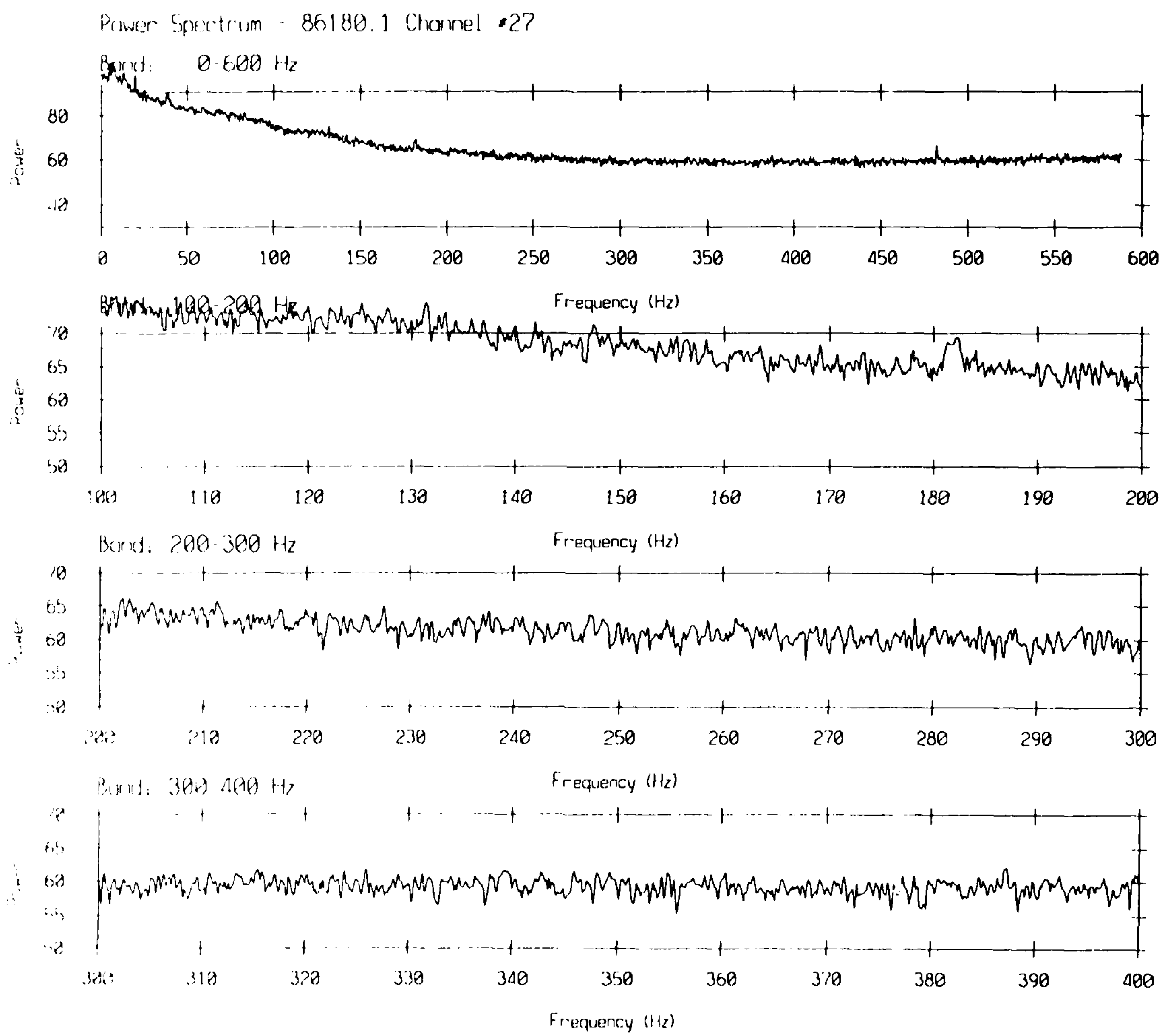

Power Spectrum - 86180.1 Channel #27
Band: 0-600 Hz
Power
80
60
40
0
50
100
150
200
250
300
350
400
450
500
550
600
Frequency (Hz)
Band: 100-200 Hz
Power
70
65
60
55
50
100
110
120
130
140
150
160
170
180
190
200
Frequency (Hz)
Band: 200-300 Hz
70
65
60
210
220
230
240
250
260
270
280
290
300
Frequency (Hz)
Band: 300-400 Hz
65
60
310
320
330
340
350
360
370
380
390
400
Frequency (Hz)

Figure 18(d).

Array Response - 86180 Bin #4271
f = 25 Hz, KB window (alpha = 1.5)

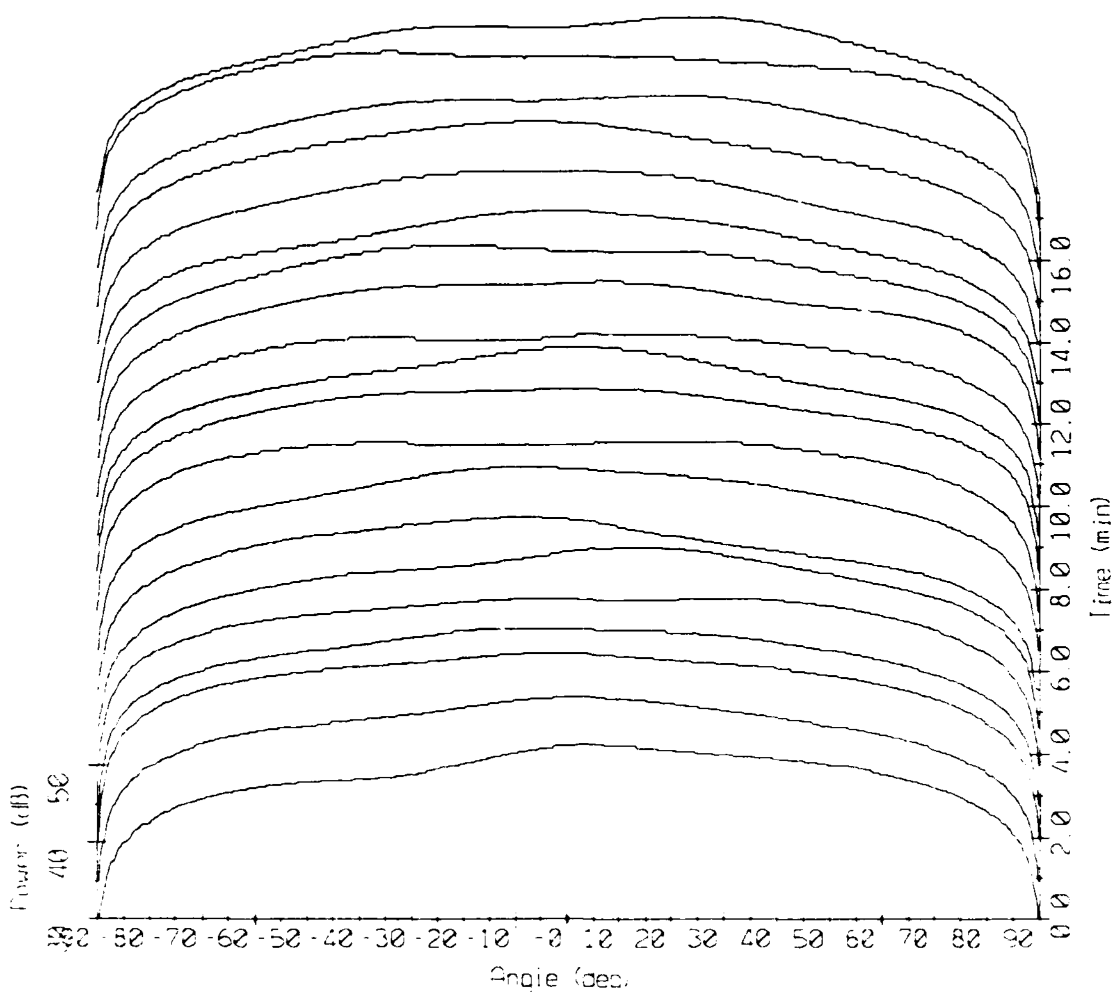

Figure 13(a).

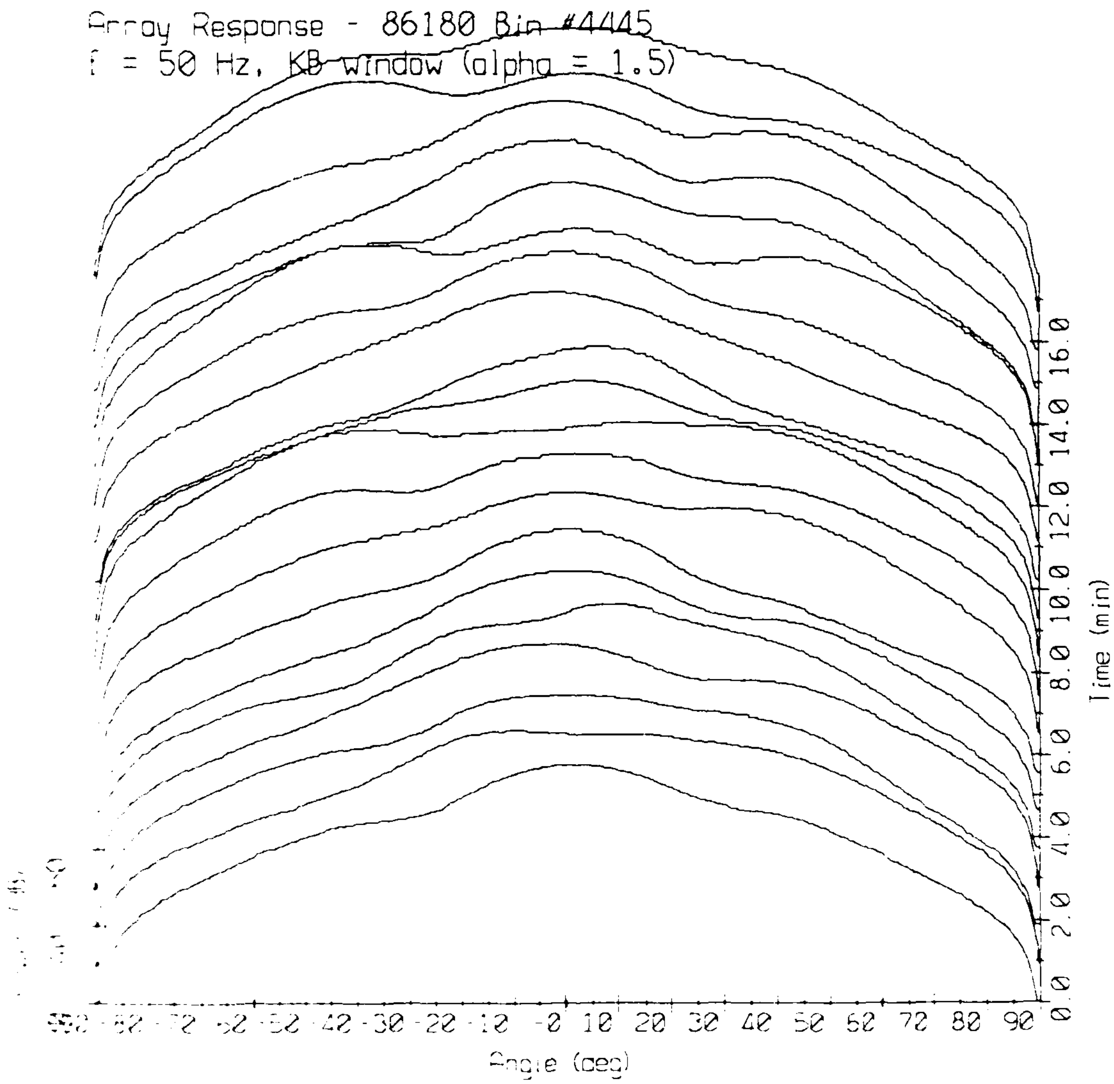

Array Response - 86180 Bin #4445
f = 50 Hz, KB window (alpha = 1.5)
Time (min)
Angle (deg)

Figure 19(b).

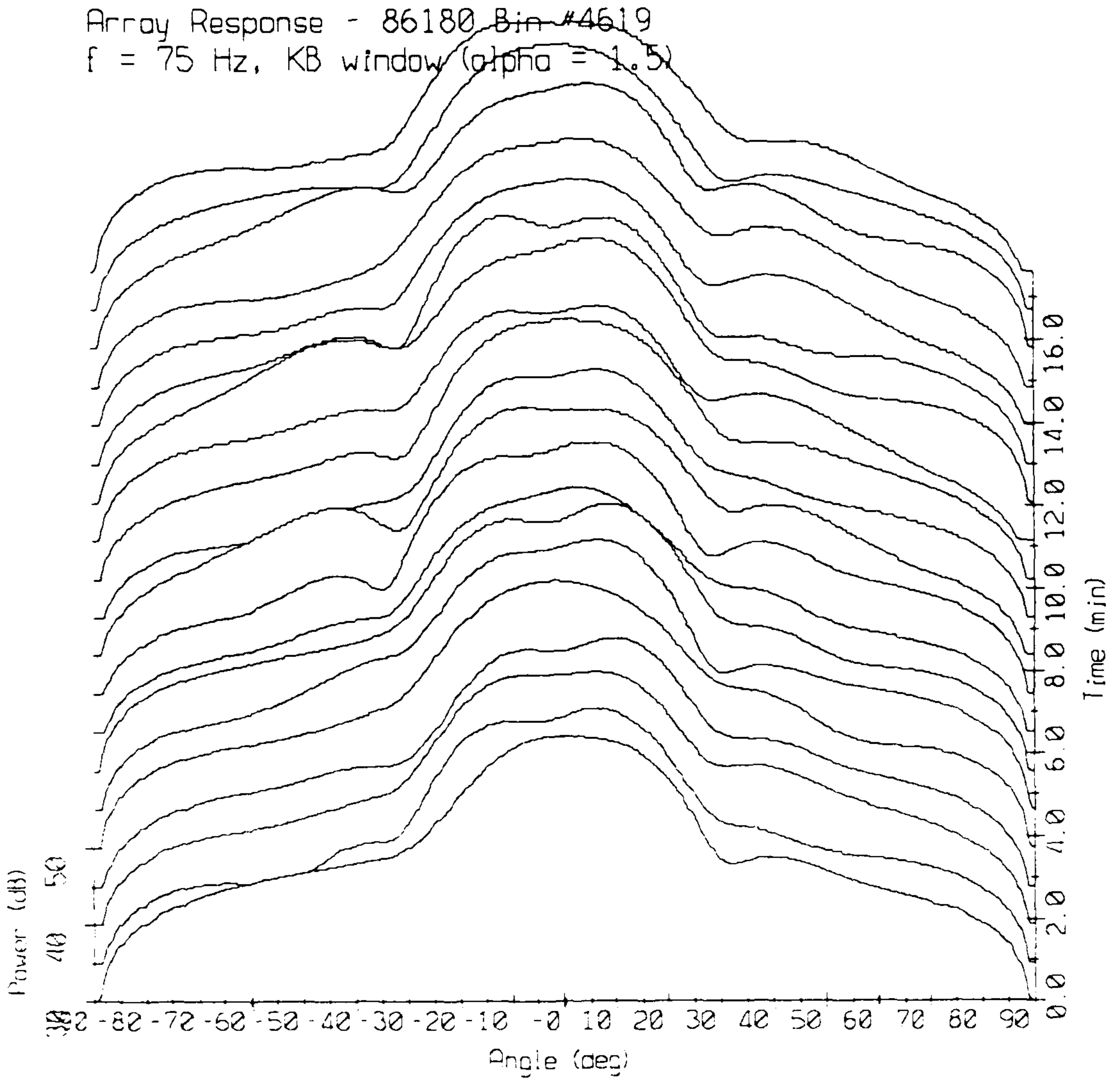

Array Response - 86180 Bin #4619
f = 75 Hz, KB window (alpha = 1.5)
Power (dB)
40
50
-82 -72 -62 -52 -42 -32 -22 -12 -0 12 22 32 42 52 62 72 82 92
Angle (deg)
0.0 2.0 4.0 6.0 8.0 10.0 12.0 14.0 16.0
Time (min)

Figure 19(c).

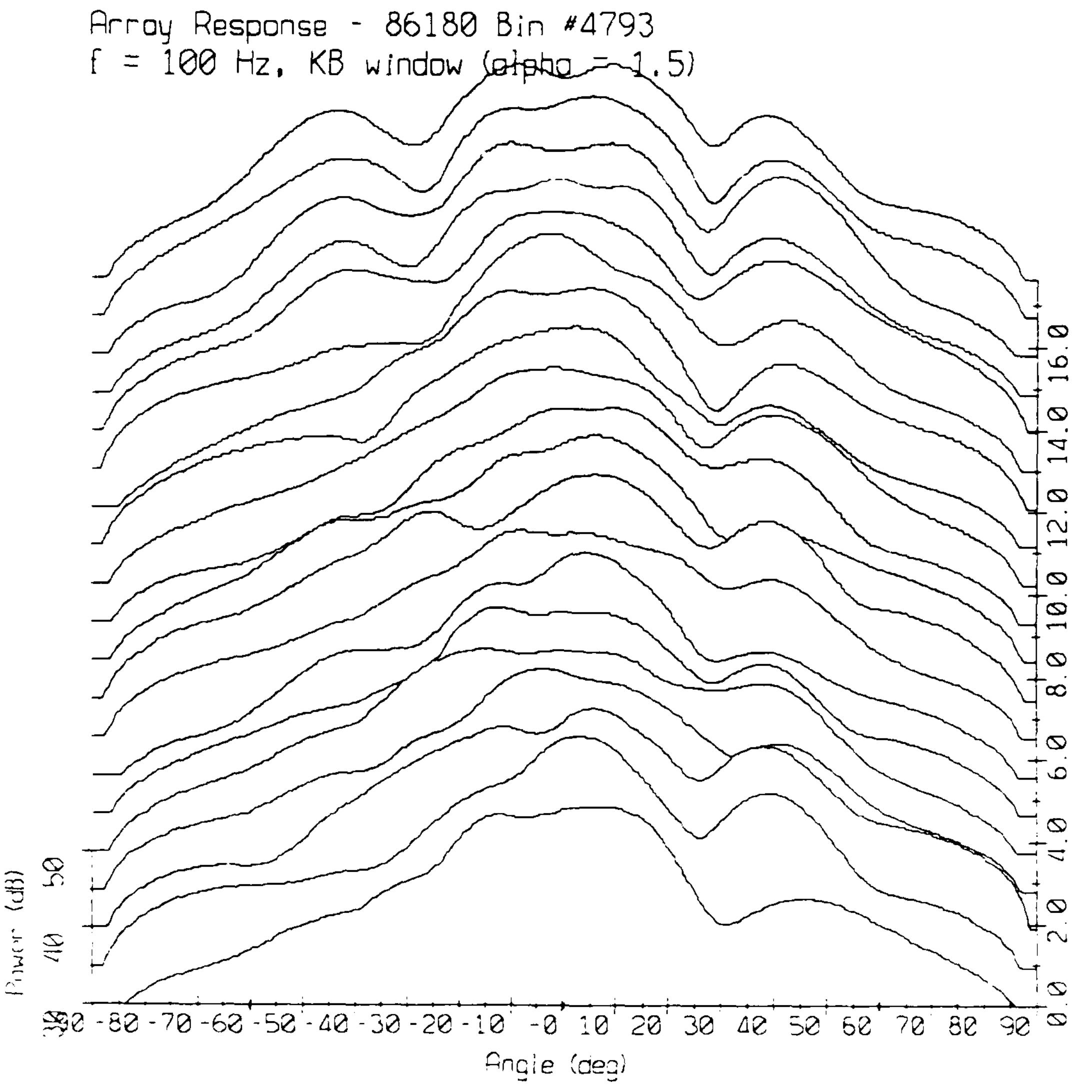

Array Response - 86180 Bin #4793
f = 100 Hz, KB window (alpha = 1.5)
Power (dB)
40
50
-90 -80 -70 -60 -50 -40 -30 -20 -10 -0 10 20 30 40 50 60 70 80 90
Angle (deg)
0.0
2.0
4.0
6.0
8.0
10.0
12.0
14.0
16.0
Time (min)

Figure 19(d).

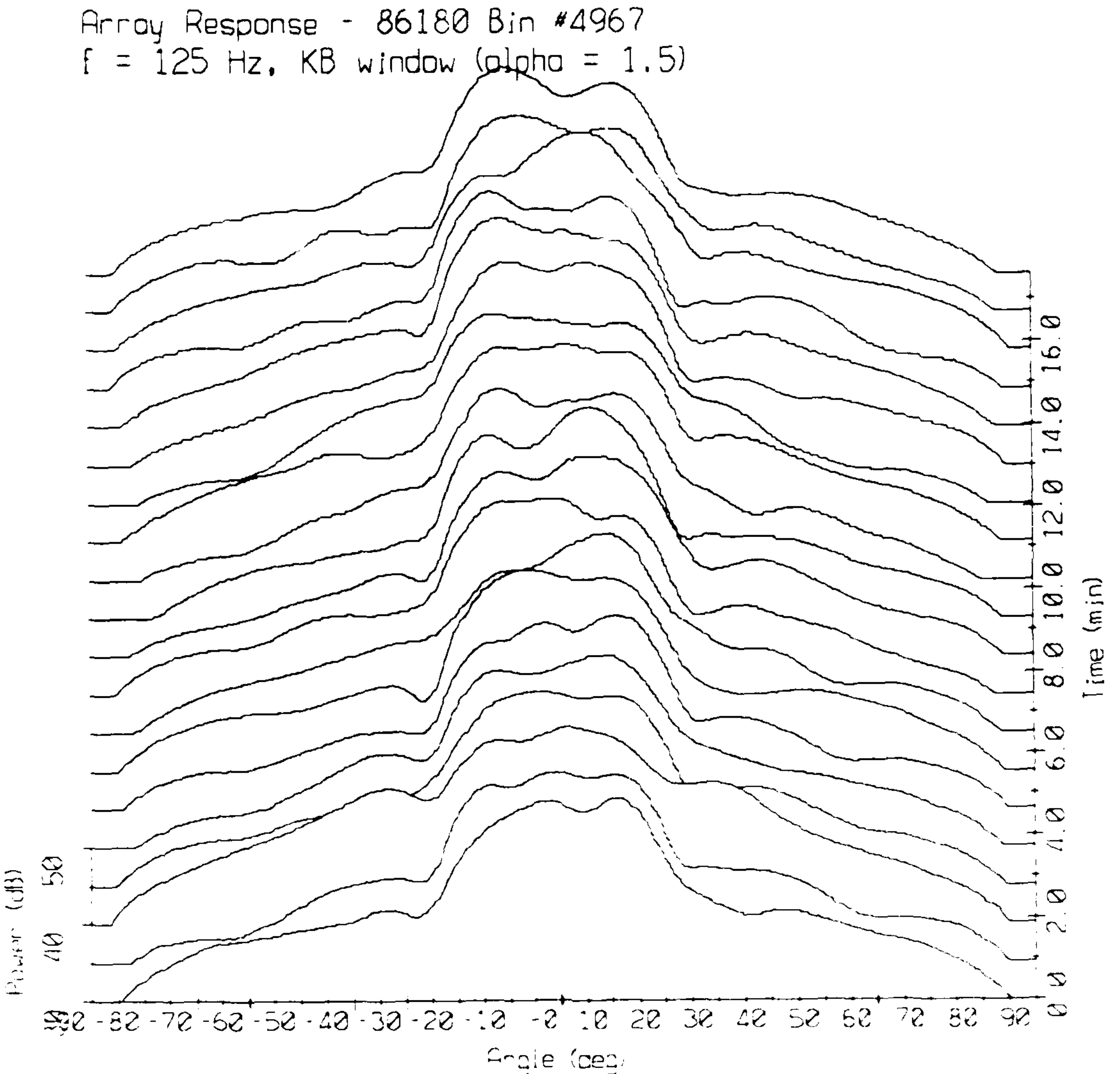
Array Response - 86180 Bin #4967
f = 125 Hz, KB window (alpha = 1.5)
Power (dB)
40
50
-90 -80 -70 -60 -50 -40 -30 -20 -10 -0 10 20 30 40 50 60 70 80 90
Angle (deg)
Time (min)
0.0 2.0 4.0 6.0 8.0 10.0 12.0 14.0 16.0

Figure 19(e).

Array Response - 86180 Bin #5141
f = 150 Hz, KB window (alpha = 1.5)

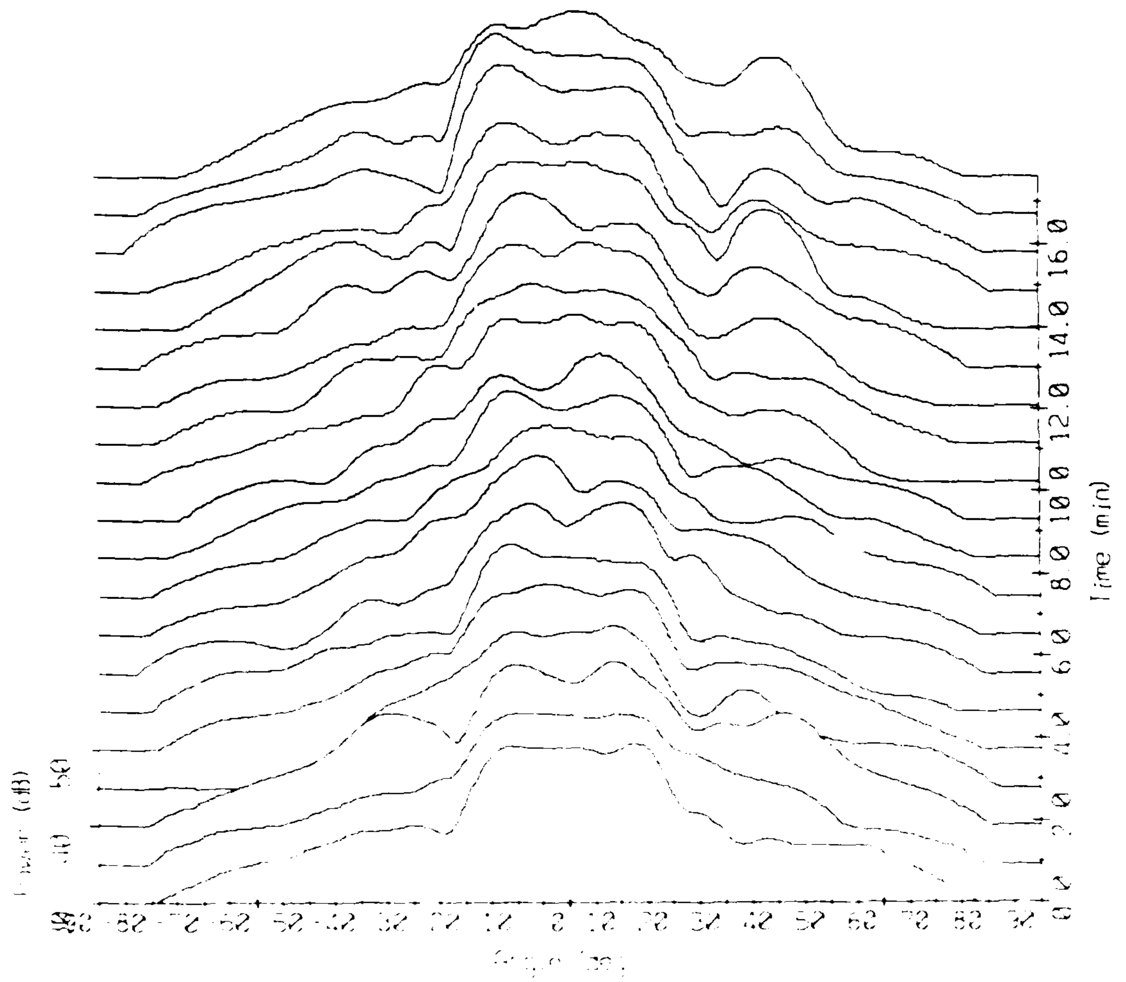

Figure 13(f).

Array Response - 86180 Bin #5316
f = 175 Hz, KB window (alpha = 1.5)

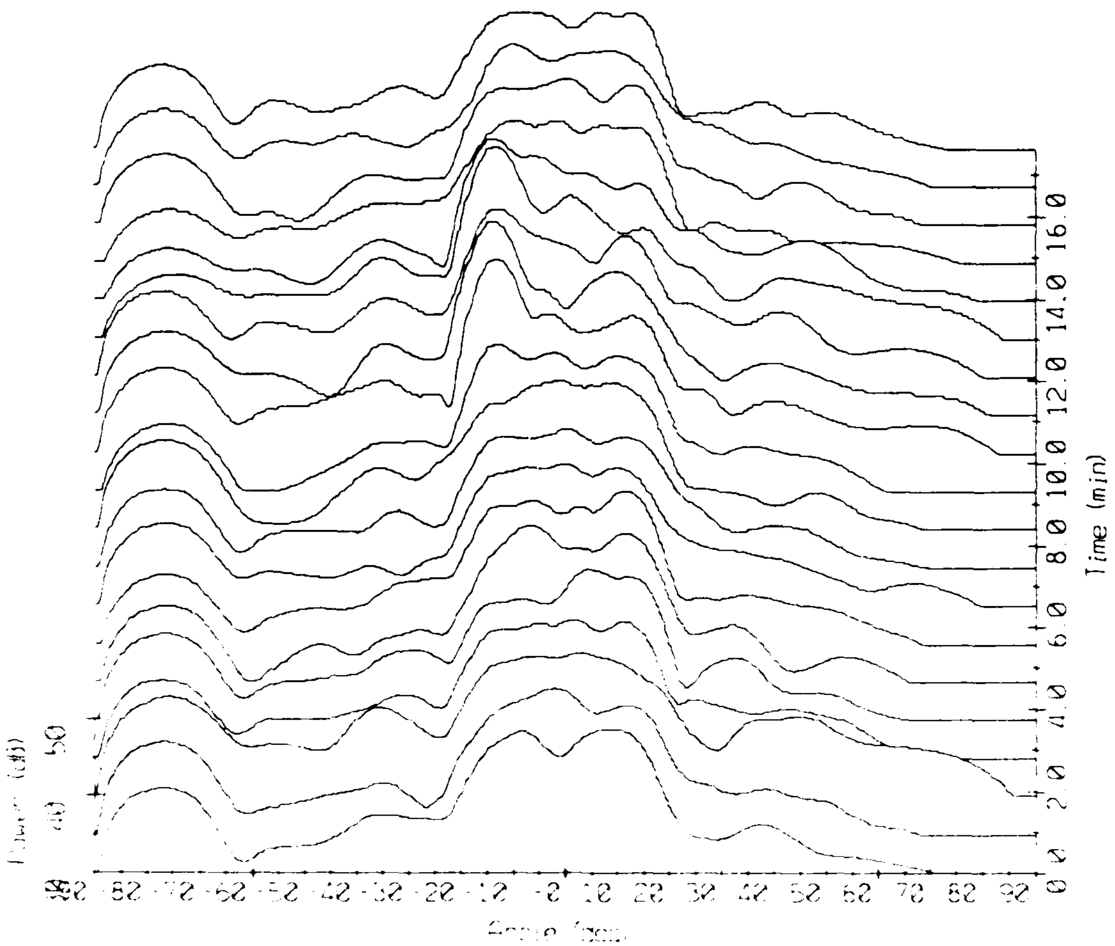

Figure 19(q).

Array Response - 86180 Bin #5490
f = 200 Hz, KB window (alpha = 1.5)

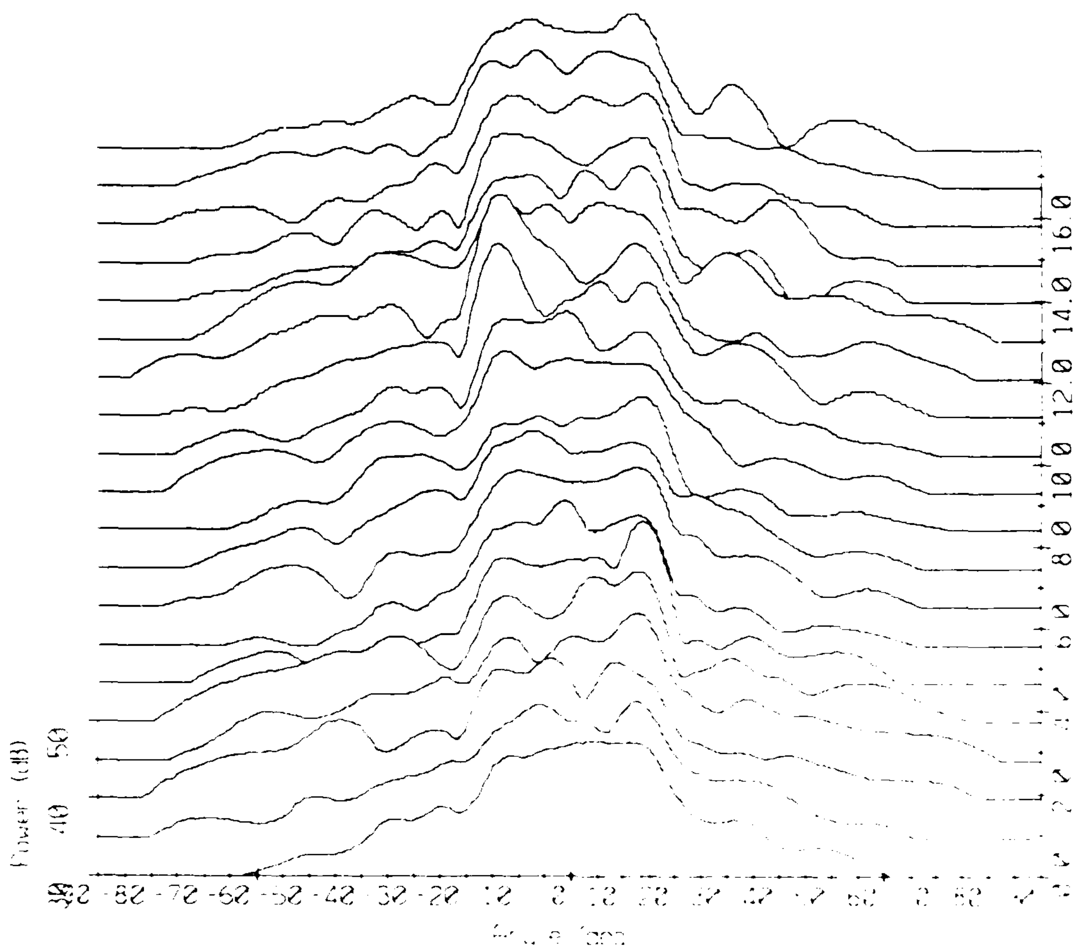

Figure 13(h).

Array Response - 86180 Bin #5664
f = 225 Hz, KB window (alpha = 1.5)

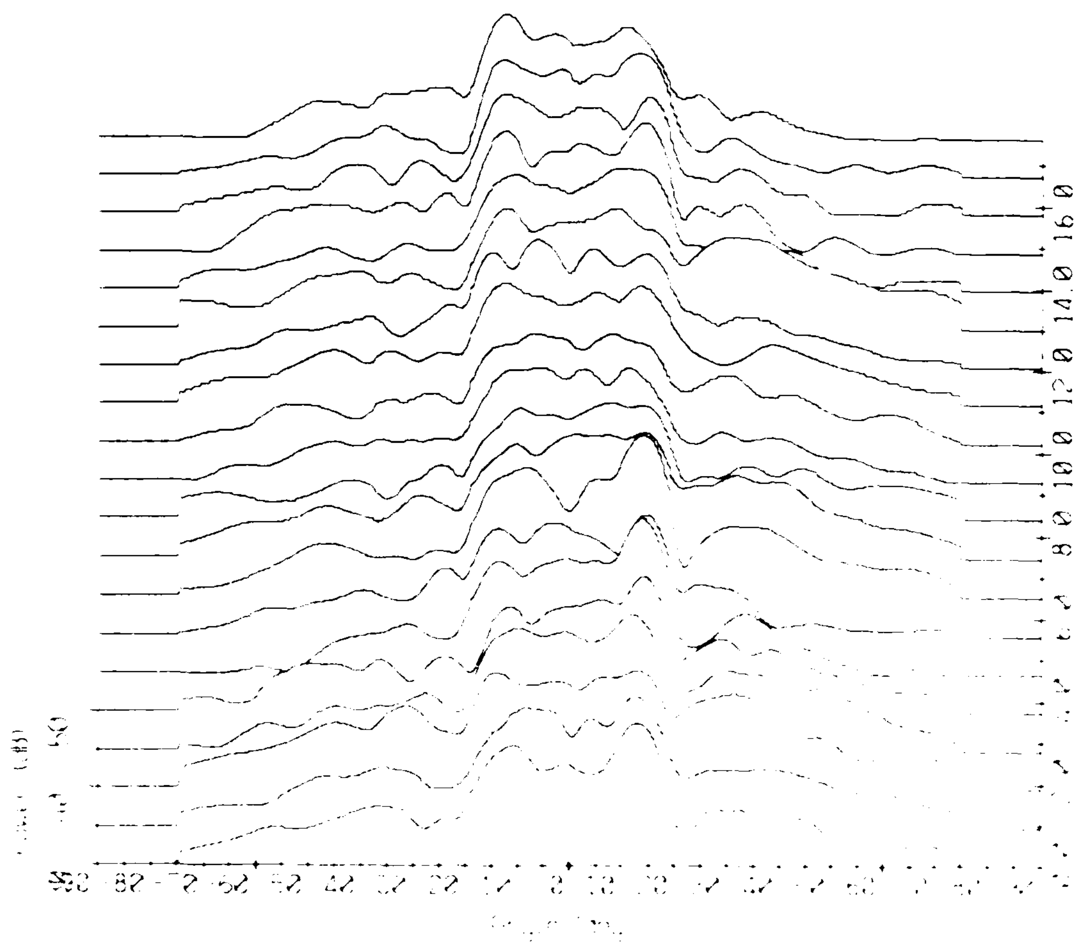

Array Response - 86180 Bin #5832
f = 250 Hz, KB window (alpha = 1.5)

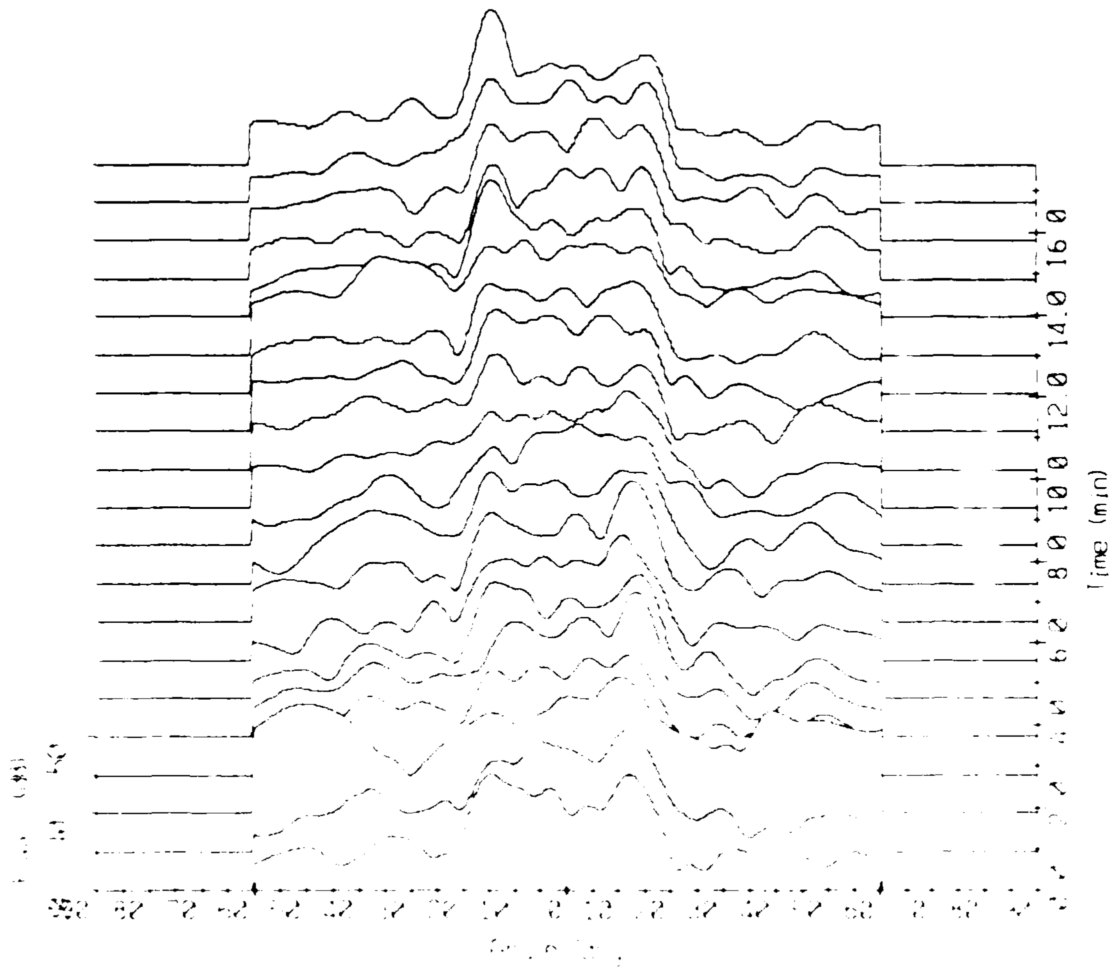

Array Response - 86180 Bin #6012
f = 275 Hz, KB window (alpha = 1.5)

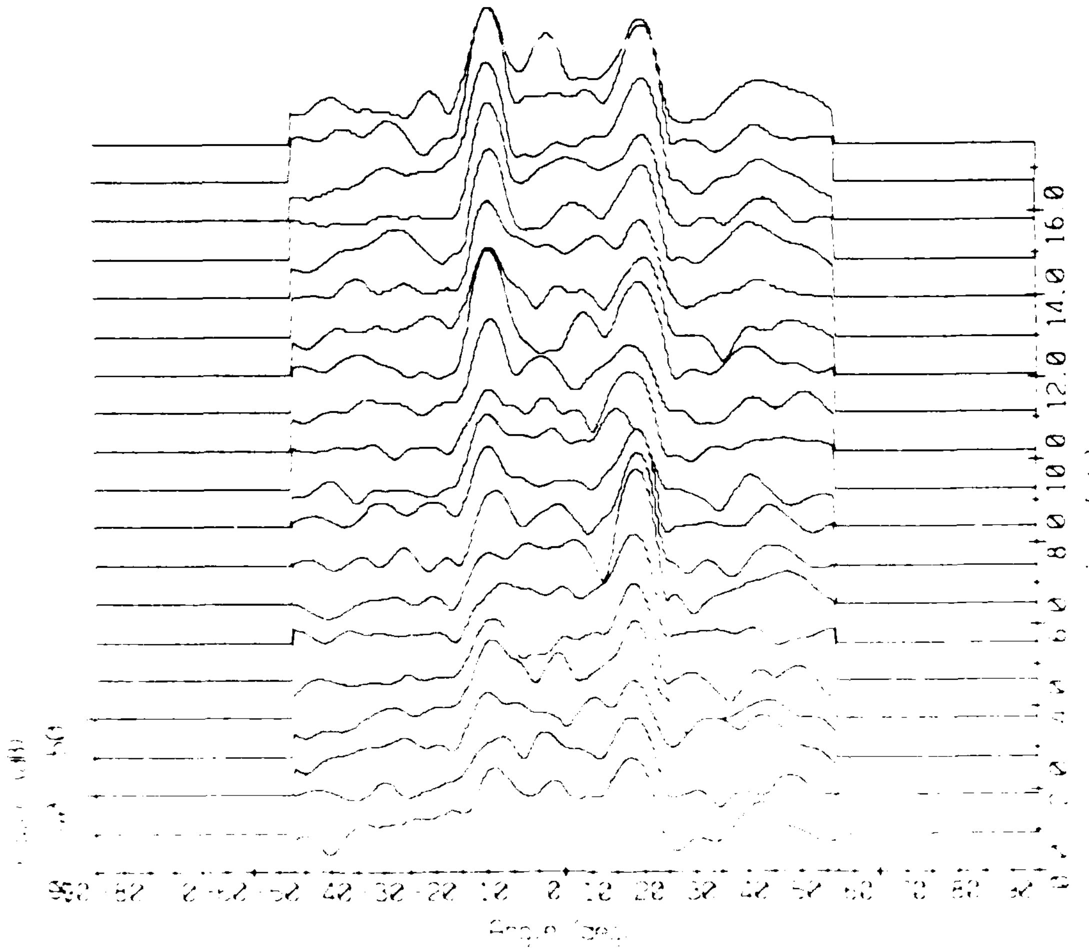

Figure 19(k).

Array Response - 86180 Bin #6186
f = 300 Hz, KB window (alpha = 1.5)

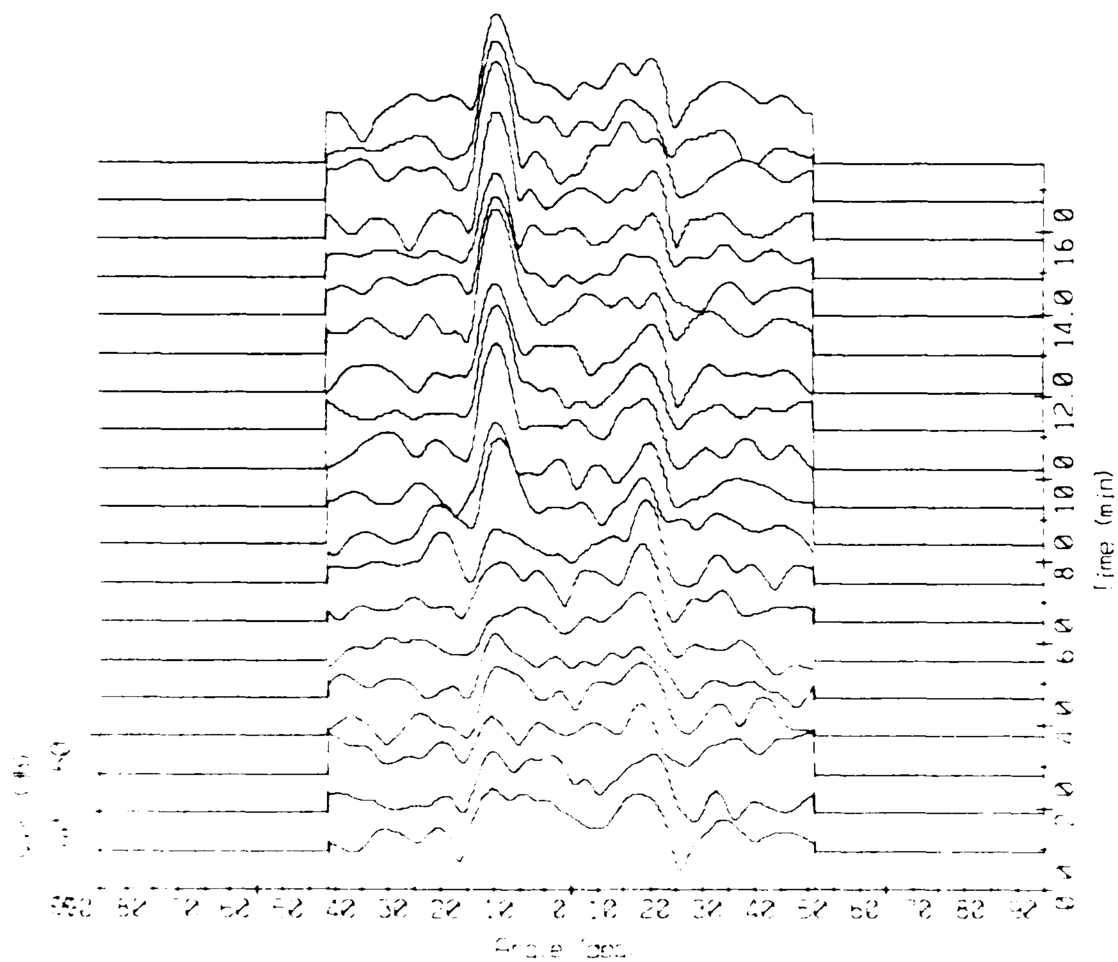

Figure 19(1).

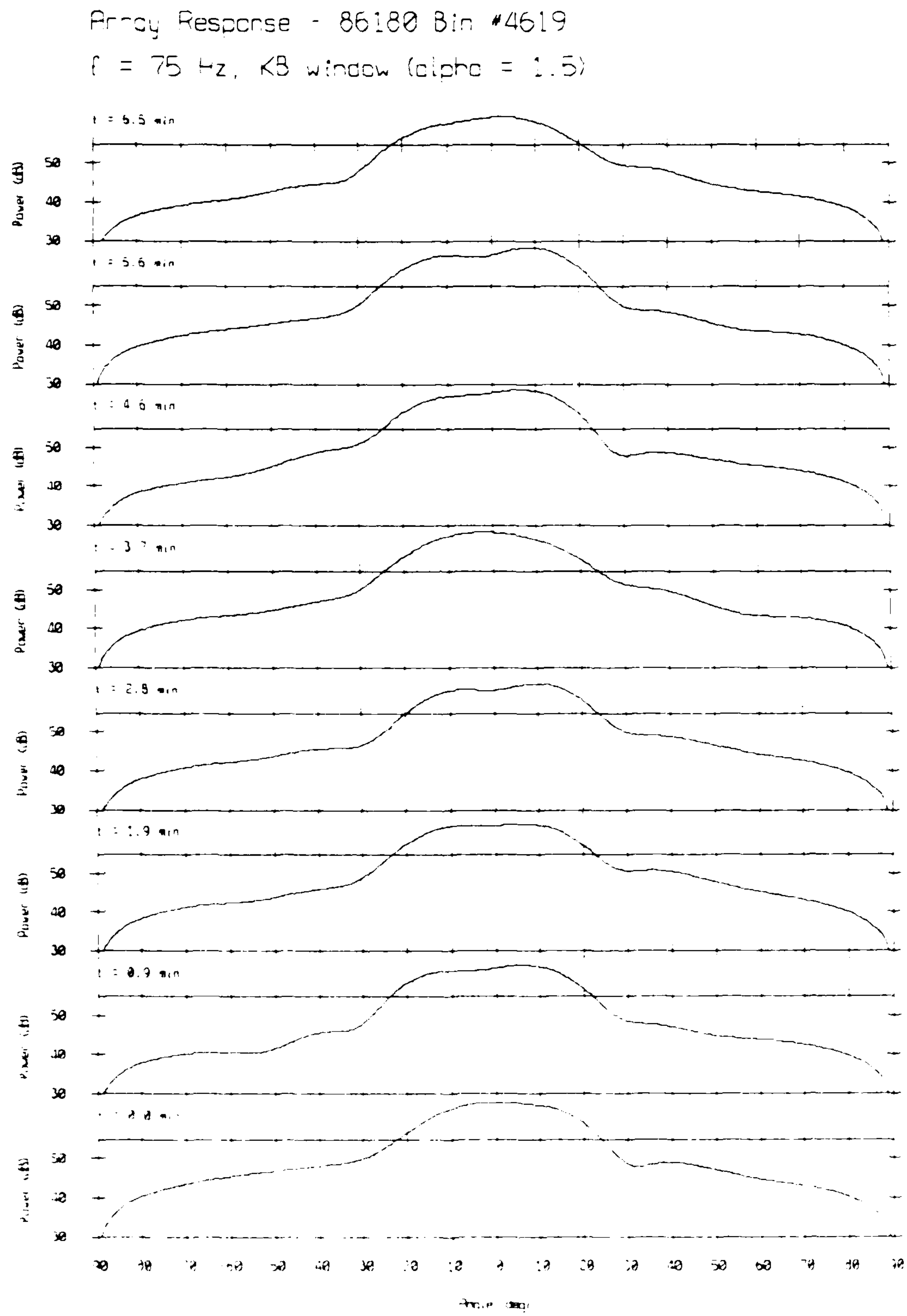
Array Response - 86180 Bin #4619
f = 75 Hz, KB window (alpha = 1.5)
t = 6.5 min
t = 5.6 min
t = 4.6 min
t = 3.7 min
t = 2.8 min
t = 1.9 min
t = 0.9 min
Power (dB)
30
40
50
90 80 70 60 50 40 30 20 10 0 10 20 30 40 50 60 70 80 90

Figure 20(a).

Array Response - 86180 Bin #4619

f = 75 Hz, KB window (alpha = 1.5)

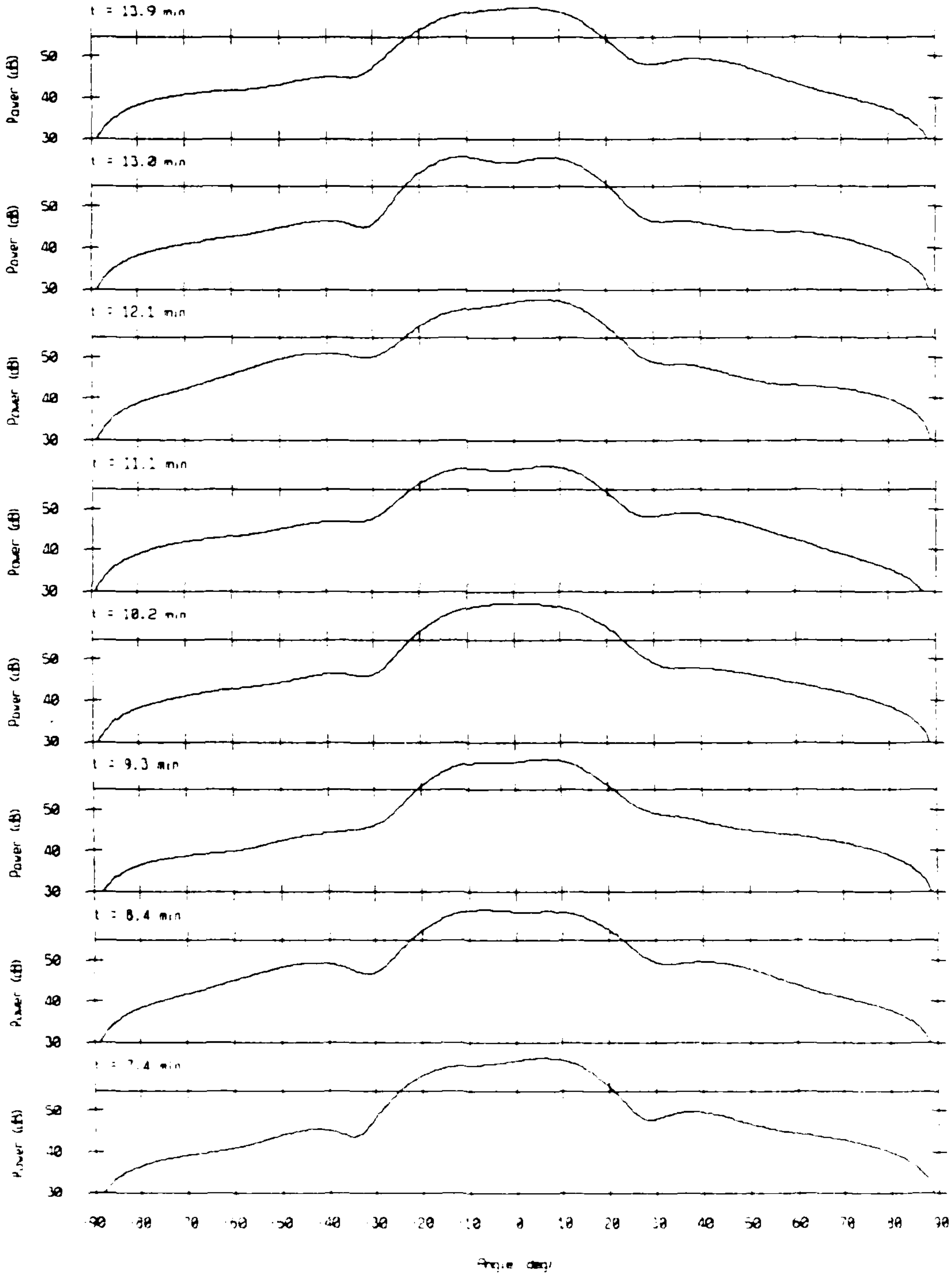

Array Response - 86180 Bin #4619

f = 75 Hz, KB window (alpha = 1.5)

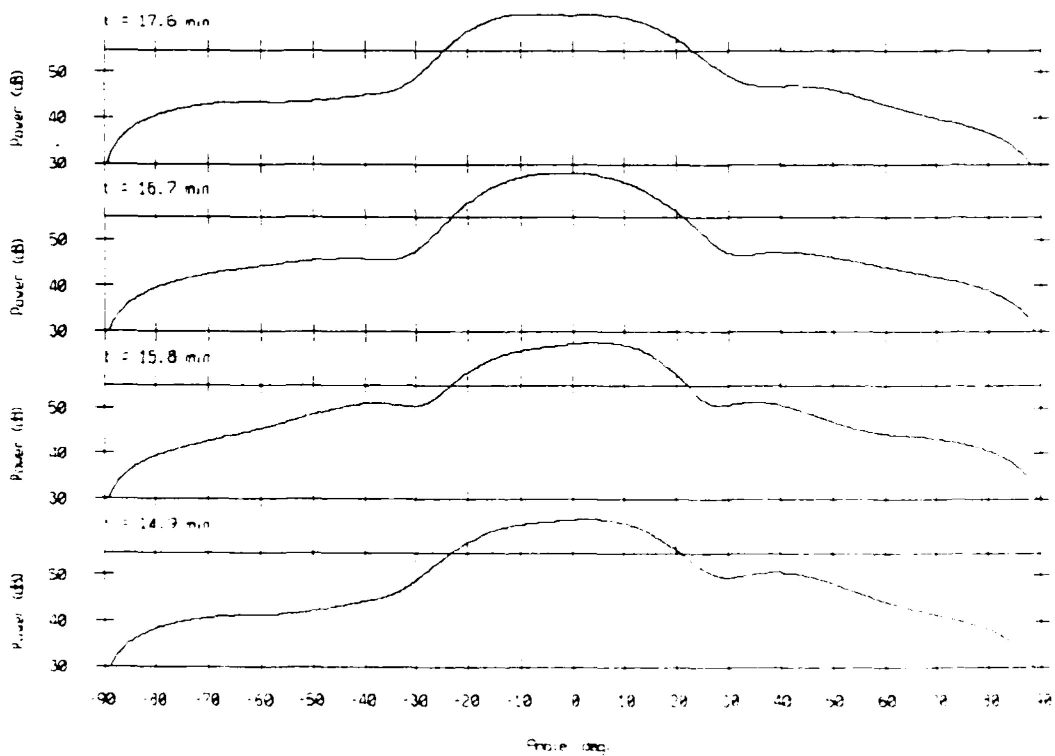

Array Response - 86180 Bin #5141

f = 150 Hz, KB window (alpha = 1.5)

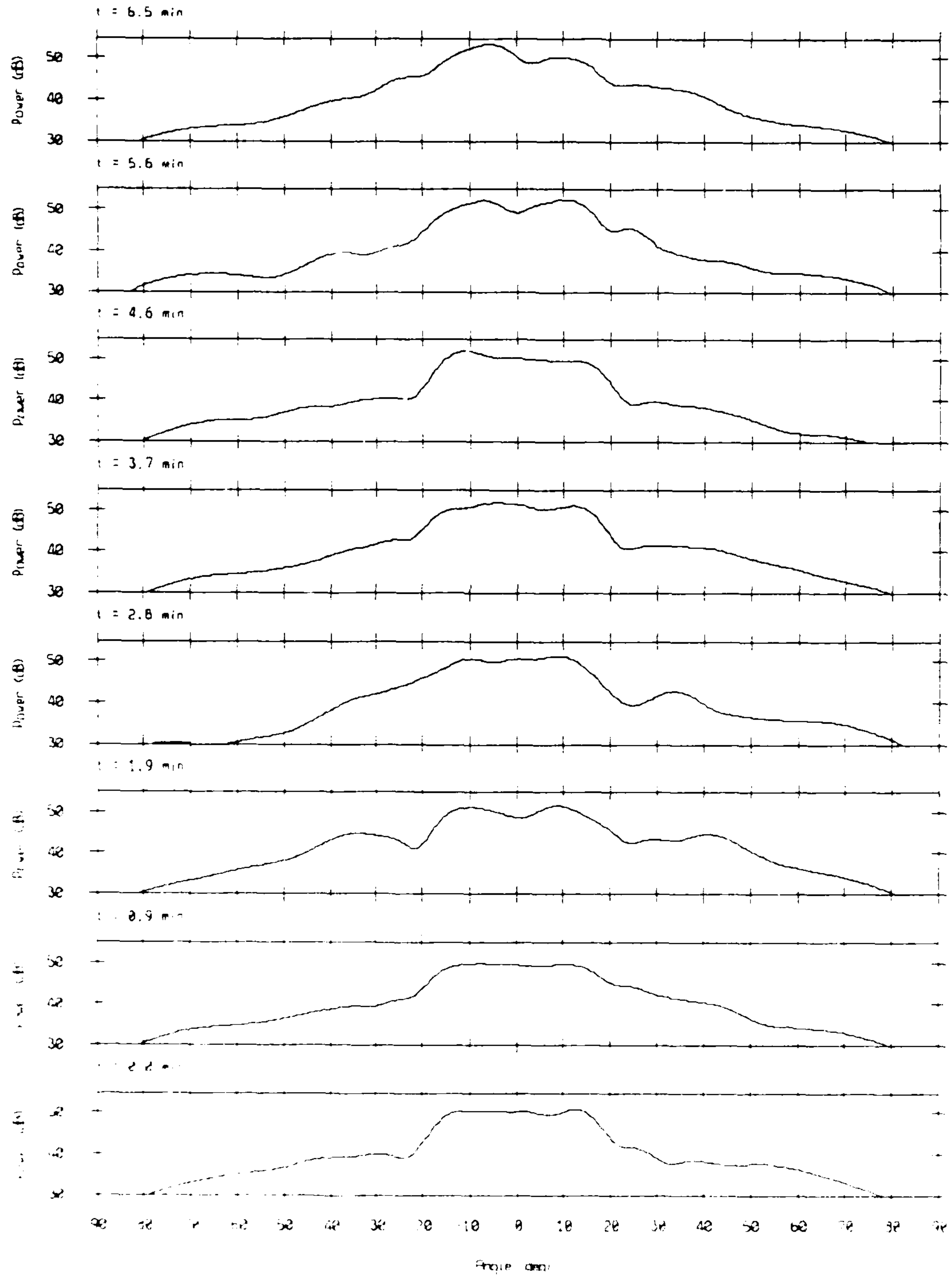

Figure 20(b).

Array Response - 86180 Bin #5141

f = 150 Hz, KB window (alpha = 1.5)

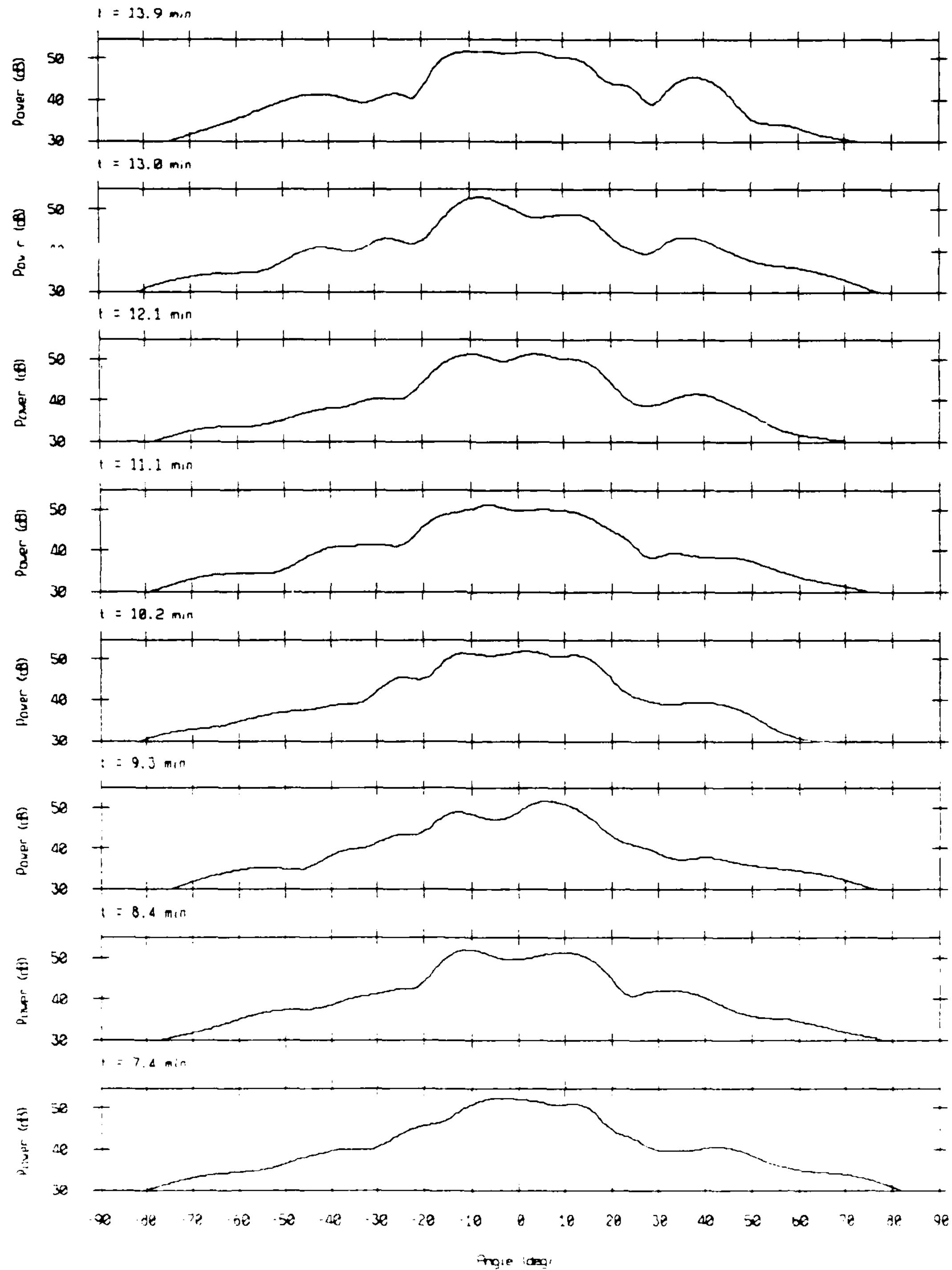

Array Response - 86180 Bin #5141

f = 150 Hz, KB window (alpha = 1.5)

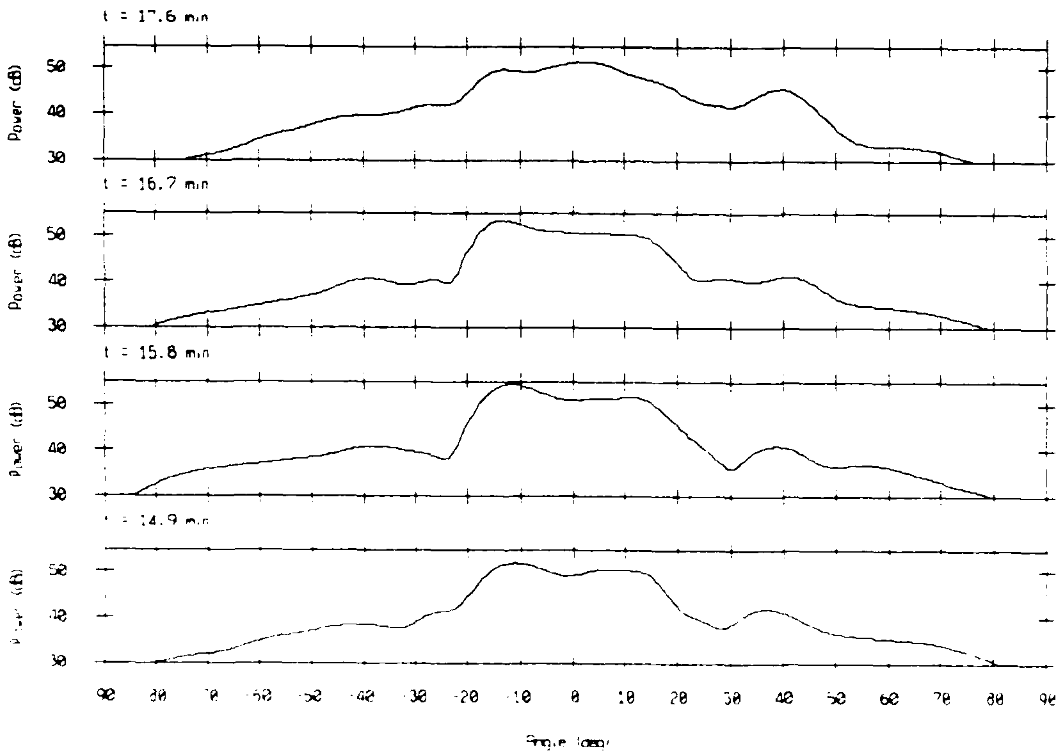

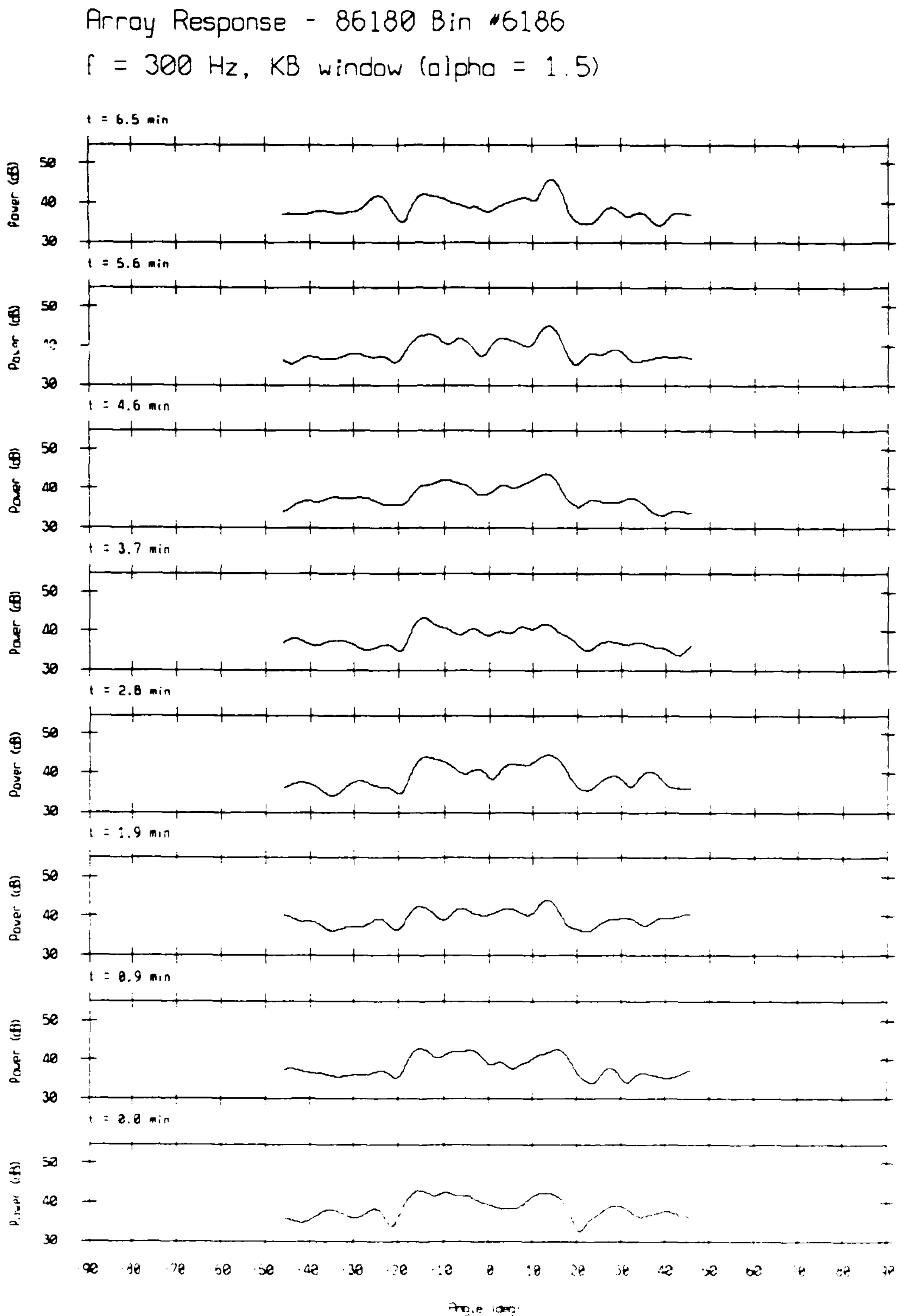
Array Response - 86180 Bin #6186
f = 300 Hz, KB window (alpha = 1.5)
t = 6.5 min
t = 5.6 min
t = 4.6 min
t = 3.7 min
t = 2.8 min
t = 1.9 min
t = 0.9 min
t = 0.0 min
Power (dB)
50
40
30
-90
-80
-70
-60
-50
-40
-30
-20
-10
0
10
20
30
40
50
60
70
80
90
Angle (deg)

Figure 20(c).

Array Response - 86180 Bin #6186

f = 300 Hz, KB window (alpha = 1.5)

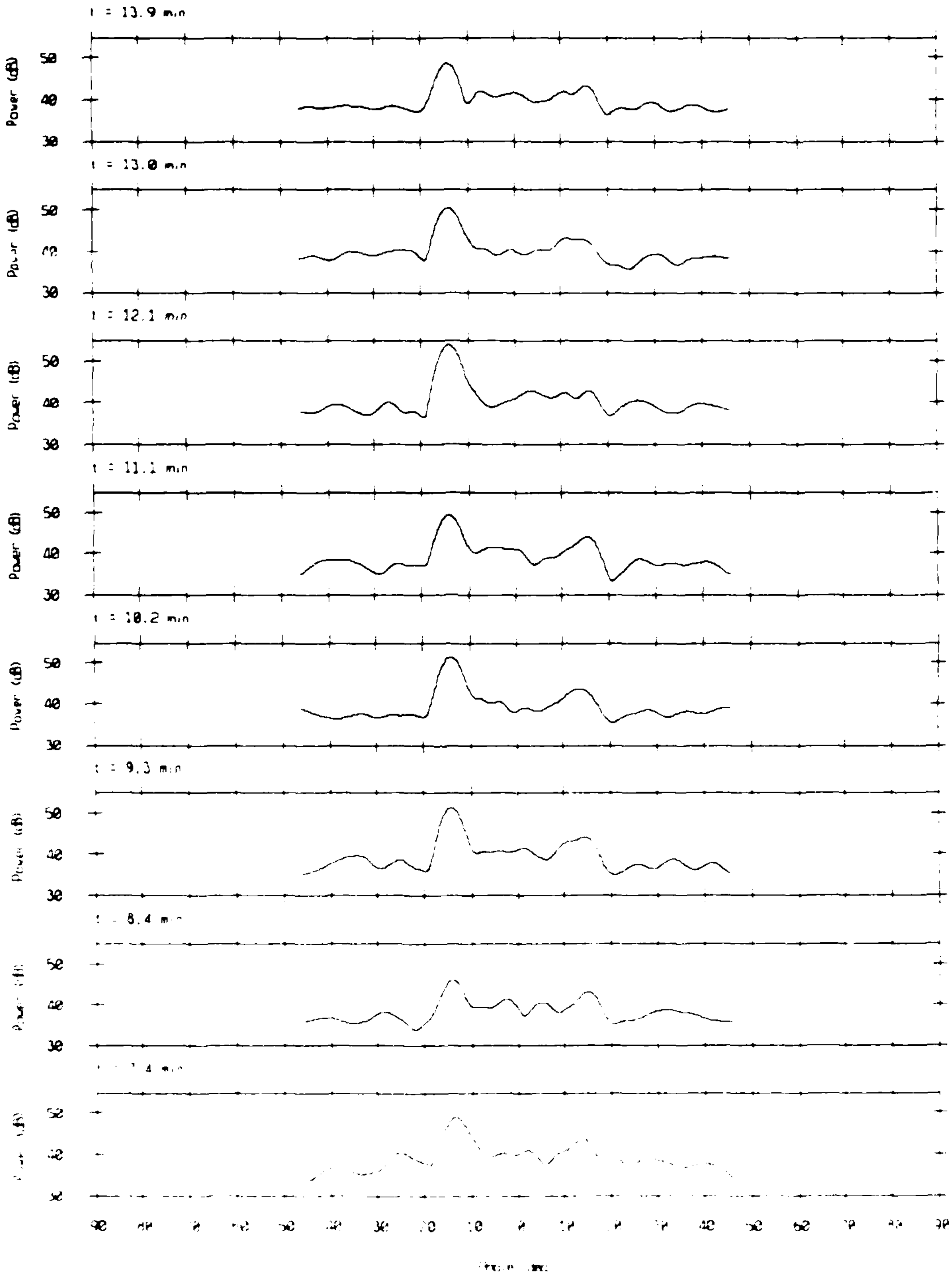

Array Response - 86180 Bin #6186

f = 300 Hz, KB window (alpha = 1.5)

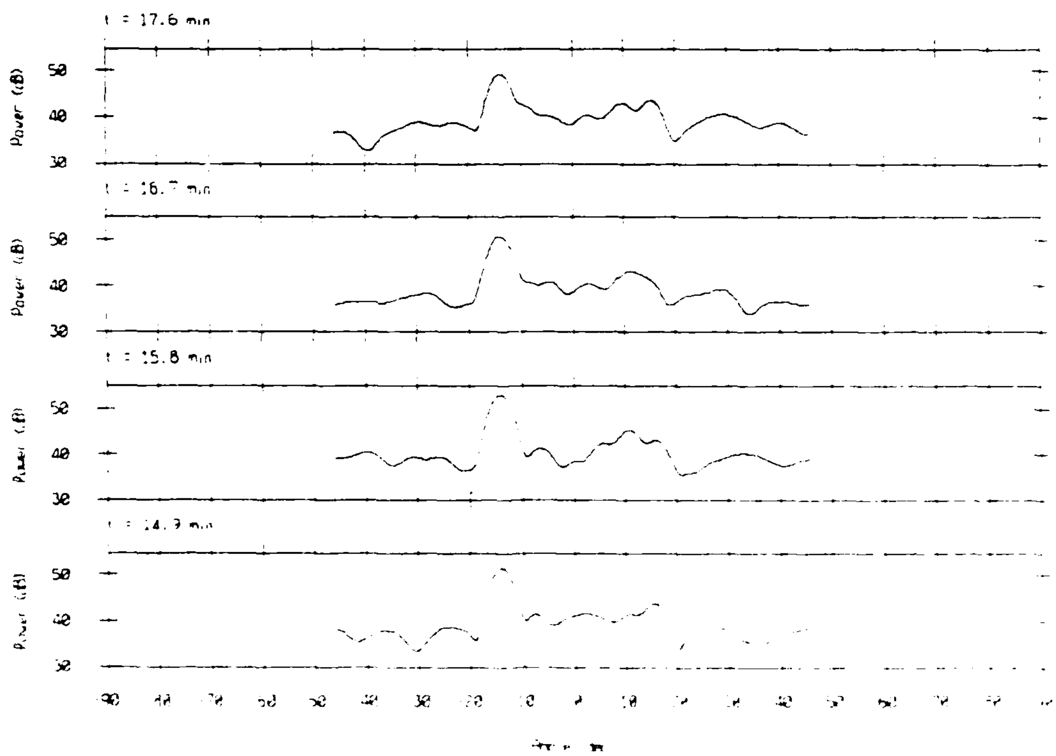

END
DATE
FILMED
DTIC
JULY 88